



January 2012

Dirhodium-Induced Intramolecular C-H Insertion On Diazosulfones/sulfonates And Its Synthetic Applications

Christian Suhngwa Jungong

[How does access to this work benefit you? Let us know!](#)

Follow this and additional works at: <https://commons.und.edu/theses>

Recommended Citation

Jungong, Christian Suhngwa, "Dirhodium-Induced Intramolecular C-H Insertion On Diazosulfones/sulfonates And Its Synthetic Applications" (2012). *Theses and Dissertations*. 1294.
<https://commons.und.edu/theses/1294>

This Dissertation is brought to you for free and open access by the Theses, Dissertations, and Senior Projects at UND Scholarly Commons. It has been accepted for inclusion in Theses and Dissertations by an authorized administrator of UND Scholarly Commons. For more information, please contact und.common@library.und.edu.

DIRHODIUM-INDUCED INTRAMOLECULAR C–H INSERTION ON
DIAZOSULFONES/SULFONATES AND ITS SYNTHETIC APPLICATIONS

by

Christian Suhngwa Jungong
Bachelor of Science (Honors), University of Buea, Cameroon, 2006

A Dissertation

Submitted to the Graduate Faculty

of the

University of North Dakota

In partial fulfillment of the requirements

for the degree of

Doctor of Philosophy

Grand Forks, North Dakota

August

2012

This dissertation, submitted by Christian Suhngwa Jungong in partial fulfillment of the requirements for the Degree of Doctor of Philosophy from the University of North Dakota, has been read by the Faculty Advisory Committee under whom the work has been done and is hereby approved.

Prof. Alexei Novikov

Prof. Irina Smoliakova

Prof. Kathryn Thomasson

Prof. Mark Hoffmann

Prof. Eric Murphy

This dissertation meets the standards for the appearance, conforms to the style and format requirements of the Graduate School of the University of North Dakota, and is hereby approved.

Prof. Wayne Swisher
Dean of the Graduate School

07/05/2012

PERMISSION

Title DIRHODIUM-INDUCED INTRAMOLECULAR C–H INSERTION
ON DIAZOSULFONES/SULFONATES AND ITS SYNTHETIC
APPLICATIONS

Department Chemistry

Degree Doctor of Philosophy

In presenting this dissertation in partial fulfillment of the requirements for a graduate degree from the University of North Dakota, I agree that the library of this University shall make it freely available for inspection. I further agree that permission for extensive copying for scholarly purposes may be granted by the professor who supervised my dissertation work or, in his absence, by the chairperson of the department or the dean of the Graduate School. It is understood that any copying or publication or other use of this thesis or part thereof for financial gain shall not be allowed without my written permission. It is also understood that due recognition shall be given to me and to the University of North Dakota in any scholarly use which may be made of any material in my dissertation.

Signature _____
Christian Suhngwa Jungong

Date 07/05/2012

TABLE OF CONTENTS

LIST OF FIGURES	VIII
LIST OF SCHEMES.....	XVIII
LIST OF TABLES	XXI
ACKNOWLEDGEMENTS.....	XXIII
ABSTRACT.....	XXVIII
CHAPTER	1
I. GENERAL INTRODUCTION AND BACKGROUND.....	1
1.1 C–H Bond Functionalization via Carbon–Carbon Bond Formation.....	1
1.2 Classes of Metal Carbenoid	8
1.3 Use of Rhodium(II) Complexes in Carbenoid C–H Insertion	9
1.4 Rhodium-Catalyzed C–H Insertion Mechanism.....	11
1.5 Synthetic Utility of Rhodium-Induced C–H Insertion.....	14
1.5.1 Intermolecular Rhodium-Induced C–H Insertion	15
1.5.2 Intramolecular Rhodium-Induced C–H Insertion	26
II. RHODIUM-CATALYZED INTRAMOLECULAR C–H INSERTION ON DIAZOSULFONES AND DIAZOSULFONATES	35
2.1 Introduction.....	35
2.3 Structural and Stereochemical Assignments of the Products	49

	2.5 Experimental Section for Rhodium-Catalyzed Intramolecular C–H Insertion Studies on Diazosulfones	52
III.	ENANTIOSELECTIVE RHODIUM-CATALYZED INTRAMOLECULAR C–H INSERTION ON DIAZOSULFONES	62
	3.1 Introduction.....	62
	3.2 Results and Discussion	64
	3.3 Experimental Section for Enantioselective Rhodium-Catalyzed Intramolecular C–H Insertion on Diazosulfones	75
IV.	SYNTHETICALLY USEFUL TRANSFORMATIONS OF CYCLIC SIX-MEMBERED SULFONES AND SULFONATES OBTAINED BY RHODIUM-CATALYZED INTRAMOLECULAR C–H INSERTION	88
	4.1 Introduction.....	88
	4.2 Results and discussion	90
	4.2.1 Direct Desulfonation of Cyclic Six-Membered Sulfonates (δ -Sulfones) to δ -Valerolactones via Samarium Iodide Reduction	90
	4.2.2 Direct Desulfonation of Cyclic Six-Membered Sulfonates (δ -Sulfones) to γ -Butyrolactones via <i>t</i> -Butyl Hydroxyperoxide (TBHP) Oxidation	93
	4.2.3 Alkylation of δ -Sulfones and Carboethoxythiane-1,1-Dioxides	96
	4.2.4 Formation of Cyclic α -Sulfonyl Oximes	100
	4.3 Conclusion	102
	4.4 Experimental Section on Synthetic Utility of Six-Membered Sulfones and Sulfonates obtained by Rhodium-Catalyzed Intramolecular C–H Insertion	103

V.	APPLICATION OF RHODIUM-CATALYZED INTRAMOLECULAR C–H INSERTION ON DIAZO SULFONES AND SULFONATES TOWARDS THE SYNTHESIS OF NATURAL PRODUCTS.....	115
	5.1 Synthesis of (+)-Bakuchiol	115
	5.1.1 Isolation and Biological activity of (+)-Bakuchiol	115
	5.1.2 Previous Syntheses of (+)-Bakuchiol	116
	5.1.3 Application of Intramolecular C–H Insertion on Diazosulfonates in the Synthesis of (+)-Bakuchiol	117
	5.2 Studies towards Synthesis of (+)-Quebrachamine.....	120
	5.2.1 Isolation and Biological Activity of (+)-Quebrachamine ...	120
	5.2.2 Previous Syntheses of Quebrachamine.....	121
	5.2.3 Application of Rhodium-Catalyzed Intramolecular C–H Insertion on Diazosulfonates towards the Synthesis of (+)- Quebrachamine.	122
	5.3 Studies towards Synthesis of (-)-Mesembrine	125
	5.3.1 Isolation and Biological Activity of (-)-Mesembrine	125
	5.3.2 Application of Rhodium-Catalyzed Intramolecular C–H Insertion on Diazosulfonates towards the Synthesis of (-)- Mesembrine.....	126
	5.4 Experimental Section on Application of Rhodium-Catalyzed Intramolecular C–H Insertion on Diazo Sulfones and Sulfonates towards the Synthesis of Natural Products	128
	APPENDICES	137
	APENDIX I: LIST OF ABBREVIATIONS AND ACRONYMS	138
	APENDIX II: SELECTED SPECTRA, FIGURES 13–150.....	141
	REFERENCES	279

LIST OF FIGURES

Figure	Page
1. Different types of C–H bonds in organic substrates; FG represents other functional groups in the substrates	3
2. Classes of diazo-based metal carbenoids	8
3. Common rhodium catalysts used for carbenoid C–H insertion of diazo compounds.....	11
4. Natural occurring lignin lactones synthesized by using rhodium-catalyzed intramolecular C–H insertion to generate γ -butyrolactones.....	31
5. Stereochemical and structural assignments of the six-membered sulfones	50
6. NOE responses (%) observed for isomers 150a , 155.2 , 156.2 , and 157.2	51
7. ^1H NMR spectrum of sulfonyl acetylmandalate showing peaks used for enantiomeric ratio determination.....	67
8. Chiral rhodium(II) carboxylate catalysts screened for enantioselective intramolecular C–H insertion.	68
9. Stereochemical assignment of alkylated products.....	99
10. Structure of (+)-bakuchiol.....	115
11. Aspidosperma alkaloids isolated from the white quebracho.....	121
12. Structure of (-)-mesembrine.	125
13. ^1H NMR (500 MHz) spectrum of ethyl (propylsulfonyl)acetate (155.1) in CDCl_3	141
14. $^{13}\text{C}\{^1\text{H}\}$ NMR (125 MHz) spectrum of ethyl (propylsulfonyl)acetate (155.1) in CDCl_3	142
15. ^1H NMR (500 MHz) spectrum of ethyl (2-methylpropylsulfonyl)acetate (156.1) in CDCl_3	143

16.	$^{13}\text{C}\{^1\text{H}\}$ NMR (125 MHz) spectrum of ethyl (2-methylpropylsulfonyl)acetate (156.1) in CDCl_3	144
17.	DEPT 135 NMR (125 MHz) spectrum of ethyl (2-methylpropylsulfonyl)acetate (156.1) in CDCl_3	145
18.	^1H NMR (500 MHz) spectrum of ethyl (3-methylbutylsulfonyl)acetate (160.1) in CDCl_3	146
19.	$^{13}\text{C}\{^1\text{H}\}$ NMR (125 MHz) spectrum of ethyl (3-methylbutylsulfonyl)acetate (160.1) in CDCl_3	147
20.	^1H NMR (500 MHz) spectrum of ethyl (propylsulfonyl)diazoacetate (158.2) in CDCl_3	148
21.	$^{13}\text{C}\{^1\text{H}\}$ NMR (125 MHz) spectrum of ethyl (propylsulfonyl)diazoacetate (158.2) in CDCl_3	149
22.	DEPT 135 NMR (125 MHz) spectrum of ethyl (propylsulfonyl)diazoacetate (158.2) in CDCl_3	150
23.	^1H NMR (500 MHz) spectrum of ethyl (2-methylpropylsulfonyl)diazoacetate (159.2) in CDCl_3	151
24.	$^{13}\text{C}\{^1\text{H}\}$ NMR (125 MHz) spectrum of ethyl (2-methylpropylsulfonyl)diazoacetate (159.2) in CDCl_3	152
25.	DEPT 135 NMR (125 MHz) spectrum of ethyl (2-methylpropylsulfonyl)diazoacetate (159.2) in CDCl_3	153
26.	^1H NMR (500 MHz) spectrum of ethyl (3-methylbutylsulfonyl)diazoacetate (160.2) in CDCl_3	154
27.	$^{13}\text{C}\{^1\text{H}\}$ NMR (500 MHz) spectrum of ethyl (3-methylbutylsulfonyl)diazoacetate (160.2) in CDCl_3	155
28.	DEPT 135 NMR (500 MHz) spectrum of ethyl (3-methylbutylsulfonyl)diazoacetate (160.2) in CDCl_3	156
29.	^1H NMR (500 MHz) spectrum of ethyl (2-methyl-2-propenylsulfonyl)acetate (161) in CDCl_3	157
30.	$^{13}\text{C}\{^1\text{H}\}$ NMR (125 MHz) spectrum of ethyl (2-methyl-2-propenylsulfonyl)acetate (161) in CDCl_3	158
31.	DEPT 135 NMR (125 MHz) spectrum of ethyl (2-methyl-2-propenylsulfonyl)acetate (161) in CDCl_3	159

32.	^1H NMR (500 MHz) spectrum of ethyl (3,3-dimethylthiotane-1,1-dioxide-2-carboxylate (159.2.2) in CDCl_3	160
33.	$^{13}\text{C}\{^1\text{H}\}$ NMR (125 MHz) spectrum of ethyl (3,3-dimethylthiotane-1,1-dioxide-2-carboxylate (159.2.2) in CDCl_3	161
34.	DEPT 135 NMR (125 MHz) spectrum of ethyl 3,3-dimethylthiotane-1,1-dioxide-2-carboxylate (159.2.2) in CDCl_3	162
35.	^1H NMR (500 MHz) spectrum of ethyl tetrahydro-2-ethyl-3,3-dimethylthiophene-1,1-dioxide-2-carboxylate (160.2.2) in CDCl_3	163
36.	$^{13}\text{C}\{^1\text{H}\}$ NMR (500 MHz) spectrum of ethyl tetrahydro-2-ethyl-3,3-dimethylthiophene-1,1-dioxide-2-carboxylate (160.2.2) in CDCl_3	164
37.	DEPT 135 NMR (500 MHz) spectrum of ethyl tetrahydro-2-ethyl-3,3-dimethylthiophene-1,1-dioxide-2-carboxylate (160.2.2) in CDCl_3	165
38.	^1H NMR (500 MHz) spectrum of (pentylsulfonyl)acetic acid (182) in CDCl_3	166
39.	$^{13}\text{C}\{^1\text{H}\}$ NMR spectrum of (pentylsulfonyl)acetic acid (182) in CDCl_3	167
40.	DEPT-135 NMR spectrum of (pentylsulfonyl)acetic acid (182) in CDCl_3	168
41.	^1H NMR (500 MHz) spectrum of methyl (pentylsulfonyl)acetate (183) in CDCl_3	169
42.	$^{13}\text{C}\{^1\text{H}\}$ NMR (125 MHz) spectrum of methyl (pentylsulfonyl)acetate (183) in CDCl_3	170
43.	DEPT 135 NMR (125 MHz) spectrum of methyl (pentylsulfonyl)acetate (183) in CDCl_3	171
44.	^1H NMR (500 MHz) spectrum of isopropyl (pentylsulfonyl)acetate (184) in CDCl_3	172
45.	$^{13}\text{C}\{^1\text{H}\}$ NMR (125MHz) spectrum of isopropyl (pentylsulfonyl)acetate (184) in CDCl_3	173
46.	DEPT 135 NMR (125MHz) spectrum of isopropyl (pentylsulfonyl)acetate (184) in CDCl_3	174
47.	^1H NMR (500 MHz) spectrum of <i>t</i> -butyl (pentylsulfonyl)acetate (185) in CDCl_3	175
48.	$^{13}\text{C}\{^1\text{H}\}$ NMR (125 MHz) spectrum of <i>t</i> -butyl (pentylsulfonyl)acetate (185) in CDCl_3	176

49.	DEPT 135 NMR (125 MHz) spectrum of <i>t</i> -butyl (pentylsulfonyl)acetate (185) in CDCl ₃	177
50.	¹ H NMR (500 MHz) spectrum of (1 <i>R</i> ,2 <i>S</i> ,5 <i>R</i>)-2-isopropyl-5-methylcyclohexyl (pentylsulfonyl)acetate (187) in CDCl ₃	178
51.	¹³ C{ ¹ H} NMR (500 MHz) spectrum of (1 <i>R</i> ,2 <i>S</i> ,5 <i>R</i>)-2-isopropyl-5-methylcyclohexyl (pentylsulfonyl)acetate (187) in CDCl ₃	179
52.	DEPT 135 NMR (500 MHz) spectrum of (1 <i>R</i> ,2 <i>S</i> ,5 <i>R</i>)-2-Isopropyl-5-methylcyclohexyl (pentylsulfonyl)acetate (187) in CDCl ₃	180
53.	¹ H NMR (500 MHz) spectrum of 2,4-dimethyl-3-pentyl (pentylsulfonyl)acetate (188) in CDCl ₃	181
54.	¹³ C{ ¹ H} NMR (125 MHz) spectrum of 2,4-dimethyl-3-pentyl (pentylsulfonyl)acetate (188) in CDCl ₃	182
55.	DEPT 135 NMR (125 MHz) spectrum of 2,4-dimethyl-3-pentyl (pentylsulfonyl)acetate (188) in CDCl ₃	183
56.	¹ H NMR (500 MHz) spectrum of methyl (pentylsulfonyl)diazoacetate (189) in CDCl ₃	184
57.	¹³ C{ ¹ H} NMR (125 MHz) spectrum of methyl (pentylsulfonyl)diazoacetate (189) in CDCl ₃	185
58.	DEPT 135 NMR (125 MHz) spectrum of methyl (pentylsulfonyl)diazoacetate (189) in CDCl ₃	186
59.	¹ H NMR (500 MHz) spectrum of isopropyl (pentylsulfonyl)diazoacetate (190) in CDCl ₃	187
60.	¹³ C{ ¹ H} NMR (125 MHz) spectrum of isopropyl (pentylsulfonyl)diazoacetate (190) in CDCl ₃	188
61.	DEPT 135 NMR (125 MHz) spectrum of isopropyl (pentylsulfonyl)diazoacetate (190) in CDCl ₃	189
62.	¹ H NMR (500 MHz) spectrum of <i>t</i> -butyl (pentylsulfonyl)diazoacetate (191) in CDCl ₃	190
63.	¹³ C{ ¹ H} NMR (125 MHz) spectrum of <i>t</i> -butyl (pentylsulfonyl)diazoacetate (191) in CDCl ₃	191
64.	DEPT 135 NMR (125 MHz) spectrum of <i>t</i> -butyl (pentylsulfonyl)diazoacetate (191) in CDCl ₃	192

65.	^1H NMR (500 MHz) spectrum of (1 <i>R</i> ,2 <i>S</i> ,5 <i>R</i>)-2-isopropyl-5-methylcyclohexyl (pentylsulfonyl)diazoacetate (193) in CDCl_3	193
66.	$^{13}\text{C}\{^1\text{H}\}$ NMR (500 MHz) spectrum of (1 <i>R</i> ,2 <i>S</i> ,5 <i>R</i>)-2-isopropyl-5-methylcyclohexyl (pentylsulfonyl)diazoacetate (193) in CDCl_3	194
67.	DEPT 135 NMR (500 MHz) spectrum of (1 <i>R</i> ,2 <i>S</i> ,5 <i>R</i>)-2-isopropyl-5-methylcyclohexyl (pentylsulfonyl)diazoacetate (193) in CDCl_3	195
68.	^1H NMR (500 MHz) spectrum of 2,4-dimethyl-3-pentyl (pentylsulfonyl)diazoacetate (194) in CDCl_3	196
69.	$^{13}\text{C}\{^1\text{H}\}$ NMR (500 MHz) spectrum of 2,4-dimethyl-3-pentyl (pentylsulfonyl)diazoacetate (194) in CDCl_3	197
70.	DEPT 135 NMR (500 MHz) spectrum of 2,4-dimethyl-3-pentyl (pentylsulfonyl)diazoacetate (194) in CDCl_3	198
71.	^1H NMR (500 MHz) spectrum of <i>trans</i> -methyl 3-methyltetrahydro-2 <i>H</i> -thiopyran-1,1-dioxide-2-carboxylate (195) in CDCl_3	199
72.	$^{13}\text{C}\{^1\text{H}\}$ NMR (125 MHz) spectrum of <i>trans</i> -methyl 3-methyltetrahydro-2 <i>H</i> -thiopyran-1,1-dioxide-2-carboxylate (195) in CDCl_3	200
73.	DEPT 135 NMR (125 MHz) spectrum of <i>trans</i> -methyl 3-methyltetrahydro-2 <i>H</i> -thiopyran-1,1-dioxide-2-carboxylate (195) in CDCl_3	201
74.	^1H NMR (500 MHz) spectrum of <i>trans</i> -isopropyl 3-methyltetrahydro-2 <i>H</i> -thiopyran-1,1-dioxide-2-carboxylate (196) in CDCl_3	202
75.	$^{13}\text{C}\{^1\text{H}\}$ NMR (125MHz) spectrum of <i>trans</i> -isopropyl 3-methyltetrahydro-2 <i>H</i> -thiopyran-1,1-dioxide-2-carboxylate (196) in CDCl_3	203
76.	DEPT 135 NMR (125MHz) spectrum of <i>trans</i> -isopropyl 3-methyltetrahydro-2 <i>H</i> -thiopyran-1,1-dioxide-2-carboxylate (196) in CDCl_3	204
77.	^1H NMR (500 MHz) spectrum of <i>trans</i> - <i>t</i> -butyl 3-methyltetrahydro-2 <i>H</i> -thiopyran-1,1-dioxide-2-carboxylate (197) in CDCl_3	205
78.	$^{13}\text{C}\{^1\text{H}\}$ NMR (125 MHz) spectrum of <i>trans</i> - <i>t</i> -butyl 3-methyltetrahydro-2 <i>H</i> -thiopyran-1,1-dioxide-2-carboxylate (197) in CDCl_3	206
79.	DEPT 135 NMR (125 MHz) spectrum of <i>trans</i> - <i>t</i> -butyl 3-methyltetrahydro-2 <i>H</i> -thiopyran-1,1-dioxide-2-carboxylate (197) in CDCl_3	207
80.	^1H NMR (500 MHz) spectrum of (1 <i>R</i> ,2 <i>S</i> ,5 <i>R</i>)-2-isopropyl-5-methylcyclohexyl (2 <i>R</i> ,3 <i>R</i>) 3-methyltetrahydro-2 <i>H</i> -thiopyran-1,1-dioxide-2-carboxylate (199) in CDCl_3	208

81.	$^{13}\text{C}\{^1\text{H}\}$ NMR (125 MHz) spectrum of (1 <i>R</i> ,2 <i>S</i> ,5 <i>R</i>)-2-isopropyl-5-methylcyclohexyl (2 <i>R</i> ,3 <i>R</i>) 3-methyltetrahydro-2 <i>H</i> -thiopyran-1,1-dioxide-2-carboxylate (199) in CDCl_3	209
82.	DEPT 135 NMR (125 MHz) spectrum of (1 <i>R</i> ,2 <i>S</i> ,5 <i>R</i>)-2-isopropyl-5-methylcyclohexyl (2 <i>R</i> ,3 <i>R</i>) 3-methyltetrahydro-2 <i>H</i> -thiopyran-1,1-dioxide-2-carboxylate (199) in CDCl_3	210
83.	^1H NMR (500 MHz) spectrum of <i>trans</i> -2,4-dimethyl-3-pentyl 3-methyltetrahydro-2 <i>H</i> -thiopyran-1,1-dioxide-2-carboxylate (200) in CDCl_3	211
84.	$^{13}\text{C}\{^1\text{H}\}$ NMR (125 MHz) spectrum of <i>trans</i> -2,4-dimethyl-3-pentyl 3-methyltetrahydro-2 <i>H</i> -thiopyran-1,1-dioxide-2-carboxylate (200) in CDCl_3	212
85.	DEPT 135 NMR (125 MHz) spectrum of <i>trans</i> -2,4-dimethyl-3-pentyl 3-methyltetrahydro-2 <i>H</i> -thiopyran-1,1-dioxide-2-carboxylate (200) in CDCl_3	213
86.	^1H NMR (500 MHz) spectrum of (<i>R</i>)-1,4-bis(4-toluenesulfonyloxy)pentane (202) in CDCl_3	214
87.	$^{13}\text{C}\{^1\text{H}\}$ NMR (125 MHz) spectrum of (<i>R</i>)-1,4-bis(4-toluenesulfonyloxy)pentane (202) in CDCl_3	215
88.	DEPT 135 NMR (125 MHz) spectrum of (<i>R</i>)-1,4-bis(4-toluenesulfonyloxy)pentane (202) in CDCl_3	216
89.	^1H NMR (500 MHz) spectrum of (<i>R</i>)-ethyl [4-(4-toluenesulfonyloxy)pentylsulfonyl]acetate (203) in CDCl_3	217
90.	$^{13}\text{C}\{^1\text{H}\}$ NMR (125 MHz) spectrum of (<i>R</i>)-ethyl [4-(4-toluenesulfonyloxy)pentylsulfonyl]acetate (203) in CDCl_3	218
91.	DEPT 135 NMR (125 MHz) spectrum of (<i>R</i>)-ethyl [4-(4-toluenesulfonyloxy)pentylsulfonyl]acetate (203) in CDCl_3	219
92.	^1H NMR (500 MHz) spectrum of 7,8,8-trimethyl-4-oxatricyclo[4.2.1.0 ^{3,7}]nonan-5-one (225) in CDCl_3	220
93.	$^{13}\text{C}\{^1\text{H}\}$ NMR (125 MHz) spectrum of 7,8,8-trimethyl-4-oxatricyclo[4.2.1.0 ^{3,7}]nonan-5-one (225) in CDCl_3	221
94.	DEPT-135 NMR (125 MHz) spectrum of 7,8,8-trimethyl-4-oxatricyclo[4.2.1.0 ^{3,7}]nonan-5-one (225) in CDCl_3	222
95.	^1H NMR (500 MHz) spectrum of 3-methyl-3-(4-methyl-3-pentenyl)dihydrofuran-2-one (226) in CDCl_3	223

96.	$^{13}\text{C}\{^1\text{H}\}$ NMR (125 MHz) spectrum of 3-methyl-3-(4-methyl-3-pentenyl)dihydrofuran-2-one (226) in CDCl_3	224
97.	^1H NMR (500 MHz) spectrum of 3-(3-benzyloxypropyl)-3-ethyldihydrofuran-2-one (227) in CDCl_3	225
98.	$^{13}\text{C}\{^1\text{H}\}$ NMR (125 MHz) spectrum of 3-(3-benzyloxypropyl)-3-ethyldihydrofuran-2-one (227) in CDCl_3	226
99.	DEPT 135 NMR (125 MHz) spectrum of 3-(3-benzyloxypropyl)-3-ethyldihydrofuran-2-one (227) in CDCl_3	227
100.	^1H NMR (500 MHz) spectrum of 2-azido-2-carbethoxy-3,3-dimethylthiane-1,1-dioxide (239) in CDCl_3	228
101.	$^{13}\text{C}\{^1\text{H}\}$ NMR (125 MHz) spectrum of 2-azido-2-carbethoxy-3,3-dimethylthiane-1,1-dioxide (239) in CDCl_3	229
102.	DEPT 135 NMR (125 MHz) spectrum of 2-azido-2-carbethoxy-3,3-dimethylthiane-1,1-dioxide (239) in CDCl_3	230
103.	^1H NMR (500 MHz) spectrum of 2-chloro-2-carbethoxy-3,3-dimethylthiane-1,1-dioxide (240) in CDCl_3	231
104.	$^{13}\text{C}\{^1\text{H}\}$ NMR (125 MHz) spectrum of 2-chloro-2-carbethoxy-3,3-dimethylthiane-1,1-dioxide (240) in CDCl_3	232
105.	DEPT 135 NMR (125 MHz) spectrum of 2-chloro-2-carbethoxy-3,3-dimethylthiane-1,1-dioxide (240) in CDCl_3	233
106.	^1H NMR (500 MHz) spectrum of 2-(4-chlorobenzyl)-2-carbethoxy-3,3-dimethylthiane-1,1-dioxide (241) in CDCl_3	234
107.	$^{13}\text{C}\{^1\text{H}\}$ NMR (125 MHz) spectrum of 2-(4-chlorobenzyl)-2-carbethoxy-3,3-dimethylthiane-1,1-dioxide (241) in CDCl_3	235
108.	DEPT 135 NMR (125 MHz) spectrum of 2-(4-chlorobenzyl)-2-carbethoxy-3,3-dimethylthiane-1,1-dioxide (241) in CDCl_3	236
109.	^1H NMR (500 MHz) spectrum of 2-methyl-2-carbethoxy-3,3-dimethylthiane-1,1-dioxide (242) in CDCl_3	237
110.	$^{13}\text{C}\{^1\text{H}\}$ NMR (125 MHz) spectrum of 2-methyl-2-carbethoxy-3,3-dimethylthiane-1,1-dioxide (242) in CDCl_3	238
111.	DEPT 135 NMR (125 MHz) spectrum of 2-methyl-2-carbethoxy-3,3-dimethylthiane-1,1-dioxide (242) in CDCl_3	239

112.	¹ H NMR (500 MHz) spectrum of 2-hydroxyimino-3-methylthiane-1,1-dioxide (254) in CDCl ₃	240
113.	¹³ C{ ¹ H} NMR (125 MHz) spectrum of 2-hydroxyimino-3-methylthiane-1,1-dioxide (254) in CDCl ₃	241
114.	DEPT 135 NMR (125 MHz) spectrum of 2-hydroxyimino-3-methylthiane-1,1-dioxide (254) in CDCl ₃	242
115.	¹ H NMR (500 MHz) spectrum of 2-hydroxyiminothiane-1,1-dioxide (255) in CDCl ₃	243
116.	¹³ C{ ¹ H} NMR (500 MHz) spectrum of 2-hydroxyiminothiane-1,1-dioxide (255) in CDCl ₃	244
117.	DEPT 135 NMR (500 MHz) spectrum of 2-hydroxyiminothiane-1,1-dioxide (255) in CDCl ₃	245
118.	¹ H NMR (500 MHz) spectrum of 2-hydroxyimino-3-ethylthiane-1,1-dioxide (256) in CDCl ₃	246
119.	¹³ C{ ¹ H} NMR (125 MHz) spectrum of 2-hydroxyimino-3-ethylthiane-1,1-dioxide (256) in CDCl ₃	247
120.	DEPT 135 NMR (125 MHz) spectrum of 2-hydroxyimino-3-ethylthiane-1,1-dioxide (256) in CDCl ₃	248
121.	¹ H NMR (500 MHz) spectrum of 2-hydroxyimino-3-butylthiane-1,1-dioxide (257) in CDCl ₃	249
122.	¹³ C{ ¹ H} NMR (125 MHz) spectrum of 2-hydroxyimino-3-butylthiane-1,1-dioxide (257) in CDCl ₃	250
123.	DEPT 135 NMR (125 MHz) spectrum of 2-hydroxyimino-3-butylthiane-1,1-dioxide (257) in CDCl ₃	251
124.	¹ H NMR (500 MHz) spectrum of ethyl 6-benzyloxy-3-ethylhexanoate (294) in CDCl ₃	252
125.	¹³ C{ ¹ H} NMR (125 MHz) spectrum of ethyl 6-benzyloxy-3-ethylhexanoate (294) in CDCl ₃	253
126.	DEPT 135 NMR (125 MHz) spectrum of ethyl 6-benzyloxy-3-ethylhexanoate (294) in CDCl ₃	254
127.	¹ H NMR (500 MHz) spectrum of 6-benzyloxy-3-ethyl-1-hexanol (289) in CDCl ₃	255

128.	$^{13}\text{C}\{^1\text{H}\}$ NMR (500 MHz) spectrum of 6-benzyloxy-3-ethyl-1-hexanol (289) in CDCl_3	256
129.	DEPT 135 NMR (500 MHz) spectrum of 6-benzyloxy-3-ethyl-1-hexanol (289) in CDCl_3	257
130.	^1H NMR (500 MHz) spectrum of ethyl [(6-benzyloxy-3-ethyl)hexyloxysulfonyl]acetate (295) in CDCl_3	258
131.	$^{13}\text{C}\{^1\text{H}\}$ NMR (125 MHz) spectrum of ethyl [(6-benzyloxy-3-ethyl)hexyloxysulfonyl]acetate (295) in CDCl_3	259
132.	DEPT 135 NMR (125 MHz) spectrum of ethyl [(6-benzyloxy-3-ethyl)hexyloxysulfonyl]acetate (295) in CDCl_3	260
133.	^1H NMR (500 MHz) spectrum of ethyl [(6-benzyloxy-3-ethyl)hexyloxysulfonyl]diazoacetate (296) in CDCl_3	261
134.	$^{13}\text{C}\{^1\text{H}\}$ NMR (125 MHz) spectrum of ethyl [(6-benzyloxy-3-ethyl)hexyloxysulfonyl]diazoacetate (296) in CDCl_3	262
135.	DEPT 135 NMR (125 MHz) spectrum of ethyl [(6-benzyloxy-3-ethyl)hexyloxysulfonyl]diazoacetate (296) in CDCl_3	263
136.	^1H NMR (500 MHz) spectrum of 3-carbethoxy-4-(3-benzyloxy)propyl-4-ethyl-1,2-oxathiane-2,2-dioxide (223) in CDCl_3	264
137.	$^{13}\text{C}\{^1\text{H}\}$ NMR (500 MHz) spectrum of 3-carbethoxy-4-(3-benzyloxy)propyl-4-ethyl-1,2-oxathiane-2,2-dioxide (223) in CDCl_3	265
138.	DEPT 135 NMR (500 MHz) spectrum of 3-carbethoxy-4-(3-benzyloxy)propyl-4-ethyl-1,2-oxathiane-2,2-dioxide (223) in CDCl_3	266
139.	^1H NMR (500 MHz) spectrum of ethyl 3-(3,4-dimethoxy)phenyl-6-heptenoate (303) in CDCl_3	267
140.	$^{13}\text{C}\{^1\text{H}\}$ NMR (125 MHz) spectrum of ethyl 3-(3,4-dimethoxy)phenyl-6-heptenoate (303) in CDCl_3	268
141.	DEPT 135 NMR (125 MHz) spectrum of ethyl 3-(3,4-dimethoxy)phenyl-6-heptenoate (303) in CDCl_3	269
142.	^1H NMR (500 MHz) spectrum of 3-(3,4-dimethoxy)phenyl-hept-6-en-1-ol (300) in CDCl_3	270
143.	$^{13}\text{C}\{^1\text{H}\}$ NMR (125 MHz) spectrum of 3-(3,4-dimethoxy)phenylhept-6-en-1-ol (300) in CDCl_3	271

144.	DEPT 135 NMR (125 MHz) spectrum of 3-(3,4-dimethoxy)phenylhept-6-en-1-ol (300) in CDCl ₃	272
145.	¹ H NMR (500 MHz) spectrum of ethyl [3-(3,4-dimethoxy)phenyl-6-heptenyloxysulfonyl]acetate (304) in CDCl ₃	273
146.	¹³ C{ ¹ H} NMR (125 MHz) spectrum of ethyl [3-(3,4-dimethoxy)phenyl-6-heptenyloxysulfonyl]acetate (304) in CDCl ₃	274
147.	DEPT 135 NMR (125 MHz) spectrum of ethyl [3-(3,4-dimethoxy)phenyl-6-heptenyloxysulfonyl]acetate (304) in CDCl ₃	275
148.	¹ H NMR (500 MHz) spectrum of ethyl [3-(3,4-dimethoxy)phenyl-6-heptenyloxysulfonyl]diazoacetate (305) in CDCl ₃	276
149.	¹³ C{ ¹ H} NMR (125 MHz) spectrum of ethyl [3-(3,4-dimethoxy)phenyl-6-heptenyloxysulfonyl]diazoacetate (305) in CDCl ₃	277
150.	DEPT 135 NMR (125 MHz) spectrum of ethyl [3-(3,4-dimethoxy)phenyl-6-heptenyloxysulfonyl]diazoacetate (305) in CDCl ₃	278

LIST OF SCHEMES

Scheme	Page
1. Direct C–H activation mechanism; “R” represents a nucleophile and ML_n represents reactive transition metal complex.....	4
2. Proposed mechanism for direct C–H bond activation of activated sp^3 C–H bonds using ruthenium complexes by Murai et al.....	5
3. Catalytic cycle for C–H functionalization by metal carbenoid insertion from diazo compounds	7
4. Proposed mechanistic pathway by Doyle et al. for rhodium-catalyzed C–H insertion from diazo precursors	12
5. Proposed mechanism by Taber et al. for rhodium-catalyzed C–H insertion from diazo precursors	13
6. Proposed mechanism by Nakamura et al. for rhodium-catalyzed C–H insertion from diazo precursors	14
7. Rhodium-catalyzed intermolecular cyclopropanation in the synthesis of the antidepressant (+)-sertraline by Corey et al.....	16
8. Rhodium-catalyzed intermolecular [4 + 3] cycloaddition in the synthesis of (±)-tremulenolide A and (±)-tremulenediol by Davies and co-workers	18
9. Synthesis of cyathane and cyanthiwigin diterpenes via intermolecular rhodium-catalyzed C–H insertion.....	19
10. Intermolecular rhodium-catalyzed insertion applied to the synthesis of products classically obtained by aldol and Mannich reactions.....	20
11. Intermolecular rhodium-catalyzed C–H insertion applied to the synthesis of a β-amino ester <i>en route</i> to the synthesis of (S)-venlafaxine	21
12. Mechanistic pathway for the combined C–H activation/Cope rearrangement	22
13. Combined C–H activation/Cope rearrangement applied to the synthesis of (-)-colombiasin A and (-)-elisapterosin B	23

14.	Intermolecular rhodium-catalyzed C–H insertion applied to the synthesis of (+)-cetiedil.....	24
15.	Intermolecular rhodium-catalyzed insertion applied to the synthesis of (+)-methylphenidate.....	25
16.	Intermolecular rhodium-catalyzed insertion applied to the synthesis of (+)-indatraline.	26
17.	Formation of β - and γ -lactams by intramolecular rhodium-catalyzed insertion.....	27
18.	Intramolecular rhodium-catalyzed insertion applied to the synthesis of (-)-hamigeran B.	28
19.	Intramolecular rhodium-catalyzed insertion applied to the synthesis of (-)-ephedrine.	29
20.	Synthesis of γ -butyrolactones and γ -lactams by intramolecular rhodium-catalyzed insertion.	30
21.	Use of intramolecular rhodium-catalyzed insertion in the synthesis of pentalenolactone E by Taber and co-workers.....	32
22.	Use of intramolecular rhodium-catalyzed insertion to construct carbocycles in strained and fused systems.....	32
23.	Synthesis of neopupekeananes via intramolecular rhodium-catalyzed insertion.	33
24.	Synthesis of (-)-2-pupekeanone via intramolecular rhodium-catalyzed insertion....	34
25.	Preparation of diazosulfones.....	43
26.	Isomerization of a four-membered ring sulfone to an alkenylsulfone.	47
27.	Formation of six- and five-membered sulfones by intramolecular C–H insertion reported by Jungong and co-workers.	65
28.	Synthesis of sulfonyl acetylmandalates for determination of enantiomeric ratio.....	66
29.	Synthesis of enantiopure sulfone 149	74
30.	Nucleophilic substitution reactions of δ -sulfones reported by Du Bois and co-workers.....	89
31.	Desulfonation of δ -sulfones to form substituted lactols reported by Du Bois and co-workers.....	90
32.	Remote alkylation of alcohols leading to the formation of 5-hydroxyesters.....	90

33.	Mechanism for SmI ₂ /DMPU reduction of δ -sultones to form δ -valerolactones.....	93
34.	Oxidative desulfonation of δ -sultones to 5-hydroxy-2-oxoesters.....	93
35.	Mechanism of TBHP oxidative desulfonation of δ -sultones to γ -butyrolactones. ...	96
36.	Rearrangement of alkylated sulfones.....	100
37.	Mechanism of formation of cyclic α -sulfonyl oximes.....	102
38.	Construction of the quaternary chiral center by Sharpless epoxidation and Yamamoto rearrangement reported by Du and co-workers.....	116
39.	Retrosynthetic disconnection for (+)-bakuchiol.	117
40.	Synthesis of δ -sultone 207 via rhodium-catalyzed intramolecular C–H insertion following procedure by Wolckenhauer and co-workers.....	118
41.	Synthesis of aldehyde 272	119
42.	Synthesis of (+)-bakuchiol from an aldehyde following the procedure by Du and co-workers.....	120
43.	Total synthesis of (\pm)-quebrachamine via [3+2] cycloaddition and efficient chloroacetamide photocyclization reported by Bajtos and co-workers	122
44.	Retrosynthetic analysis for the synthesis of (+)-quebrachamine.	123
45.	Preparation of alcohol 289	124
46.	Preparation of substituted γ -butyrolactone 223	125
47.	Retrosynthetic disconnection for (-)-mesembrine.	126
48.	Preparation of alcohol 300	127
49.	Preparation of substituted δ -sultone 299	128

LIST OF TABLES

Table	Page
1. Studies on non-directed sp ³ C–H bond activation using ruthenium complexes reported by Sames et al	6
2. Rhodium-catalyzed intramolecular C–H insertion resulting in the formation of γ -sulfones fused to phenyl, thiophene and indole ring compounds reported by Durst and co-workers	36
3. Rhodium-catalyzed intramolecular C–H insertion of aliphatic diazosulfones and diazosulfonates leading to the formation of six-membered rings by Novikov and co-workers.....	38
4. Formation of six-membered sulfonates from the corresponding diazosulfonates via intramolecular rhodium-catalyzed C–H insertion reported by Wolckenhauer and co-workers.....	39
5. Effect of catalyst on five- versus six-membered sulfone selectivity reported by Jungong et al.	42
6. Effects of structure of diazosulfone on selectivity of rhodium-catalyzed intramolecular C–H insertion leading to the formation of five- and six-membered rings reported by Jungong et al.	44
7. Preparation of diazosulfones.....	46
8. Studies on the formation of four-membered sulfones.....	48
9. Enantioselective intramolecular copper-catalyzed C–H insertion reactions of diazosulfones reported by Maguire and co-workers.....	63
10. Effect of chiral rhodium(II) carboxylate catalyst on the enantioselectivity of intramolecular C–H insertion on diazosulfones.....	69
11. Effect of temperature and solvent on the enantioselectivity of rhodium-catalyzed intramolecular C–H insertion of diazosulfones.	71
12. Preparation of diazosulfonyl acetates	72

13.	Effect of diazosulfone substrates on the enantioselectivity of rhodium-catalyzed intramolecular C–H insertion.....	73
14.	SmI ₂ reduction of δ -sultones to form δ -valerolactones reported by Jungong and coworkers.....	91
15.	TBHP oxidative desulfonation of δ -sultones to γ -butyrolactones.	94
16.	Alkylation of δ -sultones and carbethoxythiane-1,1-dioxides.	97
17.	Formation of α -sulfonyl oximes from carbethoxythiane-1,1-dioxides.....	101

ACKNOWLEDGEMENTS

The dissertation journey has ups and downs, and though the cover of this write-up bears only my name, I would never have been able to complete its production without the help of several individuals who made invaluable and countless contributions directly and indirectly. Regrettably, I cannot acknowledge them all by name. Many thanks to all those who have made my graduate experience one that I would cherish and remember forever.

I would like to express my deepest gratitude to my advisor, Prof. Alexei Novikov, for his excellent mentorship, patience, encouragement and support which were paramount to a well round collegiate experience as well as provided a conducive atmosphere for doing research. I would like to thank all the other members of my graduate committee for helping to shape and clarify my ideas, giving critical and timely feedback when needed and for not letting me take anything for granted. I would like to single out Prof. Irina Smoliakova whose insightful comments and constructive criticism at different stages of my graduate school experience were thought-provoking and helped me stay focused.

I am grateful to the Chemistry Department not just for providing all the resources that I needed to complete this dissertation, but also for financial support. The Drs. Coon and Severnson awards I received in October 2010 came at a critical time in my career and contributed significantly to this achievement. I am also thankful to the informative and dedicated staff who worked tirelessly to provide a decent learning environment. The

accessibility, ready-made answers and timely feedback they offered will always be remembered. I would like to acknowledge Dr Guadong Du for letting me use his lab for air-sensitive reactions, Dr. Quilian Chu for permitting me use his lab for photochemical reactions, and Dr. Alena Kubatov for mass spectrometry analysis. Dr. Colin Combs of the Neuroscience Department at UND deserves a special mention for the help and support he offered to enable me understand the fundamentals of Alzheimer's disease while I took my doctoral exams.

I like to thank the Chemistry Graduate Student Association for financial support and for giving me the opportunity to develop as a leader when I served as president. The end of year parties and picnics helped intersperse lab work with family-like gatherings, which contributed towards the positive and rewarding experience I had at the department.

I will always be grateful to the Graduate School for financial support, especially the Doctoral Student Travel awards I received in 2010 and 2012, which enabled me to attend the 241st American Chemical Society national meeting in Anaheim, CA and Gordon Research Conference in Andover, NH, respectively.

It would have been a lonely lab without my group members. Special thanks to Jinu Paul, Joseph Bequette and Duminda Liyange for being good friends, proofreading my write-ups, commenting on my views and helping me understand and enrich my views as a synthetic organic chemist. I would also like to thank Jean Canham and Carl Segeman for giving me the opportunity to act as mentor for two fine and hardworking chemists. I appreciate the honest effort you put in towards the realization of the projects you participated in.

I owe my gratitude to all my teachers, especially Dr. Promise Yong, who at a very tender age in my educational career back in St. Bede's College, Ashing, successfully instilled in me a burning desire and confidence to pursue a career in organic synthesis. I remain thankful to my former principal at St. Bede's College, Rev. Father Michael Kintang, for his understanding, care, patience and encouragement. His stewardship was outstanding as it set out avenues I have followed to become a better person.

I am indebted to my family for the moral support, sacrifices and encouragement they offered while I worked on this dissertation. Above all, I express my sincere gratitude to my parents Clement Suh and Elizabeth Kubili for the thankless and countless sacrifices they made to ensure that I get a sound education. This achievement is truly yours. I cannot thank my uncle and Godfather, Richard Abongnelah, enough for his kindness, help and support at every step of the way. I will always be grateful to my brothers and sisters Julius, Ivans, Wilfred, Valentine, Akongnwi, Abiinwi, Phyllis, Edith, Emmaculate and Joy who have always believed in me and supported me morally and financially throughout my educational career.

I thank my friends in Yannick Elame, Ellis Kilo, Kenneth Ndumbe, Frankline Fru, Willy Njabon, Alain Foryim, Eunice Ogbuji, Arinoh Kwajoh, Armand Nkemtsa and Ruth Tomah who provided moral support, encouragement and helped with other responsibilities while I focused on this work.

Most of all, I would like to thank my wife Nadine for her personal support and great patience at all times. As for my daughter Bryelle, her broad smile each time I got

home from school made it easier getting over failed reactions. Last but not least, I want to thank God for everything he has done in my life.

To Bryelle and Nadine

ABSTRACT

This work explores the use of rhodium-catalyzed intramolecular C–H insertion on diazosulfones and sulfonates as a tool to simplify the synthesis of organic molecules. Dirhodium-induced intramolecular C–H insertion on diazo carbonyl compounds is a relatively well-studied reaction. It occurs with an overwhelming bias for the formation of five-membered carbocycles or heterocycles, with the order of reactivity of C–H bonds being methine > methylene >> methyl. This intrinsic preference can be overridden by dissimilar factors such as substrate conformation, insertion site electronic effects and the reactivity of the dirhodium catalyst.

This study has disclosed that when diazo- sulfones and sulfonates are employed, dirhodium-induced intramolecular C–H insertion preferentially forms six-membered heterocycles. Apparently, the difference in bond lengths and bond angles around the SO₂ fragment incorporated into the newly forming ring allows more distant C–H bonds to be targeted for insertion. The preference for formation of six- versus five-membered heterocyclic sulfones, however, is tenuous in nature, and is dependent on the substrate structure and the nature of the dirhodium catalyst used. Dirhodium catalysts bearing electron poor ligands shift the preference back to formation of five-membered rings, presumably due to forming more reactive carbenoid intermediates. The presence of methyl substituents on the carbon atom adjacent to the sulfone fragment also favors the formation of five-membered sulfones, likely due to the steric compression of the bond angle. Rh₂(S-pttl)₄ [dirhodium(II)tetrakis(*N*-phthaloyl-*S*-*tert*-leucinate)] catalyst has

been identified as the current best lead to the development of chiral catalysts for this reaction. Selectivity of 3:1 (50% ee) was achieved with its use, and 20:1 (91% de) when combined with the use of a (-)-menthol-based chiral auxiliary.

The synthetic utility of these novel six-membered heterocycles has also been explored. To which end, the enantioselective synthesis of bakuchiol has been achieved in 14 linear steps by employing intramolecular C–H insertion on a diazo sulfonate to install the quaternary center in its structure. The alkylation of these substrates with active electrophiles under relatively mild conditions and with excellent yields has been attained with high diastereoselectivity. Novel methodologies have been originated to transform the obtained δ -sultones into γ -butyrolactones and δ -valerolactones using TBHP/*t*-BuOK and SmI₂/DMPU, respectively. The conversion of carbethoxythiane-1,1-dioxides to cyclic α -sulfonyl oximes has also been demonstrated under relatively mild conditions (NaH, isoamyl nitrite, rt, 8 h). Currently, the versatility of these new transformations is being pursued in the synthesis of the natural products quebrachamine and mesembrine.

CHAPTER 1

GENERAL INTRODUCTION AND BACKGROUND

1.1 C–H Bond Functionalization via Carbon–Carbon Bond Formation

In 2011, the FDA approved thirty five new drugs that offered significant advances in the treatment of hepatitis C, lupus, late-stage prostate cancer, pneumonia and other life-threatening diseases.¹ Most of these drugs were small molecule (molecular weight less than 1000) organic compounds. Increased knowledge about the *in vivo* activity of these drugs will lead to the development of analogs and other new drugs, which at times is associated with increase in molecular complexity. The development of these drugs entails complex and lengthy multi-step syntheses, which are often reflected in the cost of production, availability, marketing price, and overall success of the drug. This increases the need to develop efficient synthetic strategies that would allow the synthesis of bioactive molecules in an economical fashion.

Over the years, the synthesis of organic molecules has been achieved by modifying precursors and intermediates at preexisting functional groups.²⁻⁵ This conventional approach neglects sp^3 carbon–hydrogen (C–H) bonds, which are ubiquitous in organic molecules and are usually the most prevalent “functional group”.⁶⁻⁹ The sp^3 C–H bond has a bond length of 1.09 Å, bond energy of 413 kJ/mol, and it is non-polar because of a small difference in electronegativity between carbon and hydrogen.^{9, 10} In general, the sp^3 C–H bond is inert. The inertness arises from the fact it possesses no

empty orbitals of low energy or filled orbitals of high energy that can readily participate in a chemical reaction.^{6, 11} The inertness and ubiquitous nature of sp^3 C–H bonds makes the development of synthetically useful reactions daunting. However, the advent of efficient selective C–H bond functionalization strategies, especially in the context of carbon–carbon (C–C) bond formation, could greatly improve the available methods for making organic molecules.¹²⁻¹⁴ A major challenge to the development of such strategies has been the need for reagents that are reactive enough to cleave the relatively stable C–H bonds but still sufficiently selective to distinguish between the different types of C–H bonds in organic molecules.¹⁵⁻²²

In organic substrates, the functional groups present dictate the reactivity of proximal C–H bonds. This notion has been used to classify C–H bonds on organic substrates into three groups: sp^2 hybridized C–H bonds, activated sp^3 hybridized C–H bonds, and unactivated sp^3 hybridized C–H bonds (Figure 1).⁵ C–H bonds which are sp^2 hybridized are found in arenes and alkenes, while activated sp^3 C–H bonds refer to sp^3 C–H bonds adjacent to heteroatoms or functional groups. Unactivated sp^3 C–H bonds, on the other hand, are not adjacent to a heteroatom or functional group. Activated sp^3 hybridized C–H bonds are weaker (and thus more reactive) than their unactivated counterparts and can be selectively functionalized.^{5, 6, 8, 23-28} The selective activation of sp^3 hybridized C–H bonds is known to be both kinetically and thermodynamically unfavorable. Nevertheless, huge strides have been made in recent years to selectively activate these bonds thanks to the works of Smoliakova,^{29, 30} Sames,⁵ and Murai.³¹

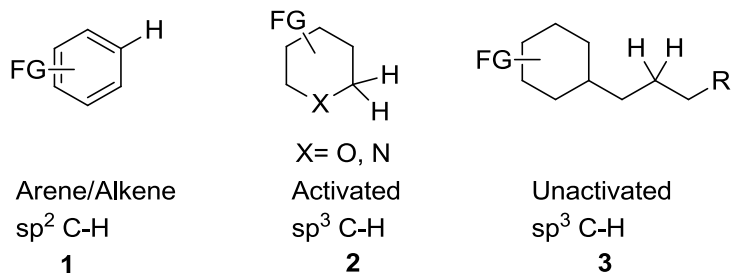
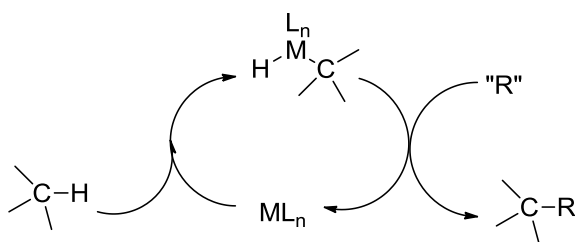


Figure 1. Different types of C–H bonds in organic substrates; FG represents other functional groups in the substrates.⁵

Historically, the functionalization of C–H bonds via C–C bond formation heavily depended on radical reactions.^{32, 33} However, the ubiquity of C–H bonds in organic substrates and the difficulties associated with controlling radical reactions significantly retarded the development of efficient and synthetically meaningful transformations. Over the past three decades, considerable progress has been made in the area of C–H bond functionalization.^{5, 6, 14, 34} Two cutting edge transition-metal-based transformations have been originated for C–H bond functionalization, specifically with respect to new C–C bond formation.

The first of these transformations is direct C–H activation, which entails adding a reactive transition metal complex (Ru, Ir, Rh or Pd) across a relatively strong C–H bond (90-105 kcal/mol) to form a weaker carbon–metal bond (50-80 kcal/mol), followed by a subsequent transformation to generate a new C–C bond (Scheme 1).^{29, 35-37} Direct C–H activation owes its roots to the pioneering work of Shilov,³⁸ Bercaw,⁶ Bergman,²⁵ Crabtree,^{39, 40} Murai³¹ and Goldman,⁴¹ and dates back to the 1970s and 1980s.

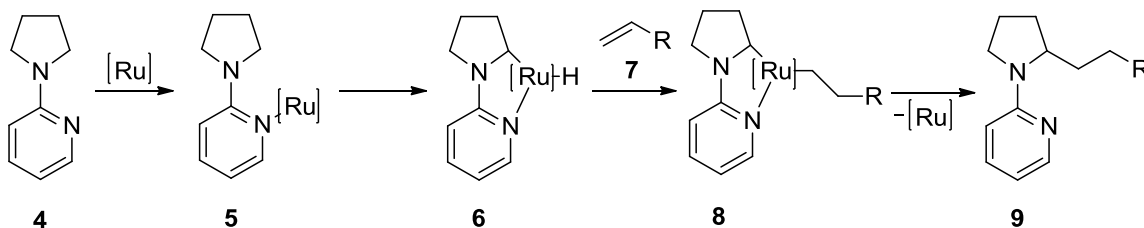


Scheme 1. Direct C–H activation mechanism; “R” represents a nucleophile and ML_n represents reactive transition metal complex.³⁴

Direct C–H activation generally involves harsh reaction conditions (high temperatures), which may not be tolerated by other functional groups on the substrate. This, alongside the fact that the reactive transition metal complex may bind too tightly with the C–H bond, has limited the use of this transformation for synthetic purposes.^{6, 37, 42} An attempted solution to this problem has been the use of neighboring functional groups to direct less reactive metal complexes to the target C–H bond activation site.^{11, 25, 43} Less reactive metal complexes tend to bind loosely and generate activated C–H bonds, which are more reactive and, thereby, creating more avenues for subsequent transformations.

For some time, direct C–H activation has been restricted to sp^2 hybridized C–H bonds (aryl and vinyl), since the activation of sp^3 hybridized C–H bonds is known to be unfavorable, both kinetically and thermodynamically. In recent years, Murai and co-workers have taken advantage of the fact sp^3 hybridized C–H bonds adjacent to heteroatoms are weaker (more reactive) to show that pyrrolidine and piperidine C–H bonds can be activated by $Ru_3(CO)_{12}$ and further coupled to unactivated alkenes.⁴⁴ In the aforementioned transformation, the 2-pyridyl nitrogen atom on compound **4** is needed to

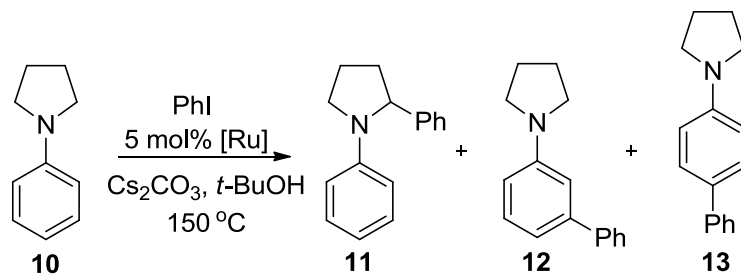
direct the ruthenium complex to the desired C–H bond resulting in the formation of ruthenium hydride complex **6**, which reacts with the unactivated alkene **7** to form alkyl ruthenium complex **8**, from which reductive elimination gives the final product **9** (Scheme 2).



Scheme 2. Proposed mechanism for direct C–H bond activation of activated sp^3 C–H bonds using ruthenium complexes by Murai et al.⁴⁴

Expanding on Murai's work, Sames and co-workers have developed the arylation of sp^3 hybridized C–H bonds without the aid of a directing group.^{28, 43} They demonstrated that *N*-phenylpyrrolidine can be arylated with iodobenzene in the presence of Cs_2CO_3 and *t*-BuOH (Table 1). Mechanistic investigations revealed an oxidative pathway for the reaction. Even though these results reveal that sp^3 hybridized C–H bonds can be directly activated, the yields for the products remain relatively low, considerably limiting the synthetic utility of this transformation.

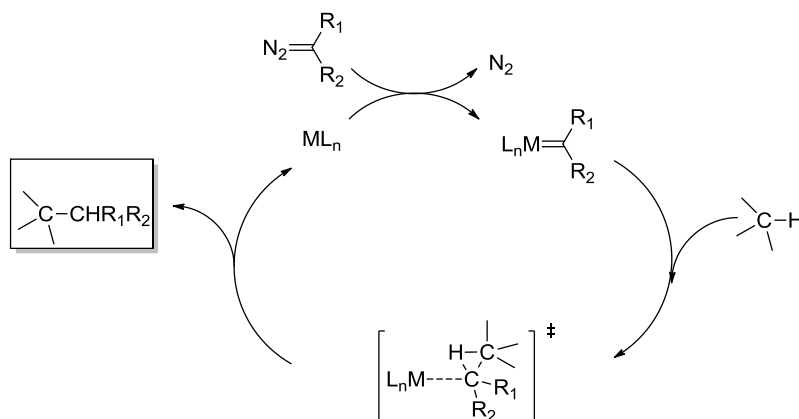
Table 1. Studies on non-directed sp^3 C–H bond activation using ruthenium complexes reported by Sames et al.²⁸



[Ru]	Yield (%)		
Ru(H ₂)(CO)(PCy ₃) ₃	32	6	4
Ru(H ₂)(H) ₂ (PCy ₃) ₃	38	6	4
Ru(H ₂) ₂ (H) ₂ (PCy ₃) ₂	40	7	4
Ru(H ₂) ₂ (H) ₂ (PCy ₃) ₂ (10 mol%)	59	9	4

The other type of transition-metal-based transformations for functionalizing C–H bonds is metal-carbenoid C–H insertion. In this case, the reactive transition metal complex inserts into a C–H bond to generate a three-centered cyclic transition state, which leads directly to the functionalized products (Scheme 3).^{3, 45-51} Unlike C–H activation, metal carbenoid C–H insertion is highly selective. The metal complexes, which initiate the reaction, are readily regenerated rendering the process highly catalytic. The metal carbenoids are masked carbenes, and require an appropriate level of electrophilicity to proficiently effect C–H insertion. If the metal carbenoid is extensively electrophilic, competing side reactions become an issue.^{4, 34} On the other hand, if the

electrophilicity is insufficient, the metal carbenoid lacks the reactivity to insert into an unactivated C–H bond.



Scheme 3. Catalytic cycle for C–H functionalization by metal carbenoid insertion from diazo compounds.³⁴

Free carbenes are overly reactive and tend to react with organic substrates in ways, which are unselective and uncontrollable.⁵²⁻⁵⁴ The binding of the metal complex to the carbene serves to modulate its reactivity, thereby allowing more control over the outcome of the reaction. The metal complex binds to the carbene through strong σ -acceptor interactions and weak π -back donation interactions, which stabilize the carbene, but still ensure that it remains active enough to insert into a C–H bond.^{14, 55} Overall, the reactivity of the carbenoid is determined by the nature of the ligands on the metal complex as well as the substituents adjacent to the carbene moiety.

1.2 Classes of Metal Carbenoid

In general, metal carbenoids are conveniently obtained by the extrusion of nitrogen from diazo compounds.⁵⁶ Depending on the substituents adjacent to the diazo moiety, three classes of metal carbenoids have been distinguished: acceptor carbenoids, acceptor/acceptor carbenoids, and donor/acceptor carbenoids (Figure 2).³ In this context, acceptor refers to an electron-withdrawing group (EWG) while donor refers to an electron-donating group (EDG). Typical acceptor groups are carbonyl, nitro, cyano, phosphonyl and sulfonyl, while typical donor groups are vinyl, aryl and heteroaryl. The presence of an EWG increases the electrophilicity and reactivity of the resulting carbenoid, while that of an EDG stabilizes the carbenoid and enhances its selectivity.^{15, 57-}

59

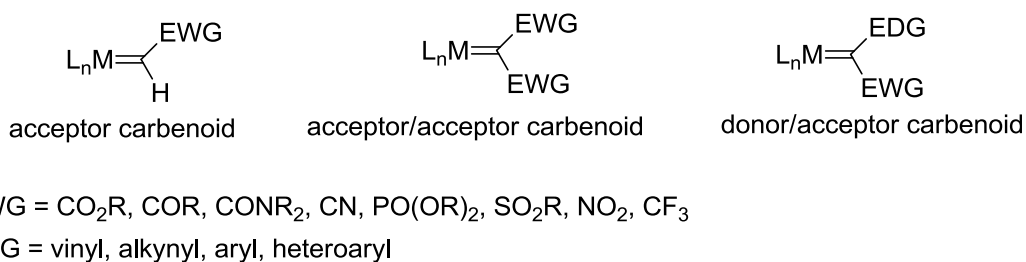


Figure 2. Classes of diazo-based metal carbenoids.³⁴

Acceptor carbenoids are highly reactive but exhibit limited selectivity since they do not bear an EDG. The high reactivity makes them susceptible to competing reactions like carbene dimerization. Acceptor carbenoids are commonly used in intramolecular and

cyclopropanation reactions, in which their reactivity can be modulated by steric effects.^{17,}

60

Acceptor/acceptor carbenoids are obtained from diazo compounds bearing two EWGs. The presence of the second EWG stabilizes the diazo compounds, and highly reactive metal catalysts are needed for the extrusion of nitrogen to form the carbenoids. Once formed, the resulting carbenoids are highly reactive and are liable to carbene dimerization. Acceptor/acceptor carbenoids can also be used for intramolecular and cyclopropanation reactions, even though they will be less selective than their acceptor counterparts.^{17, 61}

Donor/acceptor carbenoids are derived from diazo compounds that possess an EWG and a donor substituent like a vinyl or aryl group, capable of stabilizing the resulting carbenoid through resonance.^{49, 60} Again, because the diazo precursor is stabilized, very reactive metal catalysts are needed to generate the carbenoid. This class of carbenoids exhibits high chemoselectivity and is widely used for intermolecular reactions.

1.3 Use of Rhodium(II) Complexes in Carbenoid C–H Insertion

Rhodium(II) complexes are the most effective and versatile catalysts for metal carbenoid-mediated C–H insertion.^{20, 62-67} Prior to the introduction of rhodium(II) complexes by Teyssie and co-workers in the 1980s, mostly copper complexes were employed with varying levels of success.^{63, 68, 69} The superiority of rhodium(II) complexes lies in its inherent ability to form Rh–Rh bonds. This intrinsic property

permits the formation of a dirhodium-bridge, caged within a 'lantern' structure, which is thought to be the essential feature of these complexes.^{57, 70, 71} Only one of the two rhodium atoms actually binds to the carbene; the other atom serves as an electron sink to increase the electrophilicity of the carbenoid moiety, and also facilitates the cleavage of the rhodium-carbon bond upon completion of the reaction.^{15, 55} To date, four main classes of rhodium(II) complexes have been established for metal carbenoid insertion reactions. They are rhodium(II) carboxylates, rhodium(II) carboxamides, rhodium(II) phosphates, and ortho-metalated arylphosphine rhodium(II) complexes. More recently, rhodium(II) carboxylates and carboxamides have emerged at the forefront as the most effective and versatile catalysts for carbenoid C-H insertion.^{46, 47, 72} Representative examples include: Rh₂(OAc)₄ (rhodium acetate) **14**, Rh₂(*S*-DOSP)₄ (tetrakis[(*S*)-(+)-*N*-(*p*-dodecylphenylsulfonyl)prolinato]dirhodium(II) **15**, Rh₂(*S*-pttl)₄ (dirhodium(II) tetrakis[*N*-phthaloyl-(*S*)-*tert*-leucinate]) **16**, Rh₂(*S*-MEPY)₄ (dirhodium(II) tetrakis[methyl-2-pyrrolidone-5(*S*)-carboxylate]) **17** among others. The reactivity of these rhodium(II) complexes is governed by the nature of the ligands on the dirhodium bridge.^{55, 57} In general, electron-withdrawing ligands tend to increase the electrophilicity and reactivity of the catalyst, while electron-donating groups tend to enhance the selectivity.

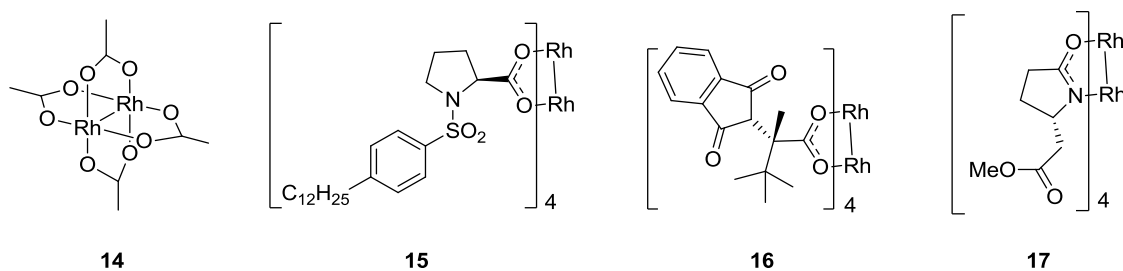
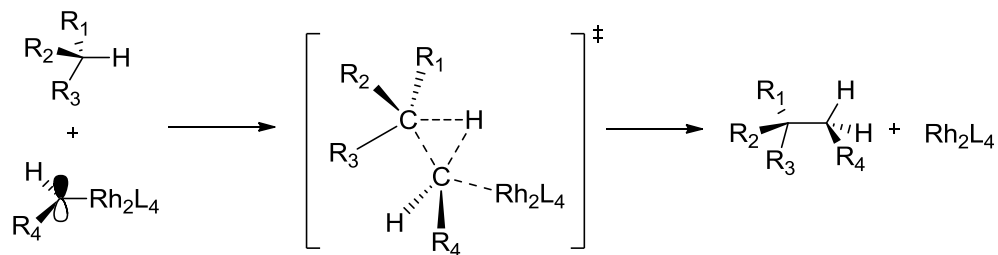


Figure 3. Common rhodium catalysts used for carbenoid C–H insertion of diazo compounds.¹⁴

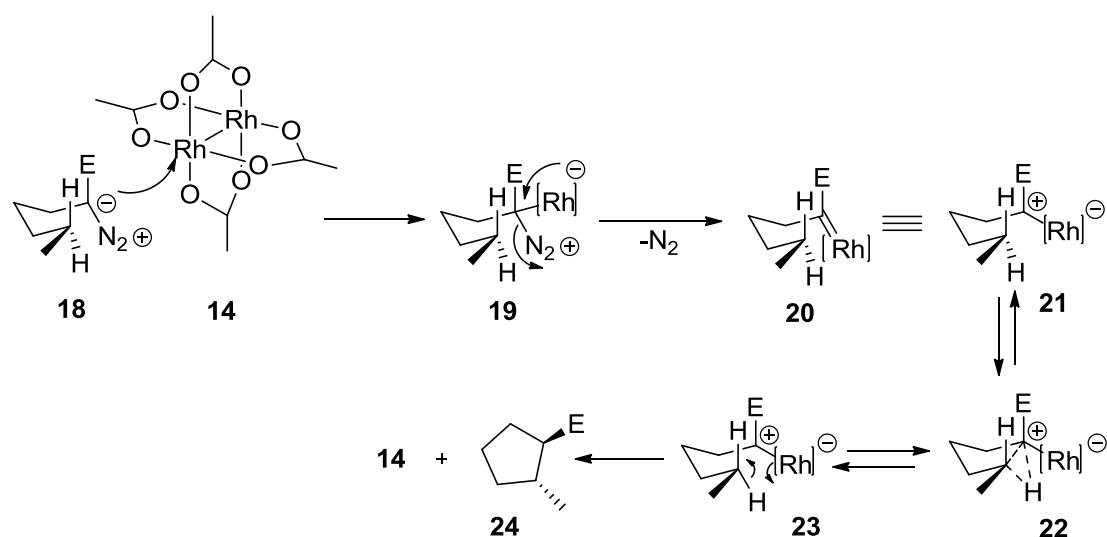
1.4 Rhodium-Catalyzed C–H Insertion Mechanism

The catalytic cycle of rhodium-catalyzed C–H insertion reactions involves three main steps: (1) rhodium-assisted nitrogen extrusion from the diazo compound, (2) activation of the C–H bond and (3) C–C bond formation.^{55, 61, 73} The sequence of occurrence of the C–H activation and C–C bond formation steps has been a subject of considerable speculation and various models of the C–H activation transition state (TS) have been proposed. Doyle and co-workers based on experimental results put forth a model, in which after nitrogen extrusion, there is overlap of the carbenoid's p-orbital with the σ -orbital of the reacting C–H bond to form a three-centered concerted transition state where C–C and C–H bond formation with the carbene carbon occurs at the same time as the ligated metal dissociates but not to the same extent (Scheme 4).¹⁵ They further emphasized that the presence of electron-withdrawing ligands on the dirhodium bridge increases the electrophilicity of the carbene and forces bond formation to occur at a greater distance, resulting in an early transition state, which leads to lower selectivity. On the other hand, the presence of electron-donating ligands favors a late transition state and leads to higher selectivity.



Scheme 4. Proposed mechanistic pathway by Doyle et al. for rhodium-catalyzed C–H insertion from diazo precursors.¹⁵

Taber and co-workers suggested a four-centered transition state whereby there is an interaction between the hydrogen of the C–H bond and one of the rhodium atoms (Scheme 5).^{21, 74} According to this model, after nitrogen extrusion, the resulting carbenoid **20** can be depicted as an inverted ylide **21**, which rapidly forms a reversible three-centered two electron intermediate complex **22**. For bond formation to proceed, a four-centered TS **23** is needed, in which the Rh–C bond is aligned with the target C–H bond. Provided sufficient overlap exists, the electron pair of the C–H bond moves to form a new C–C bond, and synchronously, the electron pair of the Rh–C bond moves to form a new C–H bond. This affords product **24** and releases initial rhodium complex **14**.

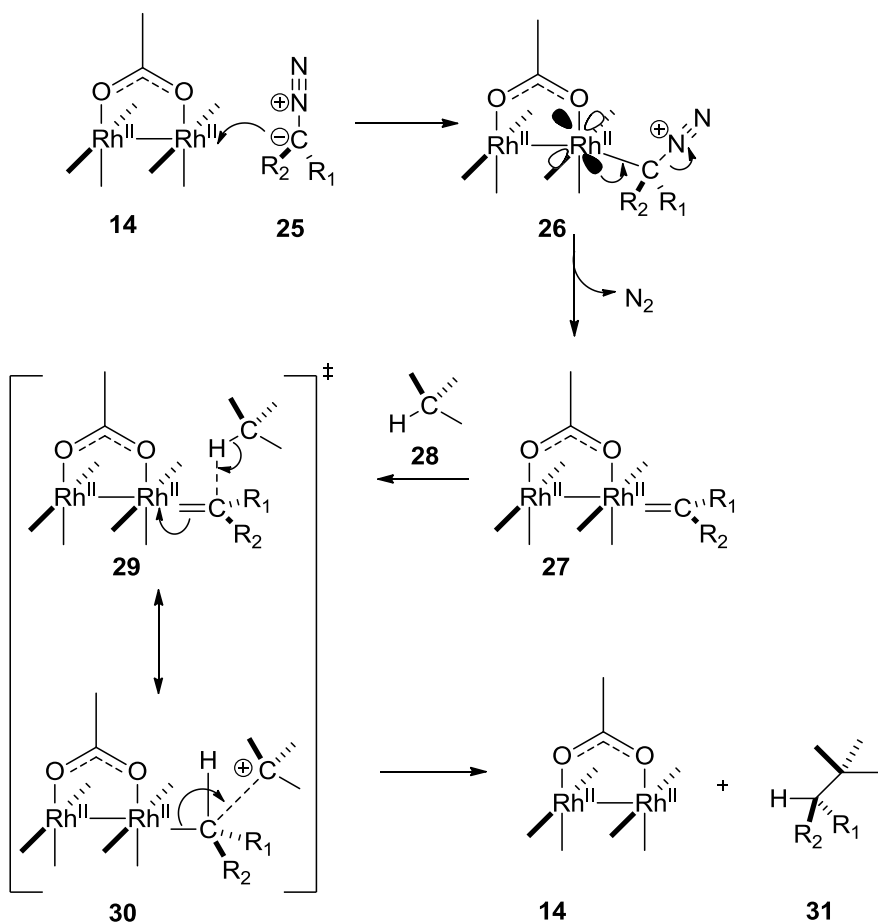


Scheme 5. Proposed mechanism by Taber et al. for rhodium-catalyzed C–H insertion from diazo precursors.²¹

A recent demonstration by Nakamura and co-workers confirmed the model advanced by Doyle and co-workers.⁵⁵ Using B3LYP density functional studies on dirhodium tetracarboxylate-catalyzed C–H bond activation, they disclosed the energetics and geometry of important intermediates and TS in the catalytic cycle. They proposed that the reaction is initiated by the formation of a complex between the rhodium catalyst and the diazo compound. This is followed by back donation of electrons from the rhodium $4d_{xz}$ orbital to the C–N σ^* -orbital, which provides the driving force for nitrogen extrusion to form the rhodium carbenoid.

The rhodium carbenoid is highly electrophilic because of its vacant 2p orbital. As such, the C–H activation and formation of the C–C bond proceed in a single step via a three-centered hydride transfer-like TS with small activation energy. Throughout the reaction, only one of the two rhodium atoms serves as a carbene binding site; the other

assists the C–H insertion reaction by enhancing the electrophilicity of the carbene bound rhodium and facilitating the cleavage of the rhodium–carbon bond. Neither of the rhodium atoms interacts directly with the target C–H bond undergoing insertion.



Scheme 6. Proposed mechanism by Nakamura et al. for rhodium-catalyzed C–H insertion from diazo precursors.⁵⁵

1.5 Synthetic Utility of Rhodium-Induced C–H Insertion

Rhodium-induced C–H insertion can either be intermolecular or intramolecular.^{58,}

⁷⁵⁻⁷⁸ For some time, regioselectivity challenges associated with intermolecular substrates and competing side reactions, like carbene dimerization, limited rhodium carbene C–H

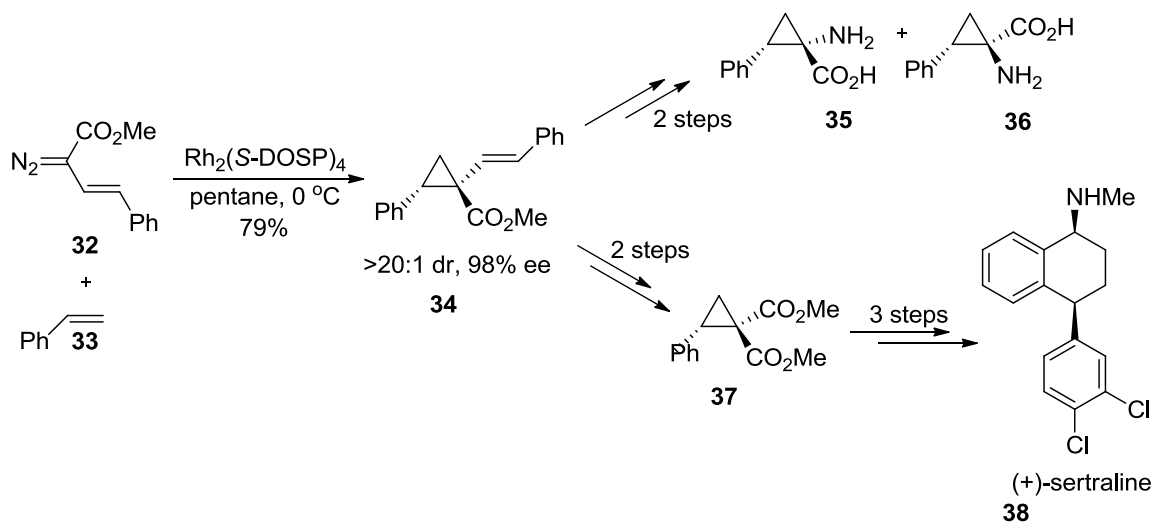
insertion to substrates capable of intramolecular reactions; whereby the target C–H bond and the rhodium carbenoid are connected by a suitable tether, which provides close proximity leading to favorable regioselectivities.⁴² However, vigorous research in the area of intermolecular rhodium-catalyzed C–H insertion has shown that this transformation is just as strategic and meaningful synthetically as the intramolecular version.^{19, 49, 75, 76, 79}

1.5.1 Intermolecular Rhodium-Induced C–H Insertion

The disclosure by Davies and co-workers that donor/acceptor carbenoids are capable of undergoing highly regio- and stereoselective intermolecular C–H insertion reactions has evolved intermolecular C–H insertion from a synthetically limited reaction to a broadly useful transformation.^{19, 49, 75} This is highlighted by a number of impressive examples, in which intermolecular C–H insertion has been employed as a strategic reaction to install stereogenic centers in natural product targets.^{3, 49, 77}

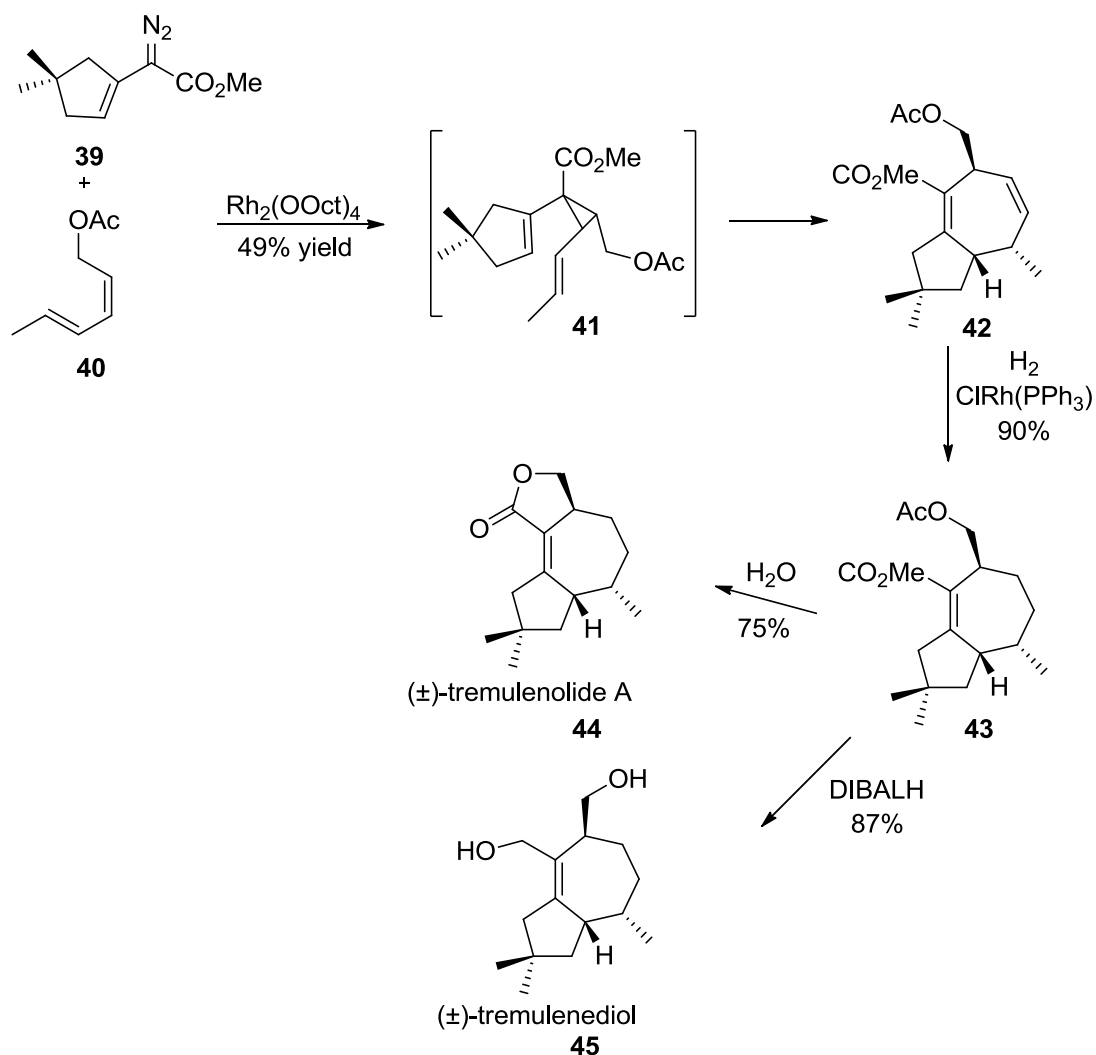
Intermolecular C–H insertion is best catalyzed by $\text{Rh}_2(\text{S-DOSP})_4$ and is highly favored at sites that stabilize positive charge.^{19, 80} It can occur at primary, secondary and tertiary C–H bonds, controlled by a tenuous balance of steric and electronic factors. Based on the ability of the substrate to stabilize positive charge, the trend of reactivity is as follows: tertiary > secondary > primary. However, because the rhodium(II) catalyst bears bulky ligands, from a steric stand point, the order of reactivity becomes primary > secondary > tertiary. Overall, secondary C–H bonds are most favored because they stabilize positive charge without being too sterically crowded.^{67, 81}

Intermolecular C–H insertion reactions can be separated into cyclopropanation,⁸² [4 + 3] cycloaddition⁵⁰ and C–H functionalization.⁸³ Intermolecular cyclopropanation routinely occurs with high diastereoselectivity (>20 : 1 dr), and the obtained cyclopropanes can be rearranged or ring-opened to allow the synthesis of other organic compounds. An illustrative example is the reaction of styryldiazoacetate **32** with styrene **33** catalyzed by $\text{Rh}_2(\text{S-DOSP})_4$ to afford vinylcyclopropane **34** in 79% yield, > 20 : 1 dr and 98% ee.⁸⁴ The resulting vinylcyclopropane **34** has been converted to amino acids **35** and **36**, and cyclopropanedicarboxylate **37**, which can be ring-expanded when subjected to Lewis acid-catalyzed conditions in the presence of an aldehyde or ring-opened by a cuprate reagent, as illustrated in the synthesis of the antidepressant (+)-sertraline **38** by Corey and coworkers.⁸²



Scheme 7. Rhodium-catalyzed intermolecular cyclopropanation in the synthesis of the antidepressant (+)-sertraline by Corey et al.⁸²

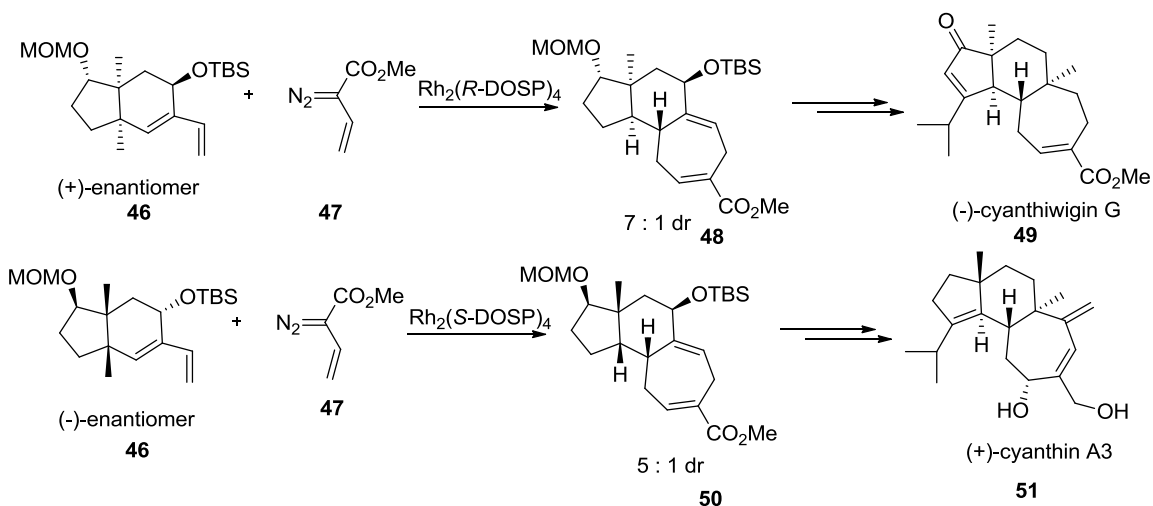
A representative example of an intermolecular [4+3] cycloaddition is that between vinyl diazoacetate **39** and the (*E,Z*)-diene **40** catalyzed by Rh₂(OOct)₄ to generate cycloheptadiene **42** as a single regioisomer and diastereomer in 49%.⁸⁵ Selective intermolecular cyclopropanation of the (*Z*) double bond occurs to generate the divinylcyclopropane **41**, which undergoes a Cope rearrangement to provide **42** as a single diastereomer. The *cis* double bond of **42** is reduced by Wilkinson's catalyst to form **43**. Base hydrolysis of the acetyl group followed by *in situ* lactonization results in the synthesis of (±)-tremulenolide A **44**. Also, DIBAL reduction of the two esters on **43** completes the synthesis of (±)-tremulenediol **45**.



Scheme 8. Rhodium-catalyzed intermolecular [4 + 3] cycloaddition in the synthesis of (±)-tremulenolide A and (±)-tremulenediol by Davies and co-workers.⁸⁵

When some chiral catalysts are used in intermolecular [4 + 3] cycloaddition, the directing ability of a chiral substrate can be overridden. This has been demonstrated by Sarpong and co-workers⁸⁶ in a parallel kinetic resolution approach used to synthesize cyathane and cyanthiwigin diterpenes. The $\text{Rh}_2(\text{S-DOSP})_4$ -catalyzed reaction of (+)-46

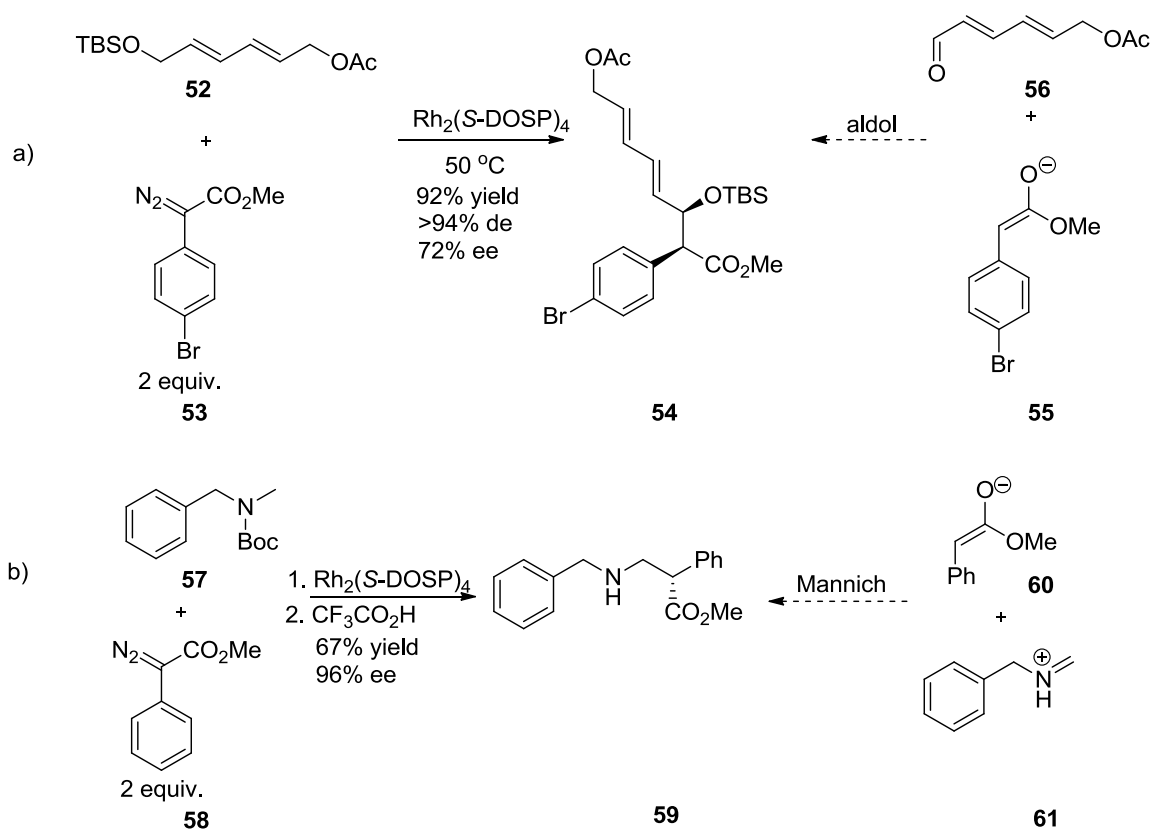
preferentially favors the formation of **48**, while that of (-)-**46** leads to **50**. Compound **48** is a precursor to (-)-cyanthiwigin G **49**, while **50** is a precursor to (+)-cyanthin A3 **51**.



Scheme 9. Synthesis of cyathane and cyanthiwigin diterpenes via intermolecular rhodium-catalyzed C–H insertion.⁸⁶

Intermolecular C–H insertion reactions can also provide complementary approaches to conventional synthetic strategies to help streamline the preparation of target natural products. For instance, intermolecular C–H insertion adjacent to oxygen forms β -hydroxy esters, which are products routinely derived from aldol reactions,⁸⁷ similarly, the same reaction on analogous leads to β -amino esters, products of a Mannich reaction (Scheme 10).⁸⁸ In Scheme 10a, intermolecular insertion is preferentially favored at the C–H bond adjacent to the siloxy group of compound **52** rather than the acetoxy group. This stems from the fact that the electron-withdrawing acetoxy group deactivates the adjacent C–H bonds towards insertion, while the electron-donating siloxy group

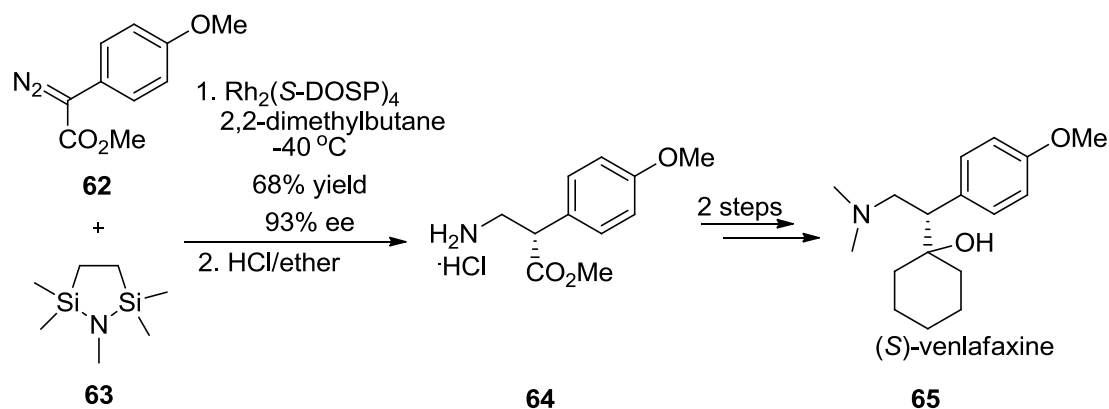
activates the adjacent C–H bonds towards insertion. In Scheme 10b, the benzylic C–H bonds in compound **57**, which are electronically most activated, are sterically inaccessible so the insertion occurs at the methyl C–H bonds.



Scheme 10. Intermolecular rhodium-catalyzed insertion applied to the synthesis of products classically obtained by aldol and Mannich reactions.^{87, 88}

The synthesis of the antidepressant (*S*)-venlafaxine by Davies and co-workers is an impressive example where this chemistry has been put to use.⁸⁹ In the synthesis, $\text{Rh}_2(\text{S-DOSP})_4$ -catalyzed reaction of aryldiazoacetate **62** with *N*-methyl-1-aza-2,5-

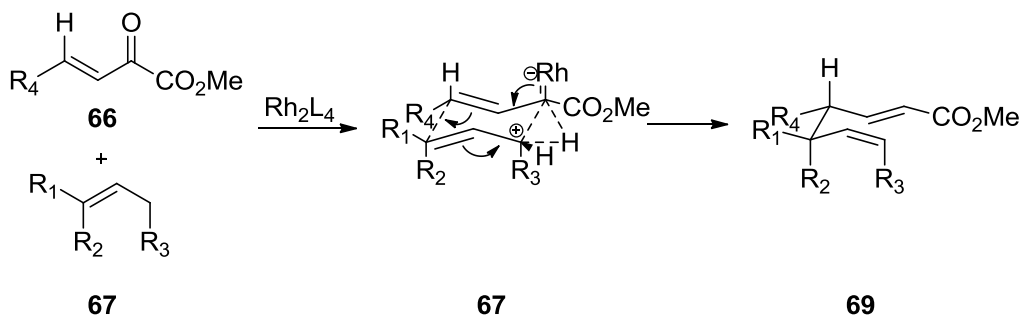
disilacyclopentane **63**, generated β -amino ester **64** in 68% yield and 93% ee, which was further converted in two steps to (*S*)-venlafaxine **65** (Scheme 11). The disilyl protecting group in **63** serves to protect the amino group from the electrophilic carbenoid, so that just its adjacent C–H bonds can react in an intermolecular fashion with the carbenoid. Also, the disilyl group is very labile, and the β -amino ester is readily released and isolated as its hydrochloride salt.



Scheme 11. Intermolecular rhodium-catalyzed C–H insertion applied to the synthesis of a β -amino ester *en route* to the synthesis of (*S*)-venlafaxine.⁸⁹

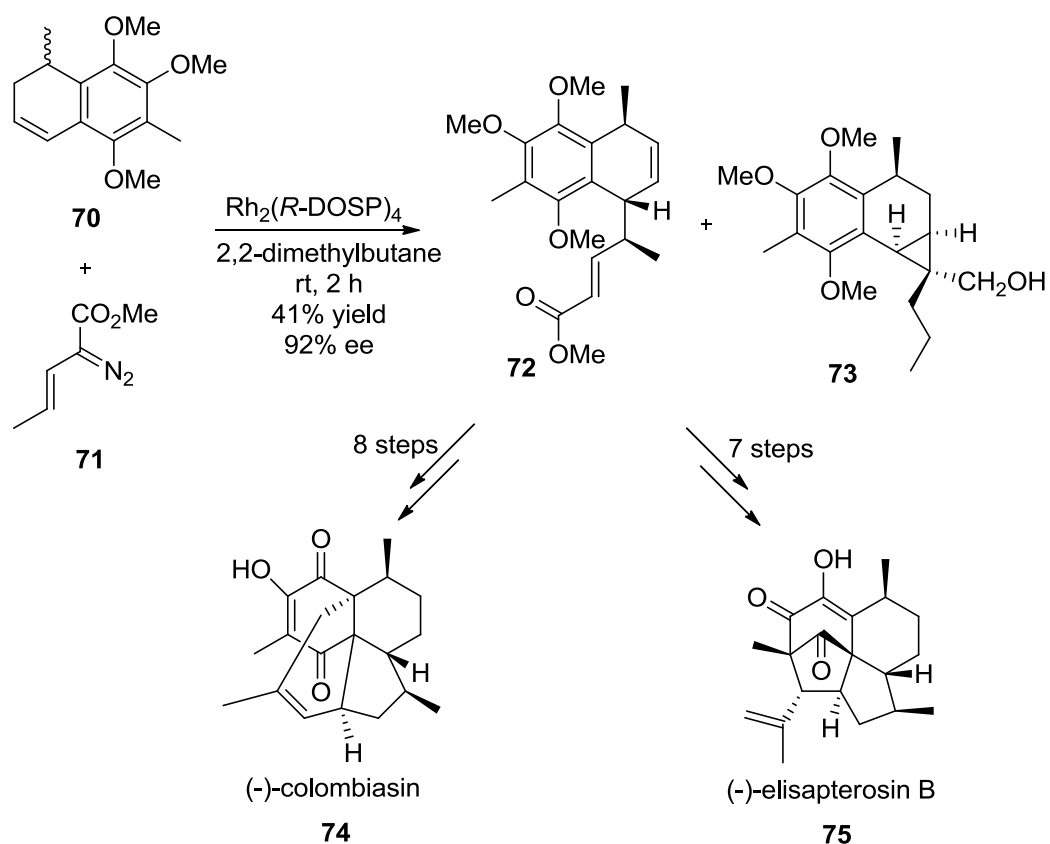
Intermolecular C–H insertion reactions are also capable of initiating cascade reactions.⁹⁰⁻⁹² An elegant example of this class of reactions has been termed the combined C–H activation/Cope rearrangement.⁹² The reaction occurs in a concerted fashion through a six-membered transition state to form products that are normally obtained from intermolecular C–H insertion followed by a Cope rearrangement. However, the intermolecular C–H insertion product was reported not to be an intermediate in this reaction because it is the most stable thermodynamic product. The pathway is thought to

be initiated by intermolecular insertion, but is interrupted by Cope rearrangement leading to the formation of product **69** (Scheme 11).



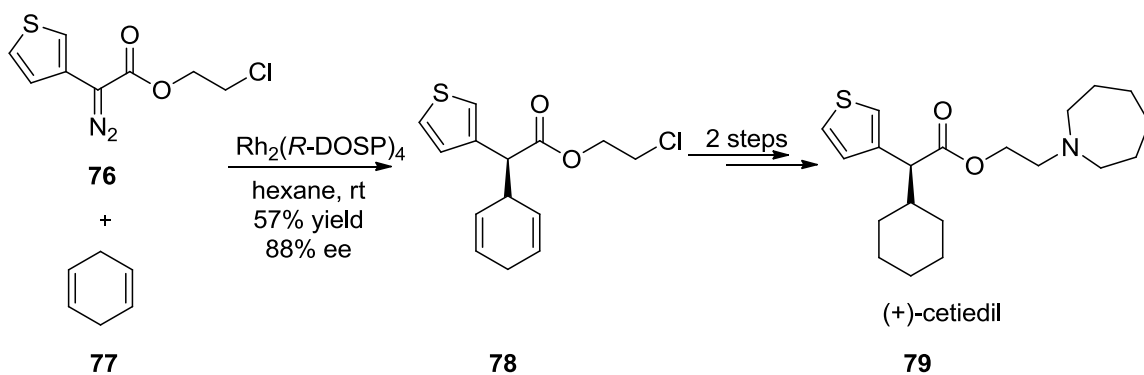
Scheme 12. Mechanistic pathway for the combined C–H activation/Cope rearrangement.⁹²

The combined C–H activation/Cope rearrangement has been employed as the key step in the synthesis of the diterpenes (-)-colombiasin A and (-)-elisapterosin B, both isolated from *Pseudopterogorgia elisabethae* (Scheme 13).⁹³ In the synthesis, dihydronaphthalene **70** and vinyl diazoacetate **71** undergo a combined C–H activation/Cope rearrangement catalyzed by $\text{Rh}_2(\text{R-DOSP})_4$ to form products **72** and **73**. Apparently, when the reaction is catalyzed by $\text{Rh}_2(\text{R-DOSP})_4$, one enantiomer of dihydronaphthalene undergoes combined C–H activation/Cope rearrangement to provide **72**, while the other enantiomer is converted by cyclopropanation to **73**. Compound **72** is obtained in 41% yield, with 92% ee. In the reaction, three chiral centers common to both natural products are obtained. Compound **72** is then transformed in seven and eight steps to (-)-colombiasin A **74** and (-)-elisapterosin B **75**, respectively.



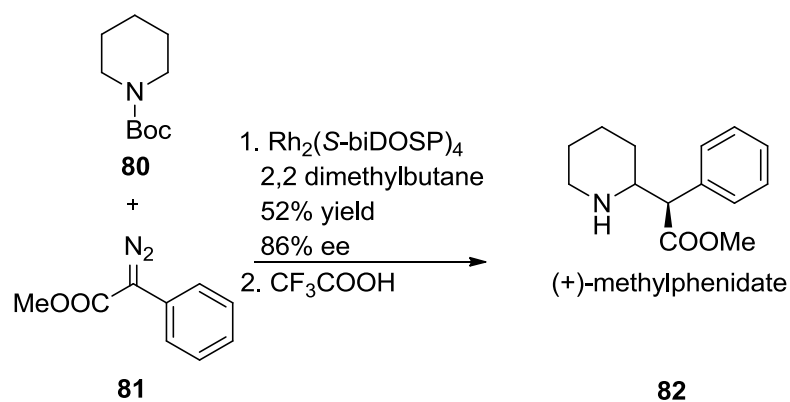
Scheme 13. Combined C–H activation/Cope rearrangement applied to the synthesis of (-)-colombiasin A and (-)-elisapterosin B.⁹³

Several pharmaceutical agents have been synthesized by applying enantioselective intermolecular C–H functionalization as a critical step in the syntheses. (+)-Cetiedil **79**,⁹⁴ (*S*)-venlafaxine **65**,⁸⁹ ritalin **82**⁹⁵ and (+)-indatraline **85**⁹⁶ are some representative examples among others. In the synthesis of (+)-cetiedil (Scheme 14), thiophenyldiazoacetate **76** undergoes an allylic C–H insertion with 1,4 cyclohexadiene **77** catalyzed by $\text{Rh}_2(\text{R-DOSP})_4$ to form **78** in 57% yield and 88% ee. Chloride **78** is further converted in two steps to furnish the cholinesterase inhibitor (+)-cetiedil **79**.



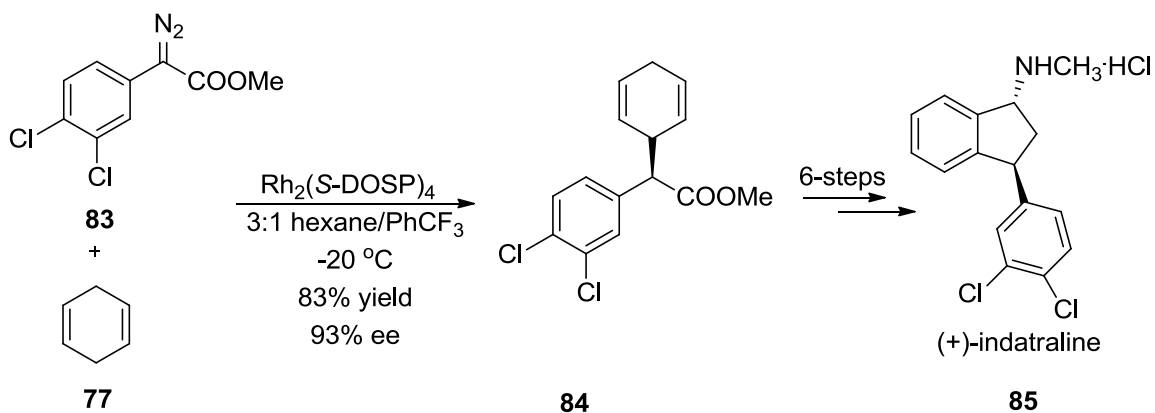
Scheme 14. Intermolecular rhodium-catalyzed C–H insertion applied to the synthesis of (+)-cetiedil.⁹⁴

Ritalin, also known as (+)-methylphenidate, is used for the treatment of attention deficit hyperactivity disorder (ADHD). Conventional synthetic approaches to this compound involve multi-step synthesis; conversely, intermolecular rhodium-catalyzed C–H insertion allowed a direct and rapid approach. The $\text{Rh}_2(\text{S-biDOSP})_4$ -catalyzed reaction of the protected piperidine **80** with methyl phenyldiazoacetate **81**, followed by removal of the protecting group, completed a rapid synthesis of (+)-methylphenidate **82** (Scheme 15).



Scheme 15. Intermolecular rhodium-catalyzed insertion applied to the synthesis of (+)-methylphenidate.⁹⁵

Indatraline is a potent psychoactive compound with a strong binding and inhibitory affinity for monoamine reuptake inhibitors such as dopamine and serotonin. The synthesis of indatraline has been completed via $\text{Rh}_2(\text{S-DOSP})_4$ -catalyzed reaction of (3,4 dichlorophenyl)diazoacetate **83** and 1,4-cyclohexadiene **77** to give C–H insertion product **84** in 83% yield and 93% ee. Product **84** was then transformed in six steps to (+)-indatraline **85** (Scheme 16).

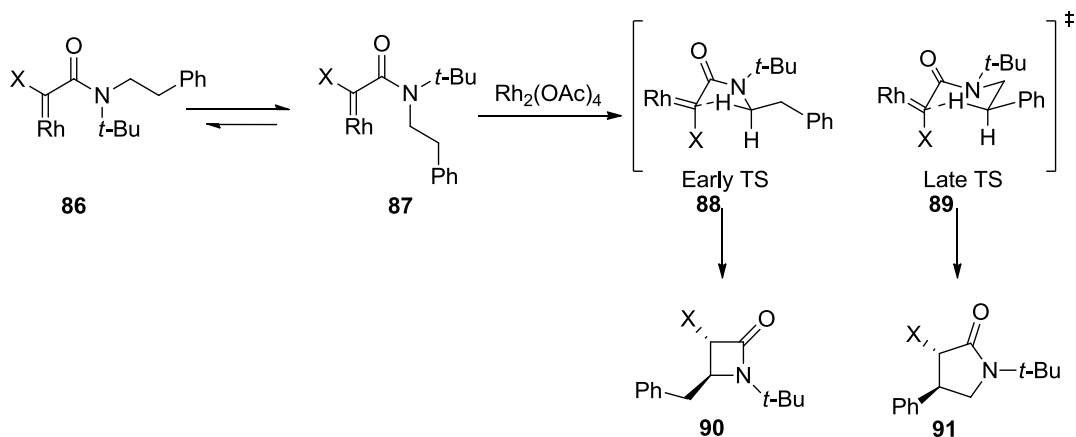


Scheme 16. Intermolecular rhodium-catalyzed insertion applied to the synthesis of (+)-indatraline.⁹⁶

1.5.2 Intramolecular Rhodium-Induced C–H Insertion

The majority of synthetically meaningful rhodium(II) catalyzed reactions are intramolecular C–H insertion reactions.⁹⁷⁻¹⁰² As mentioned earlier, this occurs when the rhodium carbenoid and the target C–H bond are in the same molecule, connected by a suitable tether. In general, rhodium-induced intramolecular C–H insertions are best catalyzed by rhodium(II) carboxamides¹⁰³ and occur with an overwhelming preference for the formation of five-membered carbocycles/heterocycles, in which the order of reactivity is tertiary > secondary >> primary.^{45, 104} This inherent preference can be overridden by substrate conformation, local electronic effects and the nature of the ligands on the rhodium catalyst to obtain four- and six-membered ring compounds on select substrates.^{57, 70} However, there is no standard procedure that dictates the application of these controlling factors. At times, competing influences may result in the formation of mixtures of products as demonstrated by Hu and co-workers in the β - and γ -

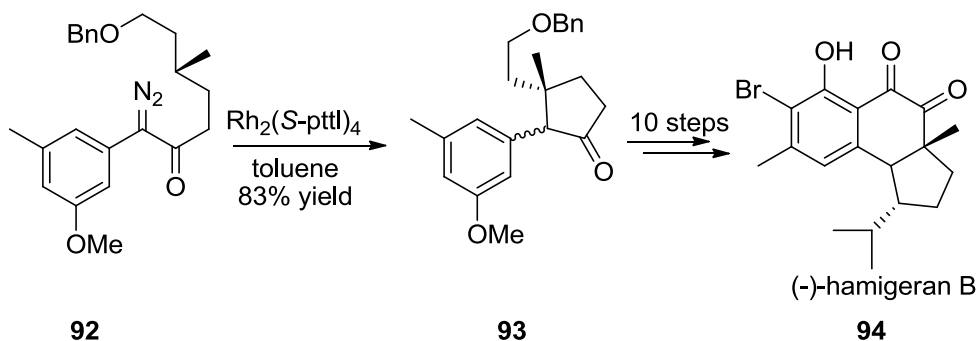
lactam synthesis via C–H insertion of diazoacetamides (Scheme 17).¹⁰⁵ The activating effect of the amide nitrogen and the strong electron-withdrawing substituent attached to the carbene favored the formation of a β -lactam. Apparently, the presence of the strong electron-withdrawing substituent leads to the early TS **88** resulting in β -lactam **90**. The absence of a strong electron-withdrawing substituent favored a late TS **89** leading to γ -lactam **91**.



Scheme 17. Formation of β - and γ -lactams by intramolecular rhodium-catalyzed insertion.¹⁰⁵

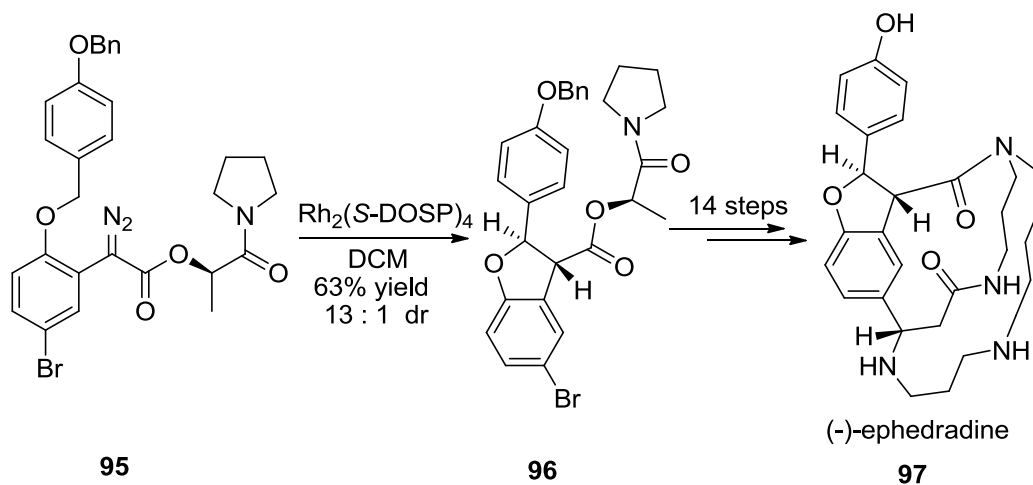
A notable feature of intramolecular C–H insertion is its inherent ability to convert an acyclic tertiary chiral center into a cyclic quaternary chiral center with retention of absolute configuration.^{74, 106} This phenomenon has been exploited by Taber and co-workers in the synthesis of (-)-hamigeran B (Scheme 18).¹⁰⁶ A key step in the synthesis was the $\text{Rh}_2(\text{S-pttl})_4$ -catalyzed reaction of α -aryl- α -diazoketone **92**, which leads to the C–H insertion product **93** in 83% yield with retention of configuration at the quaternary

center. However, a mixture of diastereomers was obtained because of the stereogenic center adjacent to the carbonyl moiety. The desired configuration was conveniently attained by equilibrating the mixture, and subsequent steps furnished the product (-)-hamigeran B **94**.



Scheme 18. Intramolecular rhodium-catalyzed insertion applied to the synthesis of (-)-hamigeran B.¹⁰⁶

During intramolecular C–H insertion, EDG and heteroatoms tend to activate adjacent C–H bonds towards insertion, while EWG deactivate adjacent C–H bonds.^{107, 108} This aspect of intramolecular C–H insertion has been utilized by Fukuyama and co-workers to generate benzofurans from α -aryl- α -diazoketones via intramolecular C–H insertion *en route* to the synthesis of the complex macrocyclic spermine alkaloid (-)-ephedradine (Scheme 19).¹⁰⁷ In one case, reaction of α -aryl- α -diazoketone **95** catalyzed by $\text{Rh}_2(\text{S-DOSP})_4$ led to C–H insertion product **96** in 63% yield. A diastereomeric ratio of 13 : 1 was obtained with the aid of a chiral auxiliary in combination with the chiral catalyst. Benzofuran **96** was converted to the product (-)-ephedradine **97** in 14 steps.

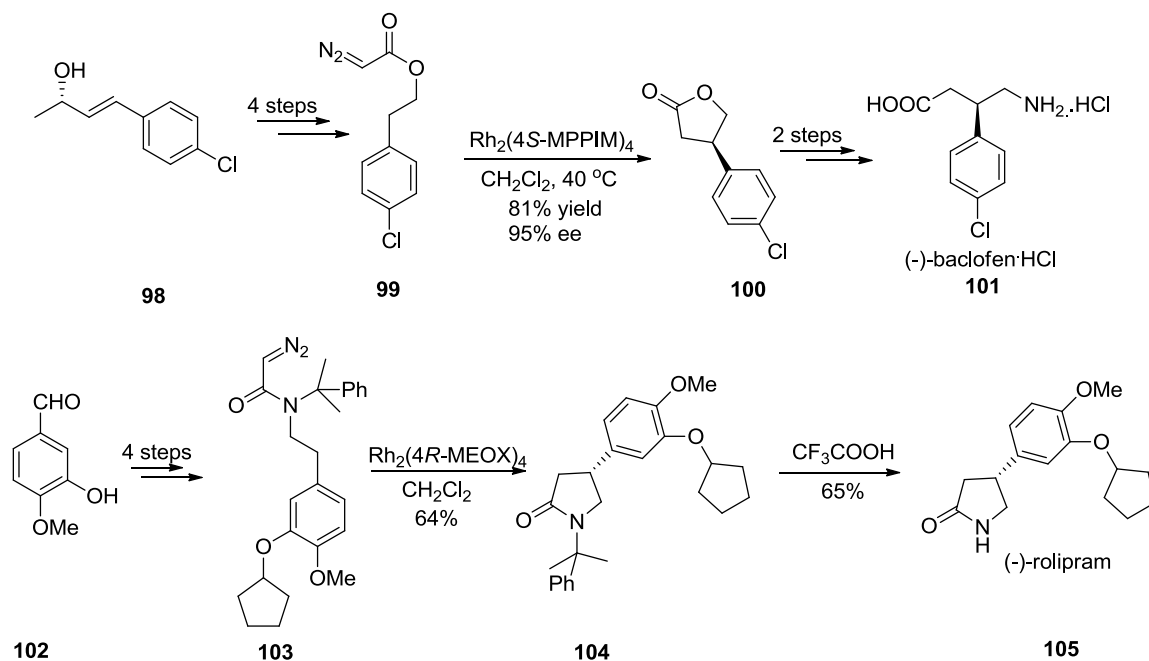


Scheme 19. Intramolecular rhodium-catalyzed insertion applied to the synthesis of (-)-ephedradine.¹⁰⁷

Intramolecular C–H insertion has been widely used in the synthesis of γ -butyrolactones and γ -lactams (Scheme 20).^{108, 109} Notable examples are the pharmaceutical agents (*R*)-baclofen HCl **101** and (*R*)-rolipram **105**, respectively. (*R*)-Baclofen HCl is a GABA_B receptor agonist, while (*R*)-rolipram is a phosphodiesterase type IV inhibitor. The synthesis of **101** begins from *p*-chlorophenethyl alcohol and involves a Rh₂(*S*-MPPIM)₄-catalyzed intramolecular C–H insertion reaction of diazoacetate **99** to afford the γ -butyrolactone **100** in 81% yield and 99% ee, which is further converted to **101** in a 60% overall yield.¹¹⁰ Hu and co-workers¹¹¹ have reported the synthesis of **105** starting from isovanillin **102** and utilizing cumyl(2,2-dimethylbenzyl) as an *N*-protecting group for a Rh₂(MEOX)₄-catalyzed intramolecular C–H

insertion of α -diazoacetamide **103** to provide the γ -lactams **104** in 64% yield and 46% ee.

Removal of the cumyl protecting group furnishes **105** in 15% overall yield.



Scheme 20. Synthesis of γ -butyrolactones and γ -lactams by intramolecular rhodium-catalyzed insertion.^{110, 111}

Naturally occurring lignin lactones such as (\pm)-enterolactone **106**, (\pm)-hinokinin **107**, (-)-arctigenin **108**, (+)-isodeoxy-podophyllotoxin **109**, (+)-isolauricerisinol **110**, and (+)-imperanene **111**, are some representative examples of natural products that have been synthesized by employing intramolecular C–H insertion to generate γ -butyrolactones as crucial steps in the syntheses (Figure 4).¹¹²

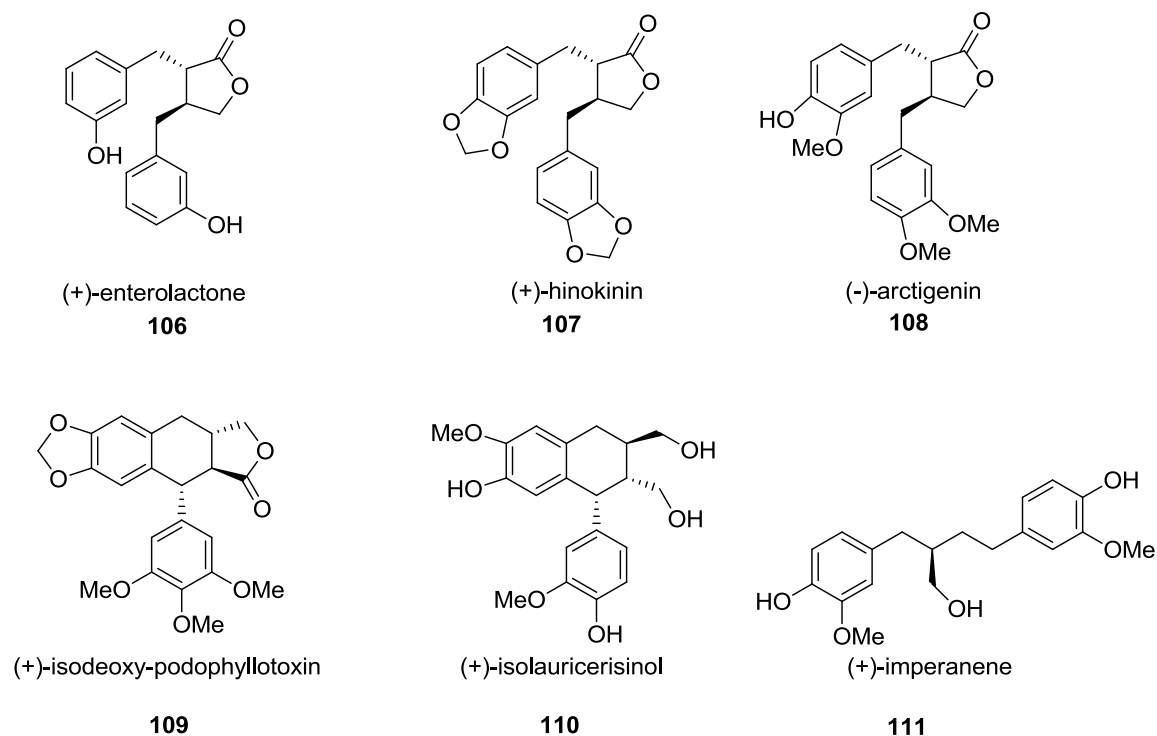
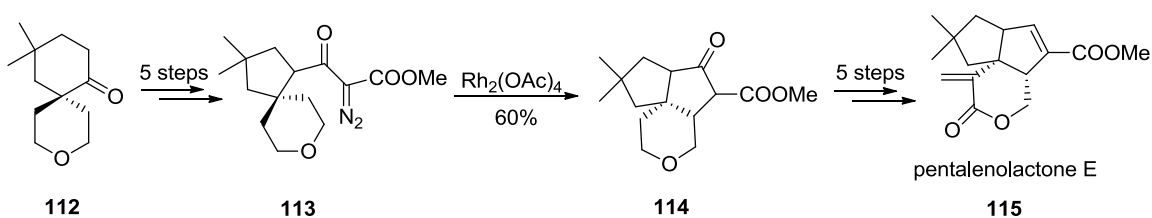


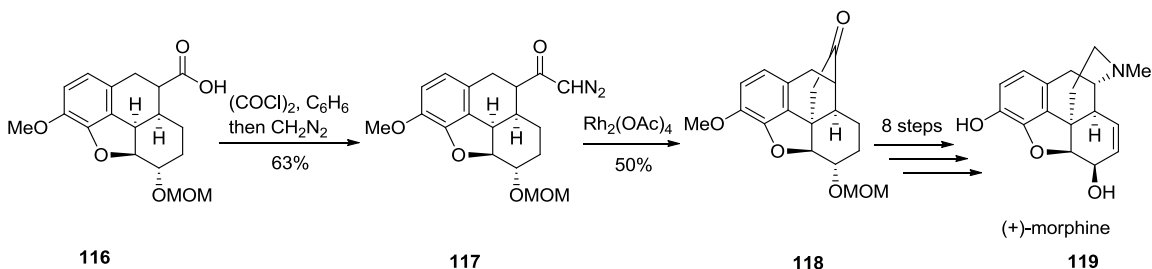
Figure 4. Natural occurring lignin lactones synthesized by using rhodium-catalyzed intramolecular C–H insertion to generate γ -butyrolactones.¹¹²

Another important aspect of intramolecular C–H insertion is that the reaction can break the symmetry of molecules, thereby generating complex products from relatively simple precursors. This aspect has been put into use by Taber and co-workers in the synthesis of the sesquiterpene antibiotic pentalenolactone E.¹¹³ In a key step of the synthetic route (Scheme 21), the tricyclic ketone **114** is furnished by $\text{Rh}_2(\text{OAc})_4$ -catalyzed intramolecular C–H insertion of α -diazo- β -ketoester **113** with a single chiral center. The ester is converted to tricyclic ketone **114** with high asymmetric induction resulting in three chiral centers. The tricyclic ketone is then converted in five steps to complete the synthesis of pentalenolactone E **115**.



Scheme 21. Use of intramolecular rhodium-catalyzed insertion in the synthesis of pentalenolactone E by Taber and co-workers.¹¹³

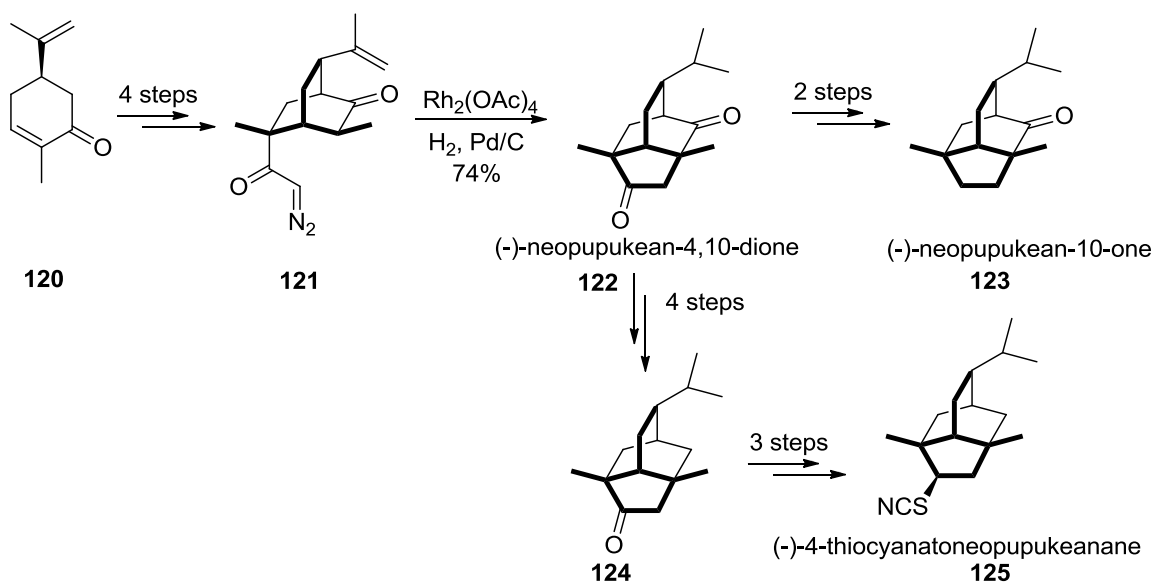
The effectiveness of rhodium-catalyzed intramolecular C–H insertion to form new C–C bonds in fused-ring systems under strained conditions has also been demonstrated.^{114, 115} In the synthesis of (+)-morphine by White et al. (Scheme 22),¹¹⁴ carboxylic acid **116** was treated with oxalyl chloride followed by diazomethane to form α -diazoketone **117** in 63% yield. $\text{Rh}_2(\text{OAc})_4$ -catalyzed intramolecular insertion of **117** afforded the fused-cyclopentanone **118** in 50% yield, from which the piperidine ring of (+)-morphine **119** was installed at a later stage in the synthesis.



Scheme 22. Use of intramolecular rhodium-catalyzed insertion to construct carbocycles in strained and fused systems.¹¹⁴

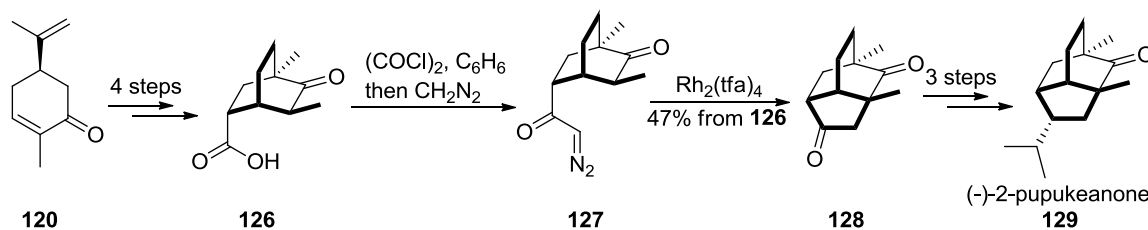
Similarly to the synthesis of (+)-morphine, Srikrishna and Gharpure¹¹⁵ have reported the synthesis of (-)-neopupukean-4,10-dione **122**, (-)-neopupukean-10-one **123**,

(-)-2-pupukeanone **129** and (-)-4-thiocyanatoneopupukeanane **125**. A characteristic feature of neopupukeananes is the presence of the subtle 9-isopropyl-3,6-dimethyltricyclo[4.3.1.0]decane (isotwistane) framework that constitutes two quaternary carbon atoms in addition to the isocyano and thiocyanato moieties. In the report, the isotwistane framework was formed via $\text{Rh}_2(\text{OAc})_4$ -catalyzed intramolecular insertion from the corresponding diazo ketone **121**. The diazo ketone is obtained from (*R*)-carvone **120** by employing double Michael reactions with LiHMDS and methyl methacrylate to get bicyclic keto esters, which are further subjected to base hydrolysis to get the corresponding keto acids. Treatment of the keto acids with oxalyl chloride followed by diazomethane results in the formation of the desired diazo ketones. The isotwistane framework is then converted to the various neopupukeananes by subsequent reactions.



Scheme 23. Synthesis of neopupukeananes via intramolecular rhodium-catalyzed insertion.¹¹⁵

Using similar transformations to the ones described above, the synthesis of (-)-2-pupukeanone was also completed starting from **120** (Scheme 24). $\text{Rh}_2(\text{tfa})_4$ -catalyzed intramolecular C–H insertion of the diazo ketone **127** gave diketone **128** in 47% yield, which was converted in three steps to (-)-2-pupukeanone **129**.



Scheme 24. Synthesis of (-)-2-pupukeanone via intramolecular rhodium-catalyzed insertion.¹¹⁵

CHAPTER 2

RHODIUM-CATALYZED INTRAMOLECULAR C–H INSERTION ON DIAZOSULFONES AND DIAZOSULFONATES

2.1 Introduction

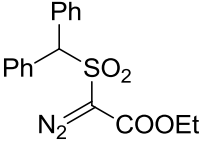
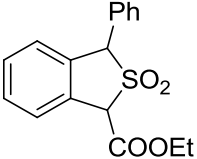
The earliest studies on rhodium-catalyzed intramolecular C–H insertion on α -diazosulfones were performed by Durst and co-workers.^{116, 117} These studies demonstrated the formation of five-membered γ -sulfones fused to phenyl, thiophene and indole ring compounds (Table 2). The products are formed from the insertion of the rhodium carbenoid carbon into an aromatic *ortho* C–H bond. However, the reaction shows a preference to products arising from insertion at the carbon atom *para* to alkoxy substituents in cases where competition between *para*- and *ortho* C–H bonds is possible (substrate **133**, Table 2). Also, *ortho*-methoxy substituted aromatic α -diazosulfones provide no identifiable products (substrate **134**, Table 2), perhaps due to competing oxygen ylide formation, followed by decomposition. The presence of an additional substituent adjacent to the sulfone fragment (substrate **135**, Table 2) result in the formation of diastereomers, but with no influence on the outcome of the reaction. While it is possible to obtain products with α -diazo esters, α -diazo ketones and sulfonyl diazomethane afford no products under the same reaction conditions. Following this initial report by Durst and co-workers, for over two decades, there have been no other reports on either intermolecular or intramolecular C–H insertion involving α -

diazosulfones and α -diazosulfonates, in which the sulfone fragment is a part of the formed ring.

Table 2. Rhodium-catalyzed intramolecular C–H insertion resulting in the formation of γ -sulfones fused to phenyl, thiophene and indole ring compounds reported by Durst and co-workers.¹¹⁶

S	Ar	P	Yield (%)
130			14-48
131			50
132			24
133			42
134			0

Table 2. Cont.

S	Ar	P	Yield (%)
135			47

Recently, Du Bois and co-workers have demonstrated that rhodium nitrenoids generated from the corresponding sulfamate esters undergo intramolecular nitrogen–hydrogen insertion to form six-membered ring sulfamates.¹¹⁸⁻¹²¹ As proposed, the difference in bond lengths and bond angles around the sulfur atom is responsible for the change of preference. Expanding on Du Bois’ work, Novikov and co-workers previously disclosed the preferential formation of cyclic six-membered sulfones and sulfonates via rhodium-catalyzed intramolecular C–H insertion of aliphatic diazosulfones and diazosulfonates (Table 3).¹²² As in the case of nitrene insertion, the preference for six-membered rings has also been attributed to longer bond lengths and larger bond angles around the sulfonyl fragment incorporated into the newly forming ring, which allows more distant C–H bonds to be targeted for insertion resulting in favorable six-membered ring.

Table 3. Rhodium-catalyzed intramolecular C–H insertion of aliphatic diazosulfones and diazosulfonates leading to the formation of six-membered rings by Novikov and co-workers.¹²²

S	X	R	P	Yield (%)
136	CH ₂			55 ^a
137	CH ₂			56
138	O			53
139	O			55 ^a
140	O			80 ^b

^a Isolated as a single isomer.

^b Diastereomeric ratio varied from experiment to experiment, ranging from complete to 2:1 in favor of the same diastereomer

A subsequent report by Wolckenhauer et al.¹²³ has shown that in the case of diazosulfonates, the preference for six-membered rings persists on a variety of substrates

(Table 4). Remarkably, the preference for six-membered rings is maintained even when formation of a strained system is required.

Table 4. Formation of six-membered sulfonates from the corresponding diazosulfonates via intramolecular rhodium-catalyzed C–H insertion reported by Wolckenhauer and co-workers.

S	R	P	Yield (%)
141			84 ^b
142			94 ^a
143			85 ^a
144			64 ^a
145			57 ^c

Table 4. Cont.

S	R	P	Yield (%)
146			66 ^d
147			68 ^a
148			77 ^a

^a: Rh₂(OAc)₄, DCM; ^b: Rh₂(esp)₂, DCM; ^c: Rh₂(tpa)₄, DCM; ^d: Rh₂(tfa)₄, CCl₄

2.2 Formation of Five- versus Six-Membered Cyclic Sulfones via Rhodium-Catalyzed Intramolecular C–H Insertion

In the initial report by Novikov and co-workers in 2007,¹²² sulfone **149a** (Table 5) was identified as the major product of intramolecular C–H insertion of the corresponding diazosulfone **136**. A more detailed analysis of the reaction mixture revealed the presence of a small amount of the cis isomer as well as isomers with a five-membered ring. This provoked follow-up studies into the contributing roles of the catalyst, structure of the diazosulfone, and the local C–H insertion site electronic effects to the selectivity of the reaction.¹²⁴

An effort to characterize the reaction mixture proved daunting as the separation of the other isomers (five-membered ring isomers and the cis six-membered ring isomer) turned out to be difficult, and was further complicated by simultaneous equilibrium between **150a** and **150b** during flash chromatography. However, it was found that the mixture of **150a** and **150b** isomerized with DBU (1,8-diazabicyclo[5.4.0]undec-7-ene) in DCM (dichloromethane) for 24 h at room temperature to provide exclusively **150a**. Also, equilibrating the mixture prior to flash chromatography separation simplified the purification of the products. Curiously, under these isomerization conditions, the six-membered ring diastereomers **149a** and **149b** formed a mixture with a ratio close to 1:1.

Mindful of the fact that the electronic properties of the ligands on the rhodium catalyst dictate the reactivity of the resultant rhodium carbenoid, the efficacy of other catalysts in the reactions of the diazosulfone substrate **136** was investigated (Table 5). Doyle's $\text{Rh}_2(\text{cap})_4$ (rhodium(II) caprolactam),¹²⁵ which is known to enhance C–H insertion selectivity, $\text{Rh}_2(\text{tpa})_4$ (rhodium(II) triphenyl acetate), and Du Bois'¹¹⁸ tethered $\text{Rh}_2(\text{esp})_4$ (bis[rhodium(α , α , $\acute{\alpha}$, $\acute{\alpha}$ -tetramethyl-1,3-benzenedipropionic acid)]) catalysts proved effective for this transformation showing results similar to $\text{Rh}_2(\text{OAc})_4$. $\text{Rh}_2(\text{cap})_4$ catalyst was unreactive at room temperature or at reflux in DCM, necessitating a switch to the higher boiling solvent dichloroethane. Unexpectedly, $\text{Rh}_2(\text{pfb})_4$ (rhodium(II) perfluorobutyrate) catalyst led to a reversal of the usual selectivity, providing exclusively the five-membered ring products. These results infer that rhodium(II) catalysts with strong electron-withdrawing ligands such as $\text{Rh}_2(\text{pfb})_4$ tend to favor the formation of five-

membered sulfones, while those with electron-donating ligands tend to favor six-membered sulfones.¹²⁴

Table 5. Effect of catalyst on five- versus six-membered sulfone selectivity reported by Jungong et al.¹²⁴

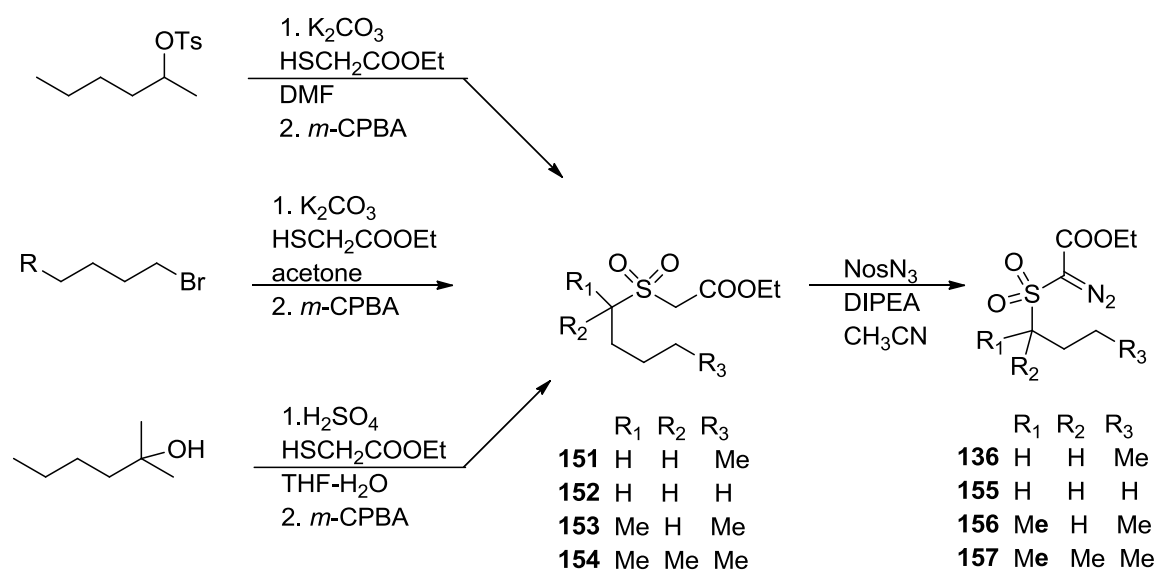
Rh ₂ L ₄ , conditions ^a	Yield of 149 ^b (%)	Yield of 150 ^b (%)
Rh ₂ (OAc) ₄ , rt, DCM	65	9
Rh ₂ (esp) ₂ , rt, DCM	70	9
Rh ₂ (tpa) ₄ , rt, DCM	50	20
Rh ₂ (cap) ₄ , 80 °C, (CH ₂ Cl) ₂	60	8
Rh ₂ (pfb) ₄ , rt, DCM	27	49

^a All reactions were carried out by slow addition of the solution of diazosulfone to 1 mol% of the catalyst.

^b Isolated yields, combined for both diastereomers

In order to explore the effect of the structure of the diazosulfone and that of the C–H insertion site on the selectivity of the transformation, the necessary diazosulfone substrates were prepared using the synthetic sequence outlined in Scheme 25. The

appropriate alkyl bromide or alkyl tosylate was subjected to a nucleophilic substitution reaction by ethyl mercaptoacetate in the presence of potassium carbonate and catalytic amounts of sodium iodide in refluxing acetone. For diazosulfone **153** (Scheme 25), the solvent was switched to DMF (dimethylformamide). The resulting sulfides were oxidized to sulfones using *m*-CPBA (*meta*-chloroperoxybenzoic acid) in DCM or oxone in a 1:1 mixture of acetone and water. The obtained sulfones were then treated with NosN_3 (4-nitrobenzenesulfonyl azide) in the presence of DIPEA (diisopropylethylamine) in CH_3CN (acetonitrile) or DMF to afford the desired diazosulfones. Preparation of diazosulfone **154** was achieved by acid-catalyzed $\text{S}_{\text{N}}1$ substitution to make the sulfide which was further converted to the corresponding diazosulfone as described above.



Scheme 25. Preparation of diazosulfones.¹²⁴

As mentioned in the previous chapter, intramolecular C–H insertion is favored at sites that stabilize positive charge. Decrease in substitution at the C–H insertion site (substrate **155**, Table 6) predictably disfavored the insertion, resulting in the preferential formation of the five-membered ring products, with only small amounts of the six-membered ring sulfone. This stems from the fact that secondary C–H bonds stabilize positive charge better than primary C–H bonds, and as such, insertion is favored at the secondary C–H bond leading to the formation of the five-membered ring sulfone, while that at the less favored primary C–H bond results in the six-membered sulfone. Remarkably, the use of $\text{Rh}_2(\text{pfb})_4$, which at this point in the study was known to favor five-membered ring sulfones, made the preference for five-membered ring sulfones complete, also greatly improving the yield of the product. No trace amounts of six-membered sulfone were detected.

Table 6. Effects of structure of diazosulfone on selectivity of rhodium-catalyzed intramolecular C–H insertion leading to the formation of five- and six-membered rings reported by Jungong et al.¹²⁴

S	R ₁	R ₂	R ₃	conditions ^a	Yield of P.1 ^b (%)	Yield of P.2 ^b (%)
136	H	H	Me	A	65	9
155	H	H	H	A	2	25

Table 6. Cont.

	R ₁	R ₂	R ₃	conditions ^a	Yield of P.1 ^b (%)	Yield of P.2 ^b (%)
155	H	H	H	B	4	45
155	H	H	H	C	Not detected	80
156	Me	H	Me	A	40	24
156	Me	H	Me	B	26	34
156	Me	H	Me	C	8	60
157	Me	Me	Me	D	5	75
157	Me	Me	Me	E	Not detected	64

^a Conditions: A: Rh₂(OAc)₄, DCM, rt; B: Rh₂(esp)₂, DCM, rt; C: Rh₂(pfb)₄, DCM, rt; D: Rh₂(OAc)₄, (CH₂Cl)₂, reflux; E: Rh₂(pfb)₄, (CH₂Cl)₂, reflux.

^b Isolated yields, combined for both diastereomers

The presence of substituents adjacent to the sulfone moiety favored the formation of five-membered ring sulfones. Monomethyl substitution (substrate **156**, Table 6) led to the formation of almost equivalent amounts of five- and six-membered sulfones. Use of Rh₂(pfb)₄ enhanced the shift in selectivity; making the five-membered ring sulfone the prevalent product. Notably, selectivity in the formation of the substitution center adjacent to the sulfone fragment (β -position) was observed for this substrate.

The formation of small amounts (5-10% combined) of several products possibly containing the opposite configuration at the β -position was observed. Definitive identification of these products was not achieved due to the difficulty encountered during

purification. The dimethyl-substituted diazosulfone **157** was stable to the rhodium catalysts screened at rt or reflux in DCM, requiring reflux in dichloroethane to react. The reaction resulted in the formation of a five-membered ring even with $\text{Rh}_2(\text{OAc})_4$. Use of $\text{Rh}_2(\text{pfb})_4$ led to complete selectivity towards the five-membered sulfone at the expense of decreased yield. These results can be explained by the decrease in the angle of C–C–SO₂ fragment due to steric compression, favoring the five-membered ring geometry.

Having established that the structure of the diazosulfone, local insertion site electronic effects, and rhodium catalyst used affect the selectivity of the reaction, the next objective was to investigate the feasibility of formation of four-membered sulfones. The necessary substrates (Table 7) were prepared as described previously.

Table 7. Preparation of diazosulfones.

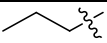
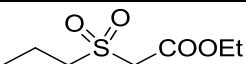
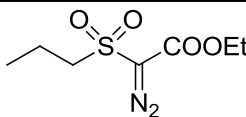
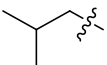
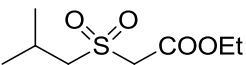
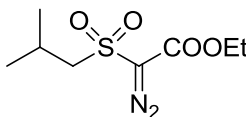
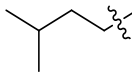
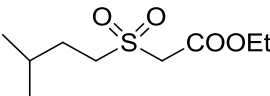
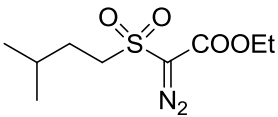
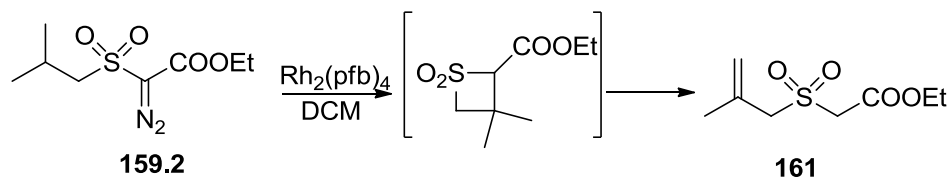
$\text{R-Br} \xrightarrow[\text{2. } m\text{-CPBA}]{\text{1. K}_2\text{CO}_3, \text{HSCH}_2\text{COOEt, acetone}} \text{R-SO}_2\text{CH}_2\text{COOEt} \xrightarrow[\text{CH}_3\text{CN}]{\text{3. NosN}_3, \text{DIPEA}} \text{R-SO}_2\text{C(=N}_2\text{)COOEt}$				
S	R	S.1	S.2	Yield (%)
158				88
159				85

Table 7. Cont.

S	R	S.1	S.2	Yield (%)
160				90

Surprisingly, $\text{Rh}_2(\text{pfb})_4$ reacted with diazosulfone **158.S.2** to form exclusively five-membered ring. Even though $\text{Rh}_2(\text{pfb})_4$ is known to favor the formation of five-membered ring, C–H insertion was expected to occur at the secondary C–H bond due to its ability to stabilize positive charge better, which would lead to the formation of a four-membered ring. When $\text{Rh}_2(\text{OAc})_4$ was used, decomposition of the diazosulfone was observed with no traces of a sulfone product. Increasing substitution at the secondary insertion site (diazosulfone **159.S.2**), $\text{Rh}_2(\text{pfb})_4$ reacted to form a four-membered sulfone. The obtained four-membered sulfone was stable enough to be fully characterized, but gradually isomerized via elimination to alkenylsulfone **161** (Scheme 26).



Scheme 26. Isomerization of a four-membered ring sulfone to an alkenylsulfone.

As expected, the insertion was favored at the tertiary C–H bond over the primary C–H bond of diazosulfone. Again, use of $\text{Rh}_2(\text{OAc})_4$ resulted in complete decomposition of the diazosulfone with no isolatable products. Reaction of $\text{Rh}_2(\text{pfb})_4$ with diazosulfone **160.S.2**, which possesses primary, secondary and tertiary insertion sites, furnished a five-membered ring sulfone.

Table 8. Studies on the formation of four-membered ring sulfones.

S	R ₁	R ₂	R ₃	method	Yield of P.1 (%)	Yield of P.2 (%)
158.2	H	H	H	A	Not detected	67
158.2	H	H	H	B	Not detected	Not detected
159.2	Me	H	H	A	57 ^a	Not detected
159.2	Me	H	H	B	Not detected	Not detected
160.2	H	Me	Me	A	Not detected	52

A: $\text{Rh}_2(\text{pfb})_4$, DCM, rt; B: $\text{Rh}_2(\text{OAc})_4$, DCM, rt

^a Reported yield is for four-membered sulfone, which isomerized over time to alkenylsulfone **161**.

2.3 Structural and Stereochemical Assignments of the Products

The relative stereochemistry of the products was determined by employing standard NMR techniques (^1H , $^{13}\text{C}\{^1\text{H}\}$, COSY, DEPT, and NOE). The relative configuration of stereocenters in **149a** was assigned on basis of the coupling constants between H_b and H_c (Figure 5). Smaller coupling constant and appearance of another coupling constant to H_a (confirmed by COSY) indicate the equatorial position of H_b . Similarly, diaxial arrangement of H_b and H_c is established in **156.1**, while indicating the cis arrangement in **156.2**. Bidirectional NOE correlation between H_a and H_b established the configuration of the β -center. While formation of the cis isomer of **157.1** appeared to occur in the reaction of **157** (by presence of characteristic peaks in the crude spectra), it appeared to recede after equilibration, and only **157.1** was isolated. It has been verified that **157.1** does not change upon treatment with DBU, unlike **149a** and **156.1**, which produce mixtures of cis and trans isomers. This could be explained by unfavorable diaxial interaction with the methyl group that would be present in the cis isomer of **157.1**, but not in **149b** and **156.2**.

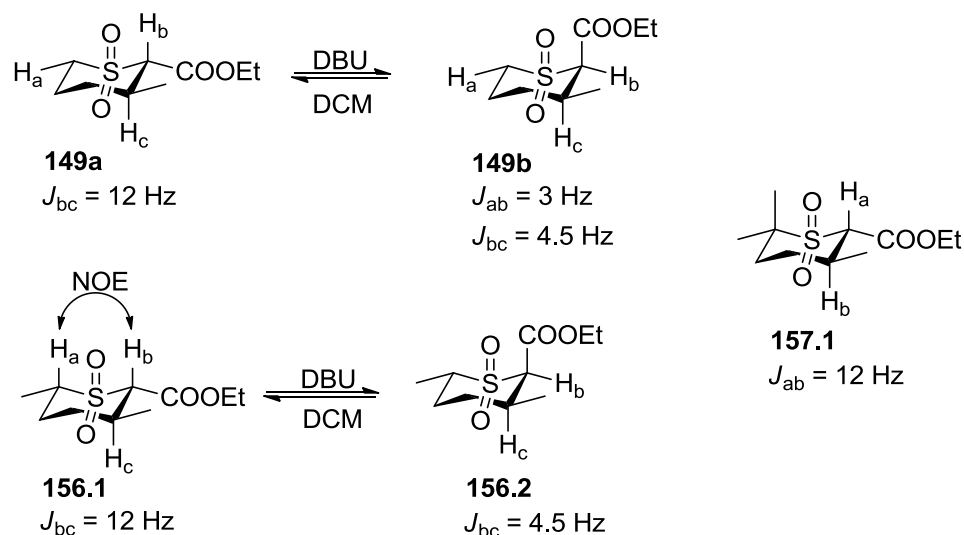


Figure 5. Stereochemical and structural assignments of the six-membered sulfones.¹²⁴

All five-membered products were isolated as single isomers after equilibration. They all show similar patterns of chemical shifts and NOE correlations between protons. The five-membered ring products have been assigned trans configuration for the Me, Et, and CO₂Et substituents on the basis of NOE data and coupling constants. Observed NOEs and their relative intensities were consistent with the proposed structures, while several disagreements can be found with the cis isomers. Additionally, the large coupling constant (10 Hz) between H_c and H_e in **150a** (H_c and H_e in **155.2**, H_d and H_h in **156.2**, H_c and H_f in **157.2**) indicate a dihedral angle that is close to either 0 or 180° (Figure 6). Weak NOE correlations between these hydrogens suggest against the small dihedral angle that would force these hydrogens to a close proximity. For **156.2**, relative configuration of the C₅ center was unambiguously confirmed by a bidirectional NOE between H_b and H_d.

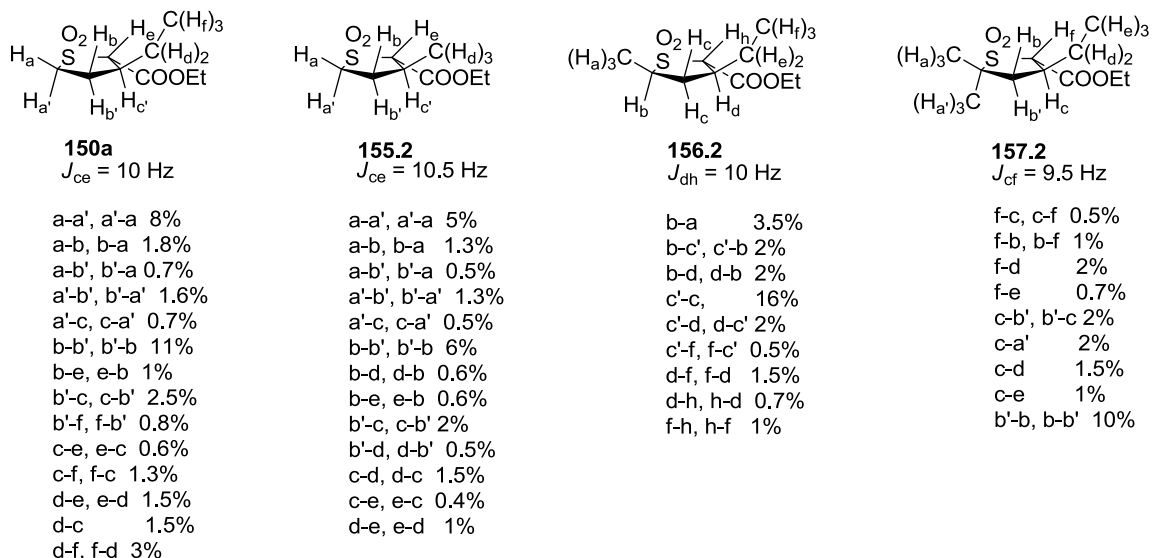


Figure 6. NOE responses (%) observed for isomers **150a**, **155.2**, **156.2**, and **157.2**.¹²⁴

2.4 Conclusion

Intramolecular rhodium-catalyzed C–H insertion on alkylsulfonyl diazoacetate substrates initially reported to favor six-membered ring compounds is sensitive to the structure of the substrate as well as the catalyst used. The presence of substituents adjacent to the sulfonyl moiety was found to tilt the selectivity of the transformation towards the formation of five-membered sulfones. Unexpectedly, the same influence was exerted by $\text{Rh}_2(\text{pfb})_4$ catalyst, apparently due to the presence of the strong electron-withdrawing ligands, which led to increased activity. This work has highlighted the fact that the selectivity of intramolecular rhodium-catalyzed C–H insertion on aliphatic alkylsulfonyl diazoacetate substrates initially reported to favor six-membered ring

compounds can be reversed by strategically installing alkyl substitutions next to the sulfone center. Also, carefully selecting the rhodium catalyst used allows more control over the selectivity of the transformation. It has also been demonstrated that it is possible to obtain four-membered ring sulfones from select diazo sulfones by intramolecular rhodium-catalyzed C–H insertion. The obtained cyclic sulfones are potentially useful intermediates in synthesis. These results will be crucial in expanding the scope of this research as well as exploring the full synthetic potential of the resulting cyclic sulfones.

2.5 Experimental Section for Rhodium-Catalyzed Intramolecular C–H Insertion Studies on Diazosulfones

All reactions were carried out under an inert nitrogen atmosphere unless otherwise stated. All reagents were used as purchased without further purification except otherwise stated. $^1\text{H-NMR}$ (500 Hz) and $^{13}\text{C}\{^1\text{H}\}$ NMR (125 Hz) spectra were recorded on an Avance 500 Bruker spectrometer and calibrated using residual undeuterated solvent as internal references. Coupling constants are given in Hz. IR spectra were recorded on a Perkin-Elmer Spectrum 400 Series FTIR spectrometer. Specific rotations were measured on an AUTOPOL III automatic polarimeter in anhydrous CHCl_3 using a 10 cm cell. HRMS data were obtained on an Agilent 61969A TOF high resolution mass spectrometer using electrospray ionization (ESI). Melting points were determined on a MEL-TEMP melting point apparatus. Analytical TLC was performed using silica gel pre-coated TLC plates (E. Merck no. 5715-7). Flash chromatography was performed using 40-63 μm silica gel (Merck, Geduran, no. 11567-1) as the stationary phase. Tetrahydrofuran (THF) was dried by distilling it from sodium and benzophenone in a continuous still under a

nitrogen atmosphere. Chloroform, dichloromethane and triethylamine were distilled from calcium hydride under an atmosphere of nitrogen.

Procedures for compounds and physical data from Scheme 25

Compounds **136**, **151**, **152**, **153**, **154**, **155**, **156**, and **157** were prepared using the literature procedure reported by John et al,¹²² except otherwise stated. Physical data for compounds **136** and **151** have already been reported; however, ¹H NMR and ¹³C{¹H} NMR are provided.

Ethyl (butylsulfonyl)acetate (151): colorless oil, ¹H NMR (500 MHz, CDCl₃): δ 4.26 (q, *J* = 7, 2H), 3.94 (s, 2H), 3.22–3.26 (m, 2H), 1.81–1.88 (m, 2H), 1.49 (q, *J* = 7.5, 2H), 1.31 (t, *J* = 7, 3H), 0.97 (t, *J* = 7.5, 3H). ¹³C{¹H} NMR (CDCl₃, 125 MHz): δ 163.3, 62.8, 57.5, 53.5, 24.0, 21.8, 14.1, 13.6.

Ethyl (hexan-2-ylsulfonyl)acetate (153): pale yellow oil, ¹H NMR (500 MHz, CDCl₃): δ 4.27 (q, *J* = 7, 2H), 3.99 (d, *J* = 14.5, 1H), 3.94 (d, *J* = 14.5, 1H), 3.35–3.43 (m, 1H), 1.99–2.07 (m, 1H), 1.52–1.66 (m, 2H), 1.47 (d, *J* = 6.5, 3H), 1.30–1.45 (m, 6H), 1.42 (t, *J* = 6.5), 1.33 (t, *J* = 7), 0.94 (t, *J* = 7, 3H). ¹³C{¹H} NMR (CDCl₃, 125 MHz): δ 163.3, 62.8, 58.2, 55.2, 28.8, 28.3, 22.6, 14.2, 14.0, 12.9. HRMS (ESI) calcd for C₁₀H₂₄NO₄S [M+NH₄]⁺ 254.1420, found 254.1404.

Ethyl (2-methylhexan-2-ylsulfonyl)acetate (154): pale yellow oil, ^1H NMR (500 MHz, CDCl_3): δ 4.28 (q, $J = 7$, 2H), 3.94 (s, 2H), 1.76–1.81 (m, 2H), 1.30–1.46 (m, 13H), 1.40 (s), 1.33 (t, $J = 7$), 0.93 (t, $J = 7$, 3H). $^{13}\text{C}\{^1\text{H}\}$ NMR (CDCl_3 , 125 MHz): δ 162.9, 65.3, 62.8, 53.3, 35.0, 26.1, 23.3, 20.7, 14.2, 14.1. HRMS (ESI) calcd for $\text{C}_{11}\text{H}_{26}\text{NO}_4\text{S}$ $[\text{M}+\text{NH}_4]^+$ 254.1577, found 254.1609.

Ethyl (propylsulfonyl)acetate (158.1): colorless oil, ^1H NMR (500 MHz, CDCl_3): δ 4.26 (q, $J = 7.2$, 2H), 3.92 (s, 2H), 3.20–3.25 (m, 2H), 1.9 (q, $J = 7.5$, 2H), 1.32 (t, $J = 7.2$, 3H), 1.09 (t, $J = 7.5$, 3H). $^{13}\text{C}\{^1\text{H}\}$ NMR (CDCl_3 , 125 MHz): δ 163.2 (C), 62.9 (CH_2), 57.8 (CH_2), 55.4 (CH_2), 16.3 (CH_2), 14.4 (CH_3), 13.5 (CH_3). HRMS (ESI) calcd for $\text{C}_7\text{H}_{15}\text{O}_4\text{S}$ $[\text{M}+\text{H}]^+$ 195.0671, found 195.0691.

Ethyl (2-methylpropylsulfonyl)acetate (159.1): colorless oil, ^1H NMR (500 MHz, CDCl_3): δ 4.28 (q, $J = 7.2$, 2H), 3.94 (s, 2H), 3.17–3.20 (m, 2H), 2.41 (m, 1H), 1.33 (t, $J = 7.2$, 3H), 1.15 (d, $J = 6.6$, 3H). $^{13}\text{C}\{^1\text{H}\}$ NMR (CDCl_3 , 125 MHz): δ 163.6, 63.1, 57.9, 52.3, 30.9, 27.9, 22.5, 14.5. HRMS (ESI) calcd for $\text{C}_8\text{H}_{17}\text{O}_4\text{S}$ $[\text{M}+\text{H}]^+$ 209.0832, found 209.0847.

Ethyl (3-methylbutylsulfonyl)acetate (160.1): colorless oil, ^1H NMR (500 MHz, CDCl_3): δ 4.28 (q, $J = 7$, 2H), 3.94 (s, 2H), 3.20–3.30 (m, 2H), 1.70–1.80 (m, 4H), 1.32 (t, $J = 7$, 3H), 0.96 (d, $J = 6.6$, 3H). $^{13}\text{C}\{^1\text{H}\}$ NMR (CDCl_3 , 125 MHz): δ 163.6 (C), 63.0 (CH_2), 61.4 (CH_2), 59.0 (CH_2), 24.3 (CH), 23.1 (CH_3), 14.1 (CH_3).

Note: The signal for the diazo carbon was not observed in $^{13}\text{C}\{^1\text{H}\}$ NMR for any of the diazo compounds, possibly due to quadrupole broadening. IR spectra showing the diazo stretch (2130 cm^{-1}) are provided for diazo compounds.

Ethyl (butylsulfonyl)diazoacetate (155): yellow oil, ^1H NMR (500 MHz, CDCl_3): δ 4.33 (q, $J = 7$, 2H), 3.35–3.43 (m, 2H), 1.77–1.86 (m, 2H), 1.48 (q, $J = 7.5$, 2H), 1.33 (t, $J = 7$, 3H), 0.96 (t, $J = 7.5$, 3H). $^{13}\text{C}\{^1\text{H}\}$ NMR (CDCl_3 , 125 MHz): δ 160.3, 62.7, 56.6, 24.8, 21.5, 14.5, 13.7. IR (neat, cm^{-1}): 2129, 1714, 1467.

Ethyl (2-hexylsulfonyl)diazoacetate (156): yellow oil, ^1H NMR (500 MHz, CDCl_3): δ 4.33 (q, $J = 7$, 2H), 3.44–3.51 (m, 1H), 1.98–2.06 (m, 1H), 1.56–1.65 (m, 1H), 1.44–1.52 (m, 1H), 1.42 (d, $J = 7$, 3H), 1.31–1.40 (m, 6H), 1.34 (t, $J = 7$), 0.94 (t, $J = 7$, 3H). $^{13}\text{C}\{^1\text{H}\}$ NMR (CDCl_3 , 125 MHz): δ 160.4, 62.7, 61.7, 28.8, 28.7, 22.6, 14.5, 14.0, 13.2. IR (neat, cm^{-1}): 2127, 1714, 1463.

Ethyl (propylsulfonyl)diazoacetate (158.2): yellow oil, ^1H NMR (500 MHz, CDCl_3): δ 4.26 (q, $J = 7$, 2H), 3.24–3.30 (m, 2H), 1.70–1.83 (m, 2H), 1.217 (t, $J = 7.2$, 3H), 1.02 (t, $J = 7.2$, 3H). $^{13}\text{C}\{^1\text{H}\}$ NMR (CDCl_3 , 125 MHz): δ 160.4 (C), 62.9 (CH_2), 58.6 (CH_2), 24.8 (CH_2), 17.1 (CH_2), 14.9 (CH_3), 13.3 (CH_3). IR (neat, cm^{-1}): 2120.

Ethyl (2-methylpropylsulfonyl)diazoacetate (159.2): yellow oil, ^1H NMR (500 MHz, CDCl_3): δ 4.34 (q, $J = 7.2$, 2H), 3.28–3.34 (m, 2H), 2.28–2.39 (m, 1H), 1.39 (t, $J = 7.2$,

3H), 1.1 (d, $J = 7.2$, 3H). $^{13}\text{C}\{^1\text{H}\}$ NMR (CDCl_3 , 125 MHz): δ 160.1 (C), 64.6 (CH_2), 62.8(CH_2), 24.7 (CH), 22.9 (CH_3), 14.7 (CH_3). IR (neat, cm^{-1}): 2123.

Ethyl (3-methylbutylsulfonyl)diazoacetate (160.2): yellow oil, ^1H NMR (500 MHz, CDCl_3): δ 4.33 (q, $J = 7.2$, 2H), 3.37–3.41 (m, 2H), 1.68–1.72 (m, 1H), 1.34 (t, $J = 7.2$), 0.96 (d, $J = 7.2$, 3H). $^{13}\text{C}\{^1\text{H}\}$ NMR (CDCl_3 , 125 MHz): δ 160.5 (C), 62.8 (CH_2), 55.4 (CH_2), 31.4 (CH), 27.7 (CH_3), 22.57(CH_3), 14.6 (CH_3). IR (neat, cm^{-1}): 2125.

General procedure for C–H insertion

To the suspension of the catalyst (1 mol%) in CH_2Cl_2 (or $\text{ClCH}_2\text{CH}_2\text{Cl}$, 4 mL/mmol), a solution of the corresponding diazo compound (1 equiv., 0.1–1 mmol) in CH_2Cl_2 (or $\text{ClCH}_2\text{CH}_2\text{Cl}$, 2 mL/mmol) was added at rt (or reflux) over a period of 1 h using a syringe pump. Upon completion of the addition, the reaction mixture was stirred at rt for additional 8 h. The volatiles were removed under reduced pressure. The crude reaction mixture was separated on silica column (ethyl acetate–hexanes, 0–40%). Typically, it was possible to divide the mixture into three parts—the unpolar decomposition products, mixture or various cyclization products, and the more polar six-membered trans isomer. In some cases, isolation of the cis six-membered product was also possible. The incompletely separated mixture of the cyclization products was dissolved in CH_2Cl_2 and treated with 1 equiv. of DBU for 24 h. 1 M HCl solution was added, and the reaction mixture was stirred for 15 min. The layers were separated, aqueous layer was washed with CH_2Cl_2 , and the combined organic layers were dried and

concentrated. The chromatography on silica column (ethyl acetate–hexanes, 0–40%) provided the trans five-membered ring product, cis six-membered ring product, and additional amount of the trans six-membered product, formed by equilibration from the cis isomer.

***cis*-Ethyl tetrahydro-3-methyl-2*H*-thiopyran-1,1-dioxide-2-carboxylate (149b)**: white flaky solid, mp 36–37 °C, ^1H NMR (500 MHz, CDCl_3): δ 4.27 (qd, $J = 7, 1$, 2H), 3.77 (dd, $J = 4.5, 3$, 1H), 3.56 (td, $J = 13, 5$, 1H), 2.93 (dq, $J = 14, 3$, 1H), 2.50–2.59 (m, 1H), 2.04–2.16 (m, 2H), 1.84 (qd, $J = 13, 5$, 1H), 1.55–1.65 (m, 1H; overlapped with water peak), 1.33 (t, $J = 7$, 3H), 1.06 (d, $J = 7$, 3H). $^{13}\text{C}\{^1\text{H}\}$ NMR (CDCl_3 , 125 MHz): δ 166.3 (C), 70.1 (CH), 62.4 (CH₂), 48.0 (CH₂), 34.4 (CH), 26.7 (CH₂), 23.3 (CH₂), 19.8 (CH₃), 14.3 (CH₃). HRMS (ESI) calcd for $\text{C}_9\text{H}_{20}\text{NO}_4\text{S}$ [$\text{M}+\text{NH}_4$]⁺ 238.1107, found 238.1095.

***trans*-Ethyl tetrahydro-3-ethylthiophene-1,1-dioxide-2-carboxylate (150a)**: pale yellow oil, ^1H NMR (500 MHz, CDCl_3): δ 4.25–4.48 (m, 2H), 3.58 (d, $J = 10$, 1H), 3.28 (ddd, $J = 13, 7, 2$, 1H), 3.10 (td, $J = 13, 7$, 1H), 2.68–2.77 (m, 1H), 2.35–2.42 (m, 1H), 1.76–1.86 (m, 1H), 1.60–1.69 (m, 1H), 1.49–1.56 (m, 1H), 1.34 (t, $J = 7$, 3H), 0.97 (t, $J = 7.5$, 3H). $^{13}\text{C}\{^1\text{H}\}$ NMR (CDCl_3 , 125 MHz): δ 165.8 (C), 70.9 (CH), 62.9 (CH₂), 52.9 (CH₂), 41.7 (CH), 27.4 (CH₂), 26.3 (CH₂), 14.3 (CH₃), 11.5 (CH₃). HRMS (ESI) calcd for $\text{C}_9\text{H}_{17}\text{O}_4\text{S}$ [$\text{M}+\text{H}$] 221.0842, found 221.0854, $\text{C}_9\text{H}_{20}\text{NO}_4\text{S}$ [$\text{M}+\text{NH}_4$] 238.1107, found 238.1121.

Ethyl tetrahydro-2*H*-thiopyran-1,1-dioxide-2-carboxylate (155.1): pale yellow oil, ¹H NMR (500 MHz, CDCl₃): δ 4.24–4.34 (m, 2H), 3.85 (ddd, *J* = 6.5, 4.5, 2, 1H), 3.45 (ddd, *J* = 14, 9, 4.5, 1H), 2.95–3.02 (m, 1H), 2.26–2.39 (m, 2H), 2.07–2.17 (m, 2H), 1.89–1.98 (m, 1H), 1.57–1.65 (m, 1H), 1.33 (t, *J* = 7, 3H). ¹³C{¹H} NMR (CDCl₃, 125 MHz): δ 166.1 (C), 65.2 (CH), 62.6 (CH₂), 51.1 (CH₂), 28.1 (CH₂), 24.3 (CH₂), 20.1 (CH₂), 14.2 (CH₃). HRMS (ESI) calcd for C₈H₁₈NO₄S [M+NH₄]⁺ 224.0951, found 224.0951.

***trans*-Ethyl tetrahydro-3-methylthiophene-1,1-dioxide-2-carboxylate (155.2)**: white flaky solid, mp 42–44 °C, ¹H NMR (500 MHz, CDCl₃): δ 4.25–4.39 (m, 2H), 3.52 (d, *J* = 10.5, 1H), 3.31 (ddd, *J* = 13, 7, 1.5, 1H), 3.13 (td, *J* = 13, 7, 1H), 2.76–2.87 (m, 1H), 2.30–2.36 (m, 1H), 1.82 (qd, *J* = 13, 7, 1H), 1.34 (t, *J* = 7, 3H), 1.22 (d, *J* = 6.5, 3H). ¹³C{¹H} NMR (CDCl₃, 125 MHz): δ 165.1 (C), 72.3 (CH), 62.9 (CH₂), 53.4 (CH₂), 35.2 (CH), 28.7 (CH₂), 19.2 (CH₃), 14.3 (CH₃). HRMS (ESI) calcd for C₈H₁₅NO₄S [M+H] 207.0686, found 207.0695; C₈H₁₄NO₄NaS [M+Na]⁺ 229.0505, found 207.0515.

(2*R*,3*R*,6*R*)-Ethyl tetrahydro-3,6-dimethyl-2*H*-thiopyran-1,1-dioxide-2-carboxylate (156.1): white solid, mp 102–103 °C, ¹H NMR (500 MHz, CDCl₃): δ 4.33 (qd, *J* = 7, 4, 2H), 3.51 (d, *J* = 12, 1H), 2.87–2.96 (m, 1H), 2.52–2.60 (m, 1H), 1.88–1.99 (m, 3H), 1.38 (d, *J* = 6.5, 3H), 1.27–1.36 (m, 4H), 1.34 (t, *J* = 7), 1.03 (d, *J* = 6.5, 3H). ¹³C{¹H} NMR (CDCl₃, 125 MHz): δ 163.8 (C), 73.0 (CH), 62.6 (CH₂), 57.6 (CH), 34.8 (CH), 33.1 (CH₂), 31.4 (CH₂), 19.9 (CH₃), 14.4 (CH₃), 10.9 (CH₃). HRMS (ESI) calcd for C₁₀H₂₂NO₄S [M+NH₄]⁺ 252.1264, found 252.1255.

(2*S*,3*R*,6*R*)-Ethyl tetrahydro-3,6-dimethyl-2*H*-thiopyran-1,1-dioxide-2-carboxylate
(156.2): white solid, mp 77–78 °C, ¹H NMR (500 MHz, CDCl₃): δ 4.27 (q, *J* = 7, 2H), 3.83 (d, *J* = 4.5, 1H), 3.60–3.68 (m, 1H), 2.51–2.59 (m, 1H), 1.81–2.02 (m, 3H), 1.55–1.61 (m, 1H; overlapped with water peak), 1.35 (δ, *J* = 7, 3H), 1.33 (t, *J* = 7, 3H), 1.06 (d, *J* = 7, 3H). ¹³C{¹H} NMR (CDCl₃, 125 MHz): δ 166.4 (C), 70.0 (CH), 62.3 (CH₂), 52.7 (CH), 34.7 (CH), 31.6 (CH₂), 27.7 (CH₂), 19.7 (CH₃), 14.3 (CH₃), 10.7 (CH₃). HRMS (ESI) calcd for C₁₀H₁₉NO₄S [M+H]⁺ 235.0999, found 235.1014.

(2*S*,3*S*,5*R*)-Ethyl tetrahydro-3-ethyl-5-methylthiophene-1,1-dioxide-2-carboxylate
(153.2): pale yellow oil, ¹H NMR (500 MHz, CDCl₃): δ 4.25–4.37 (m, 2H), 3.57 (d, *J* = 10, 1H), 3.14–3.24 (m, 1H), 2.60–2.70 (m, 1H), 2.37 (dt, *J* = 13, 6.5, 1H), 1.55–1.64 (m, 1H; overlapped with the water peak at δ 1.60), 1.42–1.52 (m, 2H), 1.39 (d, *J* = 6.5, 3H), 1.34 (t, *J* = 7, 3H), 0.94 (t, *J* = 7, 3H). ¹³C{¹H} NMR (CDCl₃, 125 MHz): δ 166.1 (C), 70.7 (CH), 62.9 (CH₂), 58.6 (CH), 39.2 (CH), 34.5 (CH₂), 27.6 (CH₂), 14.3 (CH₃), 11.4 (CH₃), 11.1 (CH₃). HRMS (ESI) calcd for C₁₀H₂₂NO₄S [M+NH₄]⁺ 252.1264, found 252.1250.

***trans*-Ethyl tetrahydro-3,6,6-trimethyl-2*H*-thiopyran-1,1-dioxide-2-carboxylate**
(157.1): pale yellow oil, ¹H NMR (500 MHz, CDCl₃): δ 4.30–4.37 (m, 2H), 3.73 (d, *J* = 12, 1H), 2.52–2.61 (m, 1H), 2.16–2.23 (m, 1H), 1.71–1.77 (m, 2H), 1.44–1.51 (m, 4H), 1.47 (s), 1.40 (s, 3H), 1.34 (t, *J* = 7, 3H), 1.03 (d, *J* = 6.5, 3H). ¹³C{¹H} NMR (CDCl₃,

125 MHz): δ 164.1 (C), 67.8 (CH), 62.6 (CH₂), 59.0 (C), 36.5 (CH₂), 34.8 (CH), 28.7 (CH₂), 21.5 (CH₃), 21.1 (CH₃), 20.0 (CH₃), 14.4 (CH₃). HRMS (ESI) calcd for C₁₁H₂₄NO₄S [M+NH₄]⁺ 266.1421, found 266.1411.

***trans*-Ethyl tetrahydro-3-ethyl-5,5-dimethylthiophene-1,1-dioxide-2-carboxylate**

(**157.2**): pale yellow oil, ¹H NMR (500 MHz, CDCl₃): δ 4.26–4.37 (m, 2H), 3.61 (d, *J* = 9.5, 1H), 2.73–2.82 (m, 1H), 2.10 (dd, *J* = 13, 6.5, 1H), 1.73 (t, *J* = 13, 1H), 1.48–1.55 (m, 2H; overlapped with the water peak at δ 1.60), 1.42 (s, 3H), 1.44 (s, 3H), 1.34 (t, *J* = 7, 3H), 0.92 (t, *J* = 7.5, 3H). ¹³C{¹H} NMR (CDCl₃, 125 MHz): δ 166.4 (C), 71.3 (CH₃), 62.8 (CH₂), 62.3 (C), 41.5 (CH₂), 37.2 (CH), 28.1 (CH₂), 22.1 (CH₃), 21.5 (CH₃), 14.3 (CH₃), 11.6 (CH₃). HRMS (ESI) calcd for C₁₁H₂₁NO₄S [M+H] 249.1155, found 249.1176; C₁₁H₂₄NO₄S [M+NH₄]⁺ 266.1421, found 266.1441.

Ethyl 3,3-dimethylthiotane-1,1-dioxide-2-carboxylate (159.2.2): pale yellow oil, ¹H NMR (500 MHz, CDCl₃): δ 2.64 (s, 1H), 4.20–4.25 (m, 2H), 3.7–3.8 (dd, *J* = 12.9, 12.6, 2H), 1.47–1.49 (s, 6H; overlapped with the water peak at δ 1.60), 1.20 (t, *J* = 7.2, 3H). ¹³C{¹H} NMR (CDCl₃, 125 MHz): δ 163.3 (C), 84.5 (CH), 74.9 (CH₂), 62.4 (CH₂), 29.4 (C), 28.5 (CH₃), 24.0 (CH₃), 14.5 (CH₃).

Ethyl (2-methyl-2-propenylsulfonyl)acetate (161): pale yellow oil, ¹H NMR (500 MHz, CDCl₃): δ 5.29–5.27 (δ , *J* = 11.3), 4.30 (q, *J* = 7.2, 2H), 3.9–4.10 (d, *J* = 23.3, 2H), 2.0 (s, 3H), 1.34 (t, *J* = 7.2, 3H), ¹³C{¹H} NMR (CDCl₃, 125 MHz): δ 163.5 (C), 134.1 (CH), 121.5 (C), 63.0 (CH₂), 61.4 (CH₂), 55.0 (CH₂), 22.9 (CH₃), 14.3 (CH₃).

Ethyl tetrahydro-2-ethyl-3,3-dimethylthiophene-1,1-dioxide-2-carboxylate (160.2.2):

pale yellow oil, ^1H NMR (500 MHz, CDCl_3): δ 4.22-4.38 (m, 2H), 3.65 (s, 1H), 3.24-3.40 (m, 2H), 2.26-2.40 (m, 1H), 1.85-2.10 (m, 1H), 1.36 (s, 3H), 1.34 (t, $J = 7.2$, 3H), 1.33 (s, 3H). $^{13}\text{C}\{^1\text{H}\}$ NMR (CDCl_3 , 125 MHz): δ 165.1 (C), 75.0 (CH_2), 62.5 (CH), 52.6 (CH_2), 40.9 (CH_2), 36.2 (CH), 29.3 (CH_3), 24.5 (CH_3), 14.7 (CH_3). HRMS (ESI) calcd for $\text{C}_9\text{H}_{17}\text{O}_4\text{S}$ [M+H] 221.0862, found 221.0847.

CHAPTER 3

ENANTIOSELECTIVE RHODIUM-CATALYZED INTRAMOLECULAR C–H INSERTION ON DIAZOSULFONES

3.1 Introduction

The factors, which determine the regioselectivity of rhodium-catalyzed intramolecular C–H insertion reactions on diazosulfones, have been disclosed by Jungong and co-workers¹²⁴ and are discussed in the previous chapter. However, the enantioselective version of these transformations remains largely unexplored. To date, there is only a single report on enantioselective intramolecular C–H insertion on diazosulfones published in 2009 by Maguire and co-workers.¹²⁶ In this report, chiral copper *bis*-oxazoline catalysts have been employed for C–H insertion reactions on diazosulfones to afford *cis*-thiopyrans in moderate yields (21-68%) but excellent enantioselectivities (85-98%) (Table 9)

Table 9. Enantioselective intramolecular copper-catalyzed C–H insertion reactions of diazosulfones reported by Maguire and co-workers.¹²⁶

S	R	R ₁	Yield (%)	ee (%)
163	OMe	Ph	47	98
164	OMe	4-tolyl	64	96
165	OMe	4-anisole	56	91
166	OMe	4-nitrophenyl	-	-
167	OMe	benzyl	42	96
168	OMe	ethyl	68	97
169	OBn	octyl	66	90
170	OBn	octyl	21	70
171	Me	Ph	30	85
172	Ph	Ph	49	97

Enantioselective rhodium-catalyzed intramolecular C–H insertion reactions have been performed on diazocarbonyl substrates using chiral rhodium catalysts.^{51, 98, 127, 128} Most of these catalysts are derived by simple ligand displacement reactions from rhodium(II) tetraacetate. Prior to the advent of chiral rhodium catalysts, control of

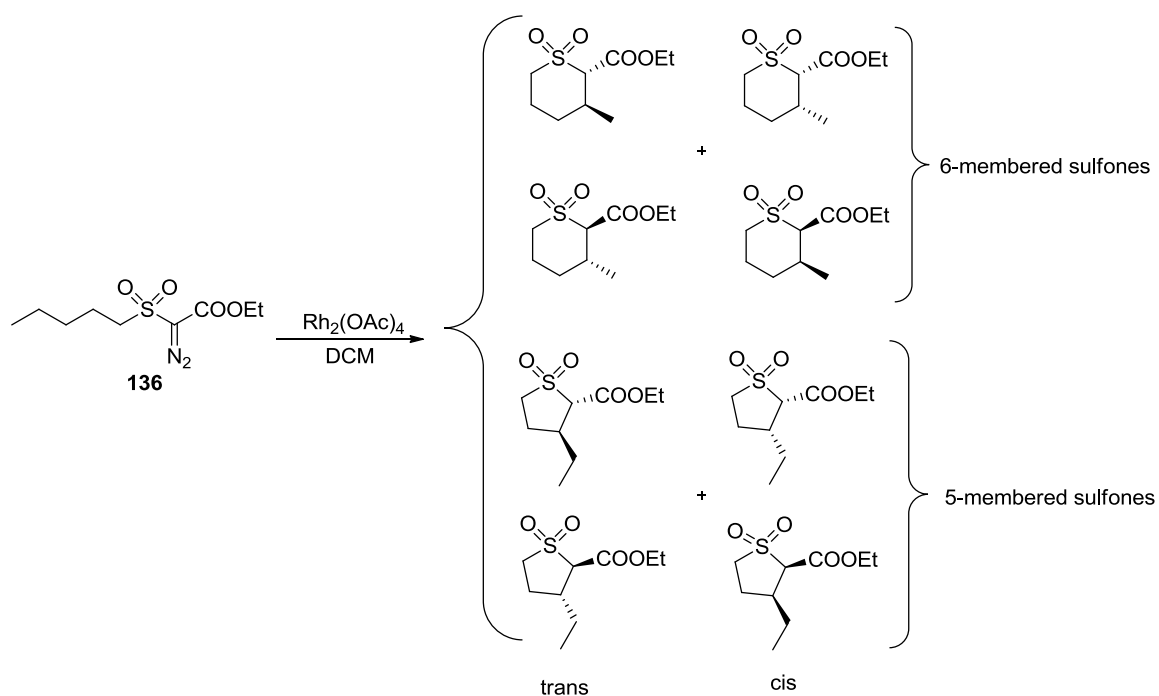
diastereoselectivity in intramolecular C–H insertion reactions had been attained by using chiral diazocarbonyl compounds, which favored 1,2- and 1,3-asymmetric inductions.¹²⁹

¹³⁰ For fused ring systems, asymmetric induction has been observed by exploiting the preferential insertion into equatorial over axial C–H bonds.¹³¹ The groups of Taber¹²⁸ and Wee¹³² have also demonstrated the use of chiral auxiliaries to control diastereoselectivity in rhodium-catalyzed intramolecular C–H insertion reactions.

Enantioselective rhodium-catalyzed intramolecular C–H insertion on diazosulfones has not yet been reported. This prompted further investigation into the feasibility of controlling diastereoselectivity during the rhodium-catalyzed intramolecular C–H insertion event on diazosulfones. For this study, diazosulfone **136** was used as the model substrate for C–H insertion. Several chiral rhodium catalysts were screened, aiming to optimize the yield and enantioselectivity of the transformation.

3.2 Results and Discussion

Jungong and co-workers¹²⁴ have demonstrated that intramolecular C–H insertion on diazosulfone **136** using achiral dirhodium catalyst Rh₂(OAc)₄ **14** would result to the formation of eight possible diastereomers: four six-membered ring sulfones and four five-membered ring sulfones (Scheme 27). The four diastereomers for each class of sulfones (six- or five-membered) comprise of two trans enantiomers (*R,R* and *S,S*) and two cis enantiomers (*R,S* and *S,R*), and the trans enantiomers were isolated as major products over the cis enantiomers.

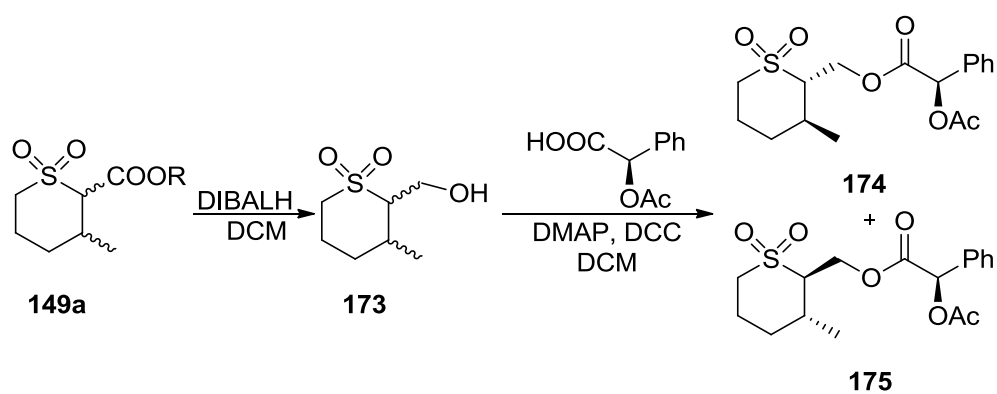


Scheme 27. Formation of six- and five-membered sulfones by intramolecular C–H insertion reported by Jungong and co-workers.¹²⁴

The formation of eight possible diastereomers greatly limits the synthetic utility of this transformation, mandating the need to establish reaction conditions that would favor the formation of a single diastereomer. To this end, the primary objective was to originate reaction conditions, which would allow the formation of just one six-membered enantiomer. The work reported by Jungong and co-workers identified diazosulfone **136** to preferentially favor the formation of six- over five-membered sulfones, which favored the decision to use it as the model substrate for these studies.

Efforts to effectively isolate and characterize the cis isomers turned out to be unexpectedly difficult, so the enantioselectivity was determined as an enantiomeric ratio

(er) between the trans enantiomers (*R,R* and *S,S*). The er for each reaction was deduced by subjecting the obtained six-membered sulfone trans isomers to a DIBALH reduction, followed by Steglich esterification of the resulting alcohol with (*S*)-acetylmandelic acid in the presence of DCC (*N,N'*-dicyclohexylcarbodiimide) and DMAP (4-dimethylaminopyridine) (Scheme 28).



Scheme 28. Synthesis of sulfonyl acetylmandalates for determination of enantiomeric ratio.

The crude reaction mixture was analyzed by ^1H NMR without prior purification to guarantee that the enantiomeric ratio remained undistorted. Two sets of peaks were used to assign enantiomeric ratios; the doublet peaks between 0.5-1 ppm corresponding to the methyl group next to the C–H insertion center, and the singlets between 5.8-6.5 ppm corresponding to the proton adjacent to the acetate moiety (Figure 7). The observed enantiomeric ratios were consistent for both peaks.

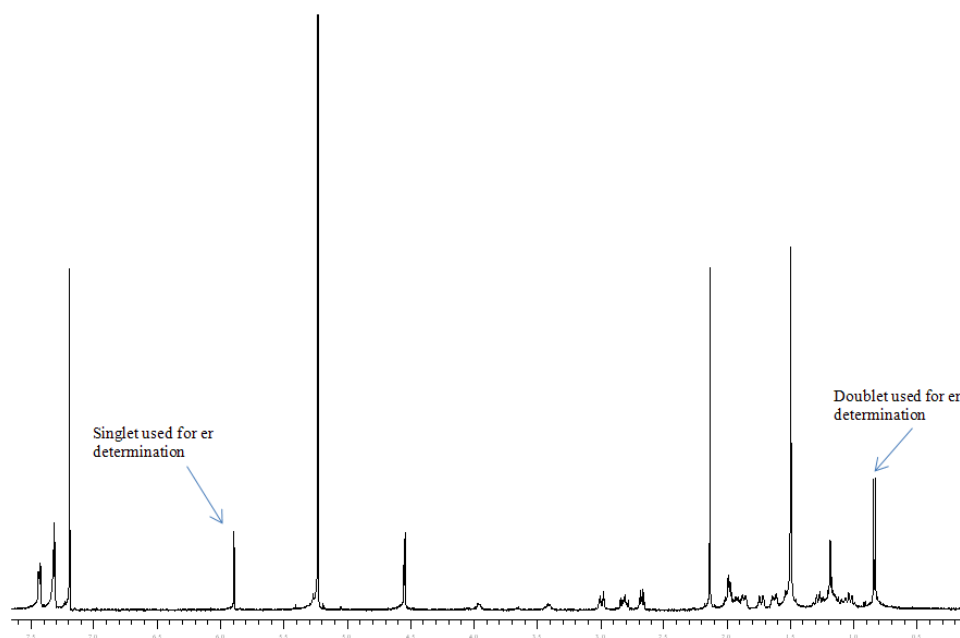


Figure 7. ^1H NMR spectrum of sulfonyl acetylmandalate showing peaks used for enantiomeric ratio determination.

The study was initiated by screening various chiral rhodium catalysts for this transformation (Figure 9). $\text{Rh}_2(\text{S-MEPY})_4$ **17** and $\text{Rh}_2(\text{S-DOSP})_4$ **15**, which have been very effective in other cases, showed poor results, providing moderate yields (45-55%), and poor enantioselectivity (1:1 to 1.2 :1 er) (Table 10).^{65, 133} Use of non-polar solvent (2,2-dimethylbutane) with **15** provided the first glimpse of selectivity (1.2 :1 er) (Table 10), although complications arose due to poor solubility of the diazo compound in this solvent. $\text{Rh}_2(\text{S-MEPY})_4$ was unreactive in DCM at room temperature, requiring reflux in the higher boiling solvent dichloroethane. Next, the class of catalysts derived from phthalimide-protected amino acids was explored, starting with $\text{Rh}_2(\text{S-pttl})_4$, derived from

tert-leucine. This provided the first encouraging result (2.5: 1 er). The additional bonus was the increased yield of the product (85%).



- 16** Rh₂(*S*-pttl)₄ (R = *t*-Bu; R₁ = H)
176 Rh₂(*S*-ptad)₄ (R = adamantyl; R₁ = H)
177 Rh₂(*S*-ptpa)₄ (R = Bn; R₁ = H)
178 Rh₂(*S*-tpttl)₄ (R = adamantyl; R₁ = *t*-Bu)

- 179** Rh₂(*S*-nttl)₄ (R = *t*-Bu)
180 Rh₂(*S*-nta)₄ (R = Me)
181 Rh₂(*S*-ntpa)₄ (R = Bn)

Figure 8. Chiral rhodium(II) carboxylate catalysts screened for enantioselective intramolecular C–H insertion.

Following this lead, it was logical to modify the backbone of Rh₂(*S*-pttl)₄ catalyst to ascertain what effect that would have on the outcome of the transformation. Increasing and decreasing the size of the substituents at the amino acid center would alter its catalytic pocket, which in turn will have an effect on the yield and the selectivity. Substituting *tert*-butyl group with a benzyl moiety (Rh₂(*S*-ptpa)₄) **177** decreased the yield and selectivity to 70% and 2:1, respectively. However, introduction of the bulky adamantyl group (Rh₂(*S*-ptad)₄) **176** at the same position improved the yield to 90% but at the detriment of the enantioselectivity which dropped to 2:1 er. Surprisingly, increasing the size of the phthaloyl group by introducing a *tert*-butyl group at the 4-position (Rh₂(*S*-tpttl)₄) **178**, slightly raised the yield to 88% but reversed the enantioselectivity to 1:2 er. When the phthaloyl substituent was replaced by the bulkier

N-naphthaloyl group (Rh₂(*S*-nttl)₄) **179**, the yield was maintained at 88%, while the enantioselectivity remained unreversed, but dropped slightly to 2.3:1 er. Maintaining the *N*-naphthaloyl group and replacing the *tert*-butyl group with a benzyl group Rh₂(*S*-ntpa)₄ **181**, held the yield at 87% but further dropped the enantioselectivity to 2:1 er. On the other hand, the use of Rh₂(*S*-nta)₄ **180**, where the *N*-naphthaloyl group is maintained, but the size of the *tert*-butyl group is decreased to a methyl group, dropped the enantioselectivity even further to 1.8:1 er, even though the yield remained at 87%. Because all modifications failed to increase the enantioselectivity compared to Rh₂(*S*-pttl)₄, it was used as the model catalyst for investigating optimal reaction conditions.

Table 10. Effect of chiral rhodium(II) carboxylate catalyst on the enantioselectivity of intramolecular C–H insertion on diazosulfones.

Entry	Rh ₂ L ₄ , conditions	Yield (%)	er
1	Rh ₂ (<i>S</i> -MEPY) ₄ , 80 °C, (CH ₂ Cl) ₂	55	1:1
2	Rh ₂ (<i>S</i> -DOSP) ₄ , rt, DCM	50	1.05:1
3	Rh ₂ (<i>S</i> -DOSP) ₄ , rt, 2,2-dimethylbutane	45	1.2:1
4	Rh ₂ (<i>S</i> -pttl) ₄ , rt, DCM	85	2.5:1
5	Rh ₂ (<i>S</i> -ptad) ₄ , rt, DCM	90	2:1
6	Rh ₂ (<i>S</i> -ptpa) ₄ , rt, DCM	70	2:1

Table 10. Cont.

	Rh ₂ L ₄ , conditions	Yield (%)	er
7	Rh ₂ (<i>S</i> -nttl) ₄ , rt, DCM	88	2.3:1
8	Rh ₂ (<i>S</i> -ntpa) ₄ , rt, DCM	86	2:1
9	Rh ₂ (<i>S</i> -nta) ₄ , rt, DCM	87	1.8:1

Enantioselective rhodium-catalyzed intramolecular C–H insertion reactions on diazocarbonyl compounds have been shown to afford better selectivities when carried out at lower temperatures.^{51, 134} In this light, the reaction temperature was decreased to 0 °C, then to -20 °C, maintaining DCM as the solvent. In both cases, the enantioselectivity was increased to 3:1 er but at the detriment to the yield which dropped to 65% and 61%, respectively. The reason appears to be the lack of decomposition of the diazosulfone at temperatures significantly below 0 °C. Switching the solvent to toluene at room temperature also raised the enantioselectivity to 3:1 er but reduced the yield to 78%.

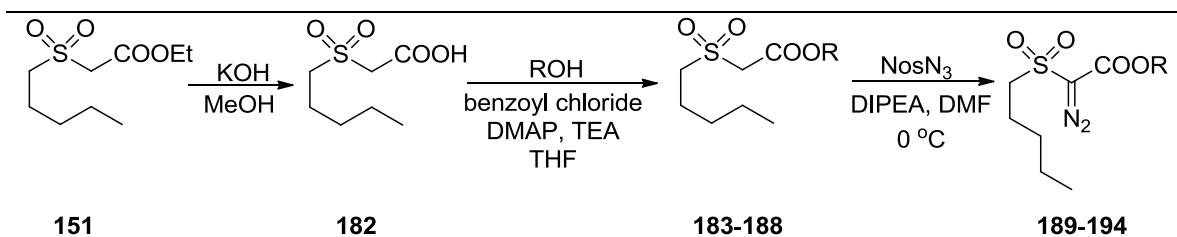
Table 11. Effect of temperature and solvent on the enantioselectivity of rhodium-catalyzed intramolecular C–H insertion of diazosulfones.

Reaction scheme: **136** (diazo sulfone) $\xrightarrow[\text{DCM}]{\text{Rh}_2(\text{S-pttl})_4}$ **149a** (sulfone)

Entry	Conditions	Yield (%)	er
1	Rh ₂ (S-pttl) ₄ , 0 °C, DCM	65	3:1
2	Rh ₂ (S-pttl) ₄ , -20 °C, DCM	61	3:1
3	Rh ₂ (S-pttl) ₄ , rt, toluene	78	3:1

The next phase of the study was to investigate the effect of the structure of diazosulfone **136** on the enantioselectivity and yield (Table 12). This entailed maintaining the catalyst as Rh₂(S-pttl)₄, while modifying the ester substituent. The necessary diazo substrates were prepared as previously described. Several transesterification conditions were tested to transform sulfone **151** to the desired sulfone esters, but were not effective. However, base-catalyzed hydrolysis of **151** using potassium hydroxide in methanol furnished sulfone acid **182**. The resulting acid **182** was then coupled to various alcohols by employing Yamaguchi esterification conditions in the presence of DMAP, benzoyl chloride and TEA (triethylamine). The obtained sulfone esters were subjected to diazo transfer conditions (NosN₃, DIPEA, DMF) to provide the desired diazosulfones, which were treated with Rh₂(S-pttl)₄ in DCM at rt.

Table 12. Preparation of diazosulfonyl acetates.



R	Sulfone	diazosulfone	Yield of sulfone (%)	Yield of diazosulfone (%)
Me	183	189	90	91
<i>i</i> -Pr	184	190	85	88
<i>t</i> -Bu	185	191	87	90
(+)-menthyl	186	192	90	92
(-)-menthyl	187	193	87	80
CH(<i>i</i> -Pr) ₂	188	194	86	94

Decreasing (methyl) or increasing (isopropyl, *tert*-butyl, and diisopropyl) the size of the ester substituent had no significant effect on the yield and selectivity. Notably, the selectivity dropped to 2:1 or when the ester substituent become even bulkier (diisopropyl).

Table 13. Effect of diazosulfone substrates on the enantioselectivity of rhodium-catalyzed intramolecular C–H insertion.

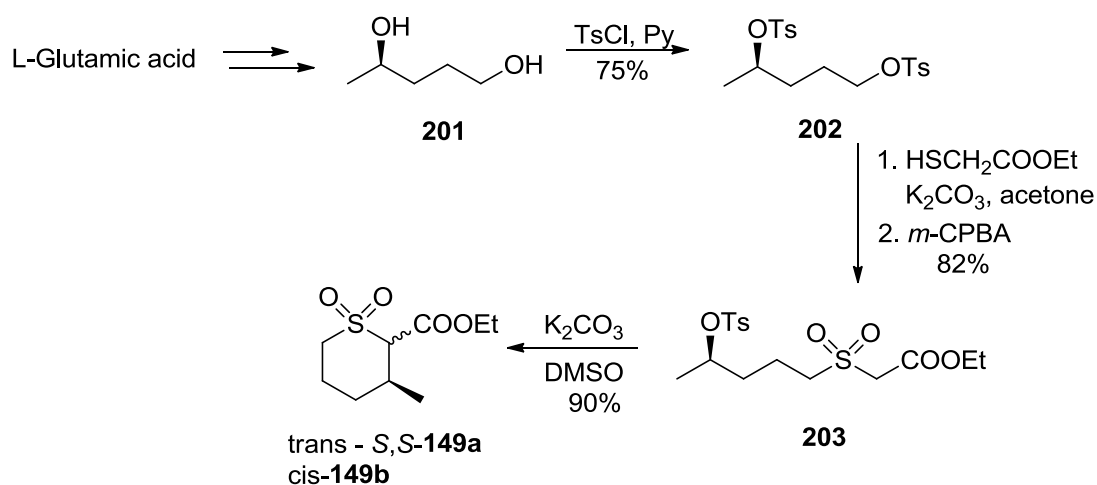
$$\text{189-194} \xrightarrow{\text{Rh}_2\text{L}_4} \text{195-200}$$

Entry	R	Product	Rh ₂ L ₄	Yield (%)	er
1	Me	195	Rh ₂ (<i>S</i> -pttl) ₄ , rt, DCM	85	2.5:1
2	<i>i</i> -Pr	196	Rh ₂ (<i>S</i> -pttl) ₄ , rt, DCM	81	2.2:1
3	<i>t</i> -Bu	197	Rh ₂ (<i>S</i> -pttl) ₄ , rt, DCM	32 (82)*	2.5:1
4	(+)-menthyl	198	Rh ₂ (<i>S</i> -pttl) ₄ , rt, DCM	82	1:2
5	(-)-menthyl	199	Rh ₂ (<i>S</i> -pttl) ₄ , rt, DCM	94	20:1
6	(-)-menthyl	199	Rh ₂ (OAc) ₄ , rt, DCM	70	1:1
7	CH(<i>i</i> -Pr) ₂	200	Rh ₂ (<i>S</i> -pttl) ₄ , rt, DCM	83	2:1

*Partial de-*tert*-butylation appeared to happen during the reaction.

The introduction of a chiral ester substituent, (-)-menthyl, amplified both the yield and enantioselectivity to 94% and 20:1 er, respectively. Unexpectedly, the use of Rh₂(OAc)₄ with the chiral menthyl diazosulfone decreased the yield to 60%, with no selectivity (1:1 er). The use of (+)-menthyl reversed the enantioselectivity towards the other enantiomer, but decreased the ratio to 1:2 er. This confirms that the (-)-menthyl group acts as a directing chiral auxiliary and not a bulky group, and the observed selectivity of 20:1 is a synergic cooperative effect.

To ascertain the absolute configuration of the obtained C–H insertion products, sulfone **149** was synthesized in enantiopure fashion by an independent method (Scheme 29). Enantiopure (*R*)-pentane-1,4-diol **201** was obtained as described from L-glutamic acid¹³⁵ and converted to ditosylate. Selective substitution of the primary tosylate with ethyl thioglycolate followed by oxidation yielded sulfone. Its treatment with a base in DMSO gave **149** via intramolecular S_N2 substitution, along with a cis isomer. The configuration of the product was assigned to be 2*S*,3*S*, assuming inversion in the course of substitution. The optical rotation of the alcohol, obtained upon reduction of this product, along with NMR analysis of its acetylmandalate indicated that it is the enantiomer of the material obtained by reduction of **199**.



Scheme 29. Synthesis of enantiopure sulfone **149**.

3.3 Experimental Section for Enantioselective Rhodium-Catalyzed Intramolecular C–H Insertion on Diazosulfones

All reactions were carried out under an inert nitrogen atmosphere unless otherwise stated. All reagents were used as purchased without further purification unless otherwise stated. ^1H -NMR (500 Hz) and $^{13}\text{C}\{^1\text{H}\}$ NMR (125 Hz) spectra were recorded on an Avance 500 Bruker spectrometer and calibrated using residual undeuterated solvent as internal references. Coupling constants are given in Hz. IR spectra were recorded on a Perkin-Elmer Spectrum 400 Series FTIR spectrometer. Specific rotations were measured on an AUTOPOL III automatic polarimeter in anhydrous CHCl_3 using a 10 cm cell. HRMS data were obtained on an Agilent 61969A TOF high resolution mass spectrometer using electrospray ionization (ESI). Melting points were determined on a MEL-TEMP melting point apparatus. Analytical TLC was performed using silica gel pre-coated TLC plates (E. Merck no. 5715-7). Flash chromatography was performed using 40-63 μm silica gel (Merck, Geduran, no. 11567-1) as the stationary phase. Tetrahydrofuran (THF) was dried by distilling it from sodium and benzophenone in a continuous still under a nitrogen atmosphere. Chloroform, dichloromethane and triethylamine were distilled from calcium hydride under an atmosphere of nitrogen.

Preparation of (pentylsulfonyl)acetic acid (182)

To a solution of ethyl (pentylsulfonyl)acetate (720 mg, 3.24 mmol), dissolved in MeOH (8 mL), was added KOH (85%, 250 mg, 3.80 mmol), dissolved in MeOH (8 mL), at rt. The resulting solution was then stirred for 3 h, after which the reaction was complete as indicated by TLC analysis. The reaction mixture was concentrated under

reduced pressure, diluted with water (20 mL), washed with dichloromethane (3 × 10 mL), diluted with 20 mL of 1N HCl solution, and extracted with ethyl acetate (3 × 20 mL). The ethyl acetate extract was washed with brine, dried over anhydrous Na₂SO₄ and evaporated under reduced pressure to afford **178** (570 mg, 91%) as a white crystalline powder that was used without further purification.

(Pentylsulfonyl)acetic acid (182): m.p. 78-79 °C. ¹H NMR (CDCl₃, 500 MHz): δ 9.20 (br s, 1H), 4.04 (s, 2H), 3.26-3.31 (m, 2H), 1.85-1.93 (m, 2H), 1.35-1.50 (m, 4H), 0.94 (t, *J* = 7.3, 3H). ¹³C{¹H} NMR (CDCl₃, 125 MHz): δ 170.0 (C), 57.3 (CH₂), 54.0 (CH₂), 30.6 (CH₂), 22.3 (CH₂), 21.7 (CH₂), 13.9 (CH₃). HRMS (ESI) calcd for C₁₇H₁₈O₄NS [M+NH₄]⁺ 212.0956, found 212.0983.

General procedure for preparation of sulfonylacetates (183-188)

(Pentylsulfonyl)acetic acid (**182**, 1 equiv.), benzoyl chloride (1 equiv.) and THF (2.5 mL/mmol) were charged to a round bottom flask, equipped with a magnetic stirrer. To the resulting solution Et₃N (2 equiv.) was added slowly, followed by the corresponding alcohol (1 equiv.), and DMAP (0.25 equiv.). The obtained mixture was stirred at rt for 6 h (TLC analysis revealed the reaction was complete). The reaction mixture was diluted with EtOAc (40 mL) and washed with water (3 × 30 mL). The organic phase was further washed with brine, dried over anhydrous Na₂SO₄ and

evaporated under reduced pressure to afford the crude product that was purified by flash chromatography on a silica gel column using EtOAc-hexanes (0:1 to 1:9).

Methyl (pentylsulfonyl)acetate (183): ^1H NMR (CDCl_3 , 500 MHz): δ 3.96 (s, 2H), 3.83 (s, 3H), 3.22-3.27 (m, 2H), 1.83-1.91 (m, 2H), 1.34-1.48 (m, 4H), 0.93 (t, $J = 7$, 3H).

$^{13}\text{C}\{^1\text{H}\}$ NMR (CDCl_3 , 125 MHz): δ 163.8 (C), 57.4 (CH_2), 53.7 (CH_2), 53.5 (CH_3), 30.6 (CH_2), 22.3 (CH_2), 21.7 (CH_2), 13.9 (CH_3). HRMS (ESI) calcd for $\text{C}_8\text{H}_{17}\text{O}_4\text{S}$ [$\text{M}+\text{H}$] $^+$ 209.0842, found 209.0848.

Isopropyl (pentylsulfonyl)acetate (184): ^1H NMR (CDCl_3 , 500 MHz): δ 5.11 (septet, $J = 6.5$, 1H), 3.91 (s, 2H), 3.22-3.27 (m, 2H), 1.84-1.92 (m, 2H), 1.34-1.48 (m, 4H), 1.31 (d, $J = 6.5$, 6H), 0.93 (t, $J = 7$, 3H). $^{13}\text{C}\{^1\text{H}\}$ NMR (CDCl_3 , 125 MHz): δ 162.8 (C), 70.9 (CH), 57.8 (CH_2), 53.7 (CH_2), 30.6 (CH_2), 22.3 (CH_2), 21.7 (CH_2), 21.8 (CH_3), 13.9 (CH_3). HRMS (ESI) calcd for $\text{C}_{10}\text{H}_{21}\text{O}_4\text{S}$ [$\text{M}+\text{H}$] $^+$ 237.1160, found 237.1158.

***t*-Butyl (pentylsulfonyl)acetate (185):** ^1H NMR (CDCl_3 , 500 MHz): δ 3.86 (s, 2H), 3.21-3.25 (m, 2H), 1.83-1.90 (m, 2H), 1.51 (s, 9H), 1.33-1.48 (m, 4H), 0.92 (t, $J = 7$, 3H). $^{13}\text{C}\{^1\text{H}\}$ NMR (CDCl_3 , 125 MHz): δ 162.3 (C), 84.3 (C), 58.6 (CH_2), 53.6 (CH_2), 30.6 (CH_2), 28.0 (CH_3), 22.3 (CH_2), 21.8 (CH_2), 13.9 (CH_3). HRMS (ESI) calcd for $\text{C}_{11}\text{H}_{26}\text{O}_4\text{NS}$ [$\text{M}+\text{NH}_4$] $^+$ 268.1582, found 268.1588.

2,4-Dimethyl-3-pentyl (pentylsulfonyl)acetate (186): ^1H NMR (CDCl_3 , 500 MHz): δ 4.69 (t, $J = 6$, 1H), 3.97 (s, 2H), 3.24-3.28 (m, 2H), 1.84-2.00 (m, 4H), 1.33-1.48 (m, 4H), 0.92 (t, $J = 7.5$, 3H), 0.91 (t, $J = 6$, 12H). $^{13}\text{C}\{^1\text{H}\}$ NMR (CDCl_3 , 125 MHz): δ 163.4 (C), 86.2 (CH), 57.5 (CH_2), 53.7 (CH_2), 30.6 (CH_2), 29.6 (CH), 22.3 (CH_2), 21.9 (CH_2), 19.6 (CH_3), 17.3 (CH_3), 13.9 (CH_3). HRMS (ESI) calcd for $\text{C}_{14}\text{H}_{32}\text{NO}_4\text{S}$ $[\text{M}+\text{NH}_4]^+$ 310.2052, found 310.2054.

(1R,2S,5R)-2-Isopropyl-5-methylcyclohexyl (pentylsulfonyl)acetate (187): $[\alpha]_{\text{D}}^{20} = -45.9^\circ$ (c 3.5, CHCl_3). ^1H NMR (CDCl_3 , 500 MHz): δ 4.79 (td, $J = 11, 4.5$, 1H), 3.93 (s, 2H), 3.20-3.29 (m, 2H), 2.01-2.07 (m, 1H), 1.84-1.96 (m, 3H), 1.68-1.74 (m, 2H), 1.34-1.55 (m, 6H), 1.02-1.12 (m, 2H), 0.85-0.96 (m, 10H), 0.77 (d, $J = 7$, 3H). $^{13}\text{C}\{^1\text{H}\}$ NMR (CDCl_3 , 125 MHz): δ 163.0 (C), 77.4 (CH), 57.9 (CH_2), 53.8 (CH_2), 47.0 (CH), 40.7 (CH_2), 34.3 (CH_2), 31.7 (CH), 30.7 (CH_2), 26.3 (CH), 23.4 (CH_2), 22.3 (CH_3), 22.1 (CH_2), 21.8 (CH_3), 20.9 (CH_3), 16.2 (CH_3), 13.9 (CH_3). HRMS (ESI) calcd for $\text{C}_{17}\text{H}_{36}\text{NO}_4\text{S}$ $[\text{M}+\text{NH}_4]^+$ 350.2365, found 350.2350.

(1S,2R,5S)-2-Isopropyl-5-methylcyclohexyl (pentylsulfonyl)acetate (188) (enantiomer of **187**, from (+)-menthol): Spectral data were identical to **187**. $[\alpha]_{\text{D}}^{20} = +45.7^\circ$ (c 3.1, CHCl_3).

General procedure for preparation of sulfonyldiazoacetates (189-194)

The corresponding alkyl (pentylsulfonyl)acetate (1 equiv.) was dissolved in THF (2.5 mL/mmol) and cooled to -45 °C. Mesityl azide (2.5 equiv.) was added, followed by dropwise addition of 1.5 equiv. of DBU. The reaction mixture was stirred for 1 h, maintaining the temperature at -45 °C, after which it was warmed up to rt over a 15-20 min interval. The obtained mixture was poured over 20 mL of a half-saturated (NH₄)₂SO₄ solution, extracted with DCM (3 × 20 mL), dried over anhydrous Na₂SO₄ and concentrated under reduced pressure to afford the crude product that was purified by flash chromatography on a silica gel column using EtOAc-hexanes (0:1 to 1:9).

Note: The diazo carbon does not appear in the ¹³C{¹H} NMR spectra of all diazo compounds. IR spectra show a strong diazo stretch at ~ 2130 cm⁻¹.

Methyl (pentylsulfonyl)diazoacetate (189): ¹H NMR (CDCl₃, 500 MHz): δ 3.87 (s, 3H), 3.35-3.40 (m, 2H), 1.80-1.87 (m, 2H), 1.32-1.46 (m, 4H), 0.92 (t, *J* = 7, 3H). ¹³C{¹H} NMR (CDCl₃, 125 MHz): δ 160.7 (C), 56.8 (CH₂), 53.3 (CH₃), 30.3 (CH₂), 22.5 (CH₂), 22.3 (CH₂), 13.9 (CH₃). IR (CH₂Cl₂, cm⁻¹): 2132, 1719, 1338, 1147.

Isopropyl (pentylsulfonyl)diazoacetate (190): ¹H NMR (CDCl₃, 500 MHz): δ 5.18 (septet, *J* = 6.5, 1H), 3.35-3.41 (m, 2H), 1.80-1.87 (m, 2H), 1.32-1.46 (m, 4H), 1.32 (d, *J* = 6.5, 6H), 0.91 (t, *J* = 7, 3H). ¹³C{¹H} NMR (CDCl₃, 125 MHz): δ 159.9 (C), 71.0 (CH), 56.7 (CH₂), 30.3 (CH₂), 22.5 (CH₂), 22.3 (CH₂), 22.0 (CH₃), 13.9 (CH₃). IR (CH₂Cl₂, cm⁻¹): 2131, 1710, 1341, 1147.

***t*-Butyl (pentylsulfonyl)diazoacetate (191):** ^1H NMR (CDCl_3 , 500 MHz): δ 3.34-3.39 (m, 2H), 1.80-1.87 (m, 2H), 1.54 (s, 9H), 1.33-1.47 (m, 4H), 0.93 (t, $J = 7$, 3H). $^{13}\text{C}\{^1\text{H}\}$ NMR (CDCl_3 , 125 MHz): δ 159.4 (C), 85.1 (C), 56.6 (CH_2), 30.3 (CH_2), 28.5 (CH_3), 22.6 (CH_2), 22.3 (CH_2), 13.9 (CH_3). IR (CH_2Cl_2 , cm^{-1}): 2128, 1708, 1338, 1146.

2,4-Dimethyl-3-pentyl (pentylsulfonyl)diazoacetate (192): ^1H NMR (CDCl_3 , 500 MHz): δ 4.75 (t, $J = 6$, 1H), 3.35-3.40 (m, 2H), 1.93-2.01 (m, 2H), 1.79-1.87 (m, 2H), 1.32-1.46 (m, 4H), 0.89-0.94 (m, 15H). $^{13}\text{C}\{^1\text{H}\}$ NMR (CDCl_3 , 125 MHz): δ 160.6 (C), 86.2 (CH), 56.7 (CH_2), 30.3 (CH_2), 29.7 (CH), 22.8 (CH_2), 22.3 (CH_2), 19.7 (CH_3), 17.4 (CH_3), 13.9 (CH_3). IR (CH_2Cl_2 , cm^{-1}): 2130, 1709, 1338, 1147.

(1*R*,2*S*,5*R*)-2-Isopropyl-5-methylcyclohexyl (pentylsulfonyl)diazoacetate (193): $[\alpha]_{\text{D}}^{20} = -56.5^\circ$ (c 2.1, CHCl_3). ^1H NMR (CDCl_3 , 500 MHz): δ 4.86 (td, $J = 11$, 4.5, 1H), 3.31-3.42 (m, 2H), 2.02-2.08 (m, 1H), 1.78-1.89 (m, 3H), 1.66-1.74 (m, 2H), 1.31-1.56 (m, 6H), 1.02-1.12 (m, 2H), 0.83-0.94 (m, 10H), 0.78 (d, $J = 7$, 3H). $^{13}\text{C}\{^1\text{H}\}$ NMR (CDCl_3 , 125 MHz): δ 160.0 (C), 77.3 (CH), 56.7 (CH_2), 47.2 (CH), 41.1 (CH_2), 34.2 (CH_2), 31.6 (CH), 30.3 (CH_2), 26.6 (CH), 23.6 (CH_2), 22.6 (CH_2), 22.3 (CH_2), 22.1 (CH_3), 20.9 (CH_3), 16.5 (CH_3), 13.9 (CH_3). IR (CH_2Cl_2 , cm^{-1}): 2131, 1705, 1336, 1146.

(1*S*,2*R*,5*S*)-2-Isopropyl-5-methylcyclohexyl (pentylsulfonyl)diazoacetate (194) (enantiomer of **193**, from (+)-menthol): Spectral data were identical to **193**. $[\alpha]_{\text{D}}^{20} = +54.7^\circ$ (c 3.5, CHCl_3).

General procedure for C-H insertion (195-200)

To the solution of Rh(II) catalyst (1 mol%) in CH₂Cl₂ (2.5 mL/mmol) was added the corresponding alkyl(pentylsulfonyl)diazoacetate (1 equiv.) dissolved in DCM (2.5 mL/mmol) over 2 h via a syringe pump. The resulting mixture was stirred at rt for 12 h after which the reaction was complete as indicated by TLC analysis. The reaction mixture was then evaporated under reduced pressure to afford the crude product that was purified by flash chromatography using EtOAc-hexanes.

***trans*-Ethyl 3-methyltetrahydro-2*H*-thiopyran-1,1-dioxide-2-carboxylate (149):** The data matched previously reported.

***trans*-Methyl 3-methyltetrahydro-2*H*-thiopyran-1,1-dioxide-2-carboxylate (195):** ¹H NMR (CDCl₃, 500 MHz): δ 3.86 (s, 3H), 3.58 (d, *J* = 11, 1H), 3.18 (dt, *J* = 14, 4, 1H), 2.88-2.96 (m, 1H), 2.52-2.62 (m, 1H), 2.09-2.23 (m, 2H), 1.94-2.01 (m, 1H), 1.23-1.33 (m, 1H), 1.07 (d, *J* = 7, 3H). ¹³C{¹H} NMR (CDCl₃, 125 MHz): δ 164.5 (C), 72.7 (CH), 53.4 (CH₃), 52.0 (CH₂), 34.5 (CH), 32.0 (CH₂), 22.9 (CH₂), 20.0 (CH₃). HRMS (ESI) calcd for C₈H₁₅O₄S [M+H]⁺ 207.0691, found 207.0668.

***trans*-Isopropyl 3-methyltetrahydro-2*H*-thiopyran-1,1-dioxide-2-carboxylate (196):** ¹H NMR (CDCl₃, 500 MHz): δ 5.18 (septet, *J* = 6.5, 1H), 3.52 (d, *J* = 11, 1H), 3.16 (dt, *J* = 14, 4, 1H), 2.86-2.94 (m, 1H), 2.51-2.61 (m, 1H), 2.08-2.23 (m, 2H), 1.93-1.99 (m, 1H), 1.33 (d, *J* = 6.5, 3H), 1.32 (d, *J* = 6.5, 3H), 1.23-1.30 (m, 1H), 1.08 (d, *J* = 6.5, 3H).

$^{13}\text{C}\{^1\text{H}\}$ NMR (CDCl_3 , 125 MHz): δ 163.5 (C), 72.9 (CH), 70.6 (CH), 52.0 (CH_2), 34.5 (CH), 32.0 (CH_2), 22.8 (CH_2), 21.9 (CH_3), 21.8 (CH_3), 19.8 (CH_3). HRMS (ESI) calcd for $\text{C}_{10}\text{H}_{22}\text{O}_4\text{NS}$ $[\text{M}+\text{NH}_4]^+$ 252.1269, found 252.1390.

***trans-t*-Butyl 3-methyltetrahydro-2*H*-thiopyran-1,1-dioxide-2-carboxylate (197):** ^1H NMR (CDCl_3 , 500 MHz): δ 3.44 (d, $J = 11$, 1H), 3.14 (dt, $J = 14$, 4, 1H), 2.84-2.92 (m, 1H), 2.46-2.56 (m, 1H), 2.06-2.21 (m, 2H), 1.90-1.97 (m, 1H), 1.53 (s, 9H), 1.20-1.30 (m, 1H), 1.08 (d, $J = 6$, 3H). $^{13}\text{C}\{^1\text{H}\}$ NMR (CDCl_3 , 125 MHz): δ 163.0 (C), 83.9 (C), 73.4 (CH), 52.0 (CH_2), 34.5 (CH), 32.0 (CH_2), 28.1 (CH_3), 22.9 (CH_2), 19.8 (CH_3). HRMS (ESI) calcd for $\text{C}_{11}\text{H}_{24}\text{O}_4\text{NS}$ $[\text{M}+\text{NH}_4]^+$ 266.1426, found 266.1383.

***trans*-2,4-Dimethyl-3-pentyl 3-methyltetrahydro-2*H*-thiopyran-1,1-dioxide-2-carboxylate (200):** ^1H NMR (CDCl_3 , 500 MHz): δ 4.75 (t, $J = 6$, 1H), 3.60 (d, $J = 11$, 1H), 3.16 (dt, $J = 14$, 4, 1H), 2.92 (td, $J = 13$, 4, 1H), 2.51-2.61 (m, 1H), 2.07- 2.23 (m, 2H), 1.91-2.01 (m, 3H), 1.23-1.33 (m, 1H), 1.10 (d, $J = 6$, 3H), 0.96 (d, $J = 7$, 3H), 0.96 (d, $J = 7$, 3H), 0.91 (t, $J = 7$, 6H). $^{13}\text{C}\{^1\text{H}\}$ NMR (CDCl_3 , 125 MHz): δ 164.1 (C), 86.1 (CH), 72.9 (CH), 52.1 (CH_2), 34.3 (CH), 32.1 (CH_2), 29.7 (CH), 29.5 (CH), 22.8 (CH_2), 20.3 (CH_3), 19.8 (CH_3), 17.7 (CH_3), 17.2 (CH_3). HRMS (ESI) calcd for $\text{C}_{14}\text{H}_{30}\text{NO}_4\text{S}$ $[\text{M}+\text{NH}_4]^+$ 308.1895, found 308.1877. Note: accidental equivalence of two methyls at 19.8.

(1*R*,2*S*,5*R*)-2-Isopropyl-5-methylcyclohexyl (2*R*,3*R*)-3-methyltetrahydro-2*H*-thiopyran-1,1-dioxide-2-carboxylate (199): $[\alpha]_D^{20} = -28.7^\circ$ (*c* 1.3, CHCl₃). ¹H NMR (CDCl₃, 500 MHz): δ 4.84 (td, *J* = 11, 4.5, 1H), 3.54 (d, *J* = 11, 1H), 3.15 (dt, *J* = 14, 4, 1H), 2.90 (td, *J* = 14, 4, 1H), 2.50-2.60 (m, 1H), 2.08-2.23 (m, 3H), 1.92-2.01 (m, 2H), 1.66-1.74 (m, 2H), 1.44-1.54 (m, 2H), 1.21-1.31 (m, 1H), 1.02-1.14 (m, 5H), 1.07 (d, *J* = 6.5), 0.84-0.95 (m, 7H), 0.92 (d, *J* = 6.5), 0.91 (d, *J* = 6.5), 0.77 (d, *J* = 7, 3H). ¹³C{¹H} NMR (CDCl₃, 125 MHz): δ 163.5 (C), 77.4 (CH), 73.1 (CH), 52.1 (CH₂), 46.9 (CH), 40.6 (CH₂), 34.4 (CH), 34.4 (CH₂), 32.1 (CH₂), 31.7 (CH), 26.2 (CH), 23.3 (CH₂), 22.9 (CH₂), 22.1 (CH₃), 21.0 (CH₃), 19.8 (CH₃), 16.1 (CH₃). HRMS (ESI) calcd for C₁₇H₃₄NO₄S [M+NH₄]⁺ 348.2208, found 348.2206.

For entries 4 and 6 in Table 13, inseparable mixtures of **199** and its diastereomer were obtained. They were directly reduced to alcohol **173** for determination of the ratio.

General procedure for the reduction of cyclized sulfonylacetates

To the corresponding thiopyran-1,1-dioxide carboxylate (1 equiv.) in DCM (2.5 mL/mmol) was added DIBALH (2.2 equiv.) and the resulting mixture stirred at rt for 12 h. The reaction was quenched with MeOH (0.7 mL). 10%-Solution of Rochelle salt (5 mL) was added and vigorously stirred for several hours, until solids disappeared. The water layer was extracted with DCM (3 × 5mL) and then EtOAc (5 mL). The combined organic extracts were washed with brine, dried over anhydrous Na₂SO₄ and concentrated

to afford a crude product that was purified by flash chromatography using EtOAc-hexanes (1:4 to 1:1).

***trans*-(3-methyltetrahydro-2*H*-thiopyran-1,1-dioxide-2-yl)methanol (173)**: m.p. 94-95 °C. ¹H NMR (CDCl₃, 500 MHz): δ 4.45 (dd, *J* = 13, 3.5, 1H), 4.00 (ddd, *J* = 5.5, 9, 14, 1H), 3.11 (dt, *J* = 14, 3.5, 1H), 2.90-2.98 (m, 1H), 2.60 (dd, *J* = 11.5, 5.5, 1H), 2.50 (dd, *J* = 9, 4.5, 1H), 2.34-2.44 (m, 1H), 2.06-2.19 (m, 2H), 1.92 (dd, *J* = 14.5, 3, 1H), 1.28-1.37 (m, 1H), 1.14 (d, *J* = 6.5, 3H). ¹³C{¹H} NMR (CDCl₃, 125 MHz): δ 68.4 (CH), 56.2 (CH₂), 52.2 (CH₂), 33.3 (CH₂), 31.8 (CH), 23.1 (CH₂), 19.1 (CH₃). HRMS (ESI) calcd for C₇H₁₅O₃S [M+H]⁺ 179.0741, found 179.0746.

(2*R*,3*R*)-(3-Methyltetrahydro-2*H*-thiopyran-1,1-dioxide-2-yl)methanol (*R,R*-173), obtained by reduction of **199**: [α]_D²⁰ = -16.7° (*c* 0.5, CHCl₃)

(2*S*,3*S*)-(3-Methyltetrahydro-2*H*-thiopyran-1,1-dioxide-2-yl)methanol (*S,S*-173), obtained by reduction of *S,S*-**194**: [α]_D²⁰ = +14.1° (*c* 0.4, CHCl₃)

Determination of enantiomeric ratio

An oven-dried round bottom flask, equipped with a magnetic stirrer, was charged with DCC (1.5 equiv.), (*S*)-acetylmandelic acid (1.5 equiv.), and DCM (2.5 mL/mmol). The resulting solution was stirred at rt for 30 min, after which alcohol **173** (1 equiv.) dissolved in DCM (2.5 mL/mmol) was added, followed by DMAP (0.5 equiv.). The

reaction mixture was stirred at rt for 8 h. The reaction mixture was taken up in EtOAc (50 mL), washed with 1N HCl solution (2 ×10 mL) and then with saturated NaHCO₃. The organic phase was further washed with brine, dried over anhydrous Na₂SO₄, and evaporated under reduced pressure to afford the crude product, which was used for ¹H NMR analysis without further purification to determine the diastereomeric ratio. The enantioselectivity or diastereoselectivity was measured by integration of the diastereomeric signals (CHCH₂-O-CO, CH₃-CH, Ph-CH(OAc)-CO) in ¹H NMR spectra of the acetylmandalates. It was shown that chromatographic purification of the product can be performed without affecting the ratio determined by NMR spectroscopy.

Preparation of (*R*)-1,4-bis(4-toluenesulfonyloxy)pentane (202)

To the solution of (*R*)-pentane-1,4-diol (**197**, 75 mg, 0.72 mmol), prepared as described from L-glutamic acid, in pyridine (1.8 mL) at 0 °C was added *p*-toluenesulfonyl chloride (345 mg, 1.80 mmol). The mixture was kept at 0 °C for 5 h, then warmed up to rt allowed to stand at this temperature for 20 h. The mixture was diluted with ethyl acetate, washed with 1N HCl solution, saturated aq. NaHCO₃ solution, brine, dried over MgSO₄ and concentrated under reduced pressure. The crude product was purified using flash chromatography to provide the pure ditosylate **198** (223 mg, 75%).

(*R*)-1,4-Bis(4-toluenesulfonyloxy)pentane (202): $[\alpha]_{\text{D}}^{20} = +15.1^{\circ}$ (*c* 2.3, CHCl₃). ¹H NMR (CDCl₃, 500 MHz): δ 7.76 (d, *J* = 8.5, 2H), 7.755 (d, *J* = 8, 2H), 7.35 (d, *J* = 8.5, 2H), 7.33 (d, *J* = 8.5, 2H), 4.57 (sextet, *J* = 6, 1H), 3.90-4.00 (m, 2H), 2.45 (s, 3H), 2.44

(s, 3H), 1.55-1.71 (m, 4H), 1.19 (d, $J = 6$, 3H). $^{13}\text{C}\{^1\text{H}\}$ NMR (CDCl_3 , 125 MHz): δ 145.1 (C), 144.9 (C), 134.4 (C), 133.1 (C), 130.1 (CH), 130.0 (CH), 128.0 (CH), 127.8 (CH), 79.3 (CH), 69.3 (CH_2), 32.6 (CH_2), 24.6 (CH_2), 21.8 (CH_3), 20.9 (CH_3). HRMS (ESI) calcd for $\text{C}_{19}\text{H}_{28}\text{NO}_6\text{S}_2$ $[\text{M}+\text{NH}_4]^+$ 430.1352, found 430.1301. Note: accidental equivalence of two methyls at 21.8 ppm.

Preparation of (*R*)-ethyl [4-(4-toluenesulfonyloxy)pentylsulfonyl]acetate (**203**)

Ditosylate **202** (18 mg, 0.040 mmol) and ethylthioglycolate (8 mg, 0.07 mmol) under nitrogen were dissolved in acetone (0.1 mL), and K_2CO_3 (10 mg, 0.07 mmol) was added. The reaction mixture was stirred at rt for 18 h, the solvent was removed under reduced pressure, and the residue was treated with water (5 mL) and ethyl acetate (10 mL). The layers were separated, the organic layer washed with brine, dried and concentrated. The crude was dissolved in CH_2Cl_2 (0.2 mL) and treated with *m*-CPBA (70%, 27 mg, 0.22 mmol), and left at rt for 20 h. After that time, the mixture was diluted with ethyl acetate, washed with NaHSO_3 , saturated aq. NaHCO_3 solution, brine, dried and concentrated. Chromatography provided **199** as a yellow oil (14 mg, 82%)

(*R*)-Ethyl [4-(4-toluenesulfonyloxy)pentylsulfonyl]acetate (203**):** $[\alpha]_{\text{D}}^{20} = +14.1^\circ$ (c 1.7, CHCl_3). ^1H NMR (CDCl_3 , 500 MHz): δ 7.80 (d, $J = 8.5$, 2H), 7.35 (d, $J = 8.5$, 2H), 4.62-4.70 (m, 1H), 4.27 (q, $J = 7$, 2H), 3.92 (s, 2H), 3.19-3.26 (m, 2H), 2.45 (s, 3H), 1.70-1.96 (m, 4H), 1.33 (t, $J = 7$, 3H), 1.26 (d, $J = 6.5$, 3H). $^{13}\text{C}\{^1\text{H}\}$ NMR (CDCl_3 , 125 MHz): δ 163.2 (C), 145.1 (C), 134.3 (C), 130.1 (CH), 127.9 (CH), 79.0 (CH), 63.0 (CH_2),

57.7 (CH₂), 53.0 (CH₂), 35.1 (CH₂), 21.9 (CH₃), 20.9 (CH₃), 17.9 (CH₂), 14.2 (CH₃).

HRMS (ESI) calcd for C₁₆H₂₈NO₇S₂ [M+NH₄]⁺ 410.1301, found 410.1315.

Preparation of (2*S*,3*S*)-ethyl 3-methyltetrahydro-2*H*-thiopyran-1,1-dioxide-2-carboxylate (149)

Sulfone **203** (35 mg, 0.089 mmol) was dissolved in DMSO (0.5 mL) under nitrogen atmosphere, and K₂CO₃ (18.5 mg, 0.134 mmol) was added. The mixture was vigorously stirred at rt for 24 h, then diluted with water (10 mL), and extracted with ethyl acetate (2 × 10 mL). The organic layer was washed with brine, dried over MgSO₄ and concentrated. Chromatography provided **149a** (12.7 g, 65%), along with the cis isomer, **149b** (5 mg, 25%). The spectral data for the compounds match previously reported.¹²²

(2*S*,3*S*)-Ethyl 3-methyltetrahydro-2*H*-thiopyran-1,1-dioxide-2-carboxylate (*S,S*-149a): $[\alpha]_{\text{D}}^{20} = +32.5^{\circ}$ (*c* 0.5, CHCl₃).

(2*R*,3*S*)-Ethyl 3-methyltetrahydro-2*H*-thiopyran-1,1-dioxide-2-carboxylate (149b):
 $[\alpha]_{\text{D}}^{20} = -36.8^{\circ}$ (*c* 0.3, CHCl₃)

CHAPTER 4

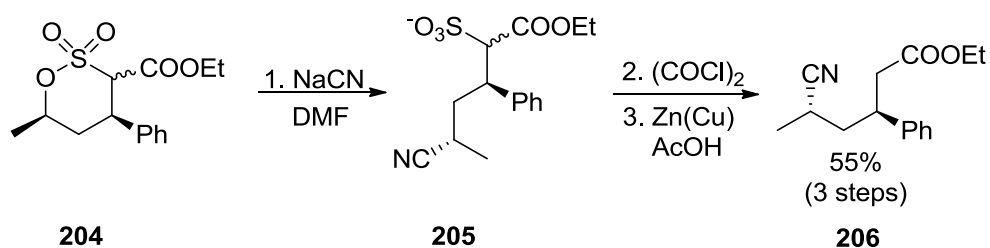
SYNTHETICALLY USEFUL TRANSFORMATIONS OF CYCLIC SIX-MEMBERED SULFONES AND SULFONATES OBTAINED BY RHODIUM-CATALYZED INTRAMOLECULAR C–H INSERTION

4.1 Introduction

Rhodium-catalyzed intramolecular C–H insertion on diazo carbonyl compounds has emerged as a powerful synthetic tool in the last three decades.^{14, 63} The potential of this reaction as a new C–C bond forming procedure, as well as its ability to streamline complex molecule synthesis are well documented.^{42, 82, 88, 136} As mentioned earlier, rhodium-catalyzed intramolecular C–H insertion on diazo carbonyl compounds occurs with overwhelming preference for five-membered carbocycles/heterocycles. This inherent preference can be overridden by factors such as substrate conformation, insertion site electronic effects and the reactivity of the rhodium catalyst. However, there is no standard procedure as to how these controlling factors can be fully explored. The extension of rhodium-catalyzed intramolecular C–H insertion to diazosulfones and diazosulfonates implicitly creates new avenues to employ C–H insertion in ways unattainable with diazo carbonyl compounds.

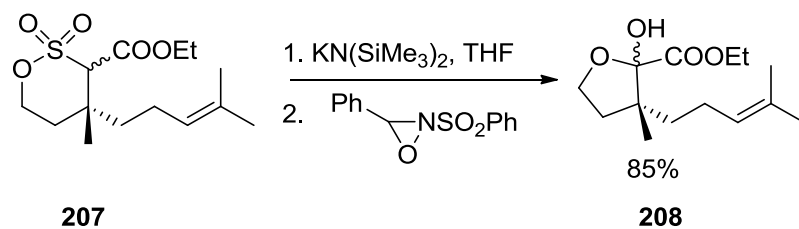
Jungong and co-workers¹²⁴ have elaborated on the formation of cyclic six-membered sulfones and sulfonates by means of rhodium-catalyzed intramolecular C–H

insertion. However, the chemistry of these novel cyclic six-membered compounds as synthetic precursors or intermediates remains largely unexplored. There is a small number of reports in the literature where cyclic six-membered sulfones and sulfonates have been converted into synthetically more relevant intermediates.¹²³ Notably, Du Bois and co-workers¹²³ have illustrated that the carbon–oxygen bond of cyclic six-membered ring sulfonates can be displaced with nucleophiles such as NaCN, NaN₃, NaOAc, and thiolates to form the corresponding sulfonate salts. Even though direct extrusion of SO₃ from the resulting salts under a variety of conditions proved futile, the salts were successfully transformed to acyclic esters in two steps (Scheme 30).



Scheme 30. Nucleophilic substitution reactions of δ -sulfones reported by Du Bois and co-workers.¹²³

Desulfonation of cyclic six-membered sulfonates under oxidative conditions to furnish five-membered lactols has also been observed by Du Bois and co-workers (Scheme 31).¹²³ The transformation is reported to involve an oxygen transfer followed by a (C–S) bond cleavage to generate an α -keto ester, which is trapped internally by the pending hydroxyl group.



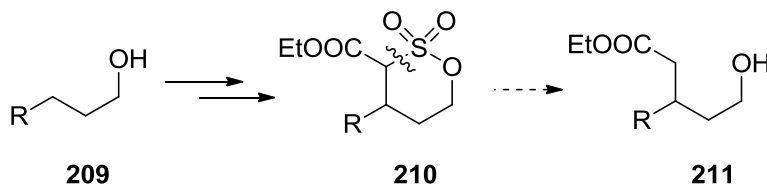
Scheme 31. Desulfonation of δ -sultones to form substituted lactols reported by Du Bois and co-workers.¹²³

The above examples depict six-membered cyclic sulfones and sulfonates as promising synthetic intermediates well-suited for complex molecule synthesis. This has provoked studies to explore synthetically meaningful transformations for these substrates, which would lead to precursors and intermediates of added value.

4.2 Results and Discussion

4.2.1 Direct Desulfonation of Cyclic Six-Membered Sulfonates (δ -Sultones) to δ -Valerolactones via Samarium Iodide Reduction

For δ -sultones, it was envisioned that direct desulfonation could be achieved by reductive cleavage of the C–S bond which would allow a “remote alkylation” at a γ -position relative to the hydroxyl group (Scheme 32).



Scheme 32. Remote alkylation of alcohols leading to the formation of 5-hydroxyesters.

Many examples of desulfonation have been demonstrated with α -arylsulfonyl esters.¹³⁷⁻¹³⁹ However, there is no such example for α -alkoxysulfonyl substituted esters. Seemingly, the aryl group on the sulfur atom is essential for this reaction, as δ -sultones did not react in the presence of known reagents for the reduction, such as Al/Hg,¹⁴⁰ Na/Hg,¹⁴¹ Mg-MeOH,¹³⁸ and SmI₂-MeOH.¹³⁷ Desulfonation of fluoroalkylsulfonyl oxindoles has been attained by using SmI₂ at prolonged reaction times.¹³⁹ In this light, Jungong and co-workers have uncovered that SmI₂ in combination with DMPU would react with δ -sultones to afford δ -valerolactones within three hours (Table 14).¹⁴²

Table 14. SmI₂ reduction of δ -sultones to form δ -valerolactones reported by Jungong and coworkers.¹⁴²

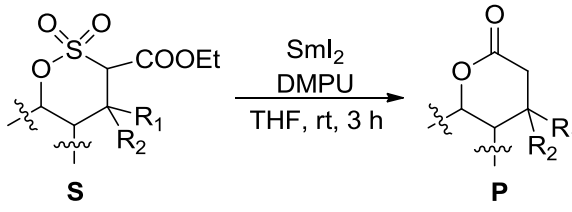
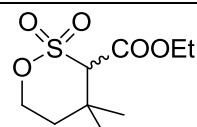
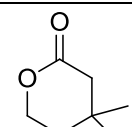
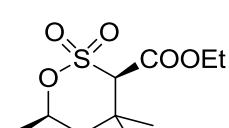
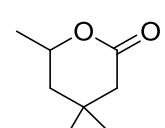
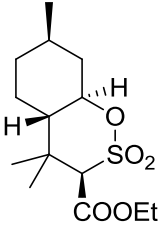
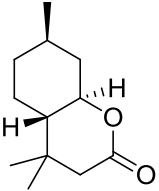
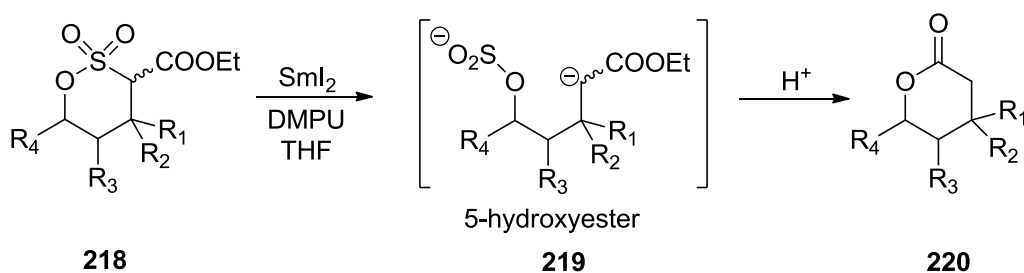
S	time	P	Yield (%)
			
 212	45 min	 215	47
 213	3 h	 216	45

Table 14. Cont.

S	time	P	Yield (%)
 214	3 h	 217	85

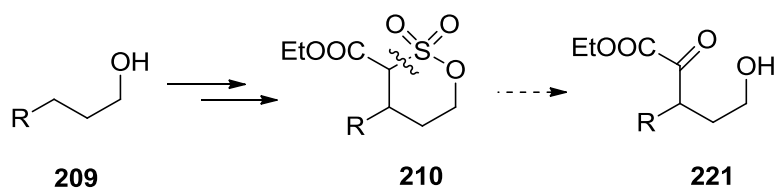
The replacement of DMPU with the relatively more toxic HMPA yielded similar results. The obtained δ -valerolactones are a consequence of the cyclization of the initially formed 5-hydroxyesters (Scheme 33). The 5-hydroxyesters are formed from the reduction of δ -sultones catalyzed by SmI_2/DMPU . The extrusion of SO_2 from these esters followed by cyclization furnishes the desired lactones. Apparently, the yields for lactones **215** and **216** are low because of the volatility of the products and a small scale of reaction. The reaction was found to be sensitive to the source of SmI_2 , as mixed success was observed with commercially available SmI_2 . However, the reaction was high yielding and worked reliably with SmI_2 prepared by the reaction of samarium metal with mercury iodide following a modification of the literature procedure for the preparation of SmCl_3 .¹⁴³



Scheme 33. Mechanism for SmI_2/DMPU reduction of δ -sultones to form δ -valerolactones.

4.2.2 Direct Desulfonation of Cyclic Six-Membered Sulfonates (δ -Sultones) to γ -Butyrolactones via *t*-Butyl Hydroxyperoxide (TBHP) Oxidation

According to literature reports,¹²³ the desulfonation of sulfonates has been examined under oxidative conditions to form lactols. It was reasoned that α -hydroxylation of δ -sultones would lead to the scission of the C–S bond, thereby permitting desulfonation and subsequent internal cyclization to 5-hydroxy-2-oxoester (Scheme 34).



Scheme 34. Oxidative desulfonation of δ -sultones to 5-hydroxy-2-oxoesters.

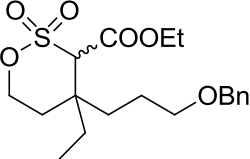
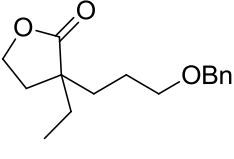
The α -hydroxylation was attained by oxidizing the corresponding enolates with TBHP (*t*-butyl hydroperoxide). While numerous bases (NaH , DBU , K_2CO_3 , KOH , *t*-

BuOLi, TEA, and NaHMDS) effect the formation of the enolates, subsequent oxidation and cyclization steps were unproductive. Eventually, TBHP in combination with *t*-BuOK or KHMDS allowed the formation of γ -butyrolactones (Table 15).

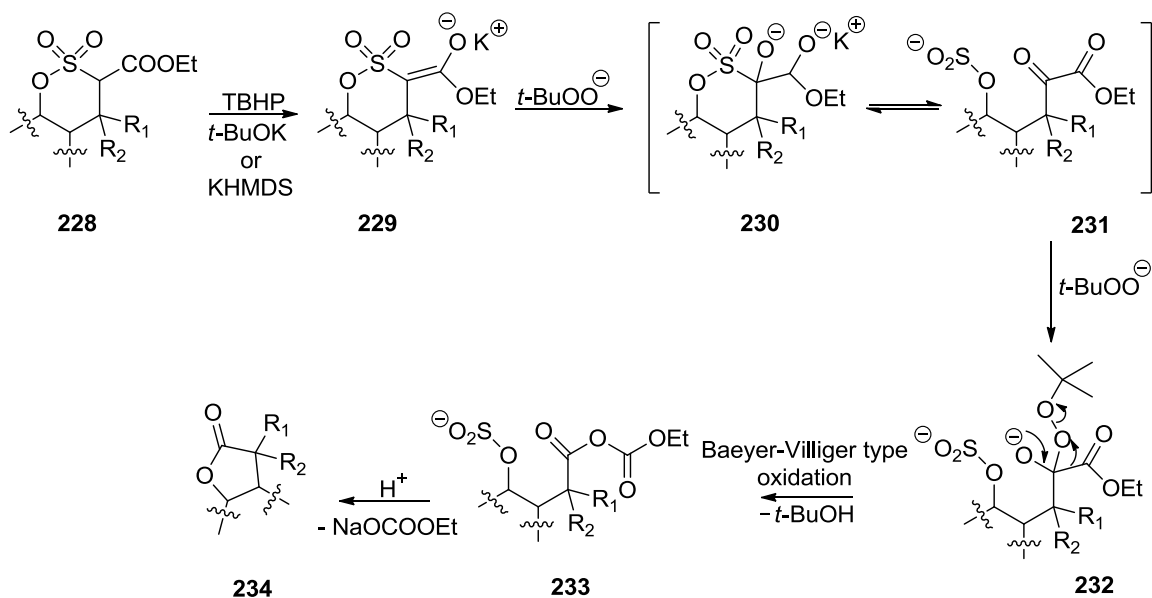
Table 15. TBHP oxidative desulfonation of δ -sulfones to γ -butyrolactones.

S	conditions	P	Yield (%)
 214	TBHP, <i>t</i> -BuOK, rt	 224	93
 222	TBHP, <i>t</i> -BuOK, rt	 225	85
 207	TBHP, KHMDS, rt	 226	70

Table 15. Cont.

S	conditions	P	Yield (%)
 223	TBHP, KHMDS, rt	 227	74

Even though δ -sultone esters in the presence of *t*-BuOK and KHMDS both form enolates, the transformations were found to be high yielding when *t*-BuOK was used to deprotonate δ -sultones derived from secondary alcohols and KHMDS for those derived from primary alcohols. Presumably, the reported γ -butyrolactones are obtained from the cyclization of the trapped 5-hydroxy-2-oxoesters (Scheme 35). Deprotonation of TBHP forms a *t*-butyl hydroperoxyl nucleophile, which reacts with the potassium enolate to form an alkoxide, which is eventually ring-opened, forcing the cleavage of the C–S bond to provide the 5-hydroxy-2-oxoester **227** that is further oxidized, presumably via a Baeyer-Villiger type of process, to form the mixed anhydride **233**. Anhydride **233** undergoes SO₂ extrusion followed by cyclization to yield the final lactone **234**.



Scheme 35. Mechanism of TBHP oxidative desulfonation of δ -sultones to γ -butyrolactones.

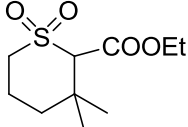
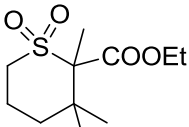
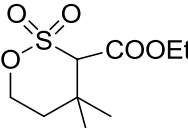
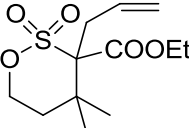
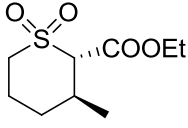
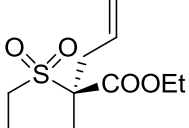
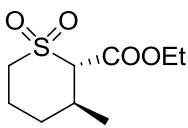
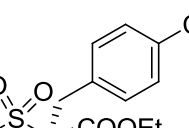
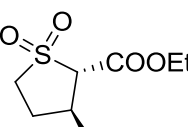
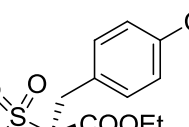
4.2.3 Alkylation of δ -Sultones and Carboethoxythiane-1,1-Dioxides

In general, δ -sultones and carboethoxythiane-1,1-dioxides are fairly strong C–H acids, which are configurationally stable in the absence of a base. Focusing on the C–H center adjacent to the SO_2 moiety, the alkylation of these compounds with active electrophiles under relatively mild conditions (NaH, alkylating agent, THF, rt, 16 h) was observed (Table 16). Interestingly, under these conditions, it was possible to selectively alkylate sultone **234**, although Du Bois and co-workers have demonstrated that δ -sultones can themselves act as electrophiles in nucleophilic substitutions. Also, high diastereoselectivity was witnessed in the alkylation of substrates **149a** and **155.2**.

Table 16. Alkylation of δ -sultones and carbethoxythiane-1,1-dioxides.¹⁴²

S	X	alkylating agent	P	Yield (%)
 235	CH ₂	allyl bromide	 237	95
 235	CH ₂	ethyl iodide	 238	80
 235	CH ₂	tosyl azide	 239	90
 235	CH ₂	hexachloroethane	 240	80
 235	CH ₂	<i>p</i> -chlorobenzyl bromide	 241	81

Table 16. Cont.

S	X	alkylating agent	P	
 235	CH ₂	diiodomethane	 242	86
 236	O	allyl bromide	 243	85
 149a	CH ₂	allyl bromide	 244	95
 149a	CH ₂	<i>p</i> -chlorobenzyl bromide	 245	95
 155.2	CH ₂	<i>p</i> -chlorobenzyl bromide	 246	90

The stereochemistry of alkylation products **244**, **245** and **246** was deduced from NOE correlations (Figure 9). In the case of **246**, the alcohol **246b**, obtained after DIBALH reduction was used.

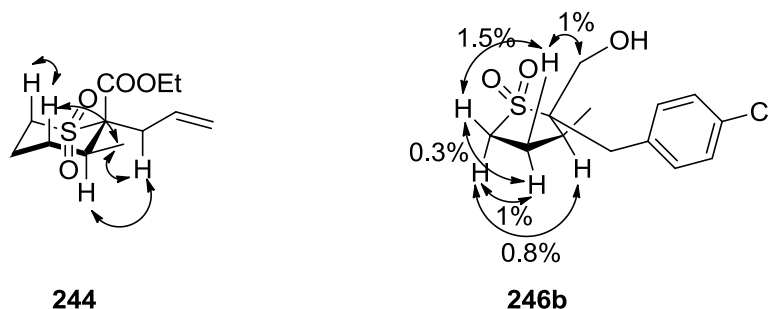
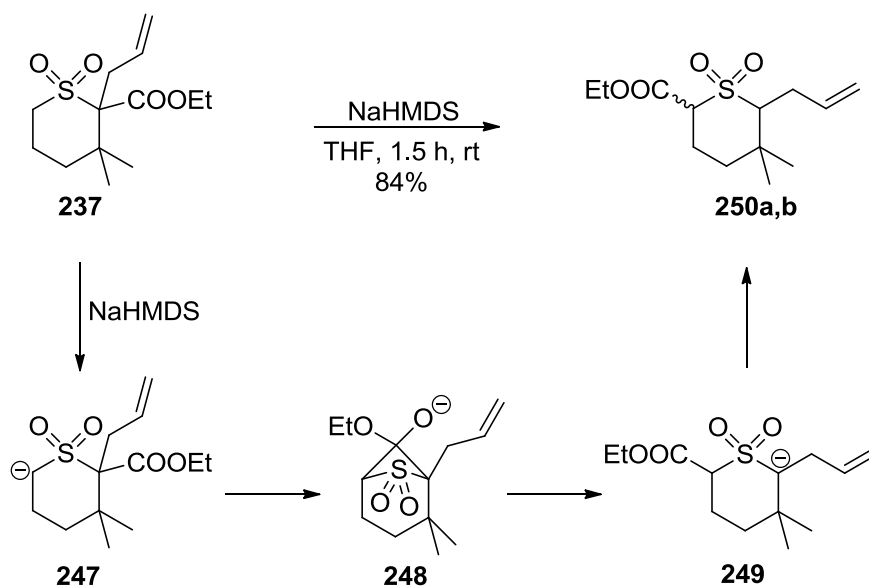


Figure 9. Stereochemical assignment of alkylated products.¹⁴²

It was found that the ester functionality of the δ -sultones can be selectively reduced by DIBALH without affecting the sultone moiety, although care must be taken as prolonged reaction times degrade the yield. While borane-dimethyl sulfide also proved effective, LAH was ineffective with both sulfones and sulfonates resulting in complete hydrogenolysis of the ester functionality to the methyl group.

Most notably, it has been uncovered that alkylated products, upon treatment with NaHMDS, could be rearranged by migration of the carbethoxy group in a manner similar to that of β -ketoesters (Scheme 36).



Scheme 36. Rearrangement of alkylated sulfones.¹⁴²

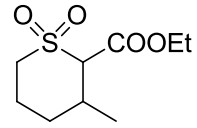
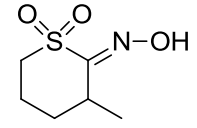
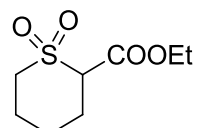
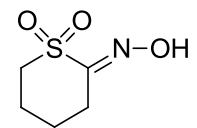
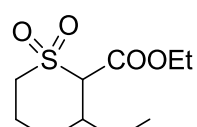
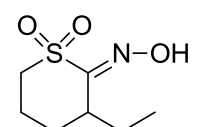
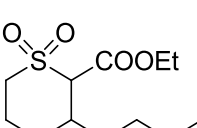
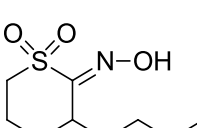
4.2.4 Formation of Cyclic α -Sulfonyl Oximes

Sulfonyl oximes constitute an important group of organic intermediates capable of undergoing nucleophilic substitution reactions to provide oxime ethers, which in turn lead to amines and carbonyl compounds.¹⁴⁴⁻¹⁴⁶ The synthetic potential of α -sulfonyl oximes is well known, however that of cyclic α -sulfonyl oximes remains limited, perhaps due to a little diversion within this group of compounds. A novel transformation of carbethoxythiane-1,1-dioxides to the corresponding cyclic α -sulfonyl oximes under relatively mild conditions (isoamyl nitrite, NaH, THF) is herein reported (Table 17). For δ -sulfones, under the same conditions, the reaction was met with complications resulting in a mixture of undesirable products.

Table 17. Formation of α -sulfonyl oximes from carbethoxythiane-1,1-dioxides.

$$\text{S} \xrightarrow[\text{THF, isoamyl nitrite}]{\text{NaH}} \text{P}$$

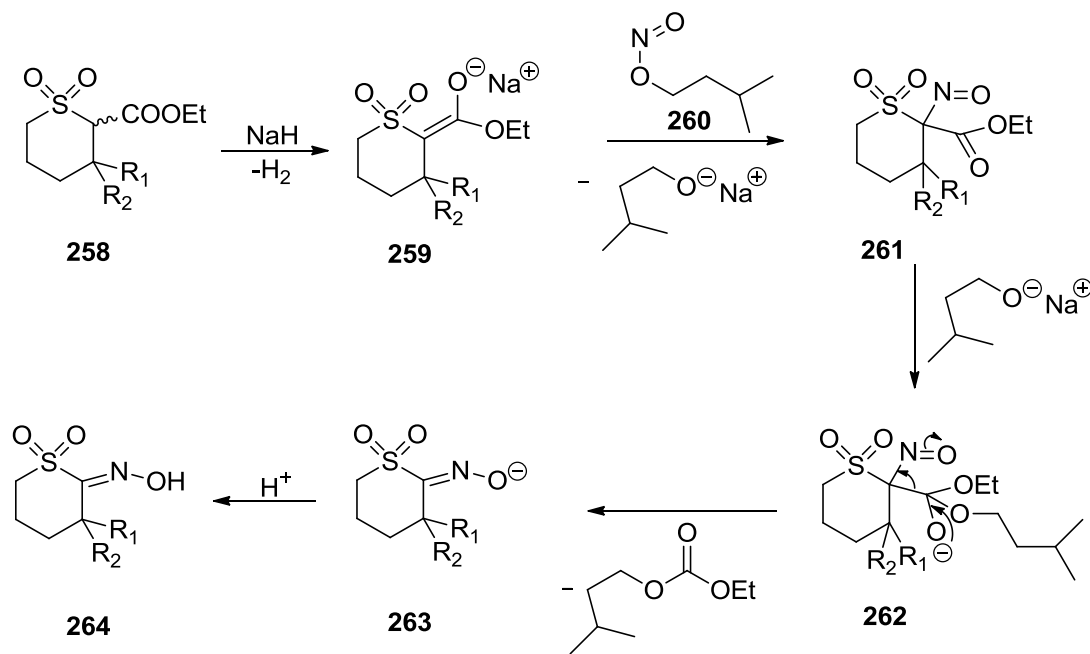
$$\text{X} = \text{CH}_2 \text{ or } \text{O}$$

Substrate	X	Product	Yield (%)
 149a	CH ₂	 254	87
 251	CH ₂	 255	82
 252	CH ₂	 256	85
 253	CH ₂	 257	90

The obtained cyclic α -sulfonyl oximes are formed as depicted on Scheme 37.

Alkylation of carbethoxythiane-1,1-dioxide using NaH and isoamyl nitrite **260** results in the formation of sulfonyl nitrite **261**. The nitrite reacts with isoamyloxy nucleophile

generated from the alkylation step to form **262**, which undergoes rearrangement, followed by protonation to furnish the desired the cyclic α -sulfonyl oxime **264**.



Scheme 37. Mechanism of formation of cyclic α -sulfonyl oximes.

4.3 Conclusion

The conversion of δ -sultones to δ -valerolactones and γ -butyrolactones has been demonstrated. This outlines a protocol to substituted lactones, which are common intermediates in the synthesis of several natural products. The stereoselective alkylation of δ -sultones and thiane-1,1-dioxides has also been attained. This opens possibilities for simple differential alkylation of thiane-1,1-dioxides, as well as construction of bicyclic sulfur-containing heterocycles, which could be converted to medium-sized carbocycles by

desulfonation. Lastly, novel cyclic α -sulfonyl oximes have been obtained from thiane-1,1-dioxides under relatively mild conditions. The availability of these compounds would facilitate studies on cyclic sulfonyl oximes. In a nut shell, these findings will be beneficial for further studies directed at exploring the full potential of δ -sulfones and thiane-1,1-dioxides in synthesis.

4.4 Experimental Section on Synthetic Utility of Cyclic Six-Membered Sulfones and Sulfonates obtained by Rhodium-Catalyzed Intramolecular C–H Insertion

All reactions were carried out under an inert nitrogen atmosphere unless otherwise stated. All reagents were used as purchased without further purification except otherwise stated. $^1\text{H-NMR}$ (500 Hz) and $^{13}\text{C}\{^1\text{H}\}$ NMR (125 Hz) spectra were recorded on an Avance 500 Bruker spectrometer and calibrated using residual undeuterated solvent as internal references. Coupling constants are given in Hz. IR spectra were recorded on a Perkin-Elmer Spectrum 400 Series FTIR spectrometer. Specific rotations were measured on an AUTOPOL III automatic polarimeter in anhydrous CHCl_3 using a 10 cm cell. HRMS data were obtained on an Agilent 61969A TOF high resolution mass spectrometer using electrospray ionization (ESI). Melting points were determined on a MEL-TEMP melting point apparatus. Analytical TLC was performed using silica gel pre-coated TLC plates (E. Merck no. 5715-7). Flash chromatography was performed using 40-63 μm silica gel (Merck, Geduran, no. 11567-1) as the stationary phase. Tetrahydrofuran (THF) was dried by distilling it from sodium and benzophenone in a continuous still under a nitrogen atmosphere. Chloroform, dichloromethane and triethylamine were distilled from calcium hydride under an atmosphere of nitrogen.

General procedure for reduction of δ -sultones with SmI₂/DMPU

To the solution of sultone (0.1 mmol) in dry THF (0.5 mL) containing DMPU (50 mg, 0.40 mmol) was added 0.1 M solution of SmI₂ (commercially available, or prepared by dissolving solid SmI₂, obtained by reaction of samarium metal with HgI₂, in dry THF) until the blue color persisted, and 2 mL after that (typically around 5 mL). The reaction mixture was stirred at rt for the specified time, after which 1N HCl solution was added (5 mL). Hexane (30 mL) was added, and the reaction mixture was stirred for 15 min at rt. The layers were separated; the aqueous layer was washed with hexane (10 mL). The combined organic layers were washed with water (10 mL), dried over Na₂SO₄, and carefully concentrated. Flash chromatography (hexane-Et₂O) provided the product. The obtained lactones have been previously reported. The spectral data for the obtained compounds match those reported in the literature, as that of the independently prepared authentic samples.

General procedure for oxidation of δ -sultones with TBHP/*t*-BuOK

To a solution of δ -sultone in THF (2.5 mL/mmol) was added *t*-BuOK (10 equiv.) or KHMDS (10 equiv.) followed by TBHP (4 equiv.). After stirring at rt for 16 h, Na₂SO₃ was added and the resulting suspension stirred for 15 min to destroy excess TBHP. This was followed by the addition of 20 mL of 1N HCl solution and the resulting mixture taken up in Et₂O, washed with brine, dried over MgSO₄ and evaporated to afford a crude product, which was purified by flash chromatography.

Spectra data for **3,3,6-trimethylhexahydrobenzofuran-2-one (224)** matched that in literature.

7,8,8-Trimethyl-4-oxatricyclo[4.2.1.0^{3,7}]nonan-5-one (225): colorless oil. ¹H NMR (CDCl₃, 500 MHz): δ 4.35 (d, 1H), 2.12-2.30 (m, 3H), 1.87 (m, 1H), 1.5 (d, *J* = 12.6, 1H), 1.39 (d, *J* = 14.2, 1H), 1.05 (s, 3H), 0.88 (s, 3H), 0.86 (s, 3H). ¹³C{¹H} NMR (CDCl₃, 125 MHz): δ 181.5 (C), 87.1 (CH), 58.8 (C), 49.2 (C), 46.6 (CH), 46.3 (CH), 36.8 (CH₂), 33.4 (CH₂), 20.5 (CH₃), 19.4 (CH₃), 11.6 (CH₃).

3-Methyl-3-(4-methyl-3-pentenyl)dihydrofuran-2-one (226): Pale yellow oil. ¹H NMR (CDCl₃, 500 MHz): δ 4.35 (d, 1H), 2.12-2.30 (m, 3H), 1.87 (m, 1H), 1.5 (d, *J* = 12.6, 1H), 1.39 (d, *J* = 14.2, 1H), 1.05 (s, 3H), 0.88 (s, 3H), 0.86 (s, 3H). ¹³C{¹H} NMR (CDCl₃, 125 MHz): δ 181.5 (C), 87.1 (CH), 58.8 (C), 49.2 (C), 46.6 (CH), 46.3 (CH), 36.8 (CH₂), 33.4 (CH₂), 20.5 (CH₃), 19.4 (CH₃), 11.6 (CH₃).

3-(3-Benzyloxypropyl)-3-ethyldihydrofuran-2-one (227): ¹H NMR (CDCl₃, 500 MHz): δ 7.27 (m, 5H), 4.44 (s, 2H), 3.60 (t, *J* = 7, 2H), 3.40 (t, *J* = 6.6, 2H), 1.50-1.60 (m, 2H), 1.40-1.48 (m, 2H), 1.31-1.38 (m, 1H), 1.22-1.29 (m, 1H), 0.79 (t, *J* = 7, 3H). ¹³C{¹H} NMR (CDCl₃, 125 MHz): δ 139.0 (C), 128.7 (CH), 128.0 (CH), 127.9 (CH), 73.3 (CH₂), 71.1 (CH₂), 61.6 (CH₂), 36.8 (CH₂), 35.3 (C), 30.1 (CH₂), 29.9 (CH₂), 27.2 (CH₂), 26.3 (CH₂), 11.1 (CH₃).

General procedure for alkylation of δ -sultones and thiane-1,1-dioxides

Sodium hydride (20 mg, 60% dispersion in mineral oil, 0.5 mmol) was washed with THF (3×10 mL), and a solution of thiane-1,1-dioxide (0.2 mmol) in THF (1 mL) was added to it. After stirring for 15 min (when gas evolution subsided), the corresponding alkyl halide (allyl bromide, ethyl iodide or *p*-chlorobenzyl chloride, 0.4 mmol) was added, and the reaction mixture was allowed to stir at rt for 16 h. 1N HCl solution (5 mL) was added, and the mixture was extracted with EtOAc (2×20 mL). The organic layer was dried with Na₂SO₄, and concentrated under reduced pressure. The product was purified by flash chromatography (hexane-EtOAc).

2-Allyl-2-carbethoxy-3,3-dimethylthiane-1,1-dioxide (237): Pale yellow oil. ¹H NMR (CDCl₃, 500 MHz): δ 6.08-6.17 (m, 1H), 5.23 (dd, *J* = 17, 1.5, 1H), 5.14 (dd, *J* = 10, 1.5, 1H), 4.25-4.36 (m, 2H), 3.81 (td, *J* = 13.5, 4, 1H), 2.97-3.04 (m, 2H), 2.82 (dd, *J* = 15, 7, 1H), 2.12-2.29 (m, 2H), 1.92-1.99 (m, 1H), 1.33-1.39 (m, 4H), 1.36 (t, *J* = 7), 1.31 (s, 3H), 1.00 (s, 3H). ¹³C{¹H} NMR (CDCl₃, 125 MHz): δ 168.3 (C), 134.2 (CH), 118.6 (CH₂), 78.0 (C), 62.2 (CH₂), 51.2 (CH₂), 40.1 (C), 36.4 (CH₂), 31.8 (CH₂), 28.8 (CH₃), 23.0 (CH₃), 19.4 (CH₂), 14.2 (CH₃). HRMS (ESI) calcd for C₁₃H₂₆NO₄S (M+NH₄)⁺ 292.1577, found 292.1559.

2-Ethyl-2-carbethoxy-3,3-dimethylthiane-1,1-dioxide (238): Pale yellow oil. ¹H NMR (CDCl₃, 500 MHz): δ 4.33-4.39 (m, 1H), 4.24-4.32 (m, 1H), 3.84 (td, *J* = 13.5, 4, 1H), 3.00 (dt, *J* = 13.5, 3.5, 1H), 2.24-3.31 (m, 1H), 2.20 (ddd, *J* = 14, 3.5, 3, 1H), 2.03-2.11

(m, 2H), 1.90-1.96 (m, 1H), 1.36 (t, $J = 7.3$, 3H), 1.29-1.35 (m, 1H), 1.27 (s, 3H), 1.26 (t, $J = 7.3$, 3H), 0.96 (s, 3H). $^{13}\text{C}\{^1\text{H}\}$ NMR (CDCl_3 , 125 MHz): δ 168.4 (C), 78.7 (C), 62.0 (CH_2), 52.0 (CH_2), 40.2 (C), 36.3 (CH_2), 28.7 (CH_3), 23.3 (CH_3), 20.9 (CH_2), 19.4 (CH_2), 14.3 (CH_3), 11.1 (CH_3). HRMS (ESI) calcd for $\text{C}_{12}\text{H}_{26}\text{NO}_4\text{S}$ ($\text{M}+\text{NH}_4$) $^+$ 280.1577, found 280.1577.

2-Azido-2-carbethoxy-3,3-dimethylthiane-1,1-dioxide (239): Pale yellow oil. ^1H NMR (CDCl_3 , 500 MHz): δ 4.37-4.51 (m, 2H), 3.51 (td, $J = 13.5$, 4, 1H), 3.26-3.31 (m, 1H), 2.08-2.21 (m, 2H), 1.9 (td, $J = 15$, 4, 1H), 1.52-1.62 (m, 1H), 1.40 (t, $J = 7.2$), 1.20 (s, 3H), 1.08 (s, 3H). $^{13}\text{C}\{^1\text{H}\}$ NMR (CDCl_3 , 125 MHz): δ 165.3 (C), 101.0 (C), 83.9 (CH_2), 64.0 (CH_2), 50.4 (CH_2), 41.5 (C), 34.7 (CH_3), 19.7 (CH_3), 14.4 (CH_3). HRMS (ESI) calcd for $\text{C}_{10}\text{H}_{25}\text{N}_2\text{O}_4\text{S}$ ($\text{M}+\text{NH}_4$) $^+$ 269.1283, found 293.1273.

2-Chloro-2-carbethoxy-3,3-dimethylthiane-1,1-dioxide (240): Pale yellow oil. ^1H NMR (CDCl_3 , 500 MHz): δ 4.35 (q, 2H), 3.85 (td, $J = 16.4$, 3.4, 1H), 3.23 (dt, $J = 13.5$, 3.1, 1H), 2.24-3.31 (m, 1H), 2.24-2.34 (m, 1H), 2.04-2.11 (m, 1H), 1.6 (dd, $J = 12.2$, 5.6, 1H), 1.40 (s, 3H), 1.39 (t, $J = 7.3$, 3H), 1.10 (s, 3H). $^{13}\text{C}\{^1\text{H}\}$ NMR (CDCl_3 , 125 MHz): δ 165.4 (C), 92.1 (C), 64.3 (CH_2), 50.3 (CH_2), 43.4 (CH_2), 35.4 (CH_2), 27.5 (C), 24.2 (CH_3), 19.6 (CH_3), 14.2 (CH_3).

2-(4-Chlorobenzyl)-2-carbethoxy-3,3-dimethylthiane-1,1-dioxide (241): Pale yellow oil. ^1H NMR (CDCl_3 , 500 MHz): δ 7.44 (d, $J = 8.1$), 7.20 (d, $J = 8.5$), 4.28 (q, $J = 7.2$,

2H), 3.81 (td, $J = 13.5$, 4, 1H), 3.55 (t, $J = 14.5$, 2H), 3.28 (d, $J = 14.5$, 1H), 3.02 (dt, $J = 13$, 3.2, 1H), 2.25 (qt, $J = 13.8$, 3.1, 1H), 2.05 (td, $J = 14.1$, 2.8, 1H), 1.92-1.98 (m, 1H), 1.42 (s, 3H), 1.34 (t, $J = 7.3$, 3H), 1.04 (s, 3H). $^{13}\text{C}\{^1\text{H}\}$ NMR (CDCl_3 , 125 MHz): δ 167.6 (C), 134.4 (C), 134.2 (CH), 127.7 (CH), 79.5 (CH_2), 62.2 (C), 52.3 (CH_2), 40.8 (CH_3), 36.5 (CH_3), 32.1 (CH_2), 29.0 (CH_2), 23.2 (CH_3), 19.4 (CH_3), 14.2 (CH_3). HRMS (ESI) calcd for $\text{C}_{17}\text{H}_{24}\text{NO}_4\text{SCl}$ ($\text{M}+\text{NH}_4$) $^+$ 376.1442, found 359.1083.

2-Methyl-2-carbethoxy-3,3-dimethylthiane-1,1-dioxide (242): Pale yellow oil. ^1H NMR (CDCl_3 , 500 MHz): δ 4.18-4.25 (m, 2H), 3.72 (td, $J = 13.2$, 4.7, 1H), 2.92 (dt, $J = 13.5$, 3.1, 1H), 1.98-2.12 (m, 1H), 1.82 (qd, $J = 12.9$, 4, 1H), 1.6 (s, 3H), 1.3 (t, $J = 7.3$, 3H), 0.88 (d, $J = 6.6$, 3H). $^{13}\text{C}\{^1\text{H}\}$ NMR (CDCl_3 , 125 MHz): δ 168.4 (C), 72.4 (C), 62.6 (CH_2), 49.2 (CH_2), 40.9 (CH_2), 29.2 (CH_2), 23.3 (C), 17.5 (CH_3), 14.6 (CH_3), 14.5 (CH_3).

3-Allyl-3-carbethoxy-4,4-dimethyl-1,2-oxathiane-2,2-dioxide (243): Pale yellow oil. ^1H NMR (CDCl_3 , 500 MHz): δ 6.05 (ddt, $J = 14$, 10, 7, 1H), 5.27 (dd, $J = 17$, 1.5, 1H), 5.18 (dd, $J = 10$, 1.5, 1H), 4.72 (td, $J = 12$, 2, 1H), 4.44 (ddd, $J = 11.5$, 4.5, 2.5, 1H), 4.29-4.38 (m, 2H), 2.86-2.96 (m, 2H), 2.61 (td, $J = 13.5$, 4, 1H), 1.43 (s, 3H), 1.33-1.39 (m, 4H), 1.36 (t, $J = 7$), 0.99 (s, 3H). $^{13}\text{C}\{^1\text{H}\}$ NMR (CDCl_3 , 125 MHz): δ 166.5 (C), 133.4 (CH), 119.5 (CH_2), 76.8 (C), 69.3 (CH_2), 62.6 (CH_2), 39.6 (CH_2), 36.7 (CH_2), 34.3 (CH_2), 27.8 (CH_3), 23.6 (CH_3), 14.2 (CH_3). HRMS (ESI) calcd for $\text{C}_{12}\text{H}_{24}\text{NO}_5\text{S}$ ($\text{M}+\text{NH}_4$) $^+$ 294.1369, found 294.1388.

(2R,3S)-2-Allyl-2-carbethoxy-3-methylthiane-1,1-dioxide (244): Pale yellow oil. ^1H NMR (CDCl_3 , 500 MHz): δ 6.10-6.19 (m, 1H), 5.20 (dq, $J = 17, 1$, 1H), 5.14 (d, $J = 10$, 1H), 4.26-4.37 (m, 2H), 3.79 (td, $J = 13.5, 4.5$, 1H), 3.11 (dd, $J = 15, 5.5$, 1H), 2.98 (dt, $J = 13.5, 3.5$, 1H), 2.82 (dd, $J = 15.5, 8.5$, 1H), 2.24-2.31 (m, 1H), 2.03-2.17 (m, 2H), 1.80 (qd, $J = 13, 3.5$, 1H), 1.60 (dq, $J = 14.5, 3.5$, 1H, overlapped with water peak at 1.60 ppm), 1.36 (t, $J = 7.5$, 3H), 0.99 (d, $J = 6.5$, 3H). $^{13}\text{C}\{^1\text{H}\}$ NMR (CDCl_3 , 125 MHz): δ 167.5 (C), 133.3 (CH), 119.0 (CH_2), 75.5 (C), 62.4 (CH_2), 50.7 (CH_2), 39.1 (CH), 34.8 (CH_2), 29.1 (CH_2), 23.0 (CH_2), 17.4 (CH_3), 14.3 (CH_3). HRMS (ESI) calcd for $\text{C}_{12}\text{H}_{21}\text{O}_4\text{S}$ ($\text{M}+\text{H}$) $^+$ 261.1155, found 261.1171.

(2R,3S)-2-Carbethoxy-2-(4-chlorobenzyl)-3-methylthiane-1,1-dioxide (245): Pale yellow oil. ^1H NMR (CDCl_3 , 500 MHz): δ 7.42 (d, $J = 8$, 2H), 7.22 (d, $J = 8$, 2H), 4.30-4.40 (m, 2H), 3.76 (td, $J = 13.5, 4$, 1H), 3.66 (d, $J = 14.5$, 1H), 3.34 (d, $J = 14.5$, 1H), 2.96 (dt, $J = 14, 3.5$, 1H), 2.33-2.41 (m, 1H), 2.08-2.19 (m, 1H), 2.00-2.07 (m, 1H), 1.63-1.72 (m, 2H), 1.37 (t, $J = 7$, 3H), 1.07 (d, $J = 7$, 3H). $^{13}\text{C}\{^1\text{H}\}$ NMR (CDCl_3 , 125 MHz): δ 167.1 (C), 134.1 (C), 133.2 (CH), 133.1 (C), 128.0 (CH), 77.2 (C), 62.6 (CH_2), 51.5 (CH_2), 40.4 (CH), 35.6 (CH_2), 29.6 (CH_2), 22.9 (CH_2), 18.1 (CH_3), 14.4 (CH_3). HRMS (ESI) calcd for $\text{C}_{16}\text{H}_{25}\text{NO}_4\text{SCl}$ ($\text{M}+\text{NH}_4$) $^+$ 362.1187, found 362.1172.

(2R,3S)-2-Carbethoxy-2-(4-chlorobenzyl)-3-methylthiolane-1,1-dioxide (246): Pale yellow oil. ^1H NMR (CDCl_3 , 500 MHz): δ 7.39 (d, $J = 8.5$, 2H), 7.25 (d, $J = 8.5$, 2H), 4.30 (qd, $J = 7, 1.5$, 2H), 3.44-3.52 (m, 2H), 3.27 (d, $J = 14.5$, 1H), 3.14-3.21 (m, 1H),

2.47-2.55 (m, 1H), 2.21-2.29 (m, 1H), 1.96-2.05 (m, 1H), 1.33 (t, $J = 7.3$, 3H), 0.90 (d, $J = 7$, 3H). $^{13}\text{C}\{^1\text{H}\}$ NMR (CDCl_3 , 125 MHz): δ 166.6 (C), 133.6 (C), 133.3 (C), 132.6 (CH), 128.5 (CH), 74.5 (C), 62.5 (CH_2), 50.7 (CH_2), 40.1 (CH), 35.2 (CH_2), 27.0 (CH_2), 17.0 (CH_3), 14.3 (CH_3). HRMS (ESI) calcd for $\text{C}_{15}\text{H}_{23}\text{NO}_4\text{SCl}$ ($\text{M}+\text{NH}_4$) $^+$ 348.1031, found 348.1035.

DIBALH reduction of 236 and 246

To the solution of **236** or **246** (0.1 mmol) in CH_2Cl_2 (0.5 mL), solution of DIBALH (0.5 mL, 1M in hexane, 0.5 mmol) was added at 0 °C. The reaction mixture was kept at 0 °C for 1h (**236**), or 10 h at rt (**246**). Concentrated aqueous solution of sodium potassium tartrate was added (10 mL), and the reaction mixture was stirred for 1h. The layers were separated; the aqueous layer was washed with EtOAc (20 mL). The combined organic layers were washed with brine, dried over Na_2SO_4 , and concentrated. Flash chromatography (hexane-EtOAc) provided the product.

3-Hydroxymethyl-4,4-dimethyl-1,2-oxathiane-2,2-dioxide (236b): Obtained in 90% yield. Clear oil, solidified on standing. mp 62-63 °C. ^1H NMR (CDCl_3 , 500 MHz): δ 4.66 (td, $J = 11.5$, 2.5, 1H), 4.46 (dt, $J = 11.5$, 4, 1H), 4.20 (ddd, $J = 12.5$, 8, 3, 1H), 4.02-4.09 (ddd, $J = 12.5$, 8, 3, 1H), 3.11 (dd, $J = 8$, 3, 1H), 2.41 (dd, $J = 8$, 3, 1H), 1.92 (ddd, $J = 14.5$, 11.5, 4, 1H), 1.61 (ddd, $J = 14.5$, 4, 2.5, 1H), 1.27 (s, 3H), 1.22 (s, 3H). $^{13}\text{C}\{^1\text{H}\}$ NMR (CDCl_3 , 125 MHz): δ 69.9 (CH), 69.7 (CH_2), 58.3 (CH_2), 38.9 (CH_2), 35.8 (C),

29.9 (CH₃), 22.1 (CH₃). HRMS (ESI) calcd for C₇H₁₈NO₄S (M+NH₄)⁺ 212.0951, found 212.0950.

(2*R*,3*S*)-4-Chlorobenzyl-2-hydroxymethyl-3-methylthiolane-1,1-dioxide (246b):

Obtained in 94% yield. Pale yellow oil. ¹H NMR (CDCl₃, 500 MHz): δ 7.28-7.31 (m, 4H), 3.94 (dd, *J* = 13, 6, 1H), 3.75 (dd, *J* = 13, 8, 1H), 3.42 (d, *J* = 14, 1H), 3.29 (ddd, *J* = 13, 8.5, 3, 1H), 3.07 (ddd, *J* = 13, 10.5, 8.5, 1H), 2.82 (d, *J* = 14, 1H), 2.59 (dd, *J* = 8, 6, 1H), 2.31-2.39 (m, 1H), 2.13-2.21 (m, 1H), 1.90-2.00 (m, 1H), 0.85 (d, *J* = 7, 3H). ¹³C{¹H} NMR (CDCl₃, 125 MHz): δ 133.8 (C), 133.5 (C), 132.2 (CH), 128.9 (CH), 68.1 (C), 61.3 (CH₂), 51.4 (CH₂), 39.5 (CH), 36.5 (CH₂), 27.7 (CH₂), 15.8 (CH₃). HRMS (ESI) calcd for C₁₃H₂₁NO₃SCl (M+NH₄)⁺ 306.0925, found 306.0941.

Rearrangement of 237

Compound **237** (25 mg, 0.091 mmol) was dissolved in dry THF (0.2 mL), and solution of NaHMDS in THF (2M in THF, 90 μL, 0.18 mmol) was added. After stirring at rt for 1.5 h, the reaction was quenched with 1N HCl solution (5 mL), and extracted with EtOAc (2 × 20 mL). The organic layer was washed with brine, dried and concentrated. The products were isolated using flash chromatography (EtOAc-hexane). The products isomerise during chromatography (verified by resubjecting pure **250a** to chromatography). Typically, small amounts of pure **250a** and **250b** were isolated, along with a mixture of the two. **250b** (the more polar isomer) was determined to be the cis isomer by diaxial NOE correlation between H₂ and H₆. Combined yield 20 mg (84%).

***trans*-2-Allyl-6-carbethoxy-3,3-dimethylthiane-1,1-dioxide (250a)**: Pale yellow oil. ^1H NMR (CDCl_3 , 500 MHz): δ 5.94-6.03 (m, 1H), 5.16 (dd, $J = 17, 1.5$, 1H), 5.07 (dd, $J = 10, 1.5$, 1H), 4.21-4.32 (m, 2H), 3.88 (dd, $J = 5, 3$, 1H), 3.43 (dd, $J = 7, 4$, 1H), 2.78-2.87 (m, 1H), 2.50 (ddd, $J = 14, 5, 3$, 1H), 2.38-2.45 (m, 1H), 2.13 (dq, $J = 15, 3$, 1H), 2.04 (td, $J = 14, 3$, 1H), 1.39 (dt, $J = 14.5, 3.5$, 1H), 1.32 (t, $J = 7$, 3H), 1.15 (s, 3H), 1.11 (s, 3H). $^{13}\text{C}\{^1\text{H}\}$ NMR (CDCl_3 , 125 MHz): δ 167.2 (C), 136.8 (CH), 116.8 (CH_2), 66.8 (CH), 63.9 (CH), 62.4 (CH_2), 37.4 (C), 34.8 (CH_2), 31.0 (CH_3), 26.3 (CH_2), 23.4 (CH_2), 19.9 (CH_3), 14.2 (CH_3). HRMS (ESI) calcd for $\text{C}_{13}\text{H}_{23}\text{O}_4\text{S}$ ($\text{M}+\text{H}$) $^+$ 275.1311, found 275.1320.

***cis*-2-Allyl-6-carbethoxy-3,3-dimethylthiane-1,1-dioxide (250b)**: Pale yellow oil. ^1H NMR (CDCl_3 , 500 MHz): δ 5.94-6.03 (m, 1H), 5.14 (dd, $J = 17, 1.5$, 1H), 5.07 (dd, $J = 10, 1.5$, 1H), 4.25-4.37 (m, 2H), 3.81 (dd, $J = 13, 3.5$, 1H), 2.83-2.91 (m, 1H), 2.82 (dd, $J = 7, 3$, 1H), 2.37-2.51 (m, 2H), 2.14 (dq, $J = 15, 3$, 1H), 1.68 (ddd, $J = 14.5, 4.5, 3$, 1H), 1.52 (td, $J = 14, 3$, 1H), 1.33 (t, $J = 7$, 3H), 1.16 (s, 3H), 1.09 (s, 3H). $^{13}\text{C}\{^1\text{H}\}$ NMR (CDCl_3 , 125 MHz): δ 164.2 (C), 136.7 (CH), 117.1 (CH_2), 71.6 (CH), 66.1 (CH), 62.8 (CH_2), 39.6 (CH_2), 37.7 (C), 30.9 (CH_3), 26.7 (CH_2), 23.5 (CH_2), 19.5 (CH_3), 14.3 (CH_3). HRMS (ESI) calcd for $\text{C}_{13}\text{H}_{23}\text{O}_4\text{S}$ ($\text{M}+\text{H}$) $^+$ 275.1311, found 275.1319.

General Procedure for the preparation of α -sulfonyl oximes (254-257)

To a stirred solution of carbethoxythiane-1,1-dioxide (30-50 mg) in 2 mL of THF was added NaH (2 equiv.). After stirring at rt for 15 min, isoamyl nitrite (2 equiv.) is

added and the combined mixture further stirred at room for 16 h. Upon completion as indicated by TLC analysis, the reaction is acidified with 1N HCl solution, extracted with Et₂O or EtOAc, washed with brine, dried over MgSO₄, filtered and the excess solvent removed under reduced pressure to afford a crude product that was purified by flash chromatography (35% EtOAc/Hexanes).

2-Hydroxyimino-3-methylthiane-1,1-dioxide (254) : Pale yellow oil. ¹H NMR (CDCl₃, 500 MHz): δ 9.54 (s, 1H), 3.95-3.97 (m, 1H), 3.30-3.33 (m, 1H), 3.09-3.15 (m, 1H), 2.49-2.53 (m, 1H), 2.05-2.10 (m, 2H), 1.80-1.94 (m, 2H), 1.47 (d, *J* = 6.6, 3H), ¹³C{¹H} NMR (CDCl₃, 125 MHz): δ 160.9 (C), 54.8 (CH₂), 31.1 (CH), 30.8 (CH₂), 19.8 (CH₂), 16.68 (CH₃).

2-Hydroxyiminothiane-1,1-dioxide (255): Pale yellow oil. ¹H NMR (CDCl₃, 500 MHz): δ 9.37 (s, 1H), 3.14 (t, *J* = 6, 2H), 2.97 (t, *J* = 6, 2H), 2.14-2.18 (m, 2H), 1.73-1.77 (m, 2H). ¹³C{¹H} NMR (CDCl₃, 125 MHz): δ 158.1 (C), 55.23 (CH₂), 25.6 (CH₂), 25.0 (CH₂), 24.4 (CH₂).

2-Hydroxyimino-3-ethylthiane-1,1-dioxide (256): Pale yellow oil. ¹H NMR (CDCl₃, 500 MHz): δ 9.24 (s, 1H), 3.72-3.73 (m, 1H), 3.41 (q, *J* = 7, 1H), 3.20-3.30 (m, 1H), 3.00-3.10 (m, 1H), 2.30-2.42 (m, 1H), 1.96-2.10 (m, 2H), 1.80-1.90 (m, 1H), 1.70-1.80 (m, 1H), 1.60 (ddd, *J* = 20, 14, 7, 1H), 1.18 (t, *J* = 7, 3H), 0.89 (t, *J* = 7.2, 3H). ¹³C{¹H} NMR (CDCl₃, 125 MHz): δ 158.1 (C), 55.23 (CH₂), 25.6 (CH₂), 25.0 (CH₂), 24.4 (CH₂).

NMR (CDCl₃, 125 MHz): δ 160.0 (C), 66.2 (CH₂), 55.1 (CH₂), 38.2 (CH), 29.0 (CH₂), 24.3 (CH₂), 20.0 (CH₂), 15.6 (CH), 12.4 (CH₃).

2-Hydroxyimino-3-butylthiane-1,1-dioxide (257): Pale yellow oil. ¹H NMR (CDCl₃, 500 MHz): δ 9.32 (s, 1H), 3.84-3.85 (m, 1H), 3.20-3.33 (m, 1H), 3.10-3.14 (m, 1H), 2.454-2.48 (m, 1H), 2.02-2.09 (m, 2H), 1.89-1.91 (m, 1H), 1.77-1.81 (m, 1H), 1.60-1.65 (m, 5H), 0.92 (t, *J* = 7, 3H). ¹³C{¹H} NMR (CDCl₃, 125 MHz): δ 160.2 (C), 55.2 (CH₂), 36.5 (CH), 30.7 (CH₂), 30.0 (CH₂), 29.2 (CH₂), 22.8 (CH₂), 20.0 (CH₂), 14.3 (CH₃).

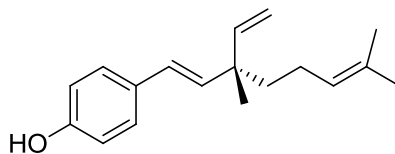
CHAPTER 5

APPLICATION OF RHODIUM-CATALYZED INTRAMOLECULAR C–H INSERTION ON DIAZO SULFONES AND SULFONATES TOWARDS THE SYNTHESIS OF NATURAL PRODUCTS

5.1 Synthesis of (+)-Bakuchiol

5.1.1 Isolation and Biological Activity of (+)-Bakuchiol

(+)-Bakuchiol is a meroterpenoid that can be found naturally in the leaves of *Psoralea glandulosa* as well as the seeds of *Psoralea corylifolia*.^{147, 148} Both plants belong to the *Fabaceae* family. *Psoralea glandulosa* is a perennial plant common along the west coast of South America, especially in Peru and Chile, while *Psoralea corylifolia* is widely distributed around India and Southeastern Asia, and has been routinely used for Chinese and Indian medicine.



265

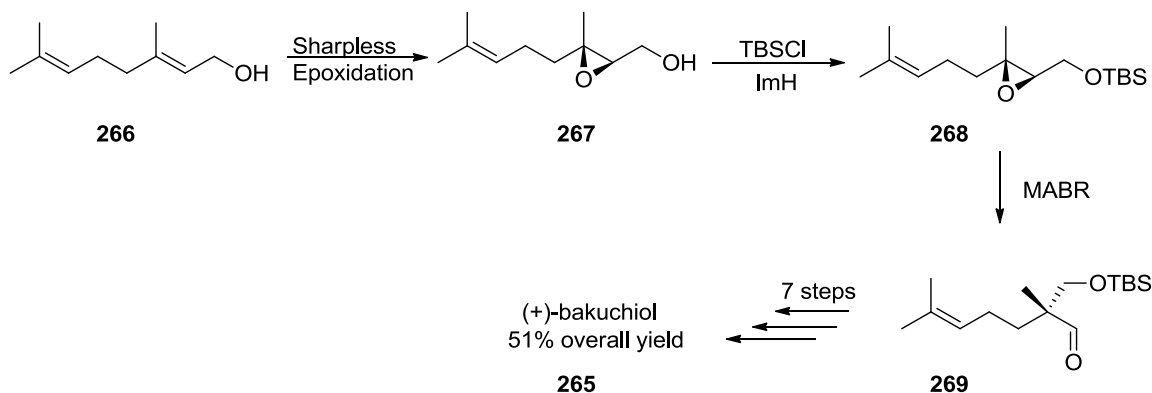
Figure 10. Structure of (+)-bakuchiol.

The urge to synthesize (+)-bakuchiol was heightened by its broad spectrum of applications, ranging from treating neurodegenerative diseases, breast cancer, oral hygiene, plant diseases, antibacterial agent, bone strength-enhancing agent and skin care

agent.¹⁴⁹ There have also been several reports describing the use of (+)-bakuchiol as an anti-inflammatory,¹⁵⁰ antioxidant,¹⁵¹ antitumor,¹⁵² and immunosuppressive agents.¹⁵³

5.1.2 Previous Syntheses of (+)-Bakuchiol

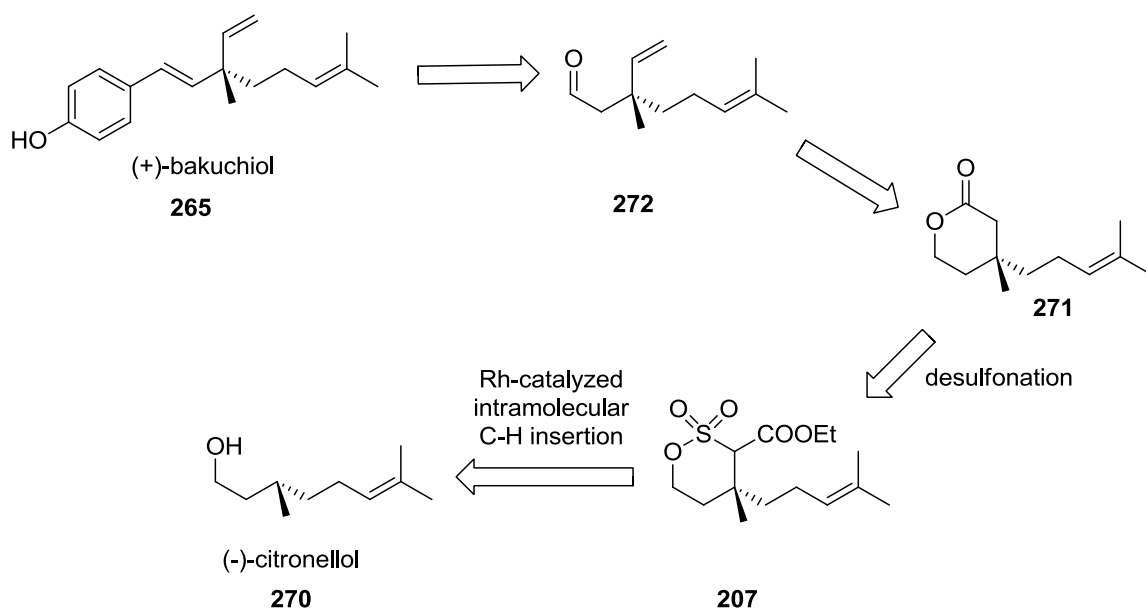
The first enantioselective total synthesis of (+)-bakuchiol was reported by Takano and co-workers in 1990.¹⁵⁴ Since then, other syntheses have been elaborated by the groups of Sakakiyama,¹⁵⁵ Esumi,¹⁵⁶ and Du.¹⁵⁷ To date, the most efficient synthesis is that developed by Du and co-workers, which resulted in a 51% overall yield (Scheme 38). The synthesis was attained in 10 steps starting from geraniol. Geraniol was converted to epoxy silyl ether via enantioselective Sharpless epoxidation, followed by protection of the hydroxyl functionality with TBSCl. The Yamamoto epoxide rearrangement induced by methylaluminum bis[4-bromo-2,6-di(*t*-butyl)phenoxide] (MABR) provided key intermediate **269** with the desired configuration of the quaternary chiral center.



Scheme 38. Construction of the quaternary chiral center by Sharpless epoxidation and Yamamoto rearrangement reported by Du and co-workers.¹⁵⁷

5.1.3 Application of Intramolecular C–H Insertion on Diazosulfonates in the Synthesis of (+)-Bakuchiol

The structure of (+)-bakuchiol is similar to that of citronellol, which is abundantly present in nature. Guided by earlier studies on the formation of δ -sultones from the corresponding alcohols, as well as the conversion of the obtained δ -sultones into δ -valerolactones,^{122, 142} it was envisioned that (+)-bakuchiol could be synthesized from commercially available citronellol by employing rhodium-catalyzed intramolecular C–H insertion to install the quaternary center in the structure (Scheme 39).



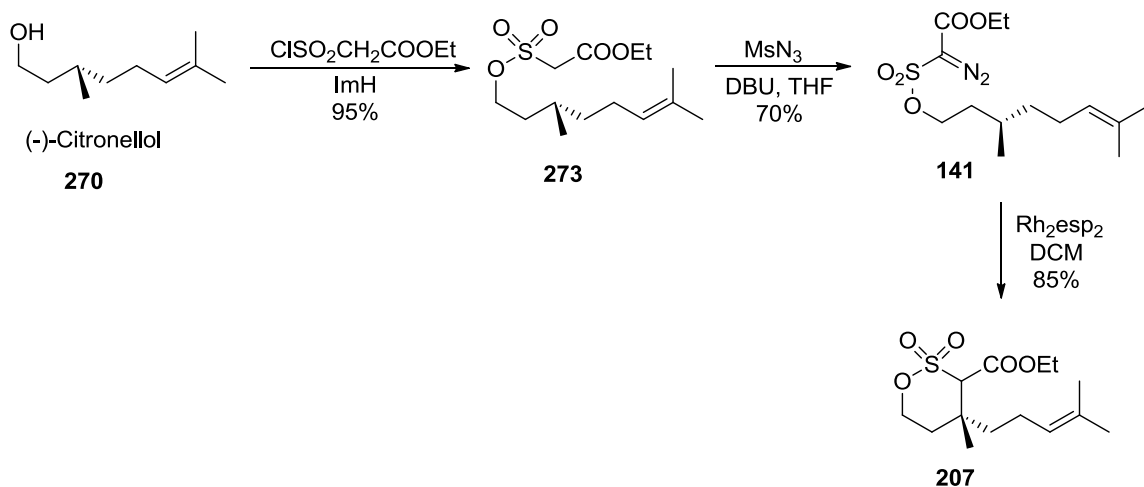
Scheme 39. Retrosynthetic disconnection for (+)-bakuchiol.

The exposure of sultone ester **207** to the SmI_2/DMPU reduction conditions was expected to form δ -valerolactone **271**. Its reduction to a diol, followed by protection of the hydroxyl groups and subsequent elimination would complete the synthesis of the key

intermediate **272**, that would then be modified to the final product (+)-bakuchiol.

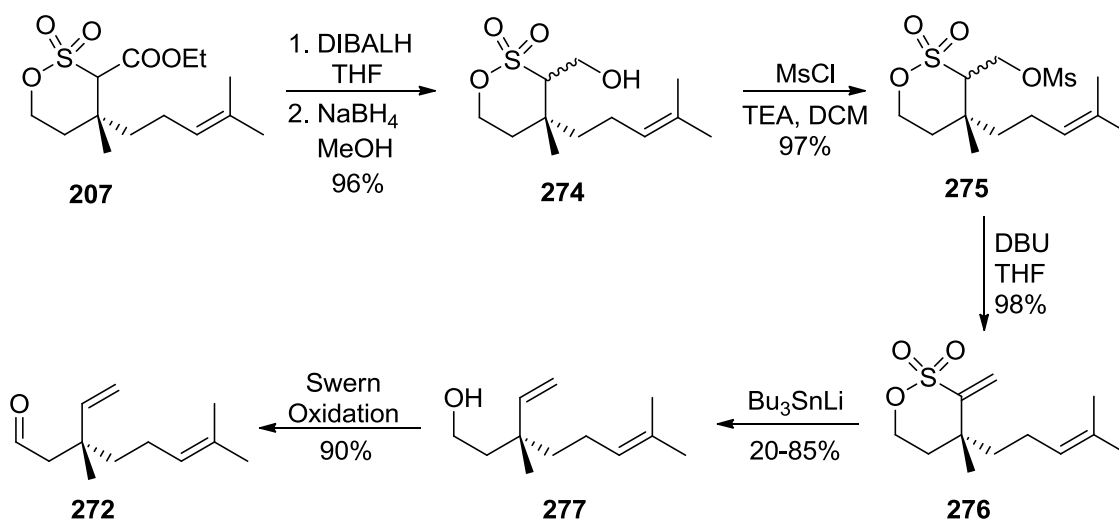
Unexpectedly, the conversion of the sultone ester to the δ -valerolactone proved futile as it afforded a mixture of inseparable products. Even so, the peaks corresponding to the more substituted double bond could not be identified by ^1H NMR – an indication that the double was sensitive to the reaction conditions and interfered in the reduction.

The enantioselective synthesis of (+)-bakuchiol was then achieved by employing the synthetic route outlined below (Scheme 40).¹³⁶ Rhodium-catalyzed intramolecular C–H insertion was used in the synthesis of sultone ester **207**. Basically, (*S*)-(-)- β -citronellol was treated with ethyl (chlorosulfonyl)acetate in the presence of imidazole in THF. The resulting sulfonate ester was exposed to diazotransfer conditions (MsN_3 , DBU, THF, 1 h, $-45\text{ }^\circ\text{C}$) to afford the diazosulfonate ester **141**. Rhodium-catalyzed intramolecular C–H insertion of **141** provided **207**.



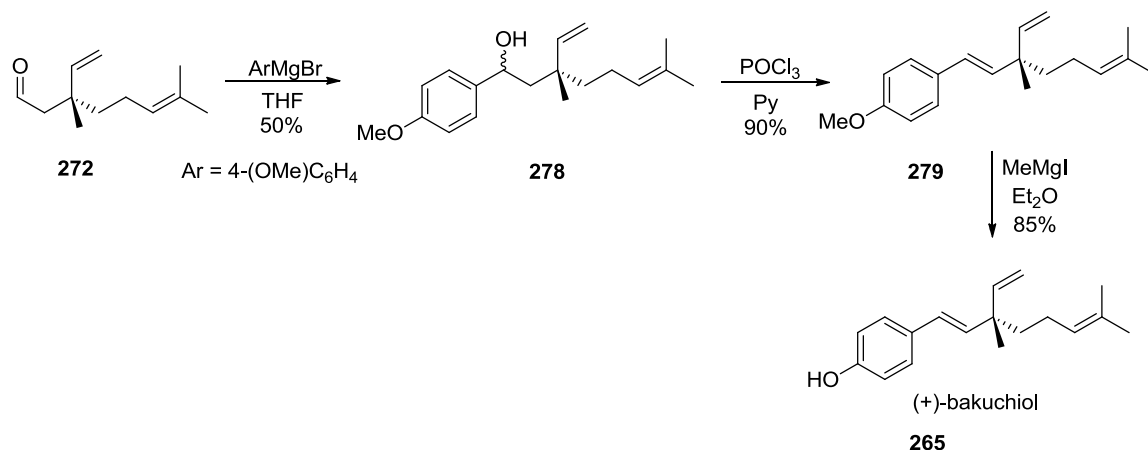
Scheme 40. Synthesis of δ -sultone **207** via rhodium-catalyzed intramolecular C–H insertion following procedure by Wolckenhauer and co-workers.¹²³

Reduction of sultone ester **207** in the presence of DIBAL followed by mesylation of the resulting alcohol provided mesylates **274**. Subsequent elimination followed by desulfonation in the presence of excess tributyltin lithium in THF resulted in alcohol **277**. Swern oxidation of **277** completed the synthesis of key aldehyde **272**.



Scheme 41. Synthesis of aldehyde **272**.¹³⁶

To complete the synthesis, the procedure reported by Du and co-workers was used. Treatment of aldehyde **272** with (4-methoxybenzyl)magnesium bromide gave alcohol **279**, which upon exposure to phosphoryl chloride in pyridine led to (+)-bakuchiol methyl ether **280**. Conversion of **280** to (+)-bakuchiol was achieved with methyl magnesium iodide at elevated temperatures.



Scheme 42. Synthesis of (+)-bakuchiol from an aldehyde following the procedure by Du and co-workers.¹⁵⁷

5.2 Studies towards Synthesis of (+)-Quebrachamine

5.2.1 Isolation and Biological Activity of (+)-Quebrachamine

(+)-Quebrachamine is an aspidosperma alkaloid, isolated from *Aspidosperma quebracho* tree bark.¹⁵⁸ The *Aspidosperma quebracho* tree, also known as white *quebracho* is common in South American countries. In general, *Aspidosperma quebracho* alkaloids (aspidospermine,¹⁵⁹ yohimbine,¹⁶⁰ quebrachamine,¹⁵⁸ and akuammidine¹⁶¹) have been reported to possess diverse pharmacological properties such as hypertensive, spasmolytic, diuretic, peripheral vasoconstrictor, arterial hypertensive, respiratory stimulant, uterine sedative, and local anesthetic.^{158, 162, 163}

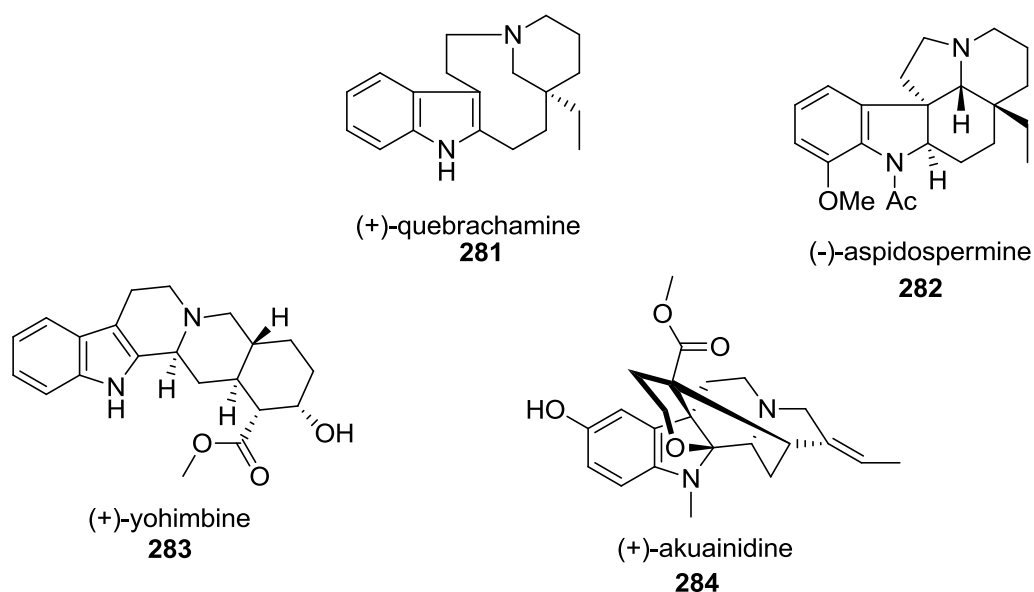
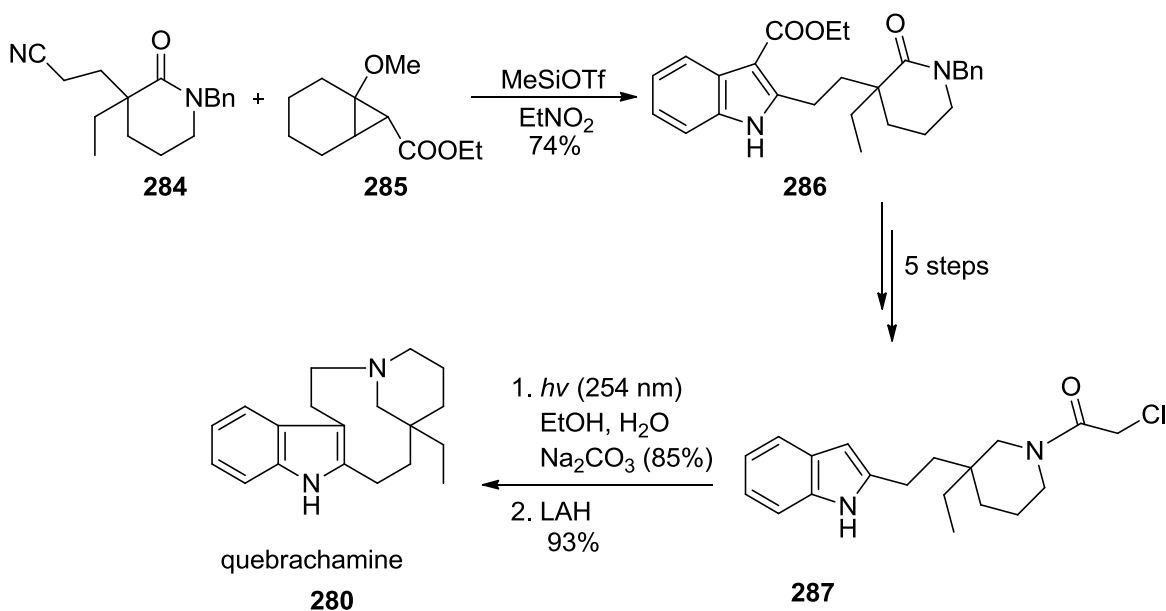


Figure 11. Aspidosperma alkaloids isolated from the white quebracho.

5.2.2 Previous Syntheses of Quebrachamine

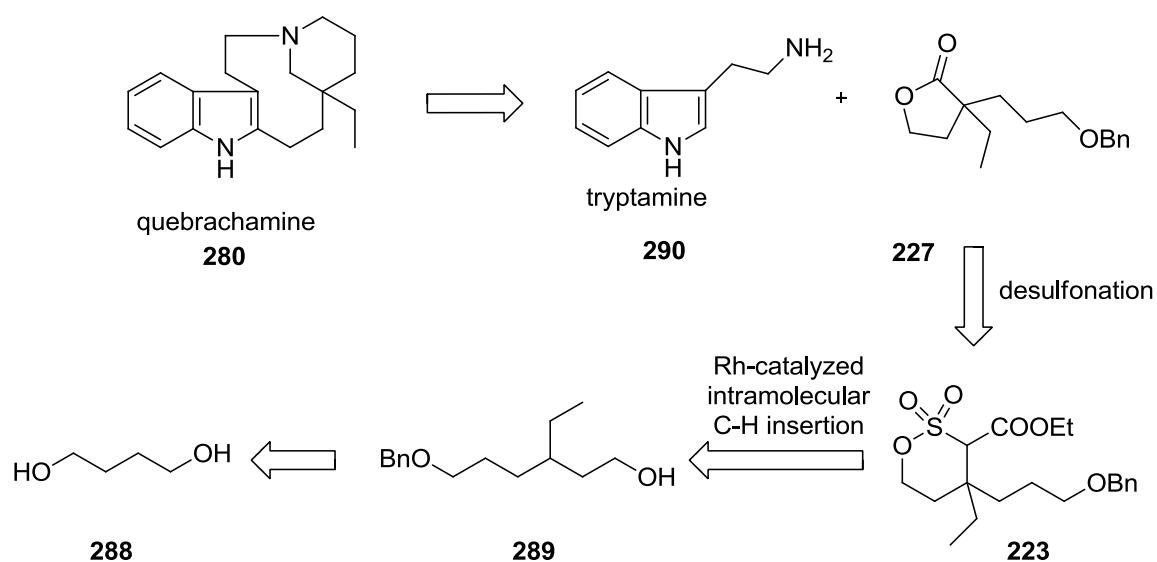
The molecular architecture of quebrachamine encompasses a synthetically challenging nine-membered ring. This, alongside its attractive pharmacological potential has attracted considerable and sustainable interest from researchers. The first total synthesis for quebrachamine was reported in 1963 by Stork and co-workers.¹⁵⁹ Since then, there have been 20 other reported syntheses for quebrachamine. To date, the most efficient synthesis for quebrachamine, elaborated by Bajtos and co-workers,¹⁶⁴ was achieved in 13 linear steps and 17.8% overall yield. The synthesis entailed forming the indole core via a formal [3+2] dipolar cycloaddition between a functionalized nitrile and donor-acceptor cyclopropane, and the synthetically challenging nine-membered ring was prepared by an efficient chloroacetamide photocyclization (Scheme 43).



Scheme 43. Total synthesis of (±)-quebrachamine via [3+2] cycloaddition and efficient chloroacetamide photocyclization reported by Bajtos and co-workers.¹⁶⁴

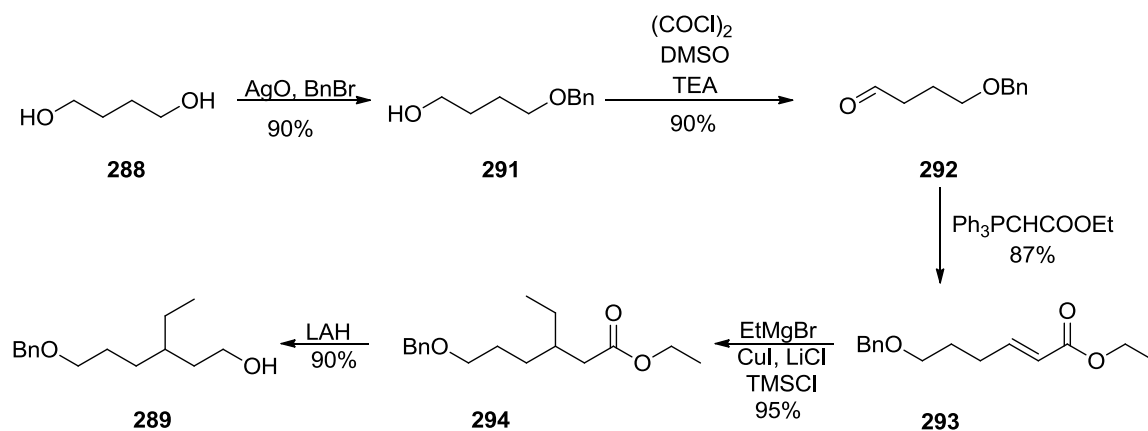
5.2.3 Application of Rhodium-Catalyzed Intramolecular C–H Insertion on Diazosulfonates towards the Synthesis of (+)-Quebrachamine

Inspired by the findings on oxidative desulfonation of δ -sultones to γ -butyrolactone using TBHP, it was envisioned that quebrachamine could be synthesized starting from commercially available 1,4-butanediol by employing the retrosynthetic disconnection shown on Scheme 44. Rhodium-catalyzed intramolecular C–H insertion will be used to implant the quaternary chiral center in the structure, followed by subsequent desulfonation to afford the key substituted γ -butyrolactone **227**.



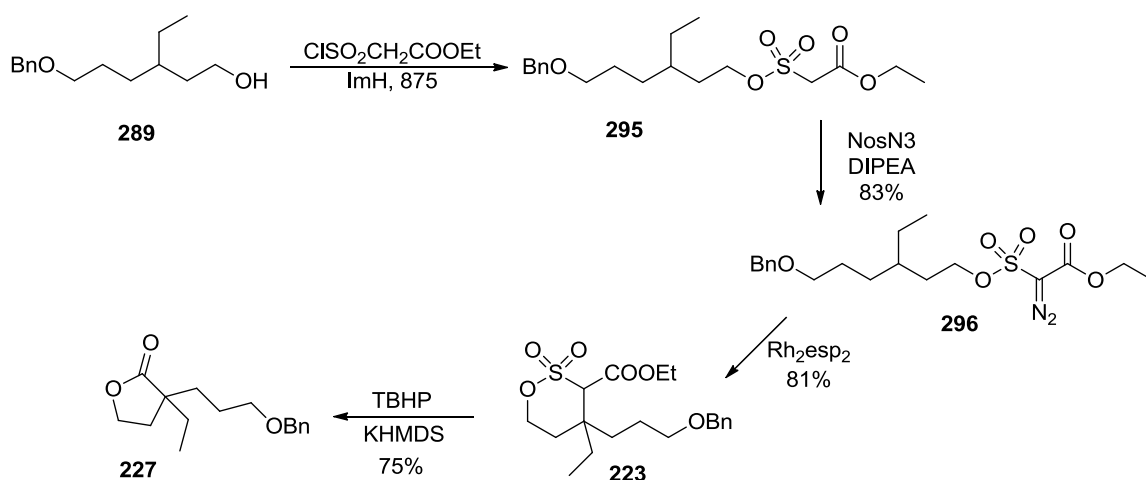
Scheme 44. Retrosynthetic analysis for the synthesis of (+)-quebrachamine.

The synthesis began with the preparation of alcohol **289**, which was completed in five steps from commercially available 1,4-butanediol **288** (Scheme 45). Mono-protection of the diol using silver oxide and benzyl chloride, followed by Swern oxidation of the resulting mono-protected alcohol led to aldehyde **292**. The Horner-Wadworth-Emmons (HWE) reaction of **292** with triethyl phosphonoacetate provided α,β -unsaturated ester **293**. Conjugate 1,4-addition of ethylmagnesium bromide to **293** followed by LAH reduction completed the synthesis of alcohol **289**.



Scheme 45. Preparation of alcohol **289**.

The coupling of alcohol **289** with ethyl (chlorosulfonyl)acetate in the presence of ImH in THF afforded sulfonate ester **295**, which was subjected to diazotransfer conditions (nosyl azide, DIPEA, DMF, 0 °C). Rhodium-catalyzed intramolecular C–H insertion of the obtained diazosulfonate **296** gave δ -sultone ester **223**. Oxidative desulfonation of **223** with TBHP/KHMDS resulted in the key substituted γ -butyrolactone **227**, which we intent in the future to couple with commercially available tryptamine **290**.



Scheme 46. Preparation of substituted γ -butyrolactone **223**.

5.3 Studies towards Synthesis of (-)-Mesembrine

5.3.1 Isolation and Biological Activity of (-)-Mesembrine

(-)-Mesembrine is the major alkaloid in *Sceletium tortuosum*, a groundcover plant native to Southern Africa.¹⁶⁵ Recent studies confirm that mesembrine is an effective serotonin re-uptake inhibitor as well as a potent inhibitor of the enzyme phosphodiesterase 4 (PDE4).¹⁶⁶ Mesembrine permits the brain to function with reduced levels of serotonin, allowing time for natural levels to build up.

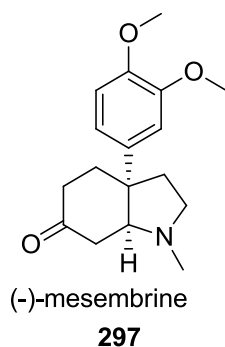
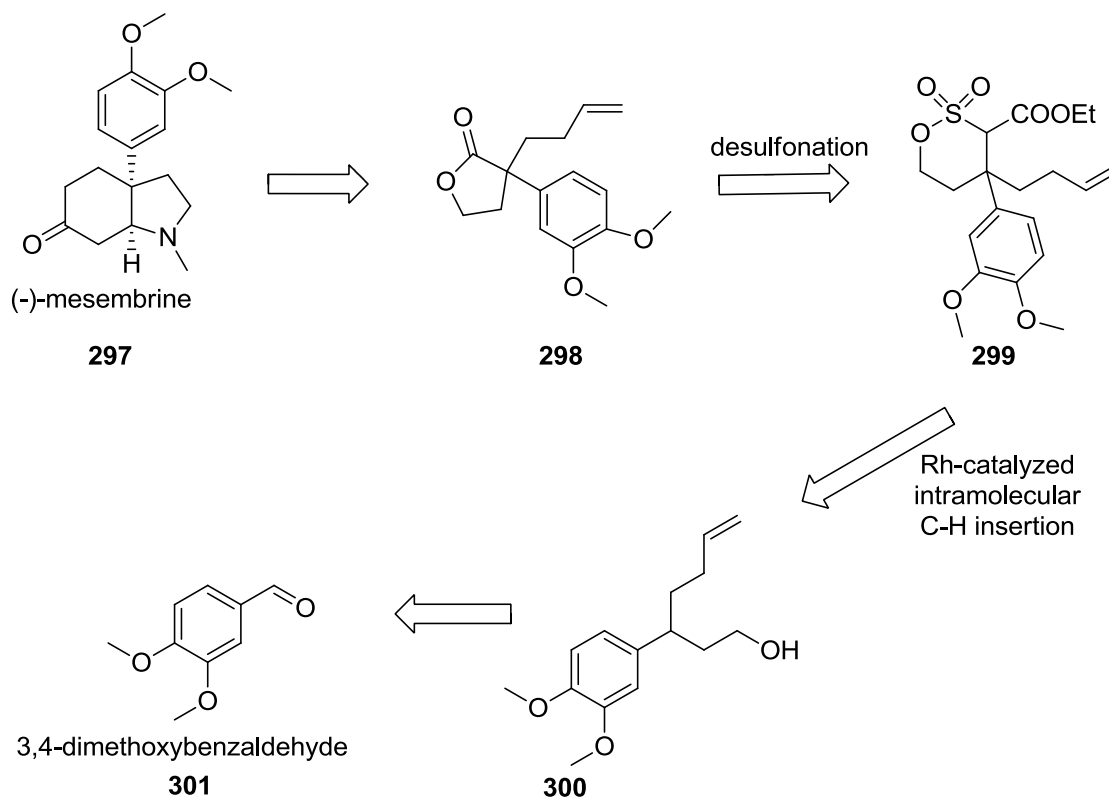


Figure 12. Structure of (-)-mesembrine.

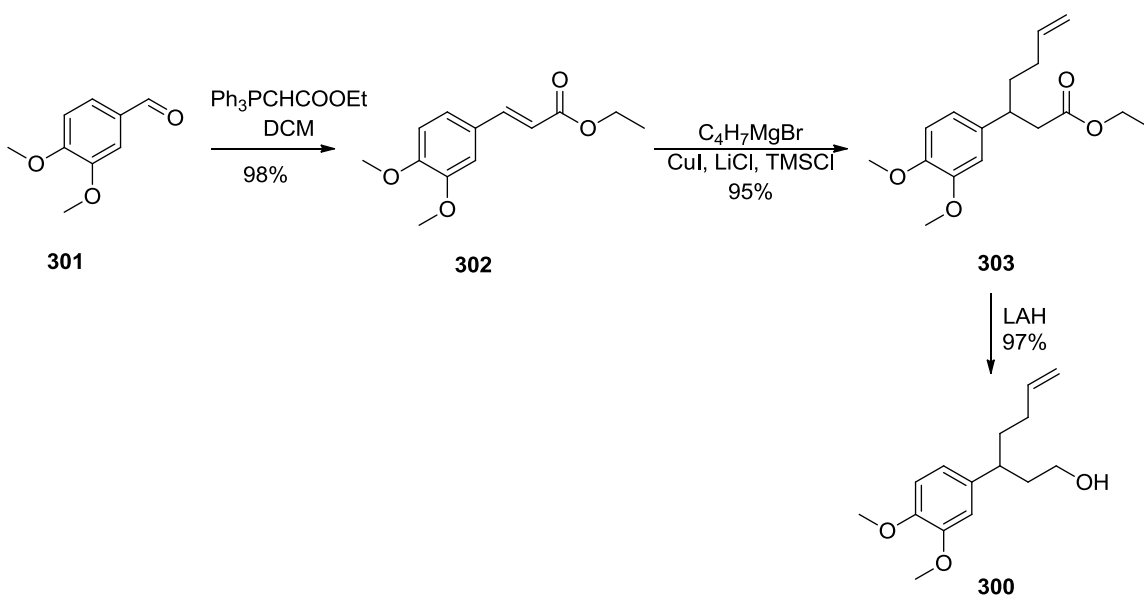
5.3.2 Application of Rhodium-Catalyzed Intramolecular C–H Insertion on Diazosulfonates towards the Synthesis of (-)-Mesembrine

The molecular structure of (-)-mesembrine and its attractive biological properties have made it one of the most interesting molecules in organic synthesis. To date, there are over 40 total and formal syntheses of this compound. In spite of the numerous syntheses of (-)-mesembrine, rhodium-catalysed intramolecular C–H insertion on diazosulfonates appeared to be a promising strategy that could be explored to install the quaternary chiral center in the structure, which upon desulfonation to a γ -butyrolactone would be critical to the completion of the synthesis (Scheme 47).



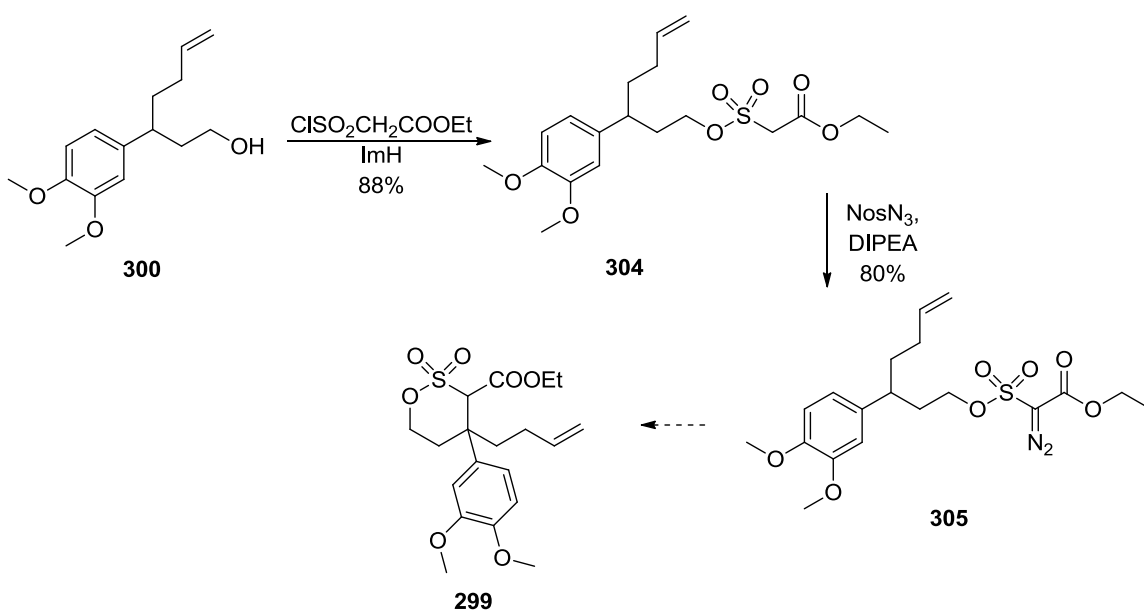
Scheme 47. Retrosynthetic disconnection for (-)-mesembrine.

The synthesis began with the preparation of alcohol **300**, which was obtained from commercially available 3,4-dimethoxybenzaldehyde **301** in three linear steps. HWE reaction of **301** afforded α,β -unsaturated ester **302**. Conjugate 1,4-addition of but-1-enylmagnesium bromide to **302**, followed by LAH reduction of the ester functionality completed the preparation of **300**.



Scheme 48. Preparation of alcohol **300**.

Treatment of alcohol **300** with ethyl (chlorosulfonyl)acetate in the presence of ImH in THF afforded sulfonate ester **304**, which upon exposure to diazotransfer condition (nosyl azide, DIPEA, DMF, $0\text{ }^\circ\text{C}$) led to diazosulfonate ester **305**. Unanticipatedly, several rhodium-catalyzed C–H insertion conditions proved futile and the insertion is still under investigation.



Scheme 49. Preparation of substituted δ -sultone **299**.

5.4 Experimental Section on Application of Rhodium-Catalyzed Intramolecular C–H Insertion on Diazo Sulfones and Sulfonates towards the Synthesis of Natural Products

All reactions were carried out under an inert nitrogen atmosphere unless otherwise stated.

All reagents were used as purchased without further purification unless otherwise stated.

$^1\text{H-NMR}$ (500 Hz) and $^{13}\text{C}\{^1\text{H}\}$ NMR (125 Hz) spectra were recorded on an Avance 500

Bruker spectrometer and calibrated using residual undeuterated solvent as internal

references. Coupling constants are given in Hz. IR spectra were recorded on a Perkin-

Elmer Spectrum 400 Series FTIR spectrometer. Specific rotations were measured on an

AUTOPOL III automatic polarimeter in anhydrous CHCl_3 using a 10 cm cell. HRMS

data were obtained on an Agilent 61969A TOF high resolution mass spectrometer using

electrospray ionization (ESI). Melting points were determined on a MEL-TEMP melting

point apparatus. Analytical TLC was performed using silica gel pre-coated TLC plates (E. Merck no. 5715-7). Flash chromatography was performed using 40-63 μm silica gel (Merck, Geduran, no. 11567-1) as the stationary phase. Tetrahydrofuran (THF) was dried by distilling it from sodium and benzophenone in a continuous still under a nitrogen atmosphere. Chloroform, dichloromethane and triethylamine were distilled from calcium hydride under an atmosphere of nitrogen.

Preparation of 4-(benzyloxy)butan-1-ol 291

To a stirred solution of 1,4-butanediol (1 equiv.) in DCM was added freshly prepared Ag_2O (1.5 equiv.) and benzyl bromide (1.1 equiv.). The reaction was stirred for 3 h and filtered through a silica gel pad. Evaporation of the solvent, followed by flash chromatography afforded **291**. Ag_2O was prepared by stirring equimolar solutions of AgNO_3 and NaOH in water for 5 min. The resulting brown precipitate was filtered and dried in for 20 min in an oven. The obtained solid was cooled to room temperature, crushed to a fine powder and used as described.

Preparation of 4-(benzyloxy)butanal 292

DMSO (1.19 g, 15.2 mmol) was added dropwise to a solution of $(\text{COCl})_2$ (0.968 g, 7.60 mmol) in CH_2Cl_2 (20 mL) at -78°C . After 15 min, a solution of alcohol **291** (0.688 g, 3.81 mmol) in CH_2Cl_2 (5 mL) was added dropwise to the reaction mixture at -78°C . After an additional 45 min, Et_3N (1.53 g, 15.2 mmol) was added dropwise to the reaction mixture. After stirring for an additional 1 h, the reaction mixture was quenched

with water, extracted with CH₂Cl₂, washed with brine, and dried with Na₂SO₄. The solvent was removed under reduced pressure to afford crude **292**. The crude product was purified by flash chromatography on silica gel using 3% ethyl acetate in hexanes as an eluent to afford **292** as colorless oil in 90% yield.

Preparation of (*E*)-ethyl 6-(benzyloxy)hex-2-enoate **293 and (*E*)-ethyl [3-(3,4-dimethoxy)phenyl]acrylate **302****

To a stirred solution of **292** or **301** (1.04 g, 9.36 mmol) in DCM (20 mL, 2.5 mL/mmol) was added (carbethoxymethylene)triphenylphosphorane (3.54 g, 1.1 equiv) and the combined reaction mixture further stirred vigorously at room temperature for 16 h. After, the reaction mixture was evaporated to afford a crude product, which was purified by flash chromatography.

Procedure for preparation of but-1-enylmagnesium bromide

An oven dried 100 mL round bottom flask equipped with a magnetic stirring bar and a septum was charged with LiCl (1.57 g, 37.0 mmol) and heated with a heat gun under high vacuum for 30 min. Magnesium turnings (1.80 g, 74.0 mmol) and THF were added and the magnesium activated with DIBALH (70.0 μL, 0.400 mmol). After stirring for 5 min, the suspension was cooled to -20 °C and 4-bromo-1-butene (4.00 g, 29.6 mmol) added slowly, after which it was further stirred at -20 °C for 1 h. The obtained solution was used for subsequent steps without purification.

Procedure for preparation of ethyl 6-benzyloxy-3-ethylhexanoate 294 and ethyl 3-[(3,4-dimethoxy)phenyl]-6-heptenoate 303

A 50 mL round bottom flask was charged with LiCl (29 mg, 0.68 mmol), CuI (65 mg, 0.34 mmol) and THF (5.0 mL, 2.5 mL/mol), and stirred at rt for 10 min until a pale yellow solution formed. The solution was cooled to 0 °C, **292** or **301** (850 mg, 3.41 mmol) was added followed by TMSCl (409 mg, 3.76 mmol) and the obtained mixture further stirred for 15 min. A solution of EtMgBr (5.0 mL, 2.1 mmol) was added dropwise until the color of the solution turned violet. After stirring for 3 h, the reaction mixture was poured onto 20 mL of saturated aqueous NH₄Cl solution, extracted with ether and dried over MgSO₄. The solvent was removed under reduced pressure and the crude product purified by flash chromatography.

Ethyl 6-benzyloxy-3-ethylhexanoate (294): Pale yellow oil. ¹H NMR (CDCl₃, 500 MHz): δ 7.3 (m, 5H), 4.40 (s, 2H), 4.02 (q, *J* = 7.2, 2H), 3.40 (t, *J* = 6.6, 2H), 2.17 (dd, *J* = 7.0, 2.2, 1H), 1.78 (q, *J* = 6.6, 1H), 1.58 (q, *J* = 6.6, 1H), 1.22-1.40 (m, 4H), 1.19 (t, *J* = 7.2, 3H), 0.82 (t, *J* = 7.5, 3H). ¹³C{¹H} NMR (CDCl₃, 125 MHz): δ 173.9 (C), 139.1 (C), 129.0 (CH), 128.0 (CH), 73.3 (CH₂), 71.0 (CH₂), 60.6 (CH₂), 39.1 (CH₂), 36.7 (CH), 30.3 (CH₂), 27.3 (CH₂), 26.6 (CH₂), 14.8 (CH₃), 11.1 (CH₃).

Ethyl 3-[(3,4-dimethoxy)phenyl]-6-heptenoate (303): Pale yellow oil. ¹H NMR (CDCl₃, 500 MHz): δ 6.76 (d, *J* = 8.1, 1H), 6.68 (ddd, *J* = 15.4, 8.1, 2.0, 2H), 5.68-5.76 (m, 1H), 4.88-4.93 (m, 2H), 4.00 (q, *J* = 7.0, 2H), 3.89 (s, 3H), 3.87(s, 3H), 3.01-3.06 (m, 1H), 2.54 (dddd, *J* = 14.8, 7.8, 7.2, 7.0, 2H), 1.86-1.90 (m, 2H), 1.62-1.74 (m, 2H), 1.11

(t, $J = 7.0$, 3H). $^{13}\text{C}\{^1\text{H}\}$ NMR (CDCl_3 , 125 MHz): δ 172.6 (C), 149.2 (CH), 147.9 (C), 138.5 (CH), 136.6 (C), 119.7 (CH), 115.1 (CH_2), 111.5 (CH_3), 111.2 (CH_3), 60.5 (CH_2), 56.2 (CH), 42.3 (CH_2), 41.6 (CH), 35.7 (CH_2), 31.8 (CH_2), 14.5 (CH_3).

Procedure for preparation of 6-benzyloxy-3-ethyl-1-hexanol 289 and 3-[(3,4-dimethoxy)phenyl]-hept-6-en-1-ol 300

A 50 mL round bottom flask charged with **294** or **303** (608 mg, 2.18 mmol) was stirred at 0 °C for 5 min followed by the addition of LAH (112 mg, 2.60 mmol). After stirring for 4 h, the reaction mixture was cooled to 0 °C and $\text{Na}_2\text{SO}_4 \cdot 10\text{H}_2\text{O}$ (5 g) added to it. The resulting suspension was further stirred for 15 min, after which it was filtered and the residue washed several times with hot EtOAc. The combined organic extract was evaporated under reduced pressure to afford a crude product which was purified by flash chromatography.

6-Benzyloxy-3-ethyl-1-hexanol (289): Pale yellow oil. ^1H NMR (CDCl_3 , 500 MHz): δ 7.4 (m, 5H), 4.53 (s, 2H), 3.68-3.72 (m, 2H), 3.50 (t, $J = 6.6$, 2H), 1.60-1.70 (m, 2H), 1.58 (q, $J = 6.6$, 2H), 1.28-1.48 (m, 6H), 0.84 (t, $J = 7.5$, 3H). $^{13}\text{C}\{^1\text{H}\}$ NMR (CDCl_3 , 125 MHz): δ 139.1 (C), 129.0 (C), 128.1 (CH), 127.9 (CH), 73.4 (CH_2), 71.3 (CH_2), 61.8 (CH_2), 36.9 (CH_2), 36.0 (CH), 30.1 (CH_2), 27.3 (CH_2), 26.4 (CH_2), 11.1 (CH_3).

3-[(3,4-Dimethoxy)phenyl]-hept-6-en-1-ol (300): Pale yellow oil. ^1H NMR (CDCl_3 , 500 MHz): δ 6.79 (d, $J = 8.1$, 1H), 6.69 (ddd, $J = 16$, 7.8, 1.8, 2H), 5.73-5.78 (m, 1H), 4.91-

4.95 (m, 2H), 3.88 (s, 3H), 3.86 (s, 3H), 3.44-3.54 (m, 2H), 2.66 (m, 1H), 1.62-1.80 (m, 3H), 1.90-1.93 (m, 3H), 1.42 (s, 1H). $^{13}\text{C}\{^1\text{H}\}$ NMR (CDCl_3 , 125 MHz): δ 149.3 (CH), 147.8 (C), 139.0 (CH), 137.7 (C), 120.0 (CH), 114.9 (CH_2), 111.6 (CH_3), 111.0 (CH_3), 61.5 (CH_2), 56.2 (CH), 41.9 (CH_2), 40.0 (CH), 36.5 (CH_2), 32.0 (CH_2).

Preparation of ethyl [(6-benzyloxy-3-ethyl)hexyloxysulfonyl]acetate 295 and ethyl [3-(3,4-dimethoxy)phenyl-6-heptenyloxysulfonyl]acetate 304

The necessary sulfonate esters were prepared following the procedure reported by Wolckenhauer and co-workers.¹²³

Ethyl [(6-benzyloxy-3-ethyl)hexyloxysulfonyl]acetate (295): Pale yellow oil. ^1H NMR (CDCl_3 , 500 MHz): δ 7.50 (m, 5H), 4.52 (s, 2H), 4.49 (t, $J = 7.0$, 2H), 4.40 (q, $J = 7.0$, 2H), 4.15 (s, 2H), 3.47 (t, $J = 6.6$, 2H), 1.74 (q, $J = 7.0$, 2H), 1.61 (q, $J = 6.6$, 2H), 1.48 (q, $J = 6.3$, 2H), 1.45-1.51 (m, 6H), 1.32-1.41 (m, 3H; overlapped with triplet), 1.31 (t, $J = 7$, 3), 0.88 (t, $J = 7$). $^{13}\text{C}\{^1\text{H}\}$ NMR (CDCl_3 , 125 MHz): δ 162.4 (C), 139.4 (C), 129.0 (C), 128.1 (CH), 127.9 (CH), 73.4 (CH_2), 71.3 (CH_2), 70.9 (CH_2), 63.2 (CH_2), 55.5 (CH_2), 36.0 (CH_2), 33.2 (CH), 29.7 (CH_2), 27.3 (CH_2), 25.9 (CH_2), 14.4 (CH_3), 11.1 (CH_3).

Ethyl [3-(3,4-dimethoxy)phenyl-6-heptenyloxysulfonyl]acetate (304): Pale yellow oil. ^1H NMR (CDCl_3 , 500 MHz): δ 6.80 (d, $J = 8.1$, 1H), 6.68 (ddd, $J = 13, 8.1, 2.2$, 2H), 5.72-5.78 (m, 1H), 4.94-4.96 (m, 2H), 4.26 (q, $J = 7.2$, 1H), 4.25 (ddd, $J = 14, 8.5, 6.3$,

1H), 4.00 (s, 2H), 3.91 (s, 3H), 3.88 (s, 3H), 2.68 (n, $J = 5$), 2H), 2.13-2.14 (m, 1H), 1.89-1.95 (m, 3H), 1.63-1.73 (m, 2H), 1.29 (t, $J = 7.2$, 3H). $^{13}\text{C}\{^1\text{H}\}$ NMR (CDCl_3 , 125 MHz): δ 162.3 (C), 149.5 (CH), 148.1 (C), 138.6 (CH), 136.0 (C), 119.9 (CH), 115.2 (CH_2), 111.8 (CH_3), 111.2 (CH_3), 71.1 (CH_2), 63.0 (CH_2), 56.2 (CH), 55.1 (CH_2), 41.2 (CH_2), 36.5 (CH_2), 36.3 (CH_2), 31.8 (CH_2), 14.3 (CH_3).

Procedure for preparation of ethyl [(6-benzyloxy-3-ethyl)hexyloxysulfonyl]diazooacetate 296 and ethyl [3-(3,4-dimethoxy)phenyl-6-heptenyloxysulfonyl]diazooacetate 305

To a solution of sulfonate **295** or **304** in DMF (2.5 mL/mmol) at 0 °C was added nosyl azide (1.1 equiv.) followed by DIPEA (2 equiv.). The temperature was maintained at 0 °C and the reaction mixture stirred for 7 h after which the reaction was complete as indicated by TLC analysis. The reaction mixture was then taken up in EtOAc, washed thrice with brine. The organic phase was dried over Na_2SO_4 and evaporated to give a crude product which was purified by flash chromatography.

Ethyl [(6-benzyloxy-3-ethyl)hexyloxysulfonyl]diazooacetate (296): Pale yellow oil. ^1H NMR (CDCl_3 , 500 MHz): δ 7.30 (m, 5H), 4.44 (s, 2H), 4.32 (t, $J = 7.0$, 2H), 4.25 (q, $J = 7.0$, 2H), 3.40 (t, $J = 6.6$, 2H), 1.66 (q, $J = 7$, 2H), 1.53 (q, $J = 6.6$, 2H), 1.40 (q, $J = 6.3$, 2H), 1.20-1.32 (m, 7H; overlapped with triplet), 0.80 (t, $J = 7$). $^{13}\text{C}\{^1\text{H}\}$ NMR (CDCl_3 , 125 MHz): δ 160.0 (C), 139.1 (C), 129.0 (C), 128.1 (CH), 73.4 (CH_2), 72.7 (CH_2), 71.2 (CH_2), 63.2 (CH_2), 35.8 (CH_2), 32.9 (CH), 29.7 (CH_2), 27.3 (CH_2), 25.9 (CH_2), 14.9 (CH_3), 11.1 (CH_3).

Ethyl [3-(3,4-dimethoxy)phenyl-6-heptenyloxysulfonyl]diazoacetate (305): Pale yellow oil. ^1H NMR (CDCl_3 , 500 MHz): δ 6.81 (d, $J = 8.1$, 1H), 6.70 (ddd, $J = 13$, 8.1, 1.8, 2H), 5.73-5.78 (m, 1H), 4.93-4.97 (m, 2H), 4.32 (q, $J = 7.2$), 4.25 (ddd, $J = 15$, 8.8, 5.6), 3.91 (s, 3H), 3.87 (s, 3H), 2.70 (n, $J = 5.0$), 2H), 2.12-2.17 (m, 1H), 1.88-1.94 (m, 3H), 1.66-1.74 (m, 2H), 1.30 (t, $J = 7.2$), 3H). $^{13}\text{C}\{^1\text{H}\}$ NMR (CDCl_3 , 125 MHz): δ 159.7 (C), 149.5 (CH), 148.1 (C), 138.6 (CH), 135.9 (C), 119.9 (CH), 115.2 (CH_2), 111.7 (CH_3), 111.1 (CH_3), 72.1 (CH_2), 63.0 (CH_2), 56.3 (CH), 56.2 (CH), 55.1 (CH_2), 41.2 (CH_2), 36.3 (CH_2), 31.8 (CH_2), 14.6 (CH_3).

Preparation of 3-carbethoxy-4-(3-benzyloxy)propyl-4-ethyl-1,2-oxathiane-2,2-dioxide 223

To a suspension of Rh_2esp_2 catalyst (1 mol%) in CH_2Cl_2 (4 mL/mmol), a solution of **296** (1 equiv.) in CH_2Cl_2 (2 mL/mmol) was added at rt over a period of 1 h using a syringe pump. Upon completion of the addition, the reaction mixture was stirred at rt for additional 8 h. All volatiles were removed under reduced pressure. The crude reaction mixture was separated on silica column (ethyl acetate–hexanes, 30%).

3-Carbethoxy-4-(3-benzyloxy)propyl-4-ethyl-1,2-oxathiane-2,2-dioxide (223): Pale yellow oil. ^1H NMR (CDCl_3 , 500 MHz): δ 7.30-7.40 (m, 5H), 4.64-4.67 (m, 2H), 4.49-4.55 (m, 2H), 4.52 (s, 2H; overlapped with multiplet), 4.48 (s, 2H), 3.93 (d, $J = 4.7$, 2H), 3.41 (t, $J = 6.6$, 2H), 3.43-3.58 (m, 2H), 3.28-3.42 (m, 2H), 1.88-1.20 (q, $J = 6.6$, 2H), 1.40-1.64 (q, $J = 6.3$, 2H), 1.22-1.38 (m, 7H; overlapped with triplet), 0.84-0.94 (t, $J = 7.0$, 3H). $^{13}\text{C}\{^1\text{H}\}$ NMR (CDCl_3 , 125 MHz): δ 160.0 (C), 139.1 (C), 129.0 (C), 128.1

(CH), 73.4 (CH₂), 72.7 (CH₂), 71.2 (CH₂), 63.2 (CH₂), 35.8 (CH₂), 32.9 (CH), 29.7 (CH₂), 27.3 (CH₂), 25.9 (CH₂), 14.9 (CH₃), 11.1 (CH₃).

APPENDICIES

APENDIX I: LIST OF ABBREVIATIONS AND ACRONYMS

1,2-DCE	1,2-dichloroethane
acam	acetamide
Ac	acetate
B3LYP	Becke, 3-parameter, Lee-Yang-Parr
BARF	tetra-aryl borate
Bn	benzyl
Bu	butyl
cap	caprolactam
DBU	1,8-diazabicyclo[5.4.0]undec-7-ene
DCC	<i>N,N'</i> -dicyclohexylcarbodiimide
DCM	dichloromethane
DEPT	distortionless enhancement by polarization transfer
DIBAL-H	diisobutylaluminum hydride
DIPEA	<i>N,N</i> -diisopropylethylamine
DMAP	dimethylaminopyridine
DMPU	<i>N,N'</i> -dimethylpropyleneurea
DMF	<i>N,N</i> -dimethylformamide
DMSO	dimethyl sulfoxide
DOSP	<i>N</i> -(<i>p</i> -dodecylphenylsulfonyl)prolinate
DPT	diisopropyltartrate
EDG	electron-donating group
EWG	electron-withdrawing group
er	enantiomeric ratio

Et	ethyl
esp	$\alpha, \alpha, \alpha, \alpha$ -tetramethyl-1,3-benzenedipropionate
FDA	food and drug administration
HMPA	hexamethylphosphoramide
HRMS	high resolution mass spectrometry
HWE	Horner-Wadsworth-Emmons
Hz	hertz
ImH	imidazole
HMDS	hexamethyldisilazane
LAH	lithium aluminum hydride
LDA	lithium diisopropylamide
MABR	methylaluminum bis[4-bromo-2,6-di(<i>tert</i> -butyl)phenoxide]
<i>m</i> -CPBA	<i>meta</i> -chloroperoxybenzoic acid
MEPY	methyl 2-pyrrolidone-5-carboxylate
MEOX	methyl 2-oxazolidone-4-carboxylate
MPPIM	methyl (3-phenylpropanoyl) imidazolidin-2-one-4-carboxylate
Ms	mesyl
NMR	nuclear magnetic resonance
NOE	nuclear overhauser effect
Nos	nosyl
nta	<i>N</i> -naphthaloyl alanate
ntpa	<i>N</i> -naphthaloyl phenylalanate
nttl	<i>N</i> -naphthaloyl <i>tert</i> -butylalanate
oct	octoate

OTF	trifluoromethanesulfonate
pfb	perfluorobutyrate
ptad	<i>N</i> -phthaloyl adamantyl leucinate
ptpa	<i>N</i> -phthaloyl phenyl leucinate
pttl	<i>N</i> -phthaloyl- <i>tert</i> -leucinate
Py	pyridine
rt	room temperature
S _N 1	unimolecular nucleophilic substitution
S _N 2	bimolecular nucleophilic substitution
TBHP	<i>tert</i> -butyl hydroxyperoxide
TBDPS	<i>tert</i> -butyldiphenylsilyl
TBDPS	<i>tert</i> -butyldiphenylsilyl
TBS	<i>tert</i> -butyldimethylsilyl
TEA	triethylamine
tfa	trifluoroacetate
THF	tetrahydrofuran
TIPS	triisopropylsilyl
TLC	thin layer chromatography
TMS	tetramethylsilane
TMS	trimethylsilyl
tpa	triphenyl acetate
TPAP	tetrapropylammonium perruthenate
Tol	tolyl
Ts	<i>p</i> -toluenesulfonyl
TS	transition state

APENDIX II: SELECTED SPECTRA, FIGURES 13–150

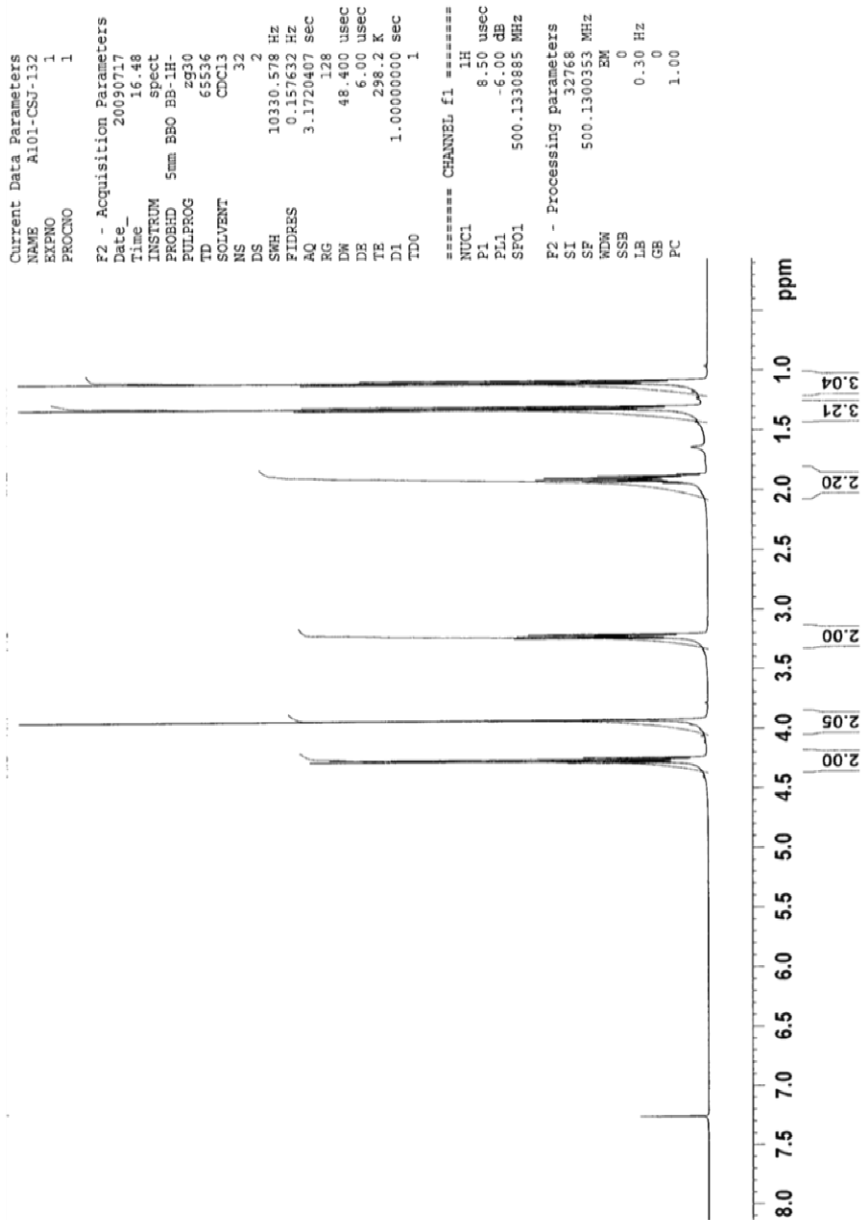


Figure 13. ^1H NMR (500 MHz) spectrum of ethyl (propylsulfonyl)acetate (**155.1**) in CDCl_3 .

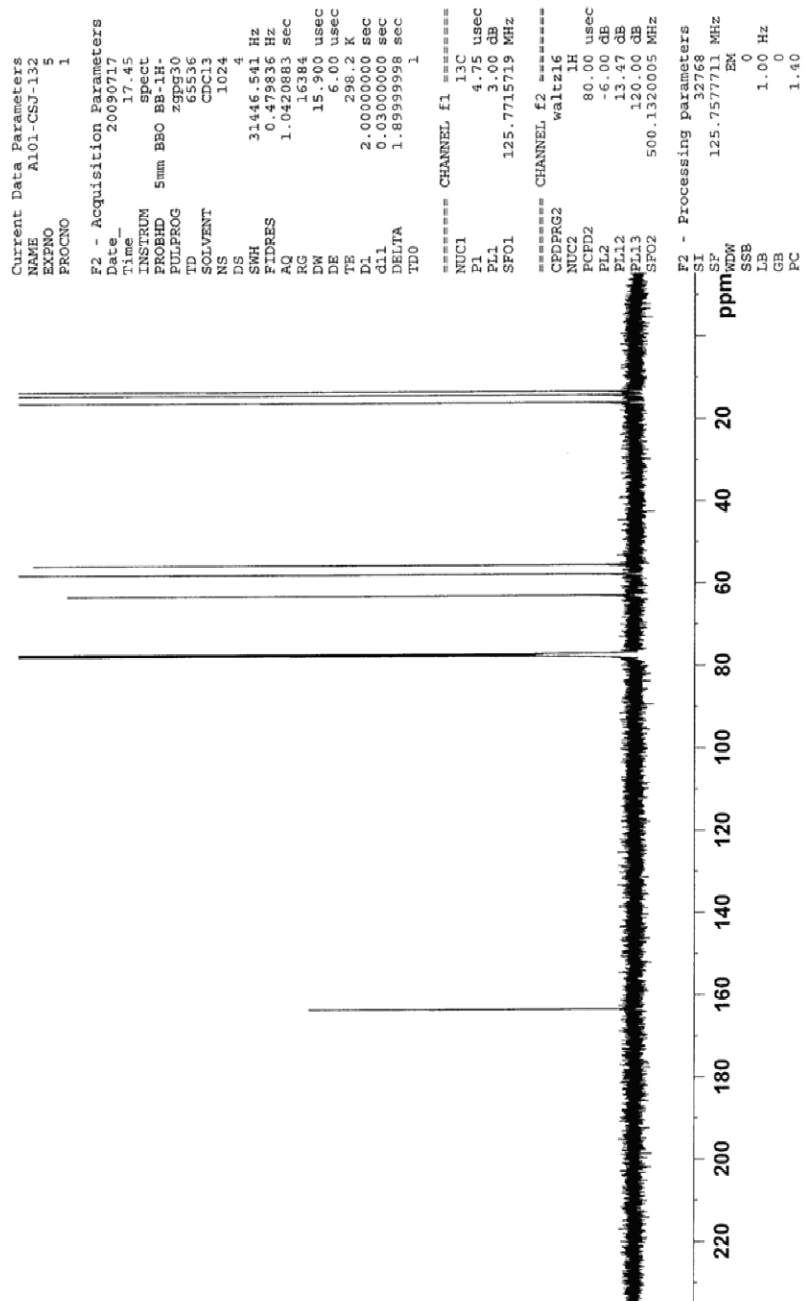


Figure 14. $^{13}\text{C}\{^1\text{H}\}$ NMR (125 MHz) spectrum of ethyl (propylsulfonyl)acetate (**155.1**) in CDCl_3 .

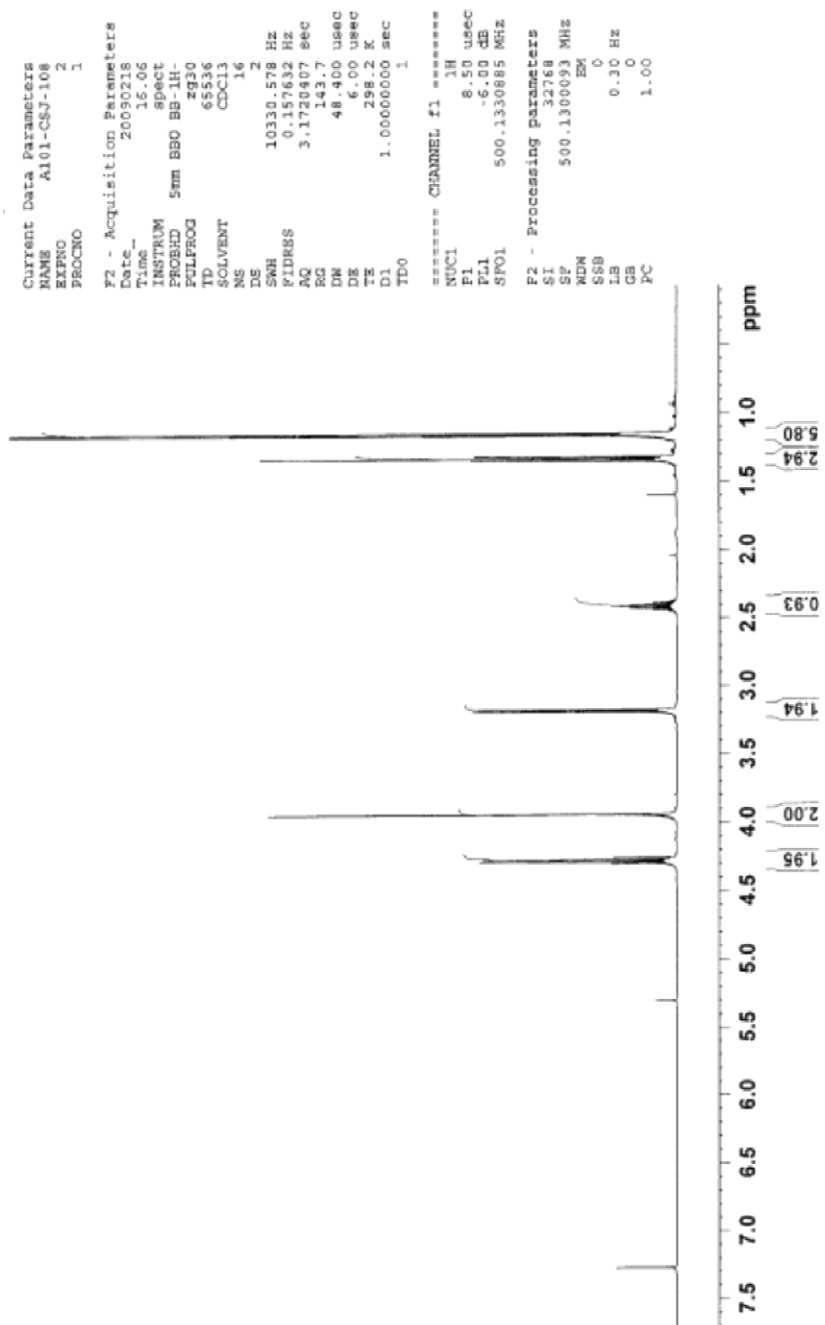


Figure 15. ^1H NMR (500 MHz) spectrum of ethyl (2-methylpropylsulfonyl)acetate (**156.1**) in CDCl_3 .

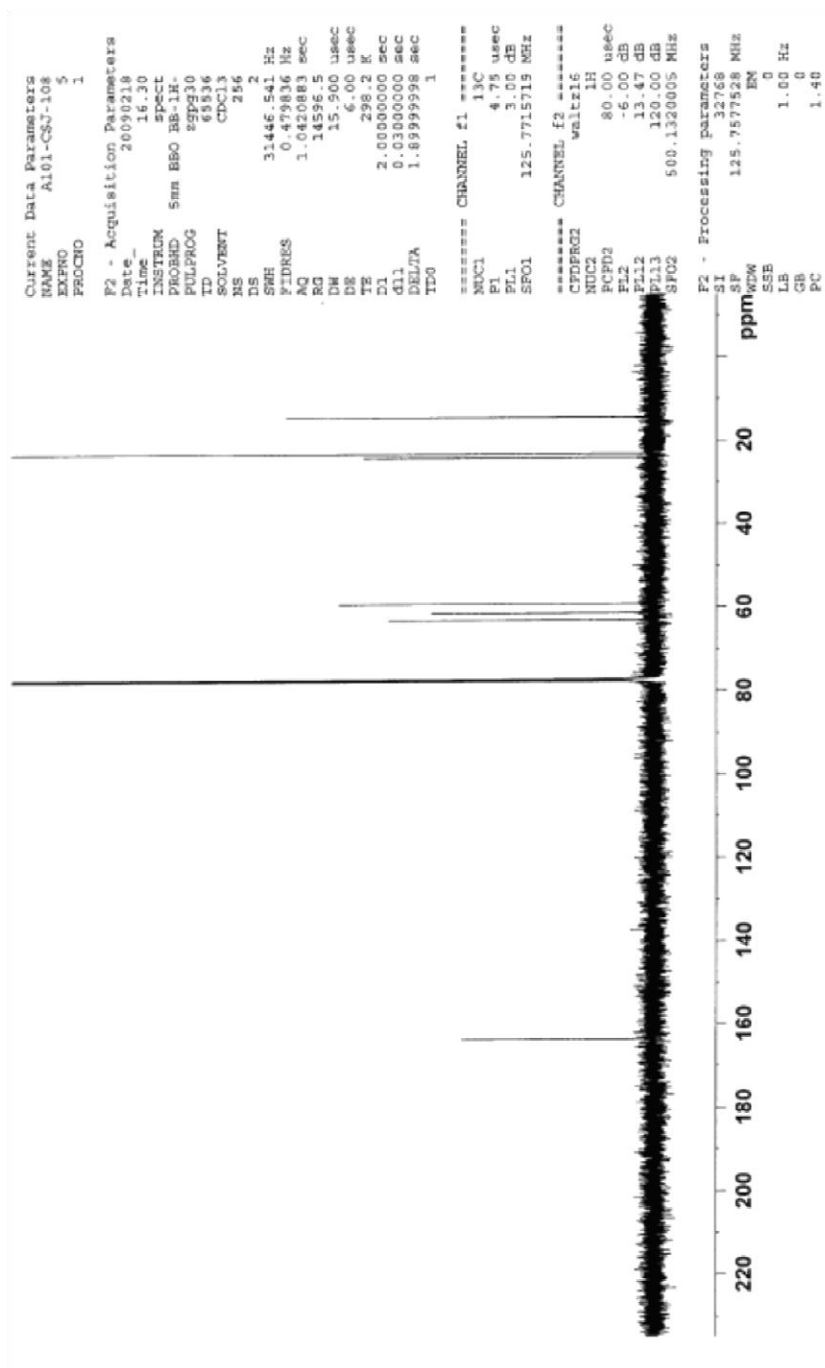


Figure 16. $^{13}\text{C}\{^1\text{H}\}$ NMR (125 MHz) spectrum of ethyl (2-methylpropylsulfonyl)acetate (**156.1**) in CDCl_3 .

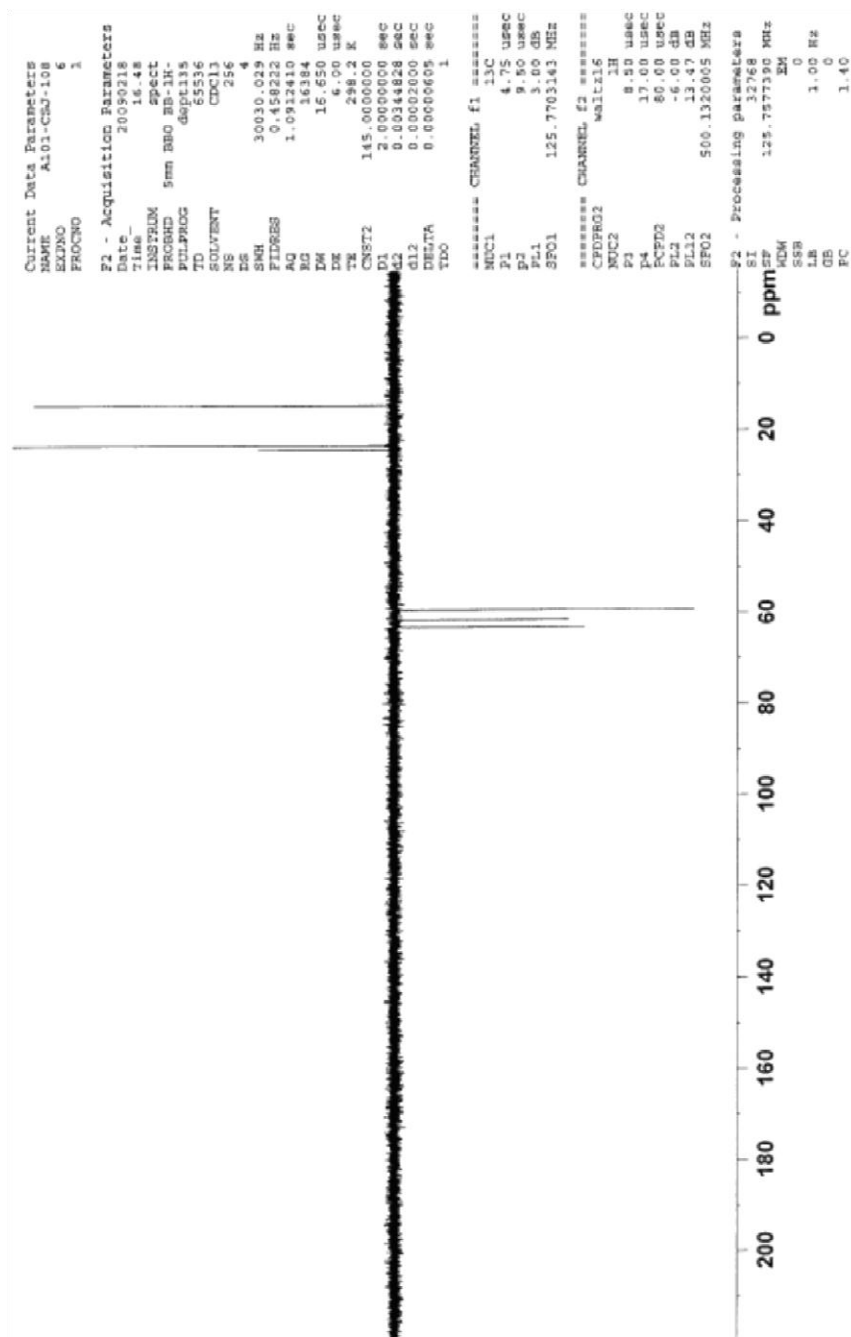


Figure 17. DEPT 135 NMR (125 MHz) spectrum of ethyl (2-methylpropylsulfonyl)acetate (**156.1**) in CDCl_3 .

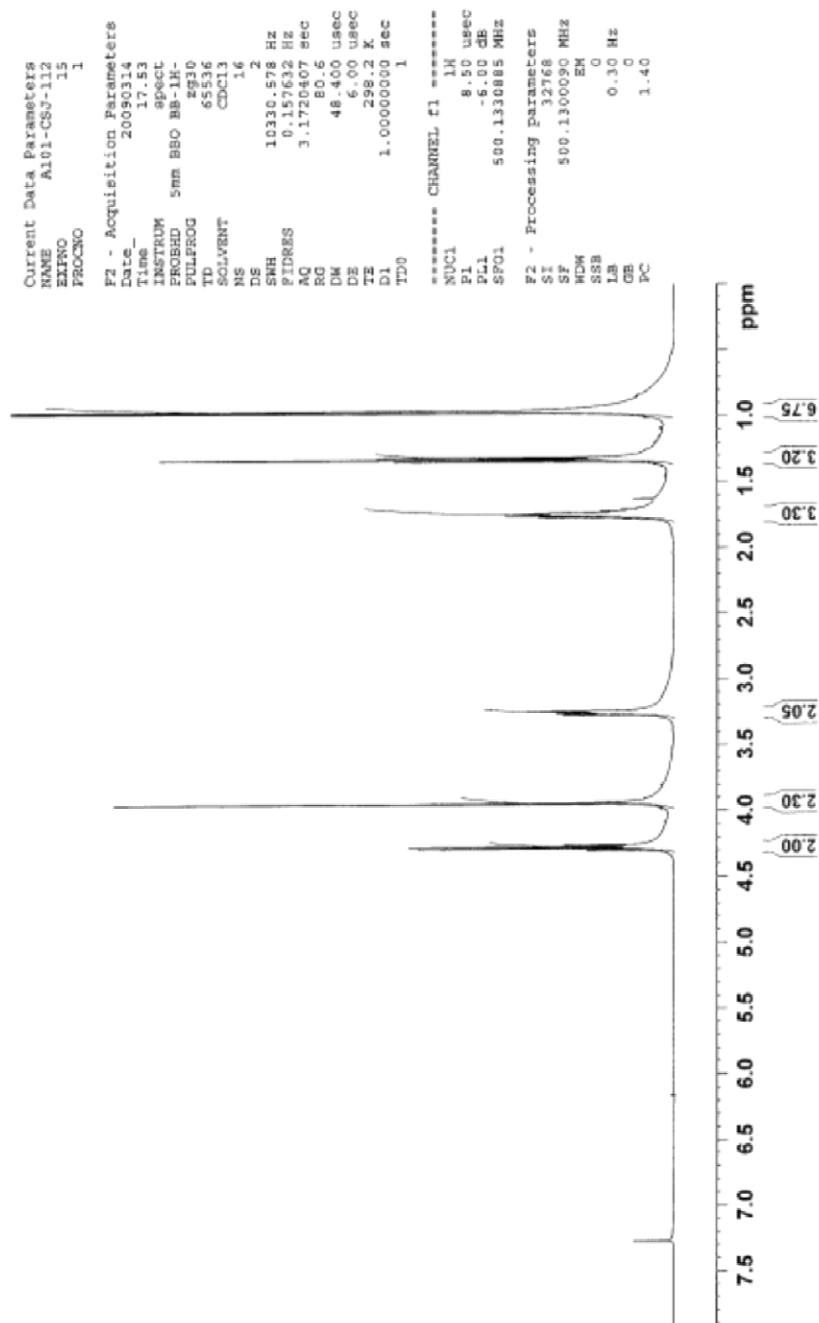


Figure 18. ^1H NMR (500 MHz) spectrum of ethyl (3-methylbutylsulfonyl)acetate (**160.1**) in CDCl_3 .

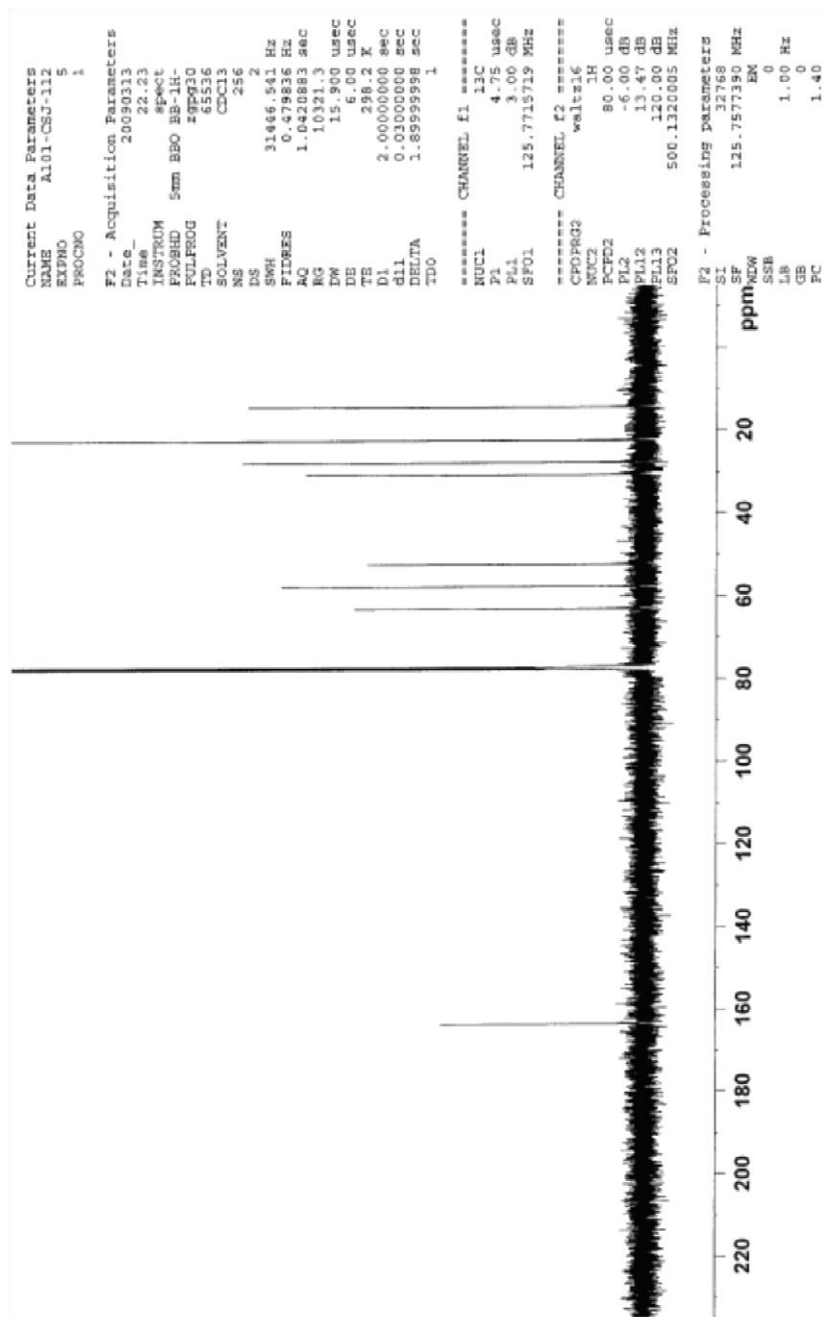


Figure 19. $^{13}\text{C}\{^1\text{H}\}$ NMR (125 MHz) spectrum of ethyl (3-methylbutylsulfonyl)acetate (**160.1**) in CDCl_3 .

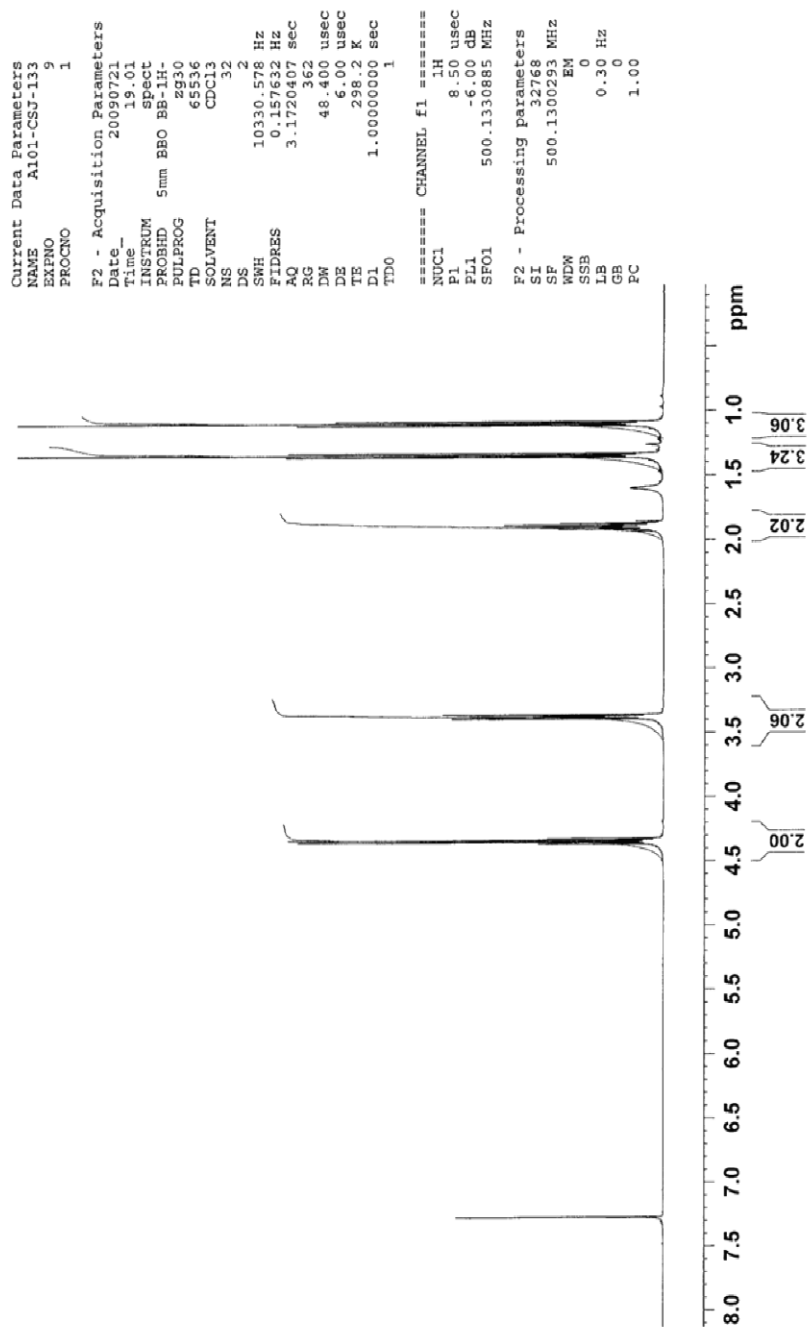


Figure 20. ^1H NMR (500 MHz) spectrum of ethyl (propylsulfonyl)diazoacetate (**158.2**) in CDCl_3 .

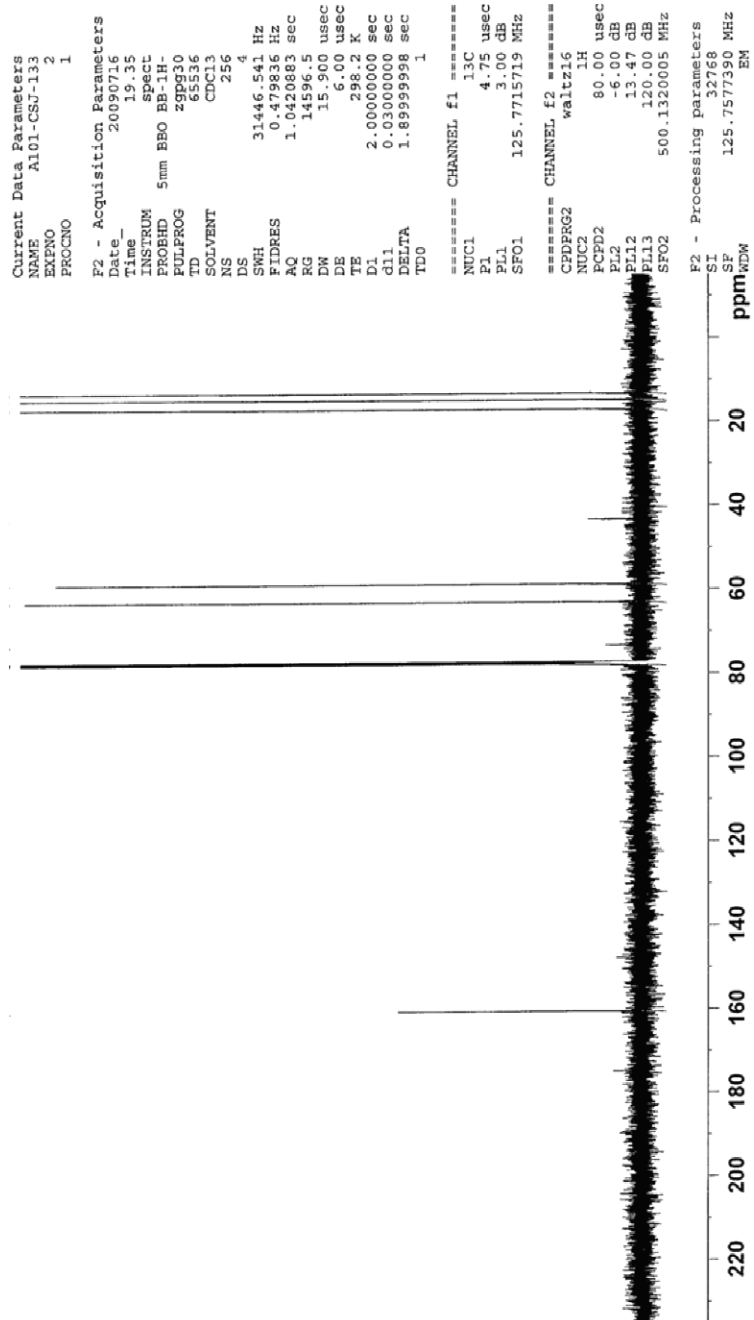


Figure 21. $^{13}\text{C}\{^1\text{H}\}$ NMR (125 MHz) spectrum of ethyl (propylsulfonyl)diazoacetate (**158.2**) in CDCl_3 .

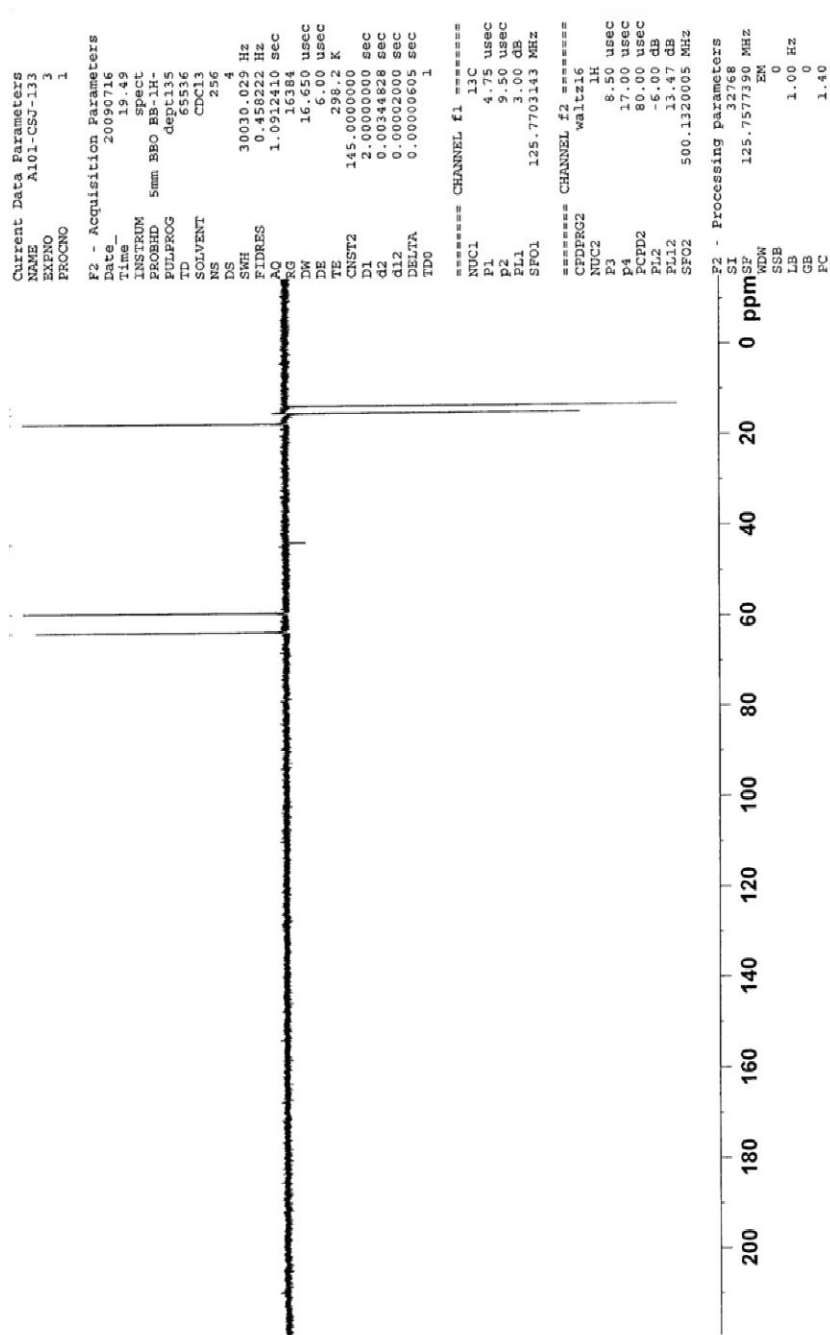


Figure 22. DEPT 135 NMR (125 MHz) spectrum of ethyl (propylsulfonyl)diazoacetate (**158.2**) in CDCl₃.

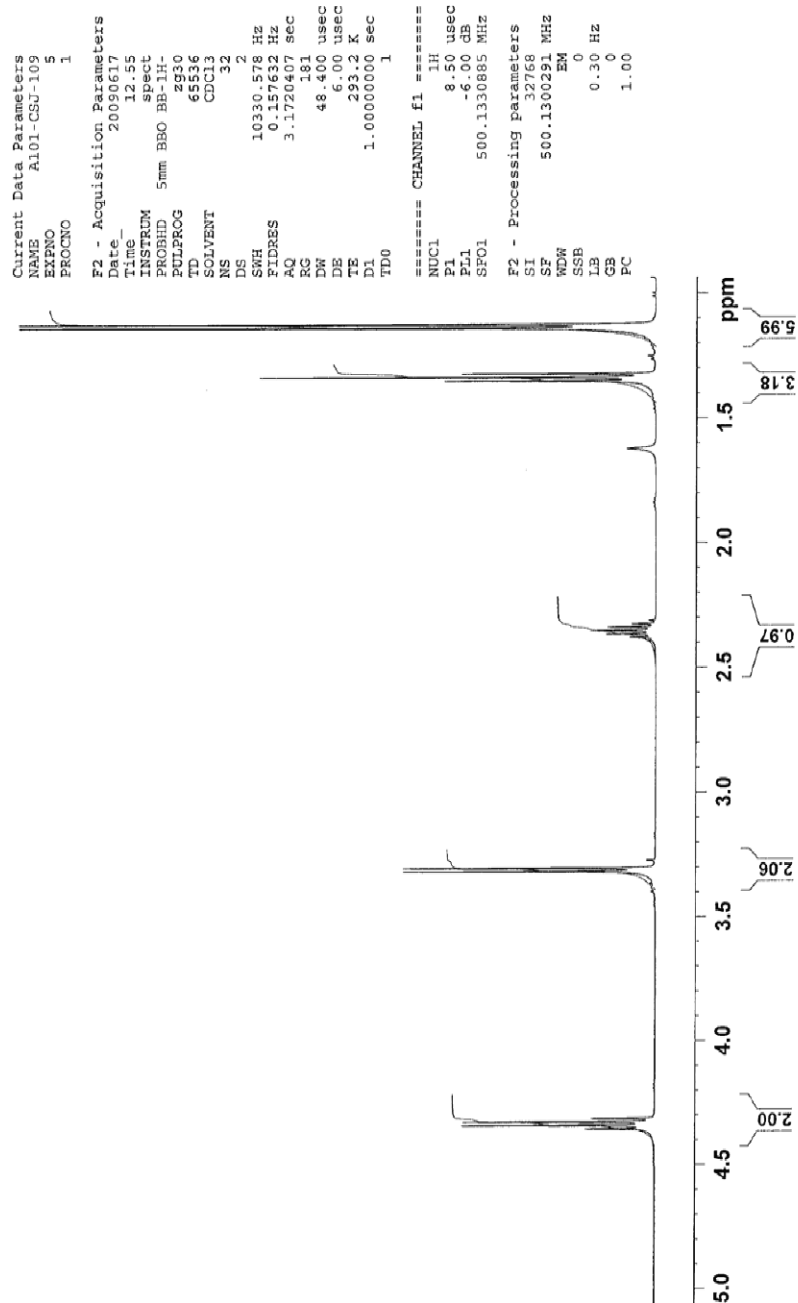


Figure 23. ^1H NMR (500 MHz) spectrum of ethyl (2-methylpropylsulfonyl)diazoacetate (**159.2**) in CDCl_3 .

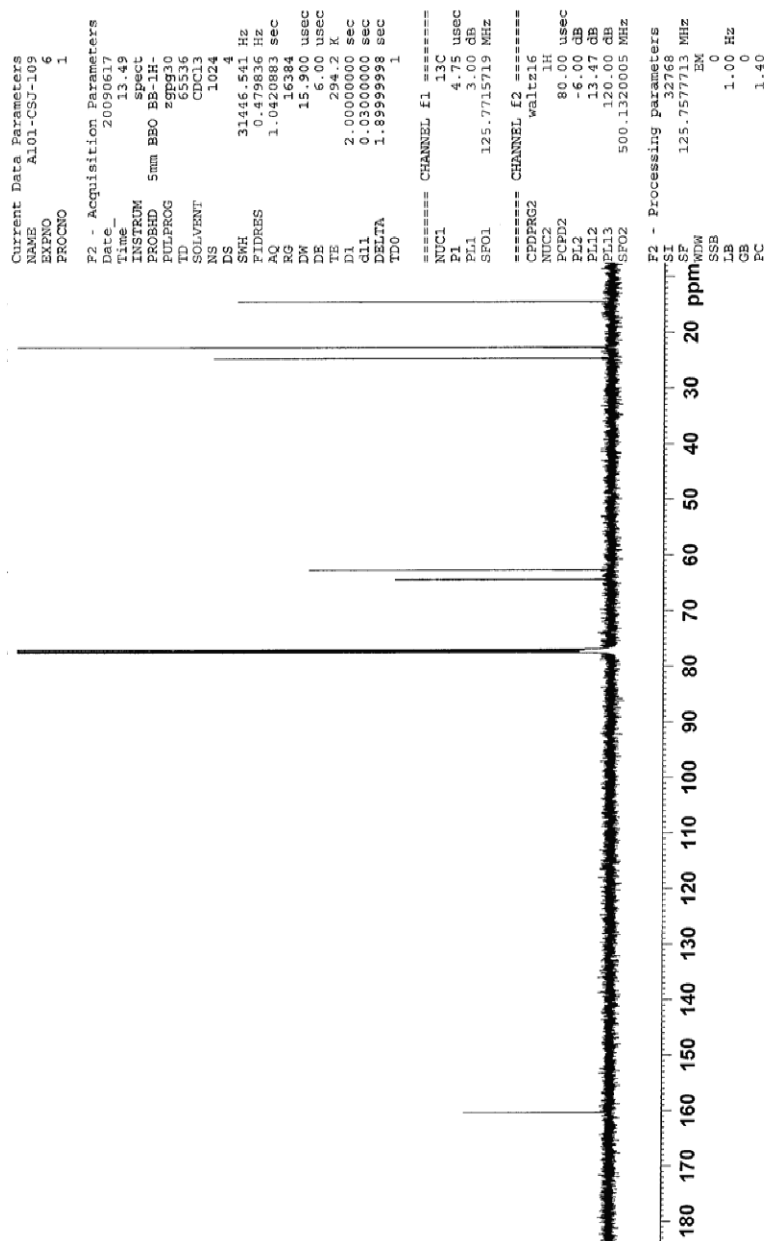


Figure 24. $^{13}\text{C}\{^1\text{H}\}$ NMR (125 MHz) spectrum of ethyl (2-methylpropylsulfonyl)diazoacetate (**159.2**) in CDCl_3 .

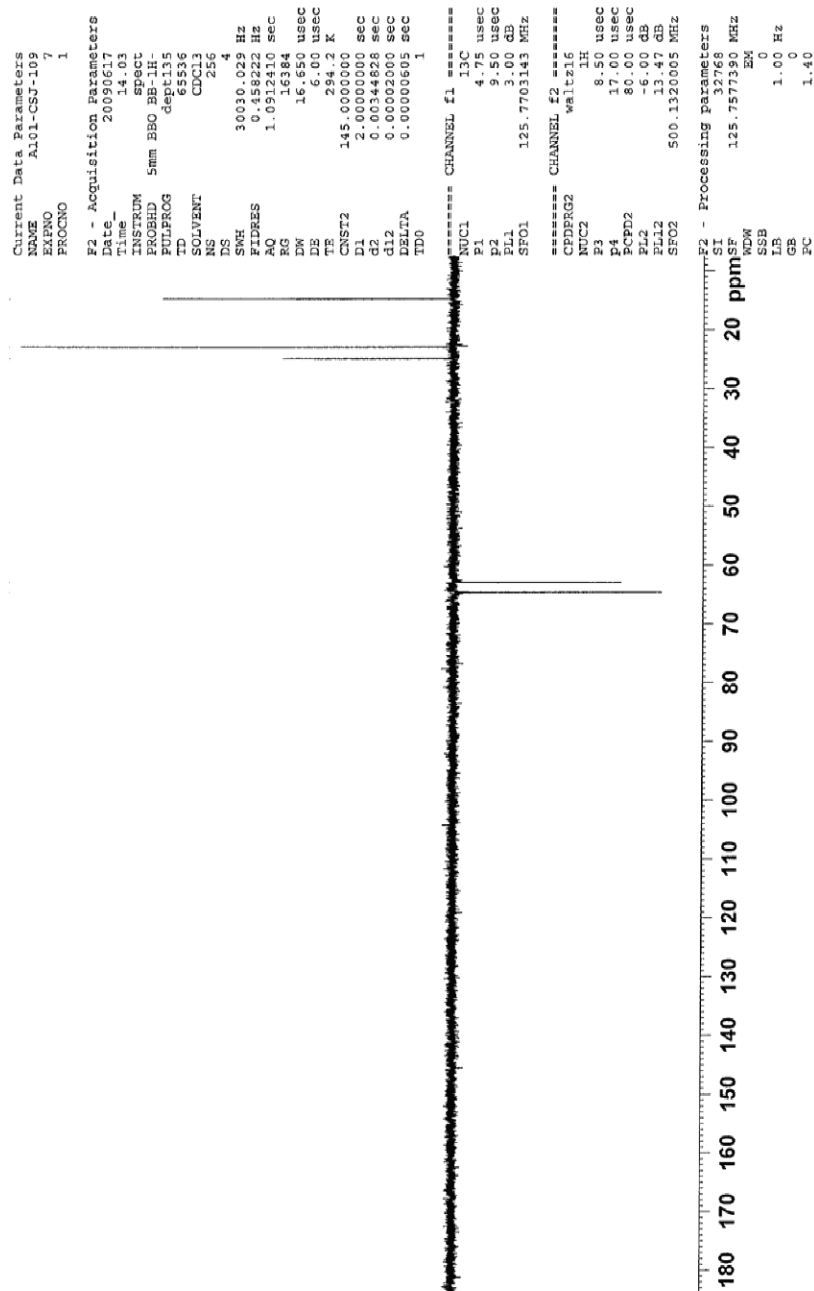


Figure 25. DEPT 135 NMR (125 MHz) spectrum of ethyl (2-methylpropylsulfonyl)diazoacetate (**159.2**) in CDCl_3 .

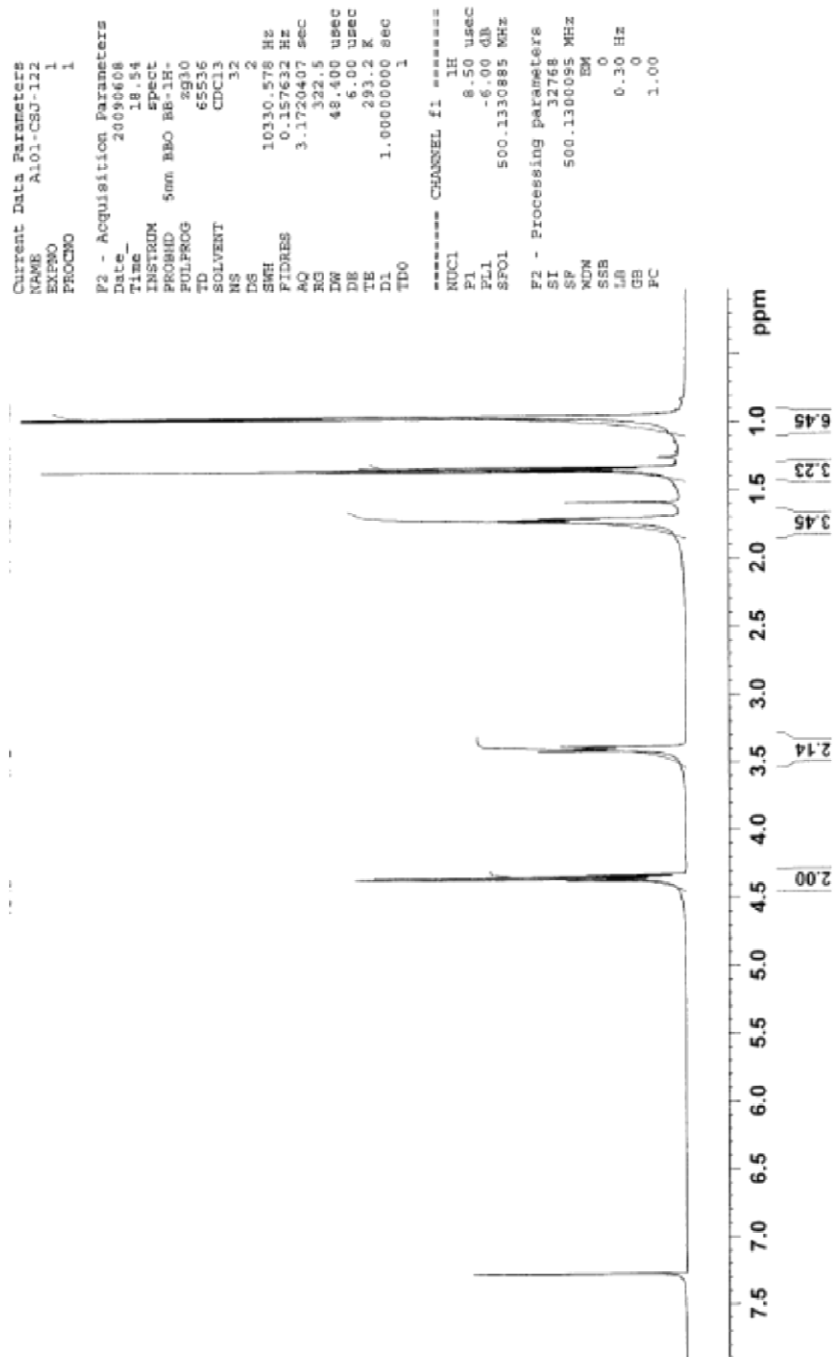


Figure 26. ^1H NMR (500 MHz) spectrum of ethyl (3-methylbutylsulfonyl)diazoacetate (**160.2**) in CDCl_3 .

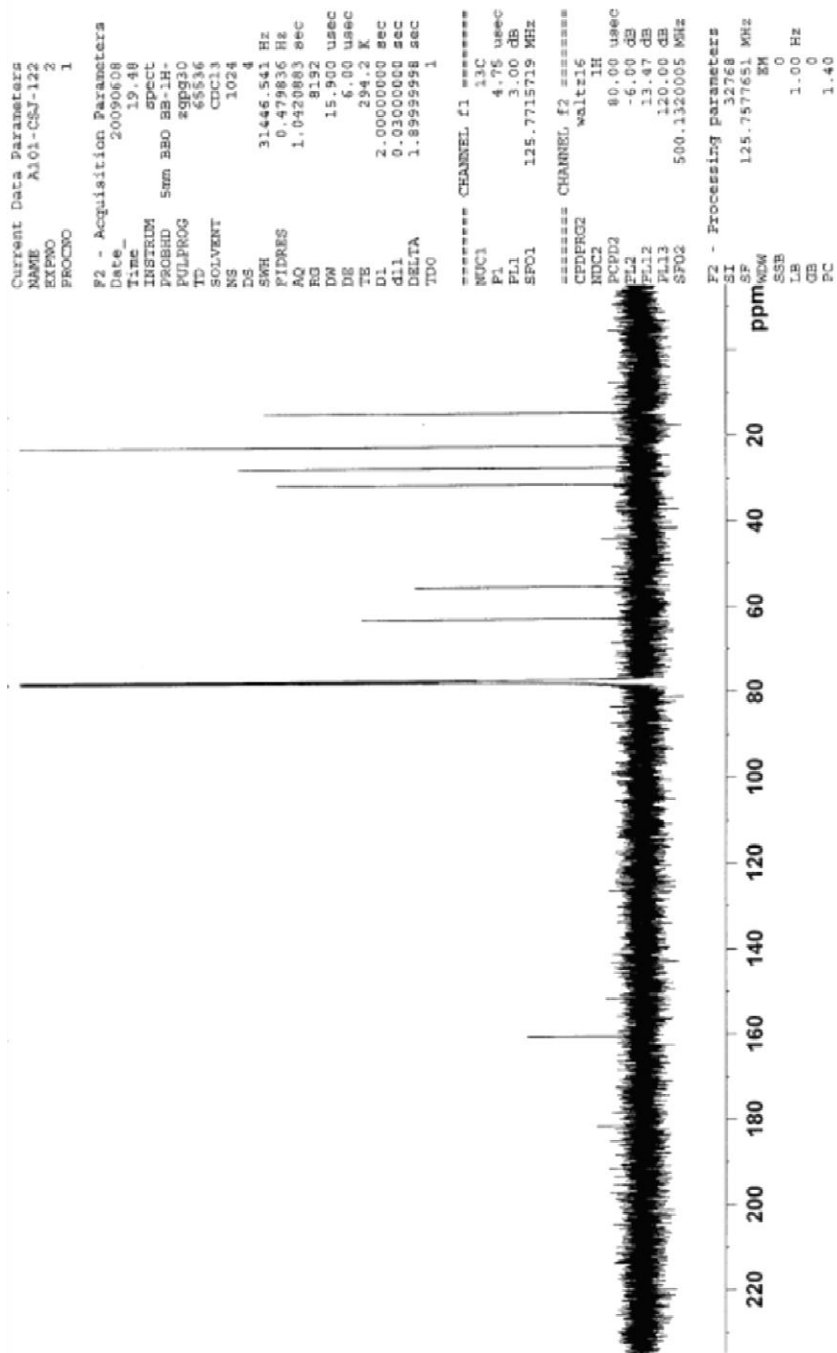


Figure 27. $^{13}\text{C}\{^1\text{H}\}$ NMR (500 MHz) spectrum of ethyl (3-methylbutylsulfonyl)diazoacetate (**160.2**) in CDCl_3 .

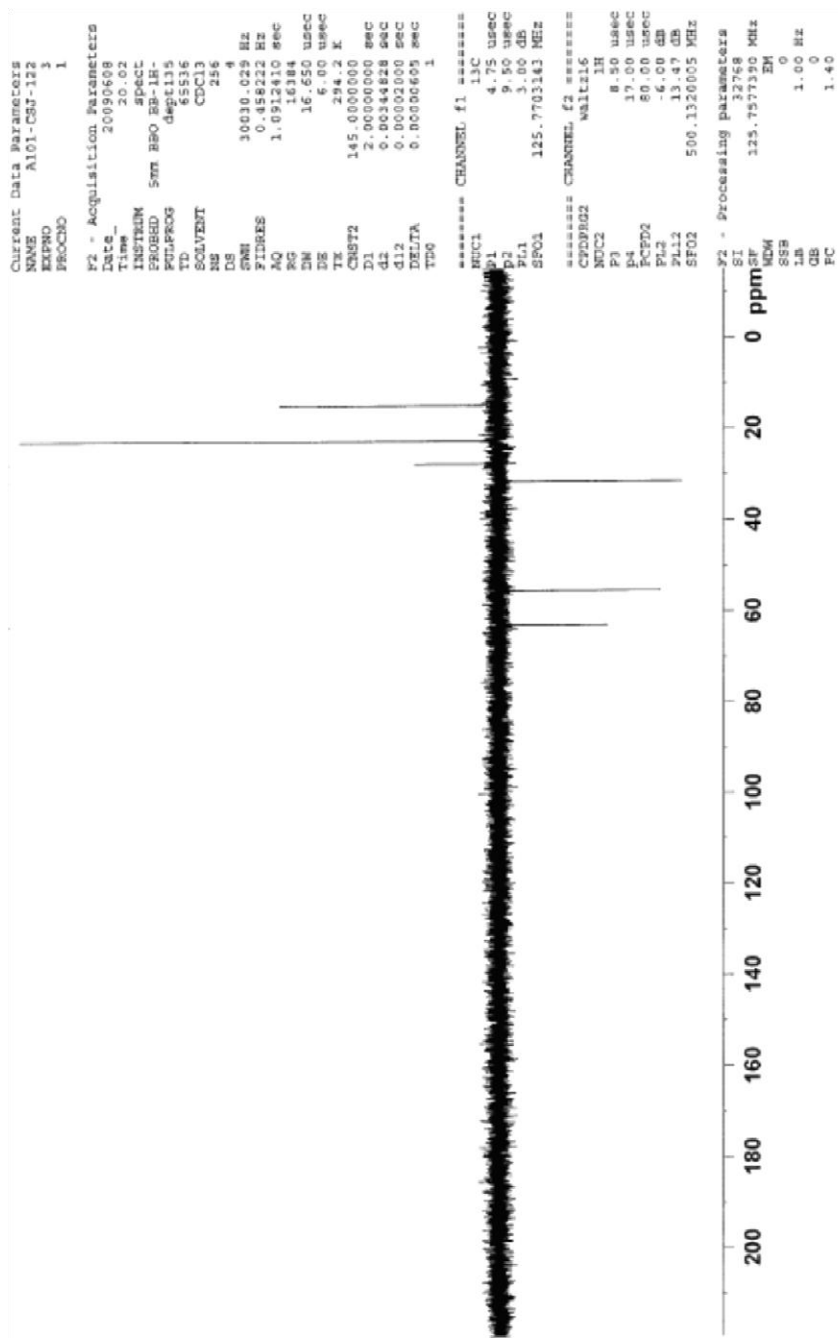


Figure 28. DEPT 135 NMR (500 MHz) spectrum of ethyl (3-methylbutylsulfonyl)diazoacetate (**160.2**) in CDCl_3 .

```

Current Data Parameters
NAME      A101-CSJ-110
EXPNO     15
PROCNO    1

F2 - Acquisition Parameters
Date_     20090622
Time      22.42
INSTRUM   spect
PROBHD    5mm BBO BB1H
PULPROG   zgpg30
TD         65536
SOLVENT   CDCl3
NS         64
DS         2
SWH        10330.578 Hz
FIDRES     0.157632 Hz
AQ         3.1729407 sec
RG         362
DW         48.400 usec
DE         6.00 usec
TE         293.2 K
D1         1.0000000 sec
TD0        1

===== CHANNEL f1 =====
NUC1       1H
P1         8.50 usec
PL1        -6.00 dB
SFO1       500.1330885 MHz

F2 - Processing parameters
SI         32768
SF         500.1300104 MHz
WDW        EM
SSB        0
LB         0.30 Hz
GB         0
PC         1.00

```

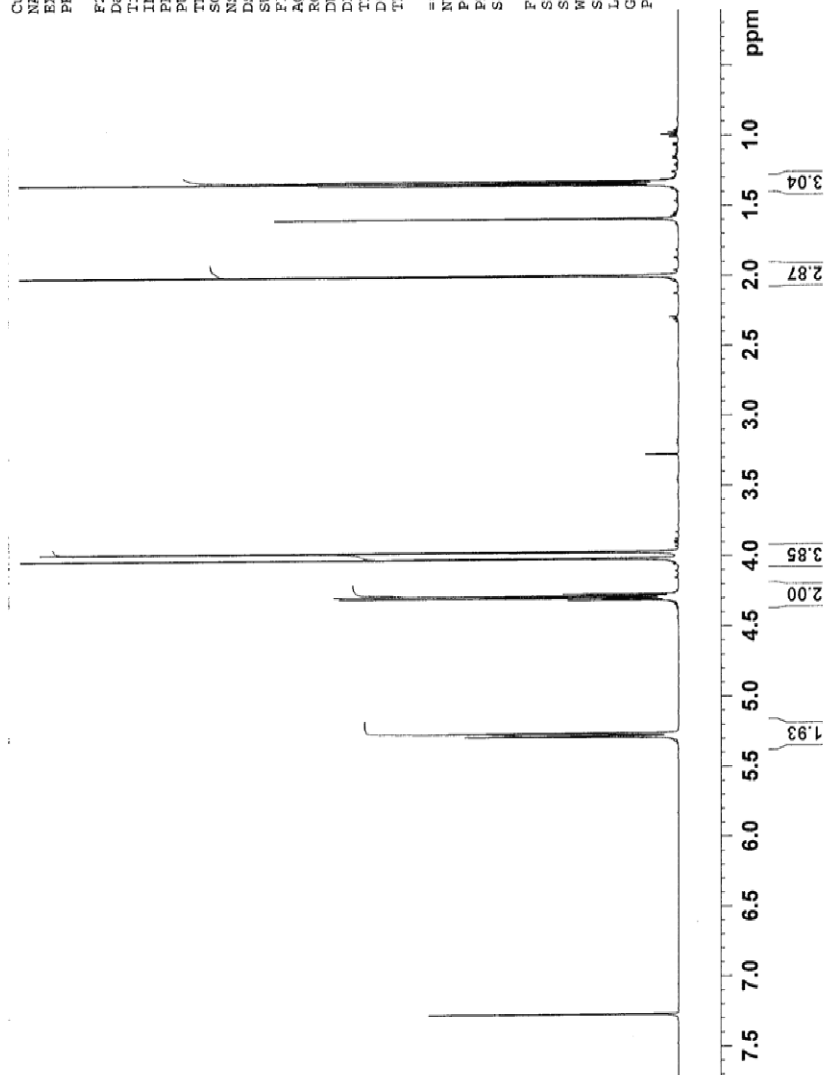


Figure 29. ¹H NMR (500 MHz) spectrum of ethyl (2-methyl-2-propenylsulfonyl)acetate (**161**) in CDCl₃.

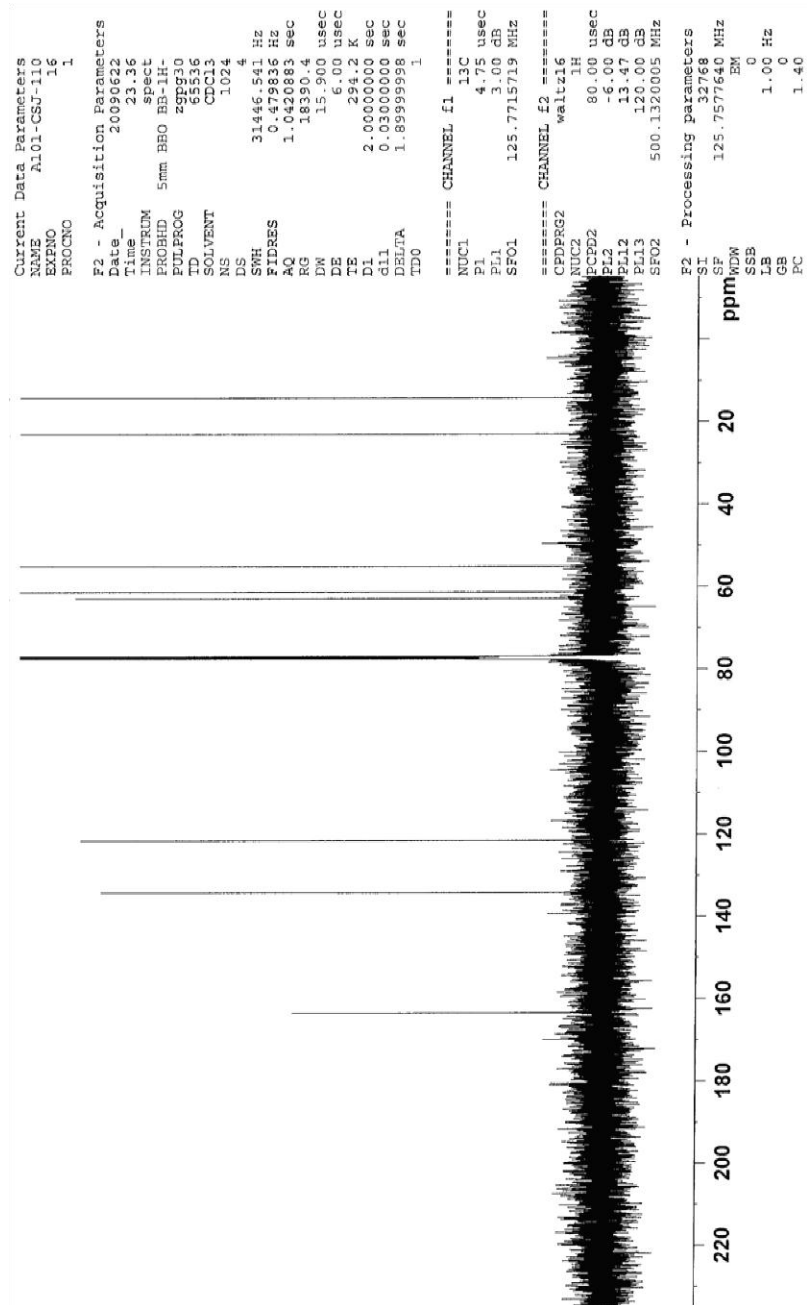


Figure 30. $^{13}\text{C}\{^1\text{H}\}$ NMR (125 MHz) spectrum of ethyl (2-methyl-2-propenylsulfonyl)acetate (**161**) in CDCl_3 .

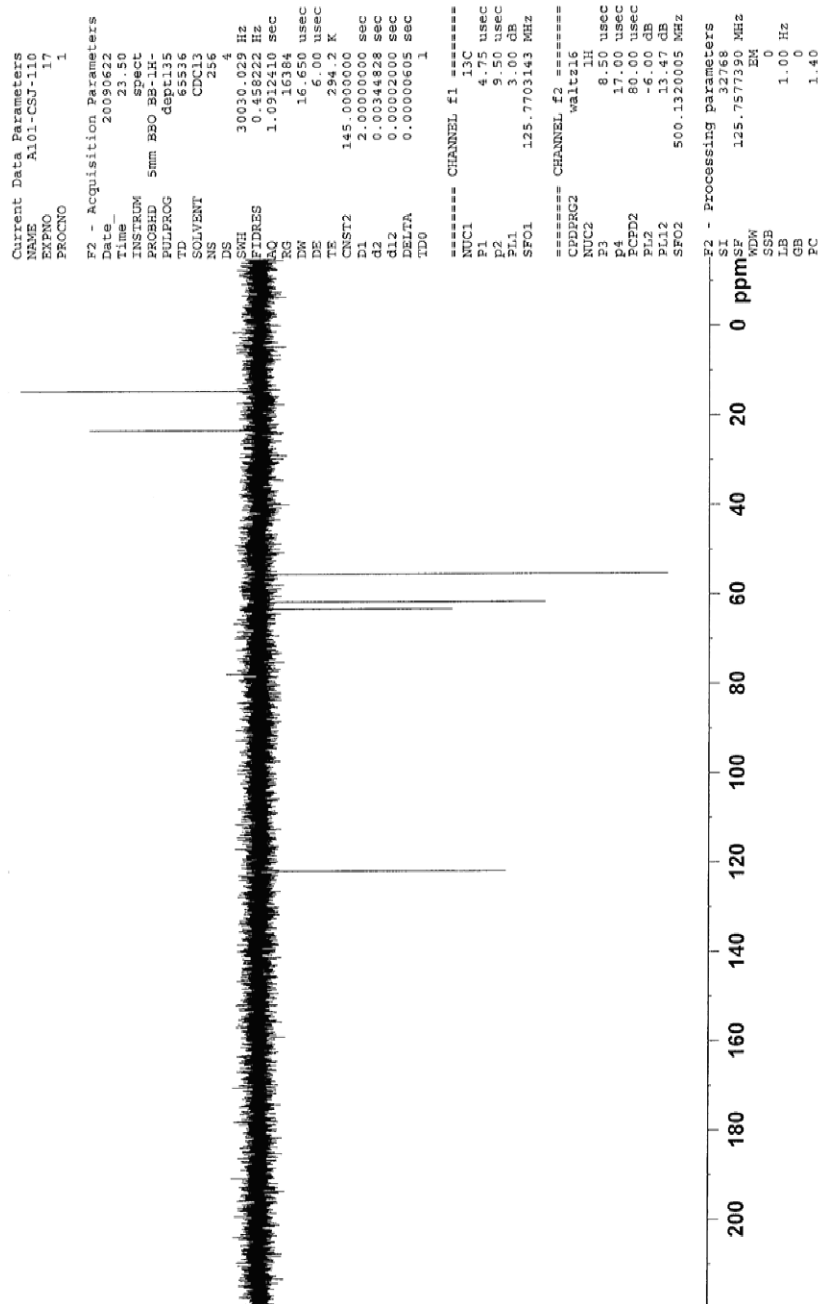


Figure 31. DEPT 135 NMR (125 MHz) spectrum of ethyl (2-methyl-2-propenylsulfonyl)acetate (**161**) in CDCl₃.

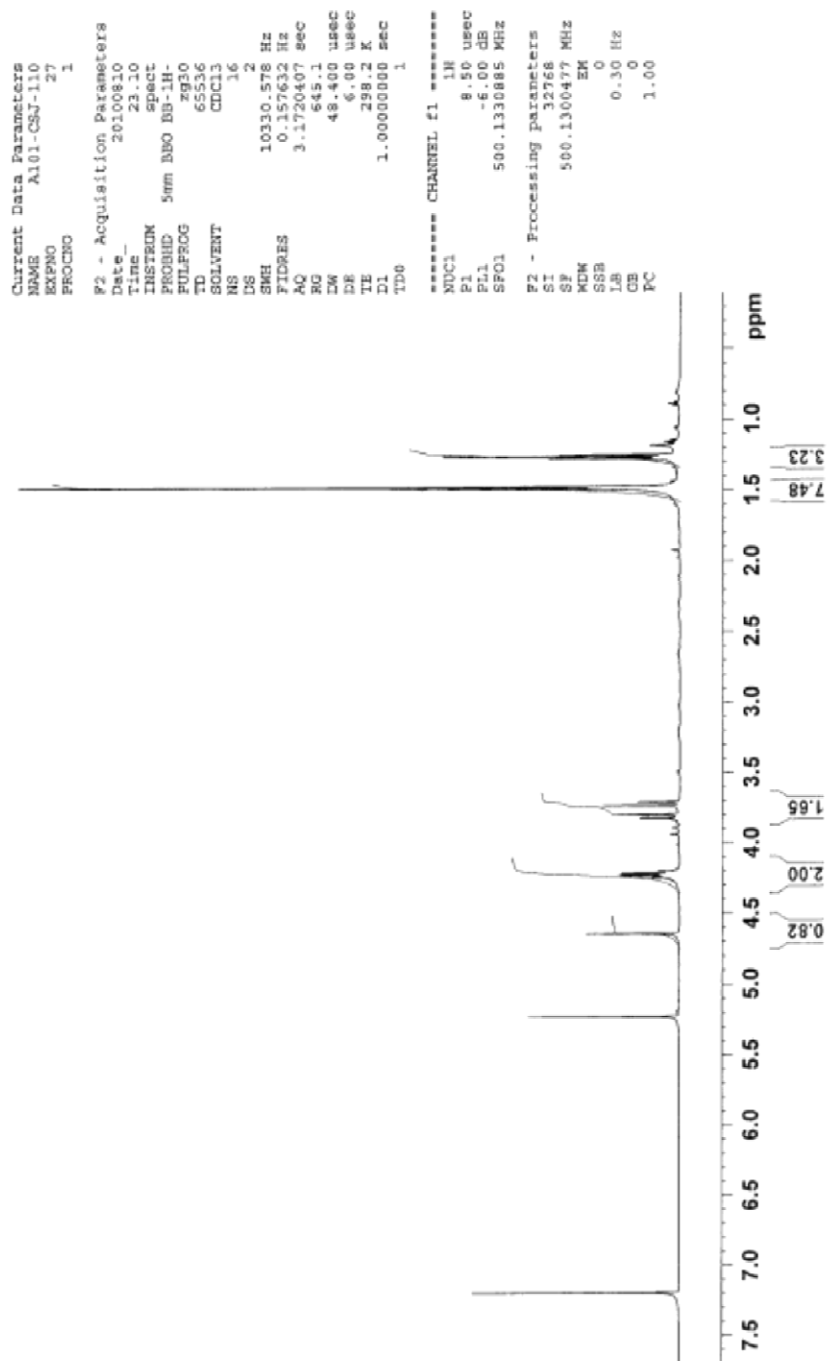


Figure 32. ^1H NMR (500 MHz) spectrum of ethyl (3,3-dimethylthiotane-1,1-dioxide-2-carboxylate) (**159.2.2**) in CDCl_3 .

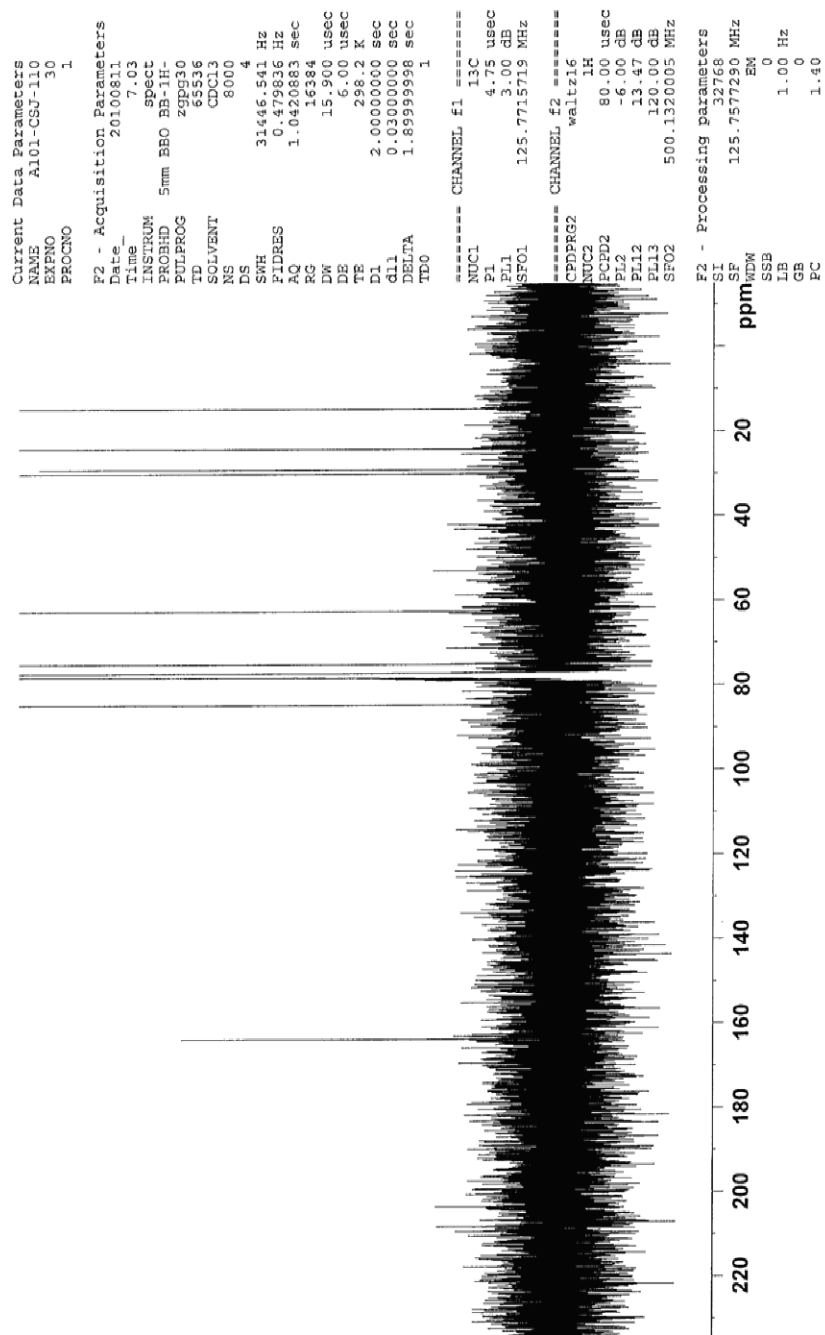


Figure 33. $^{13}\text{C}\{^1\text{H}\}$ NMR (125 MHz) spectrum of ethyl (3,3-dimethylthiotane-1,1-dioxide-2-carboxylate (**159.2.2**) in CDCl_3 .

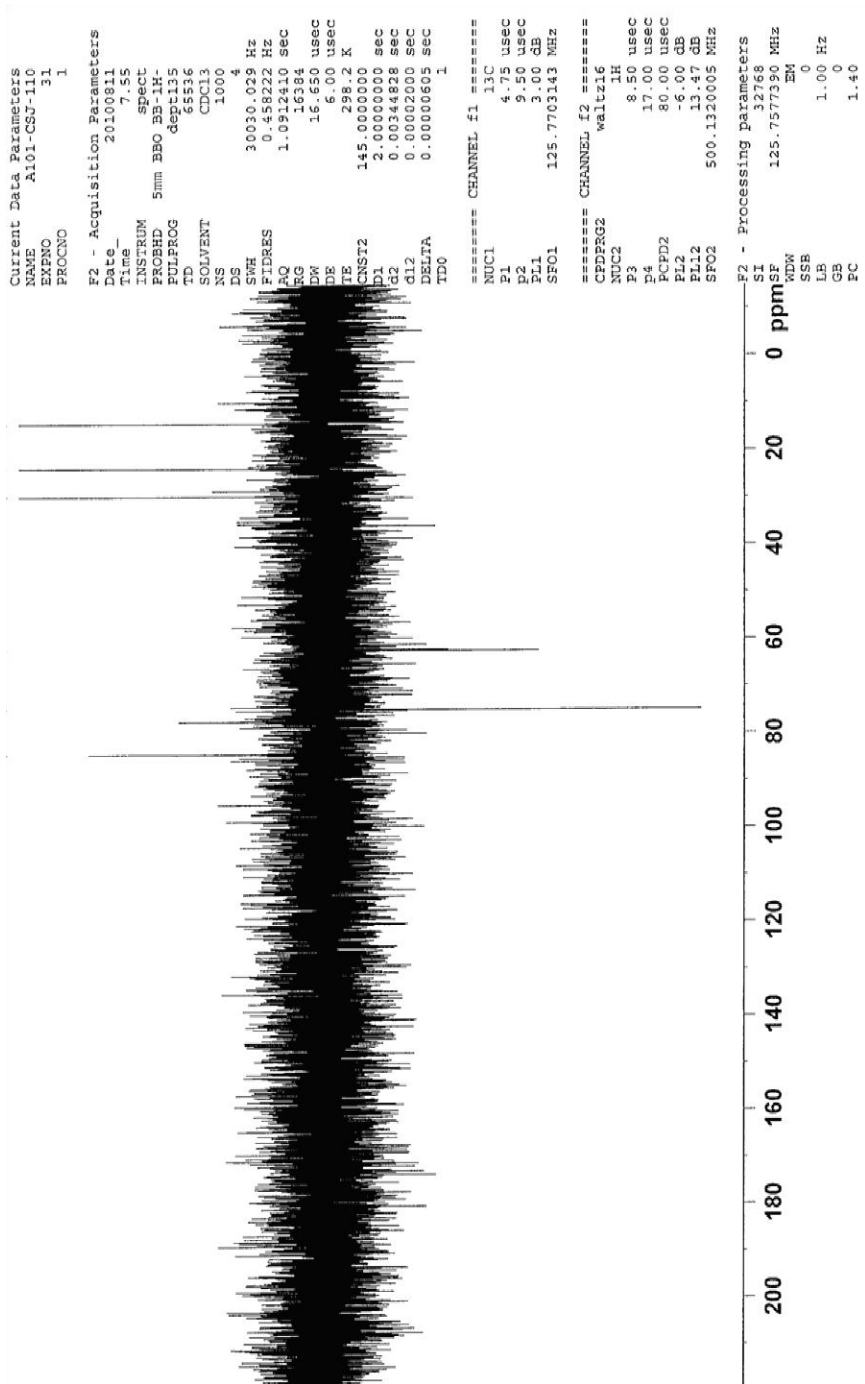


Figure 34. DEPT 135 NMR (125 MHz) spectrum of ethyl 3,3-dimethylthiotane-1,1-dioxide-2-carboxylate (**159.2.2**) in CDCl₃.

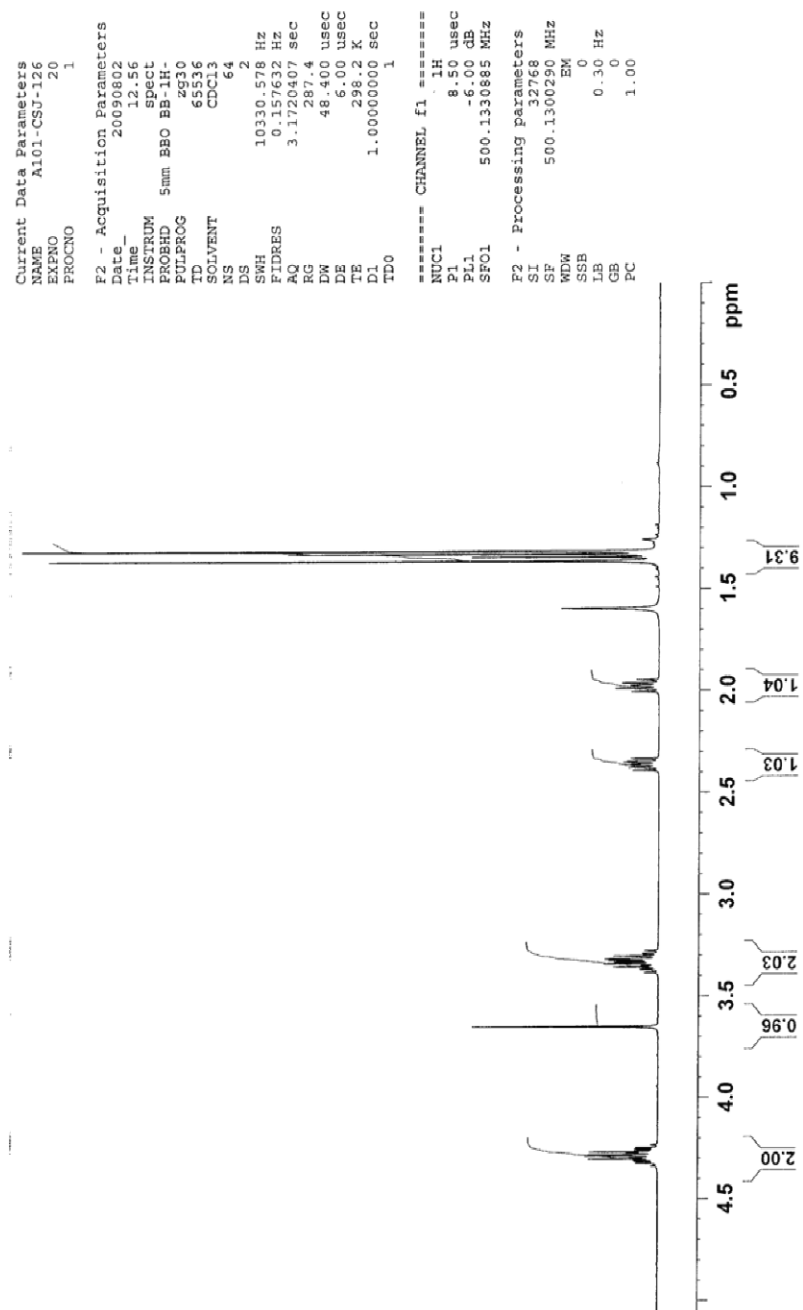


Figure 35. ^1H NMR (500 MHz) spectrum of ethyl tetrahydro-2-ethyl-3,3-dimethylthiophene-1,1-dioxide-2-carboxylate (**160.2.2**) in CDCl_3 .

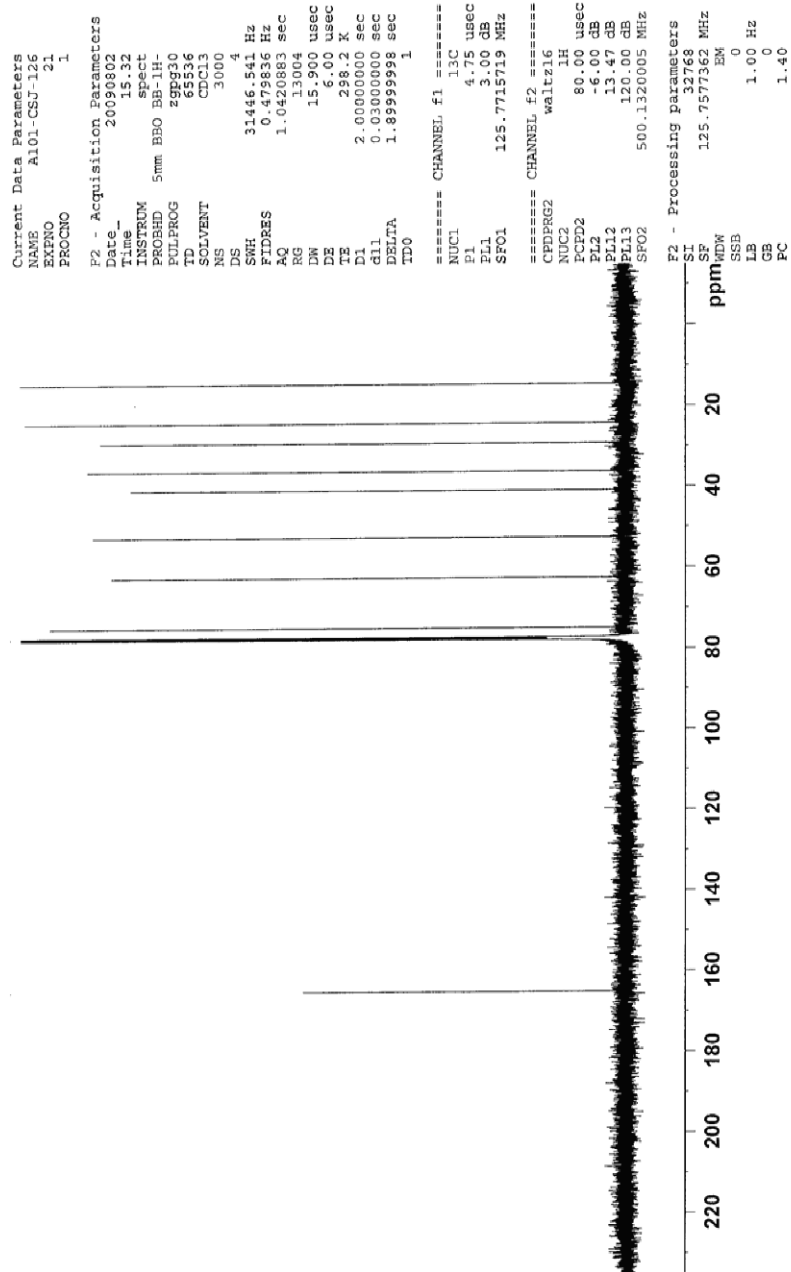


Figure 36. $^{13}\text{C}\{^1\text{H}\}$ NMR (500 MHz) spectrum of ethyl tetrahydro-2-ethyl-3,3-dimethylthiophene-1,1-dioxide-2-carboxylate (**160.2.2**) in CDCl_3 .

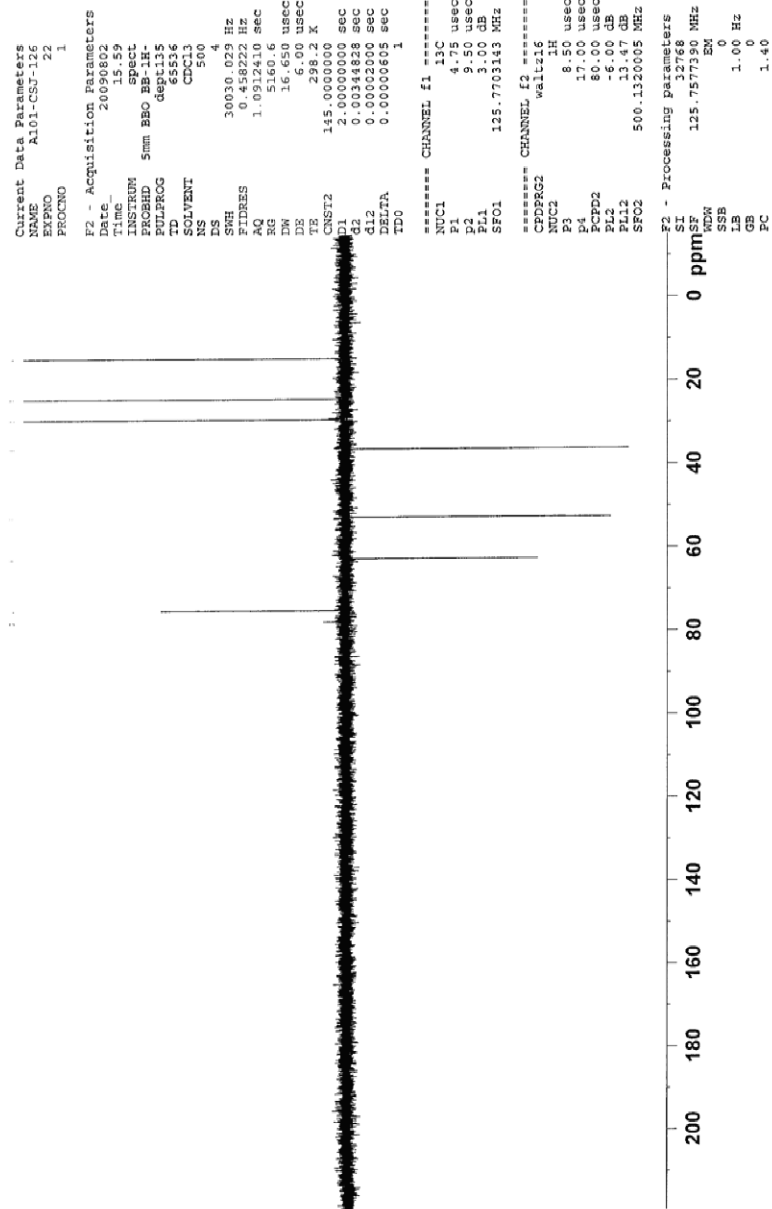


Figure 37. DEPT 135 NMR (500 MHz) spectrum of ethyl tetrahydro-2-ethyl-3,3-dimethylthiophene-1,1-dioxide-2-carboxylate (**160.2.2**) in CDCl₃.

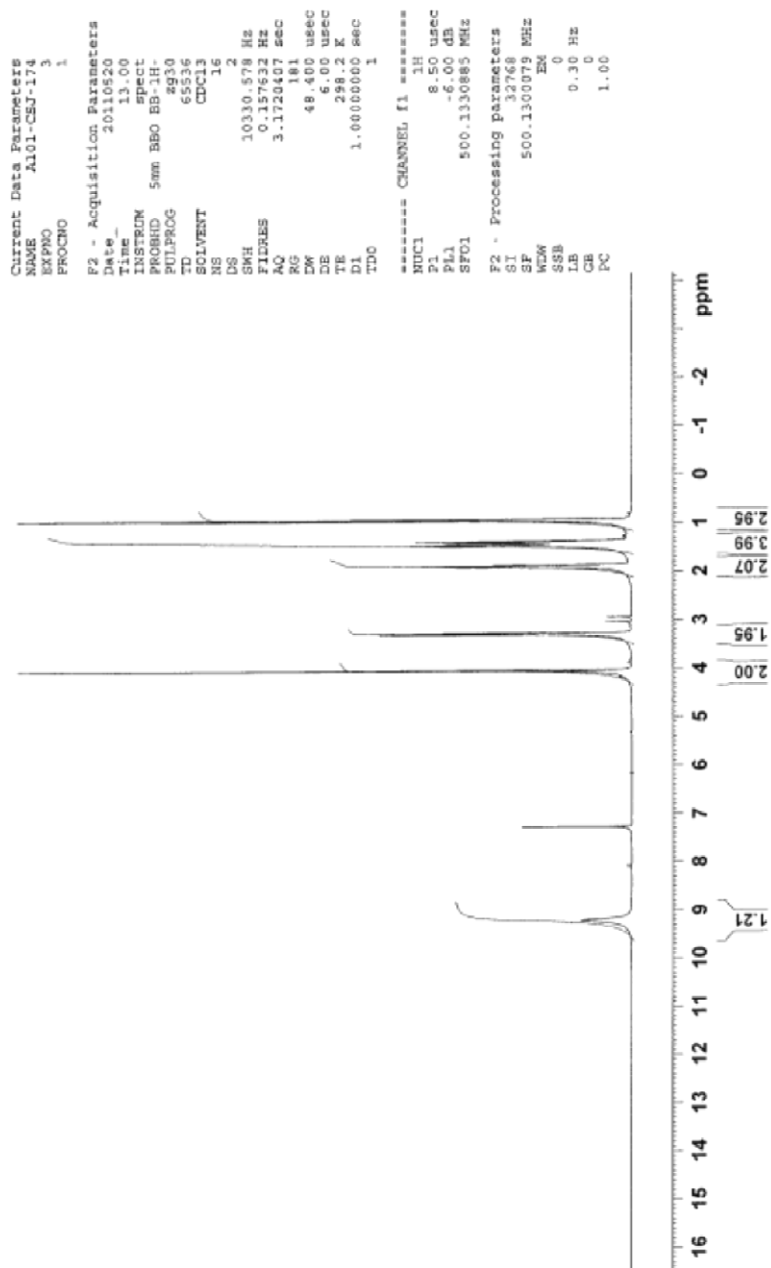


Figure 38. ^1H NMR (500 MHz) spectrum of (pentylsulfonyl)acetic acid (**182**) in CDCl_3 .

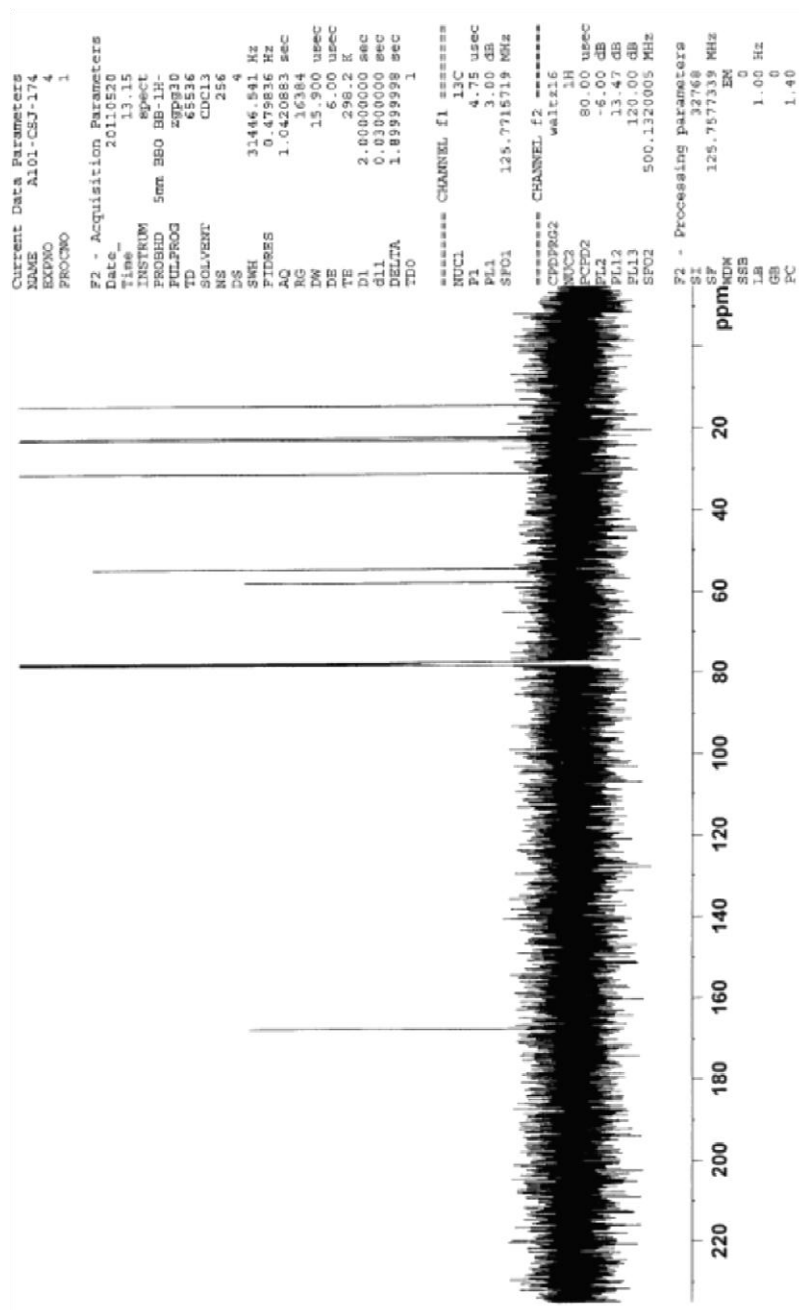


Figure 39. $^{13}\text{C}\{^1\text{H}\}$ NMR spectrum of (pentylsulfonyl)acetic acid (**182**) in CDCl_3 .

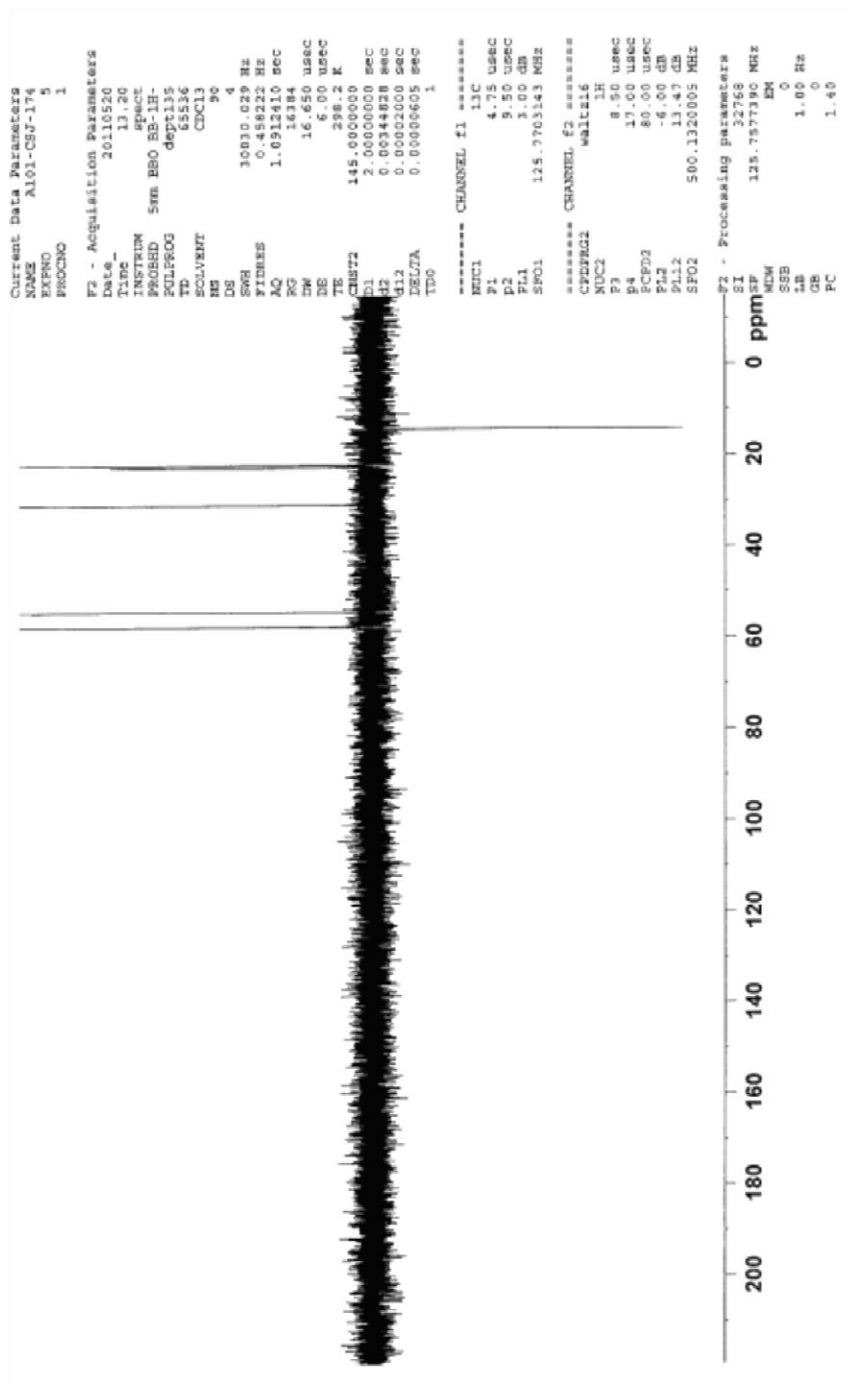


Figure 40. DEPT-135 NMR spectrum of (pentylsulfonyl)acetic acid (**182**) in CDCl₃.

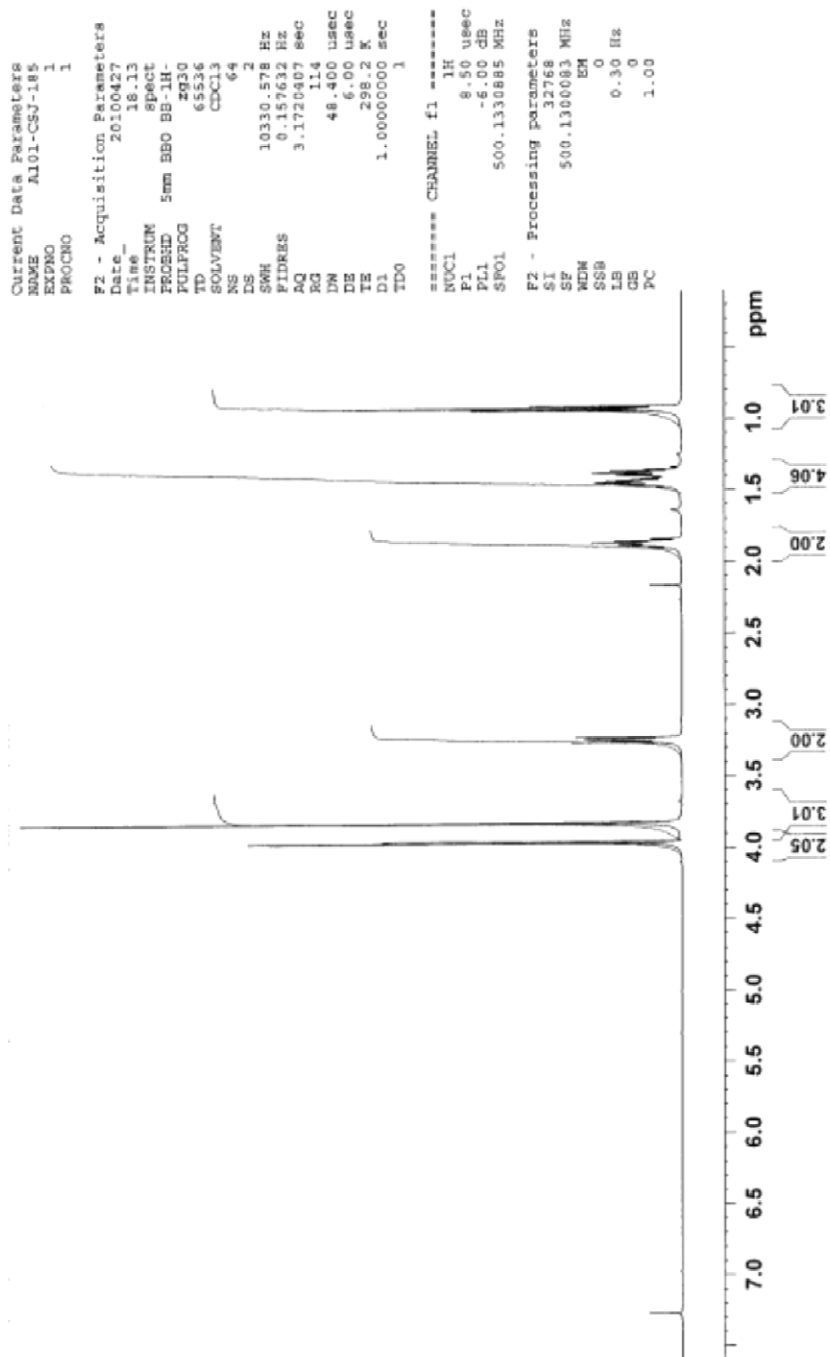


Figure 41. ^1H NMR (500 MHz) spectrum of methyl (pentylsulfonyl)acetate (**183**) in CDCl_3 .

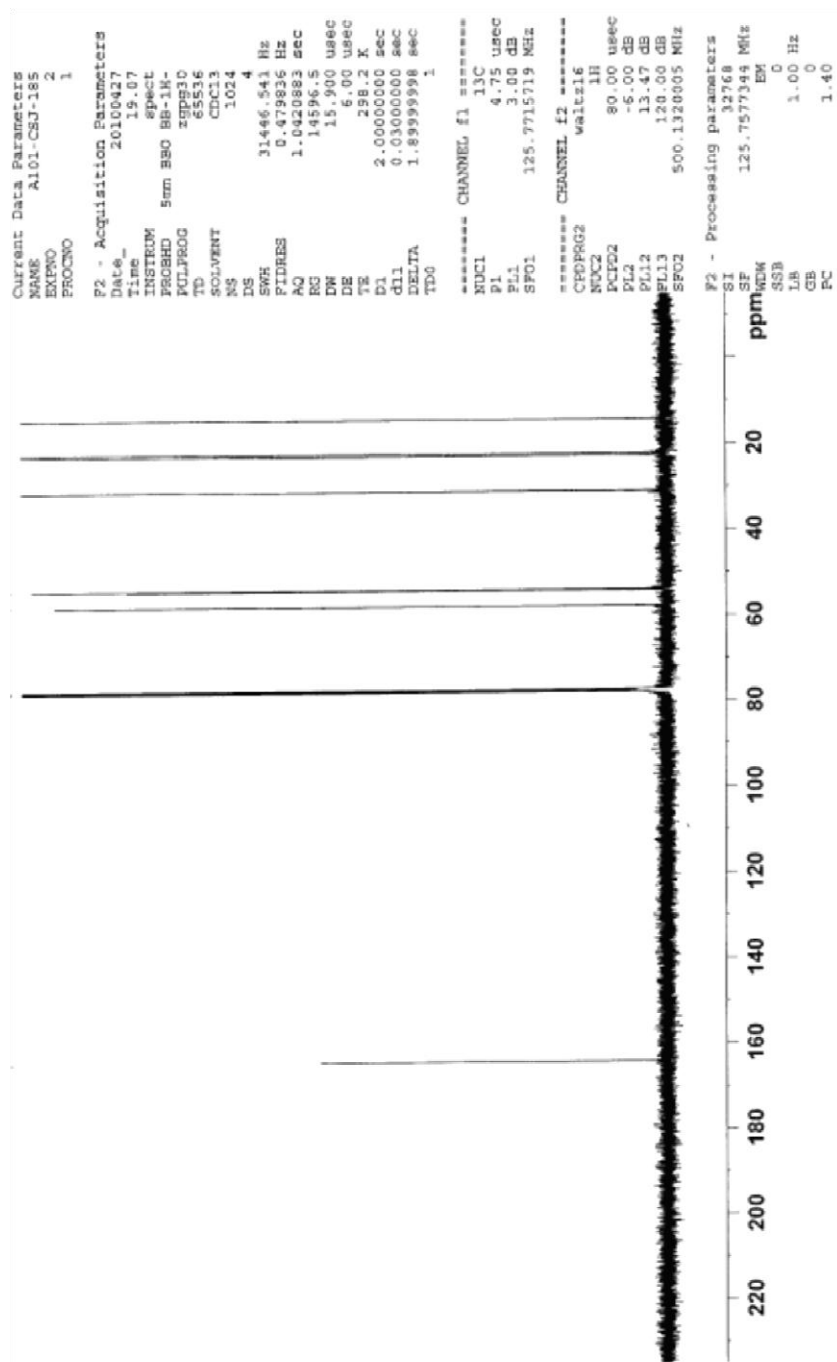


Figure 42. $^{13}\text{C}\{^1\text{H}\}$ NMR (125 MHz) spectrum of methyl (pentylsulfonyl)acetate (**183**) in CDCl_3 .

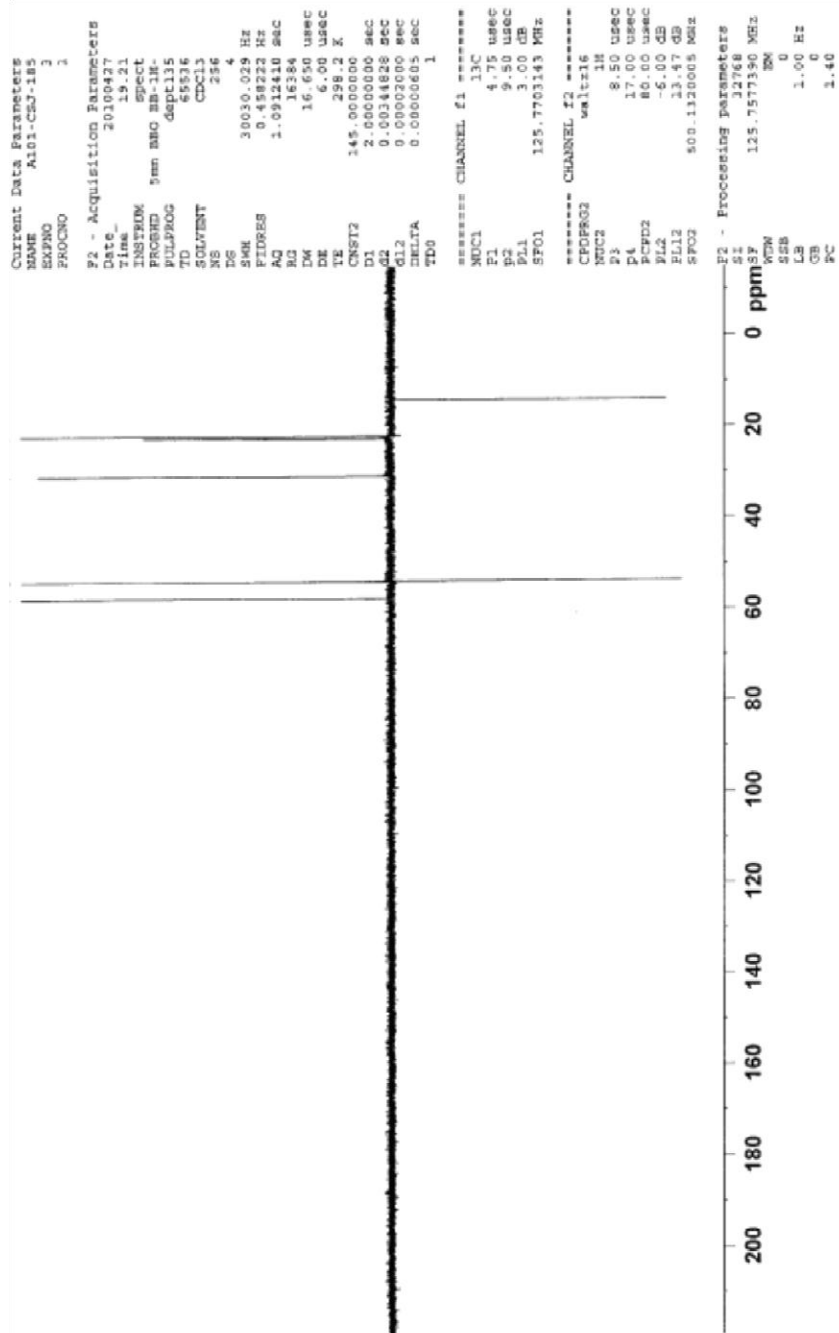


Figure 43. DEPT 135 NMR (125 MHz) spectrum of methyl (pentylsulfonyl)acetate (**183**) in CDCl₃.

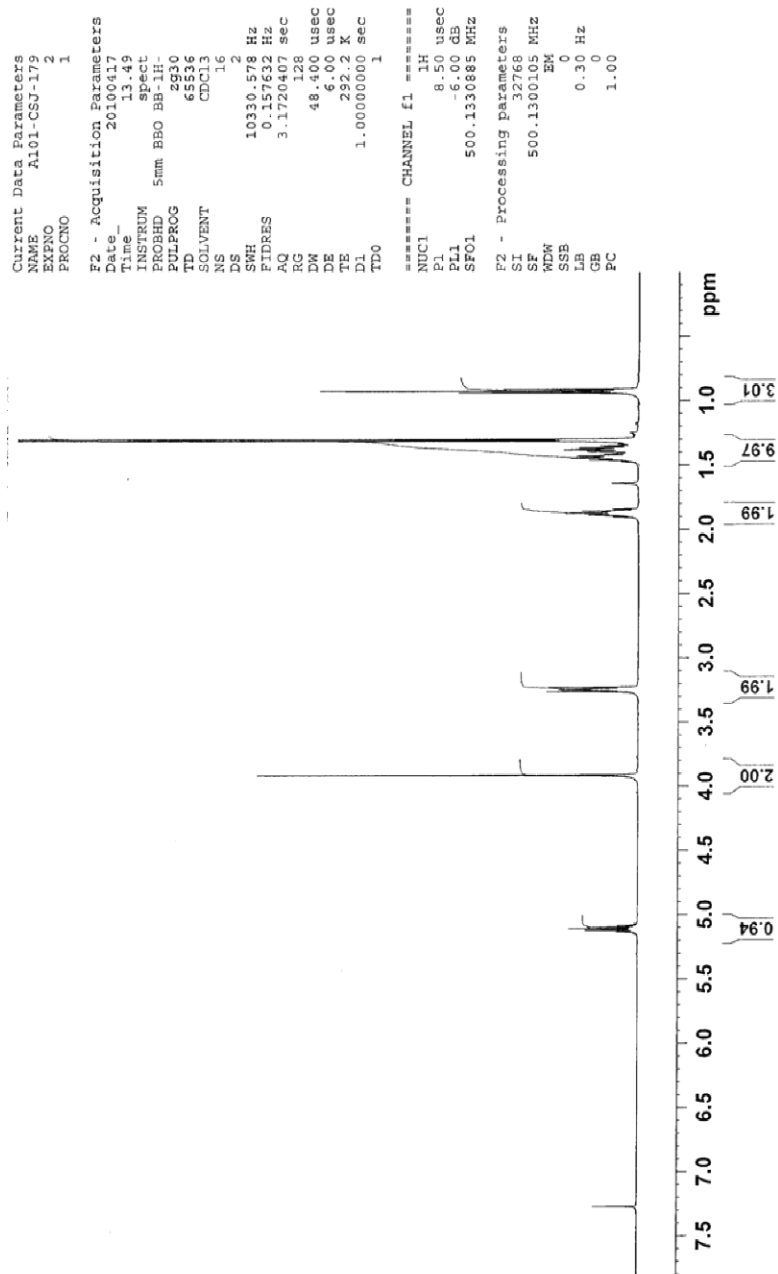


Figure 44. ^1H NMR (500 MHz) spectrum of isopropyl (pentylsulfonyl)acetate (**184**) in CDCl_3 .

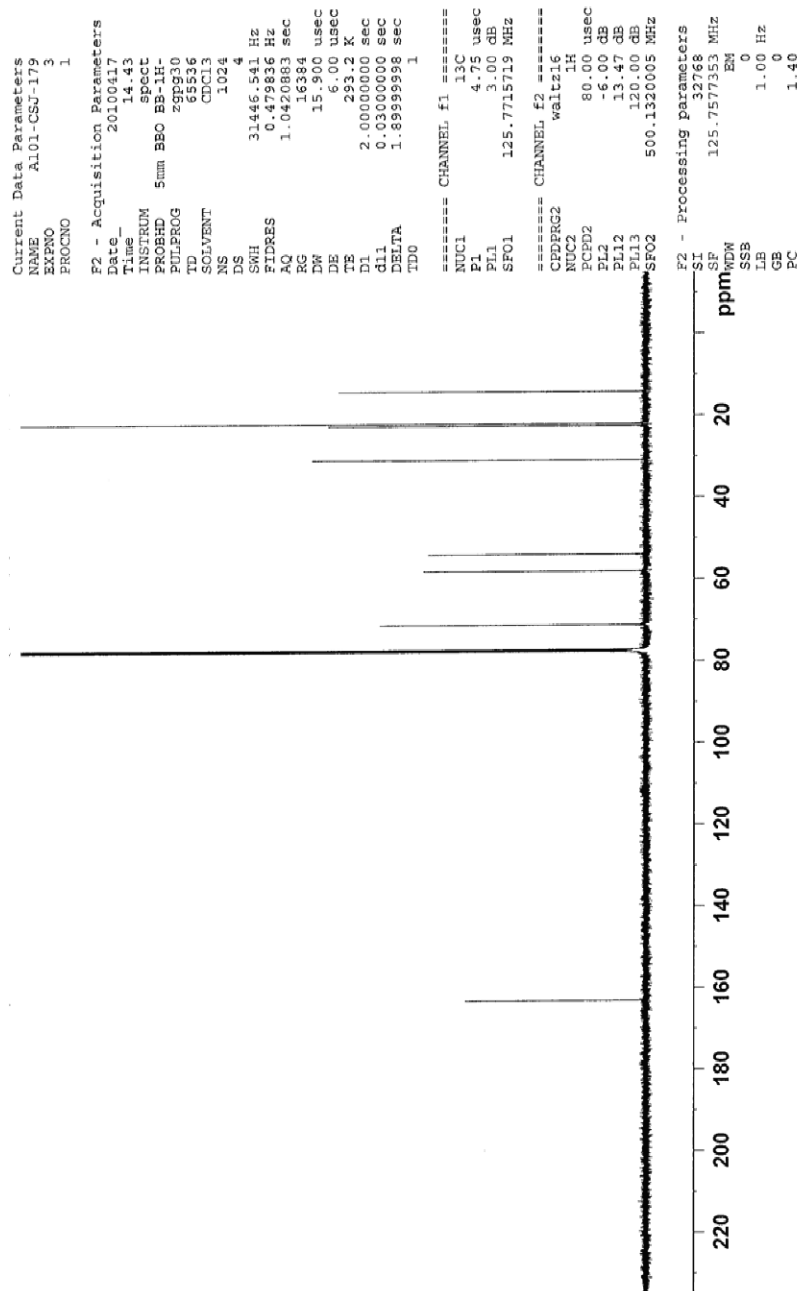


Figure 45. $^{13}\text{C}\{^1\text{H}\}$ NMR (125MHz) spectrum of isopropyl (pentylsulfonyl)acetate (**184**) in CDCl_3 .

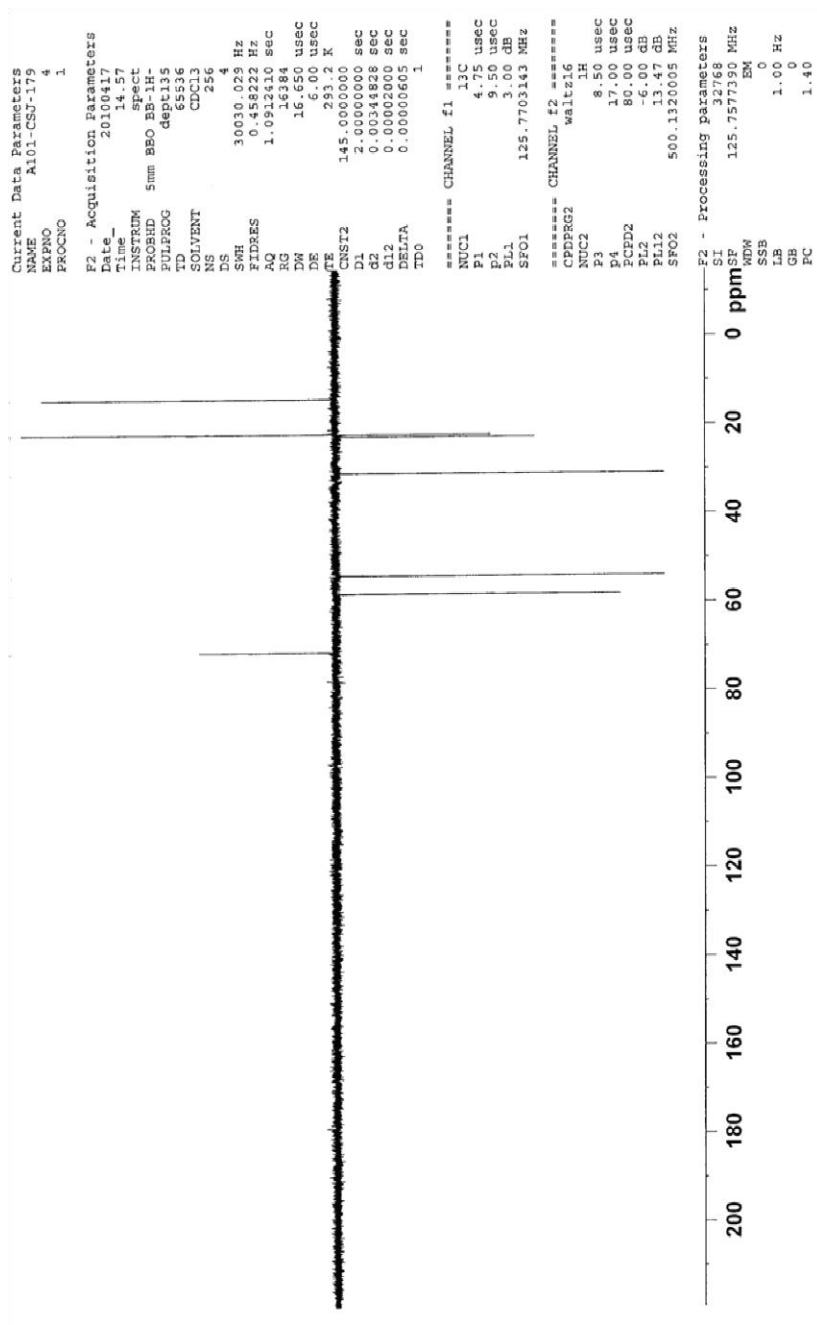


Figure 46. DEPT 135 NMR (125MHz) spectrum of isopropyl (pentylsulfonyl)acetate (**184**) in CDCl₃.

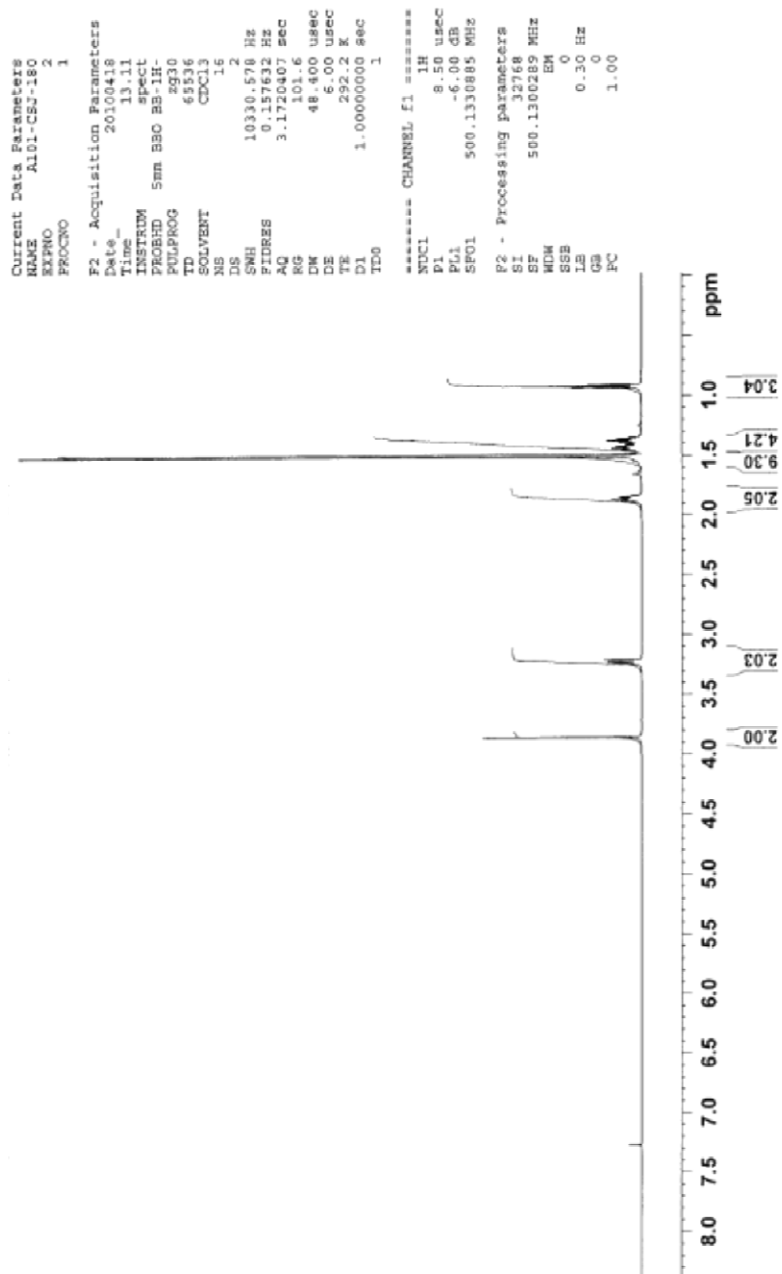


Figure 47. ^1H NMR (500 MHz) spectrum of *t*-butyl (pentylsulfonyl)acetate (**185**) in CDCl_3 .

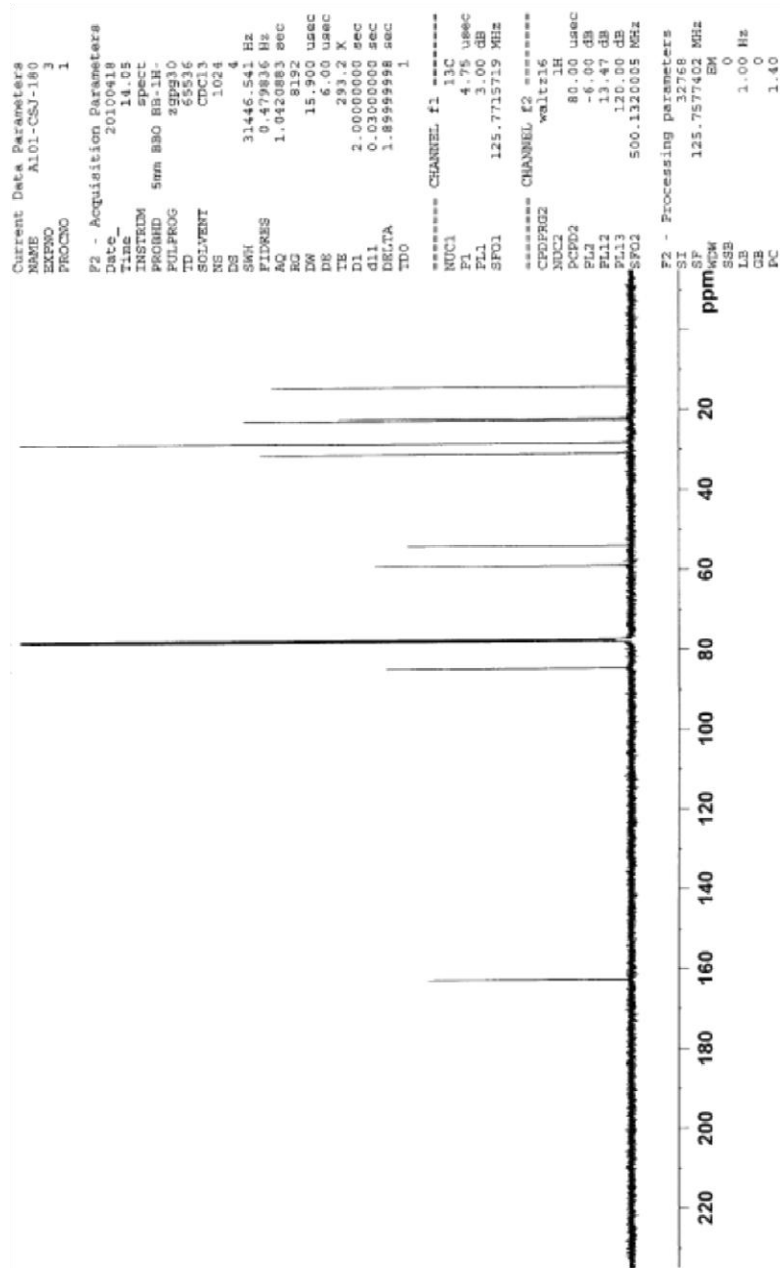


Figure 48. $^{13}\text{C}\{^1\text{H}\}$ NMR (125 MHz) spectrum of *t*-butyl (pentylsulfonyl)acetate (**185**) in CDCl_3 .

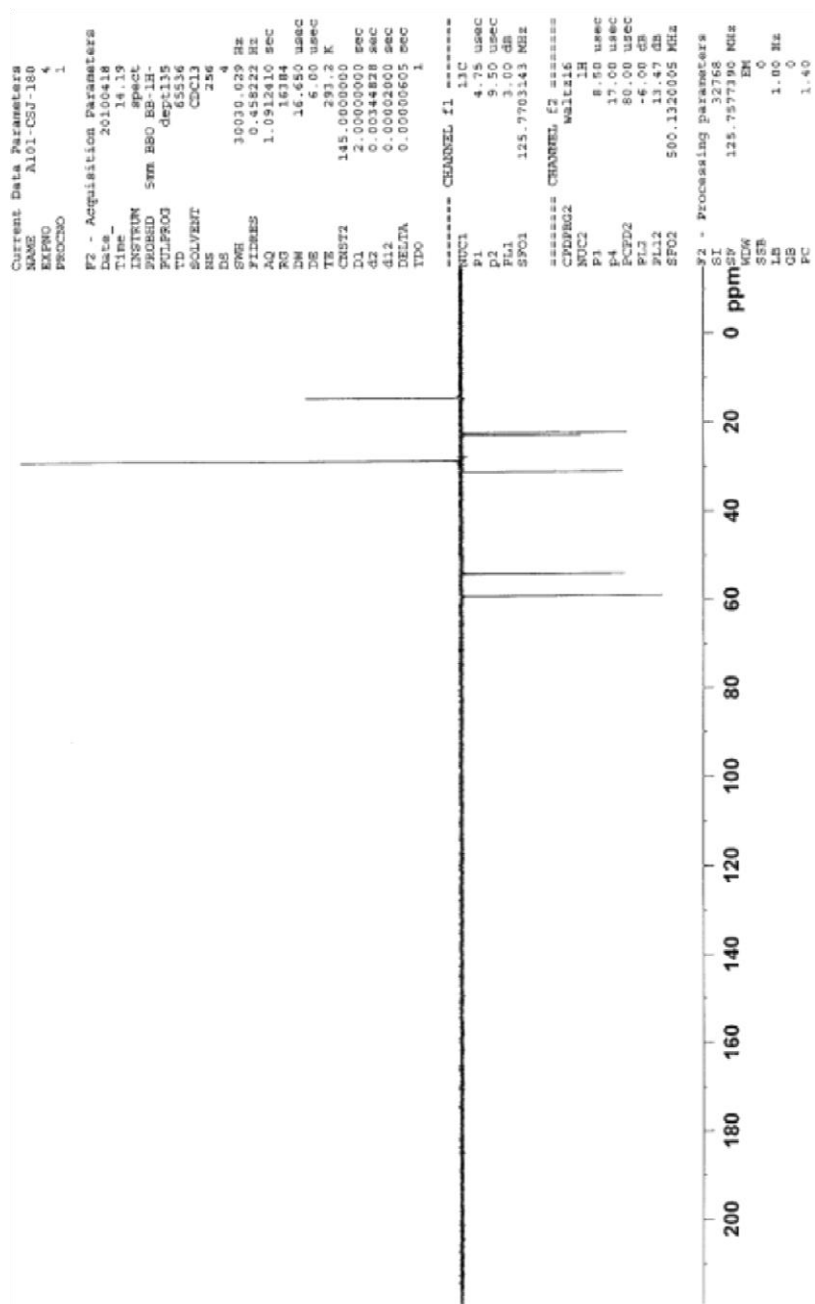


Figure 49. DEPT 135 NMR (125 MHz) spectrum of *t*-butyl (pentylsulfonyl)acetate (**185**) in CDCl₃.

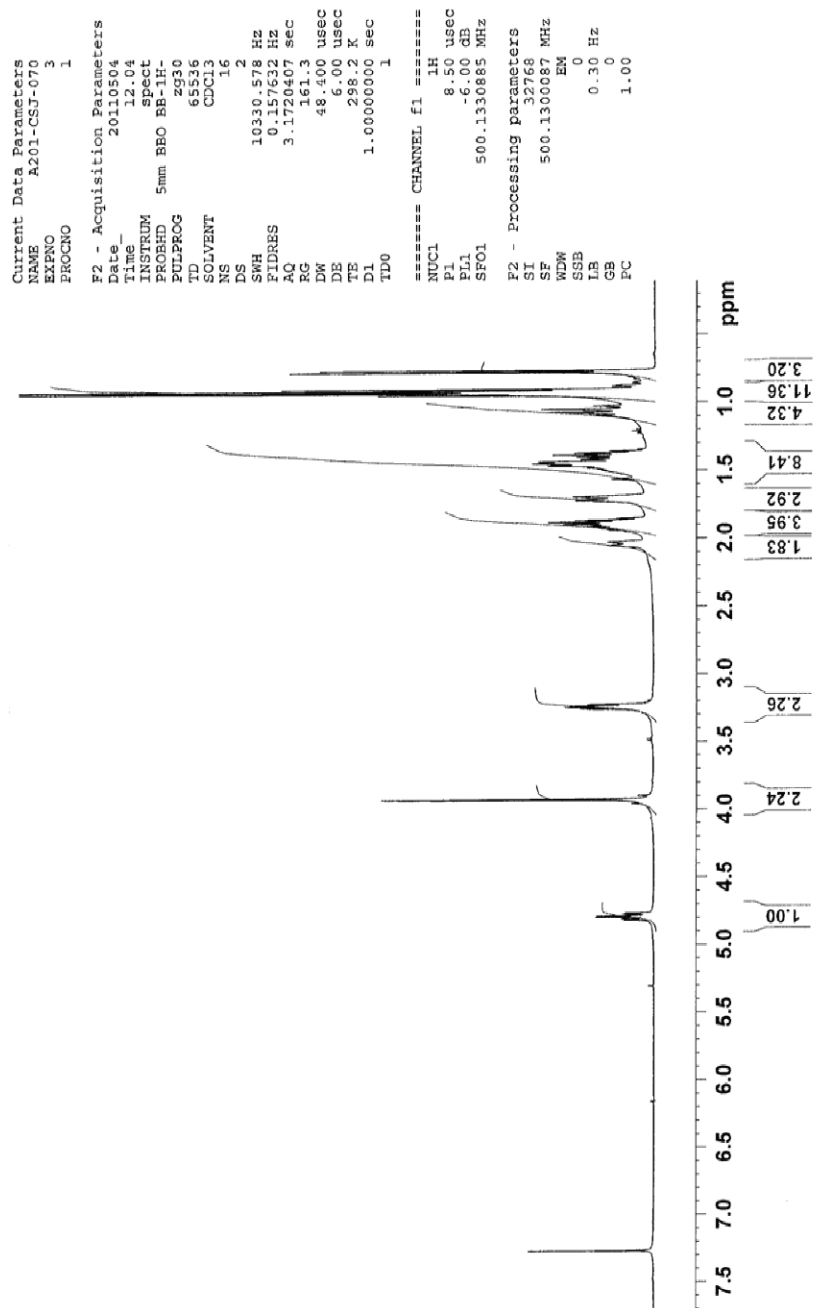


Figure 50. ^1H NMR (500 MHz) spectrum of (1*R*,2*S*,5*R*)-2-isopropyl-5-methylcyclohexyl (pentylsulfonyl)acetate (**187**) in CDCl_3 .

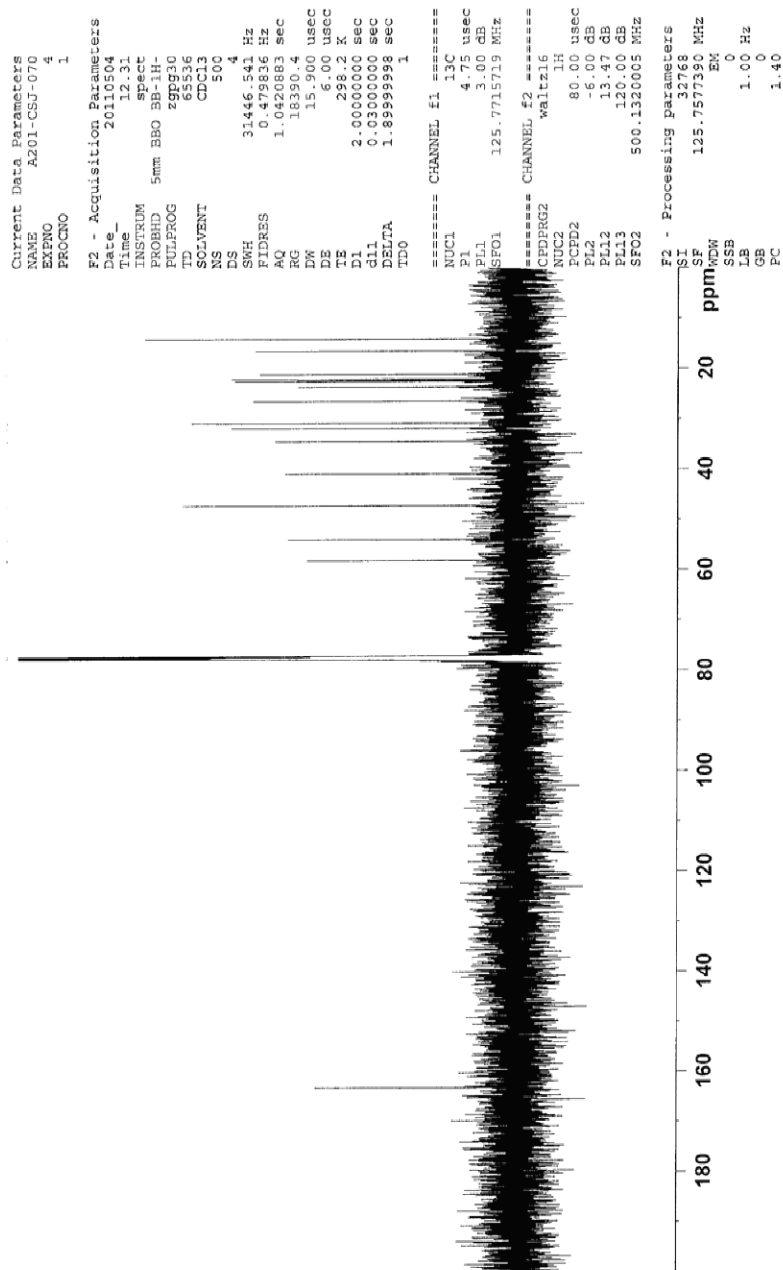


Figure 51. $^{13}\text{C}\{^1\text{H}\}$ NMR (500 MHz) spectrum of (1*R*,2*S*,5*R*)-2-isopropyl-5-methylcyclohexyl (pentylsulfonyl)acetate (**187**) in CDCl_3 .

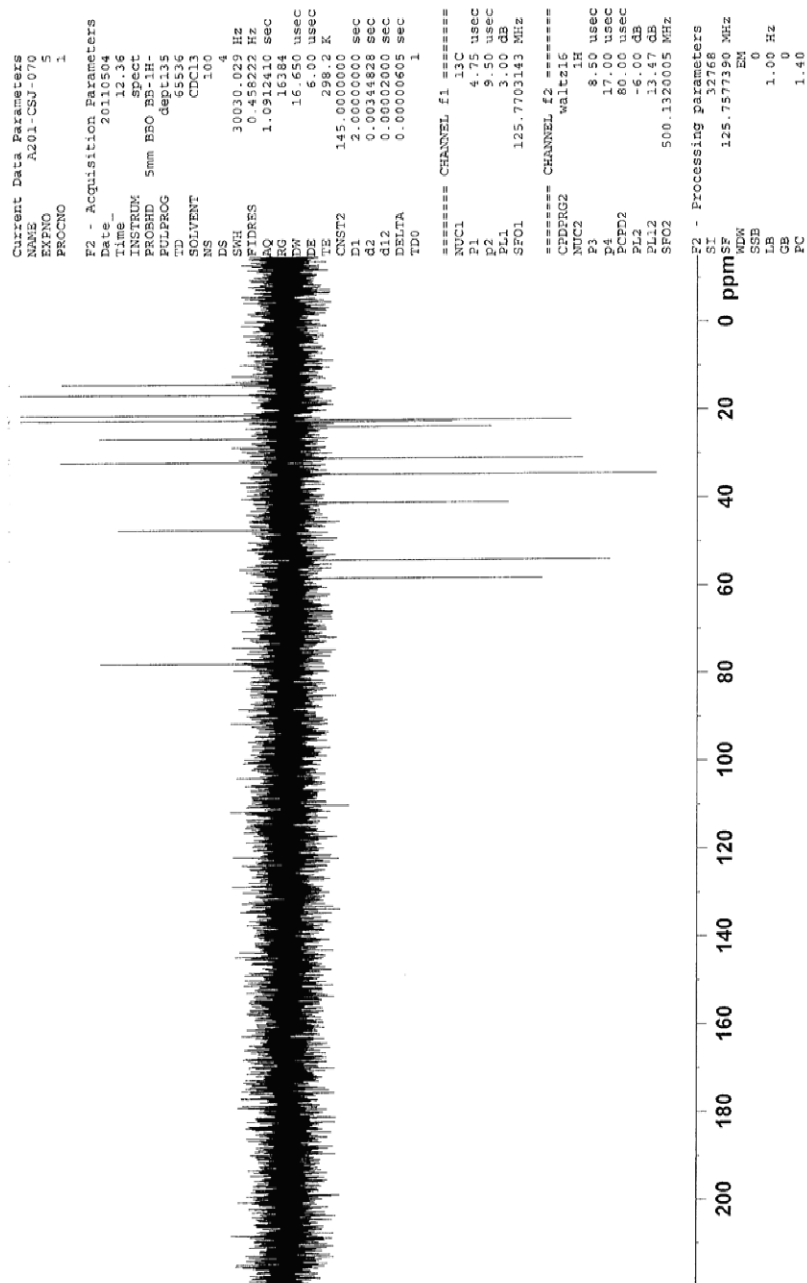


Figure 52. DEPT 135 NMR (500 MHz) spectrum of (1*R*,2*S*,5*R*)-2-Isopropyl-5-methylcyclohexyl (pentylsulfonyl)acetate (**187**) in CDCl₃.

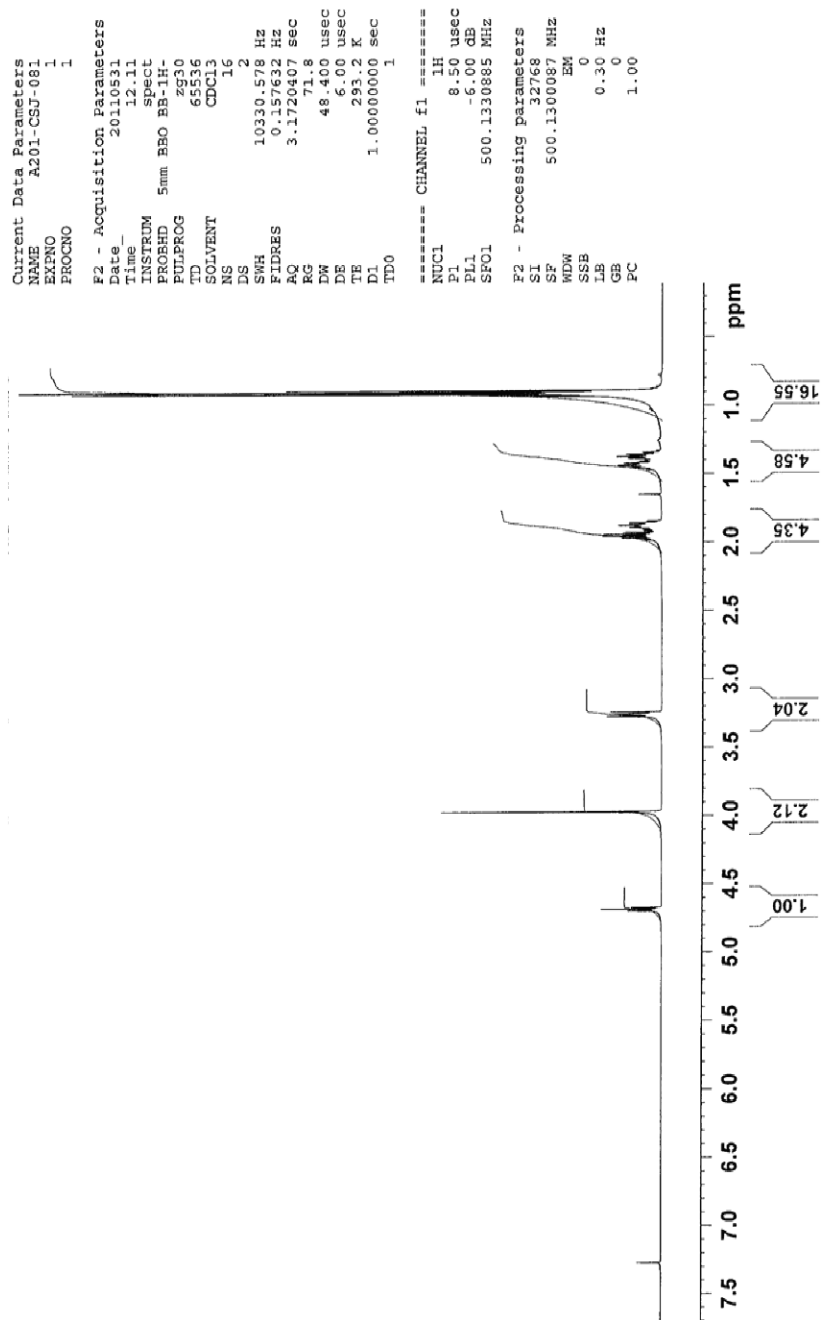


Figure 53. ^1H NMR (500 MHz) spectrum of 2,4-dimethyl-3-pentyl (pentylsulfonyl)acetate (**188**) in CDCl_3 .

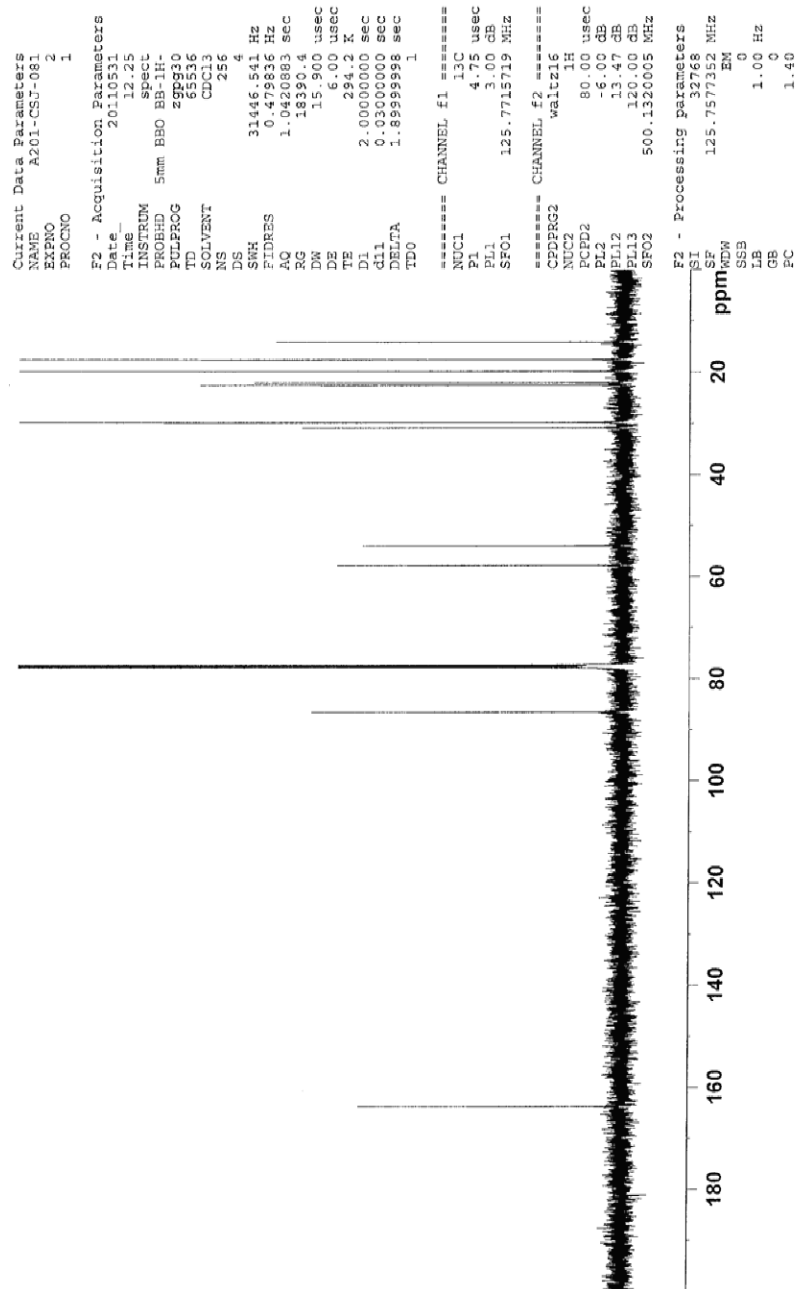


Figure 54. $^{13}\text{C}\{^1\text{H}\}$ NMR (125 MHz) spectrum of 2,4-dimethyl-3-pentyl (pentylsulfonyl)acetate (**188**) in CDCl_3 .

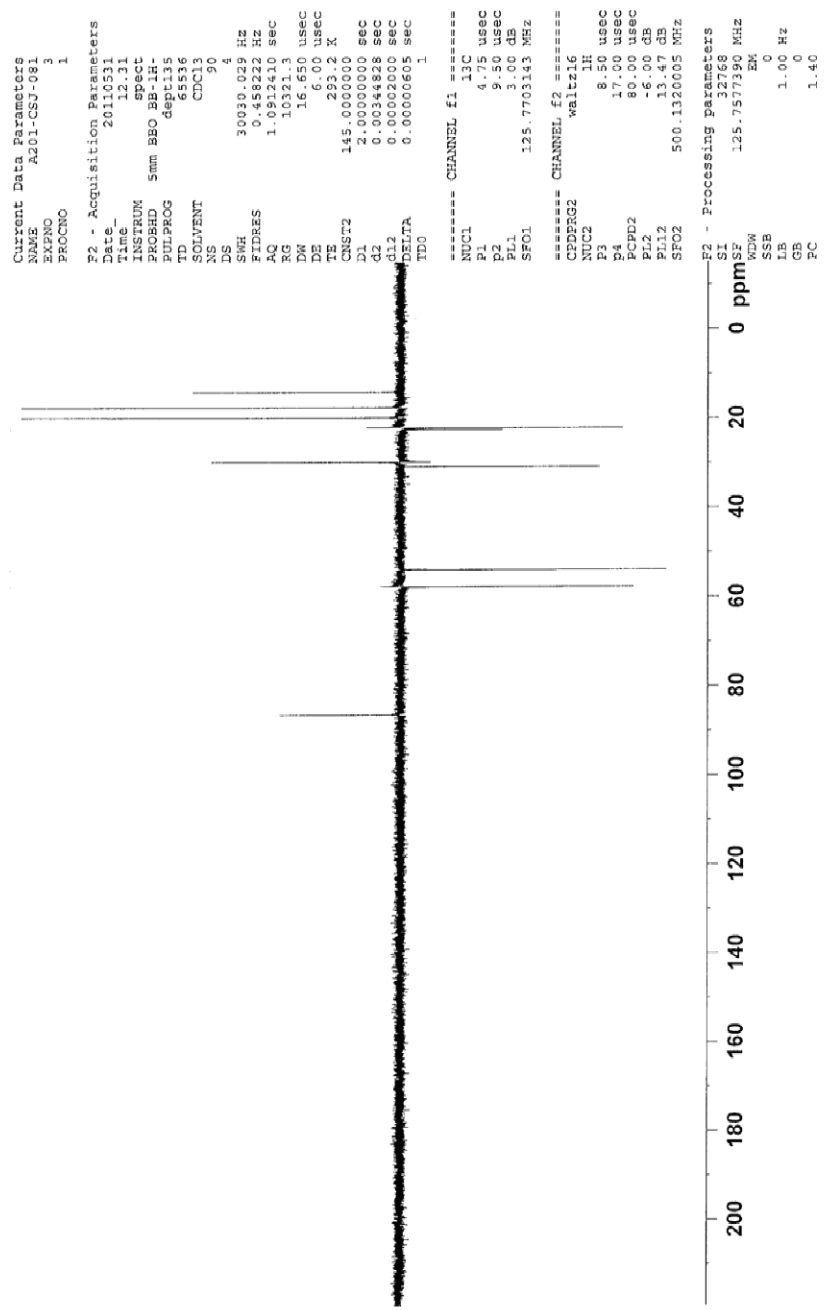


Figure 55. DEPT 135 NMR (125 MHz) spectrum of 2,4-dimethyl-3-pentyl (pentylsulfonyl)acetate (**188**) in CDCl₃.

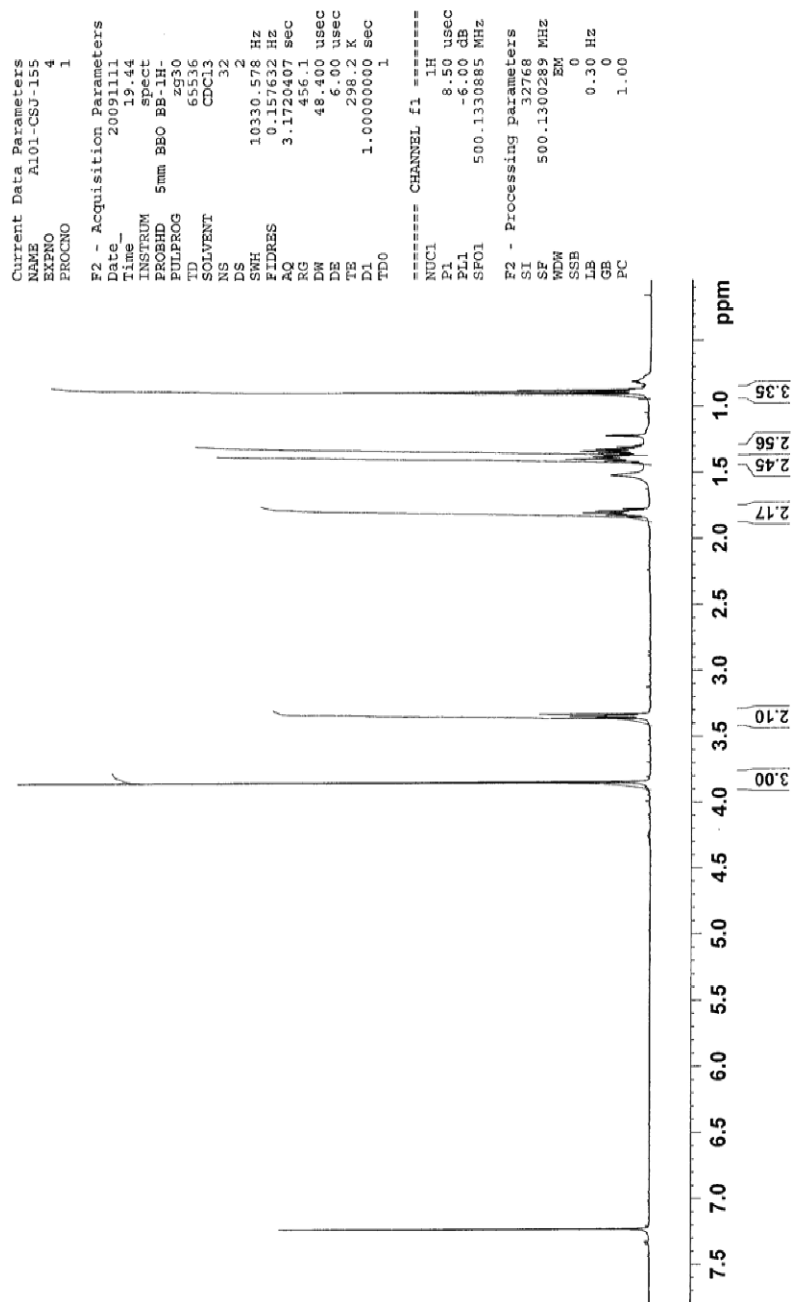


Figure 56. ^1H NMR (500 MHz) spectrum of methyl (pentylsulfonyl)diazoacetate (**189**) in CDCl_3 .

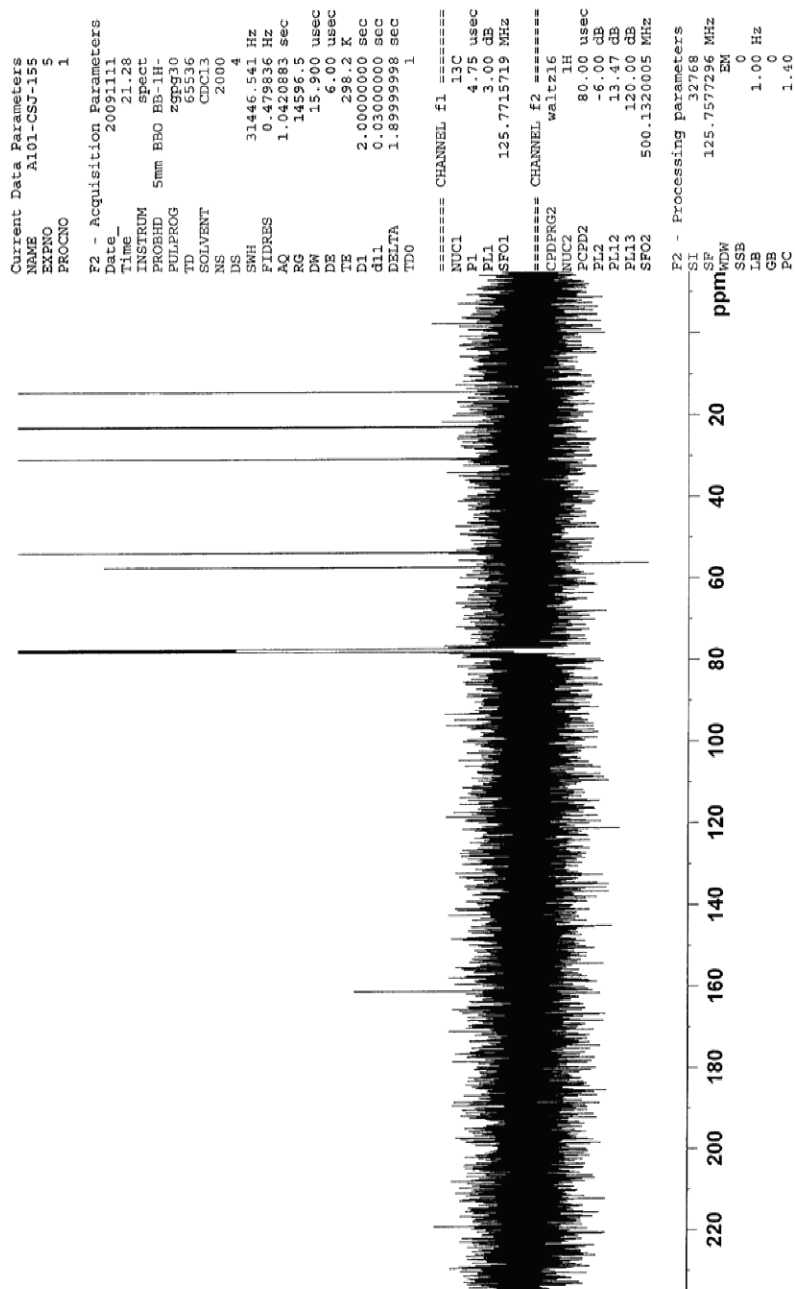


Figure 57. $^{13}\text{C}\{^1\text{H}\}$ NMR (125 MHz) spectrum of methyl (pentylsulfonyl)diazoacetate (**189**) in CDCl_3 .

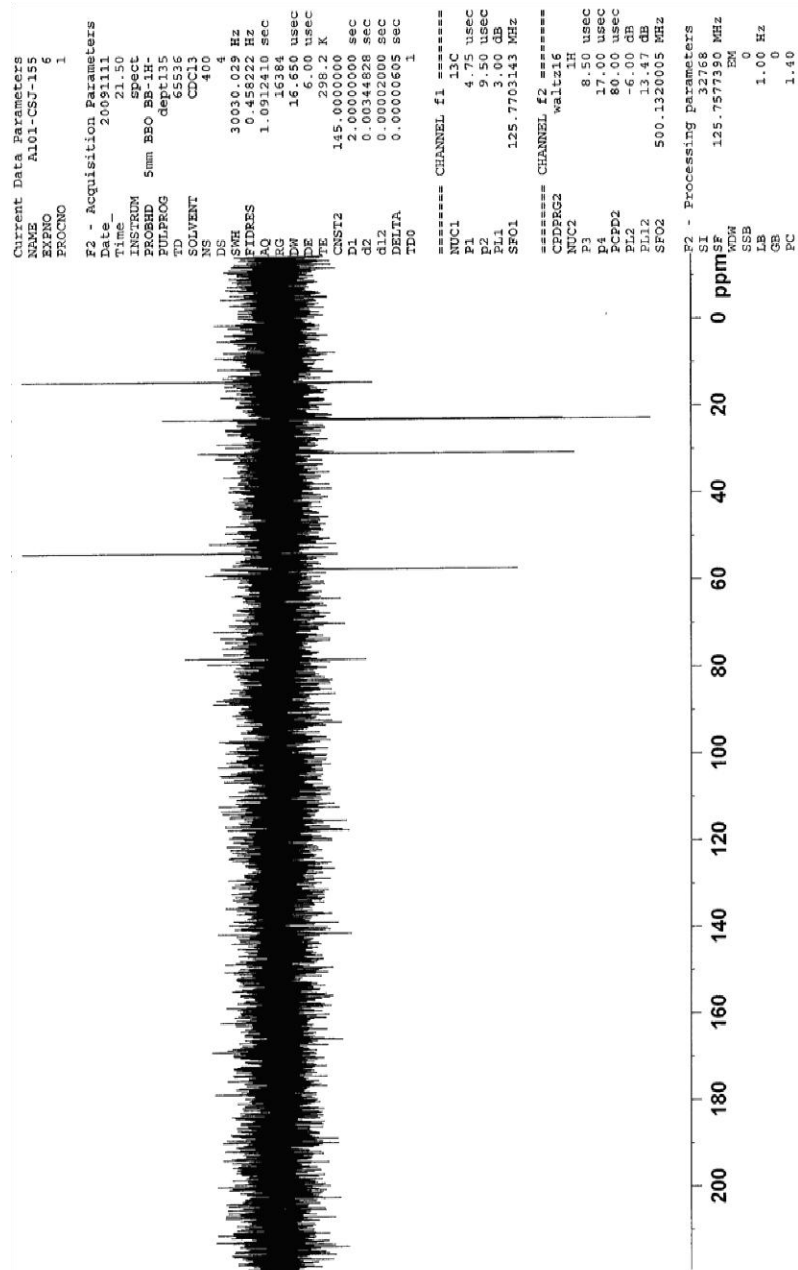


Figure 58. DEPT 135 NMR (125 MHz) spectrum of methyl (pentylsulfonyl)diazoacetate (189) in CDCl_3 .

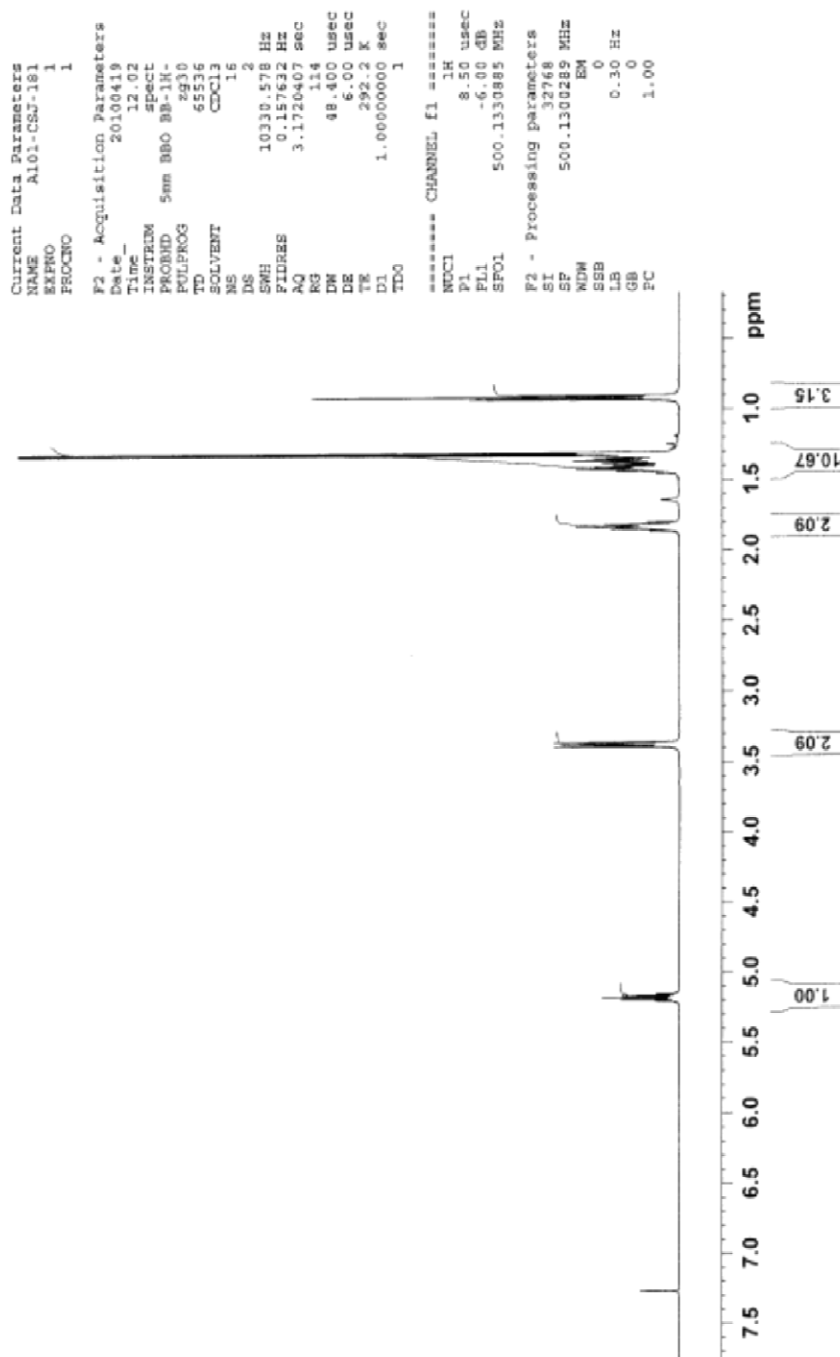


Figure 59. ^1H NMR (500 MHz) spectrum of isopropyl (pentylsulfonyl)diazoacetate (**190**) in CDCl_3 .

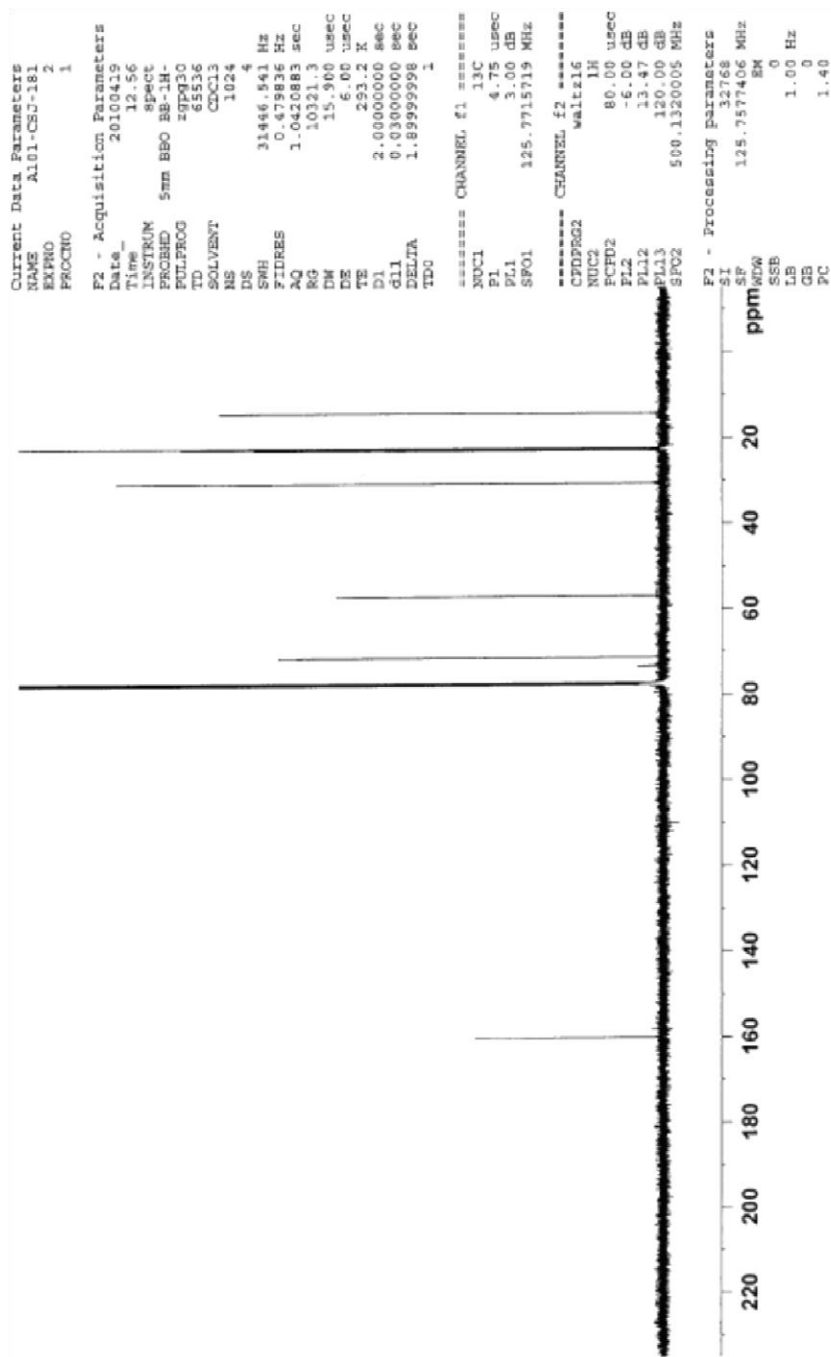


Figure 60. $^{13}\text{C}\{^1\text{H}\}$ NMR (125 MHz) spectrum of isopropyl (pentylsulfonyl)diazoacetate (**190**) in CDCl_3 .

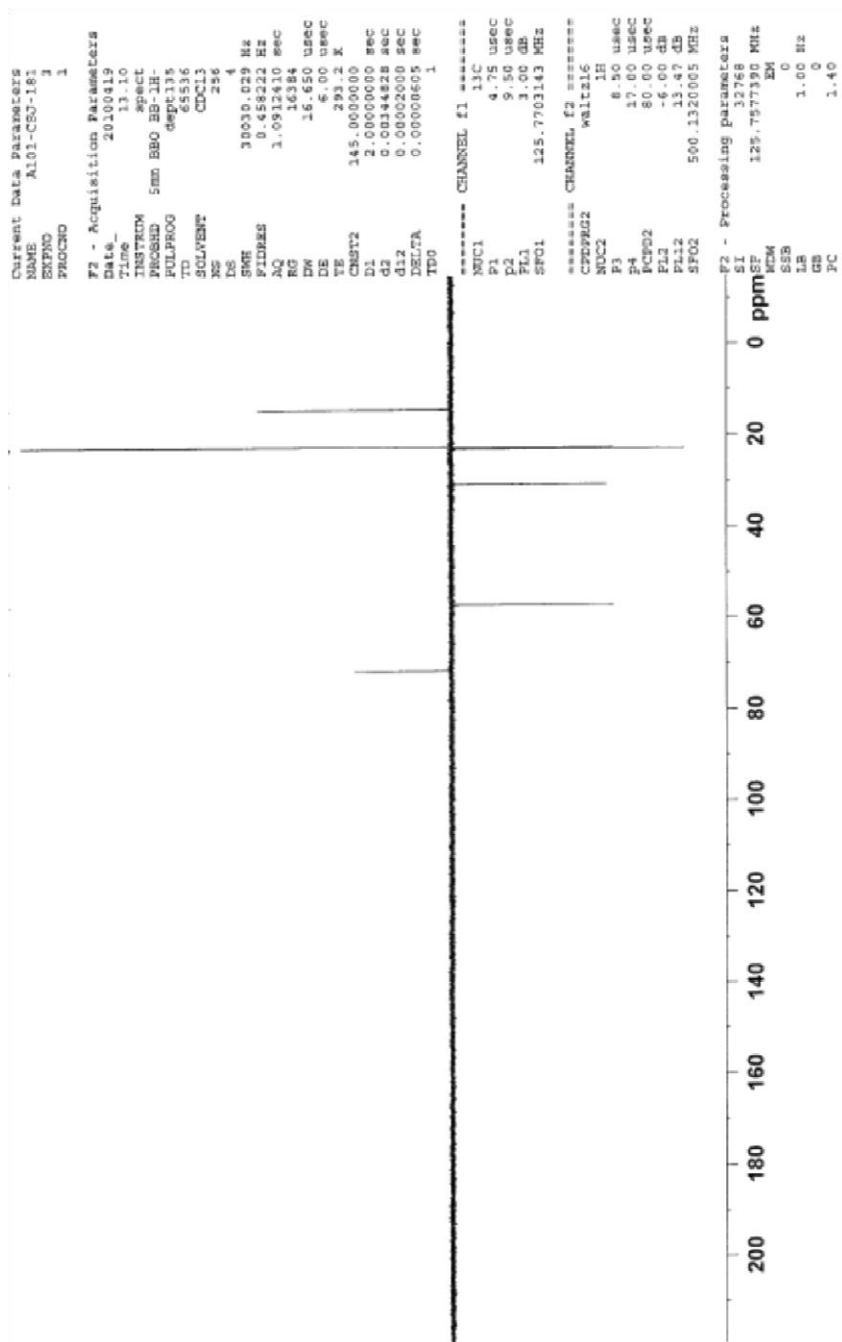


Figure 61. DEPT 135 NMR (125 MHz) spectrum of isopropyl (pentylsulfonyl)diazoacetate (**190**) in CDCl₃.

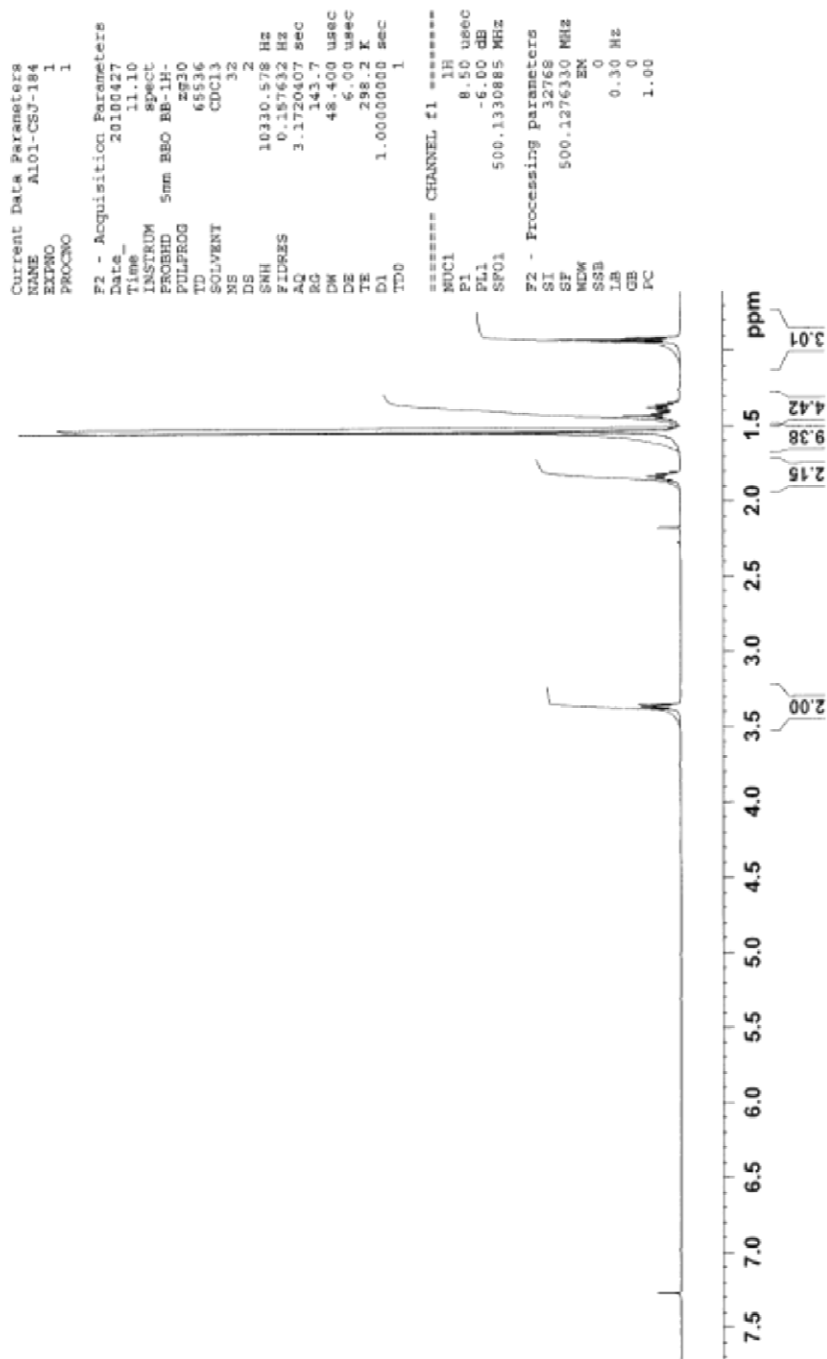


Figure 62. ^1H NMR (500 MHz) spectrum of *t*-butyl (pentylsulfonyl)diazoacetate (**191**) in CDCl_3 .

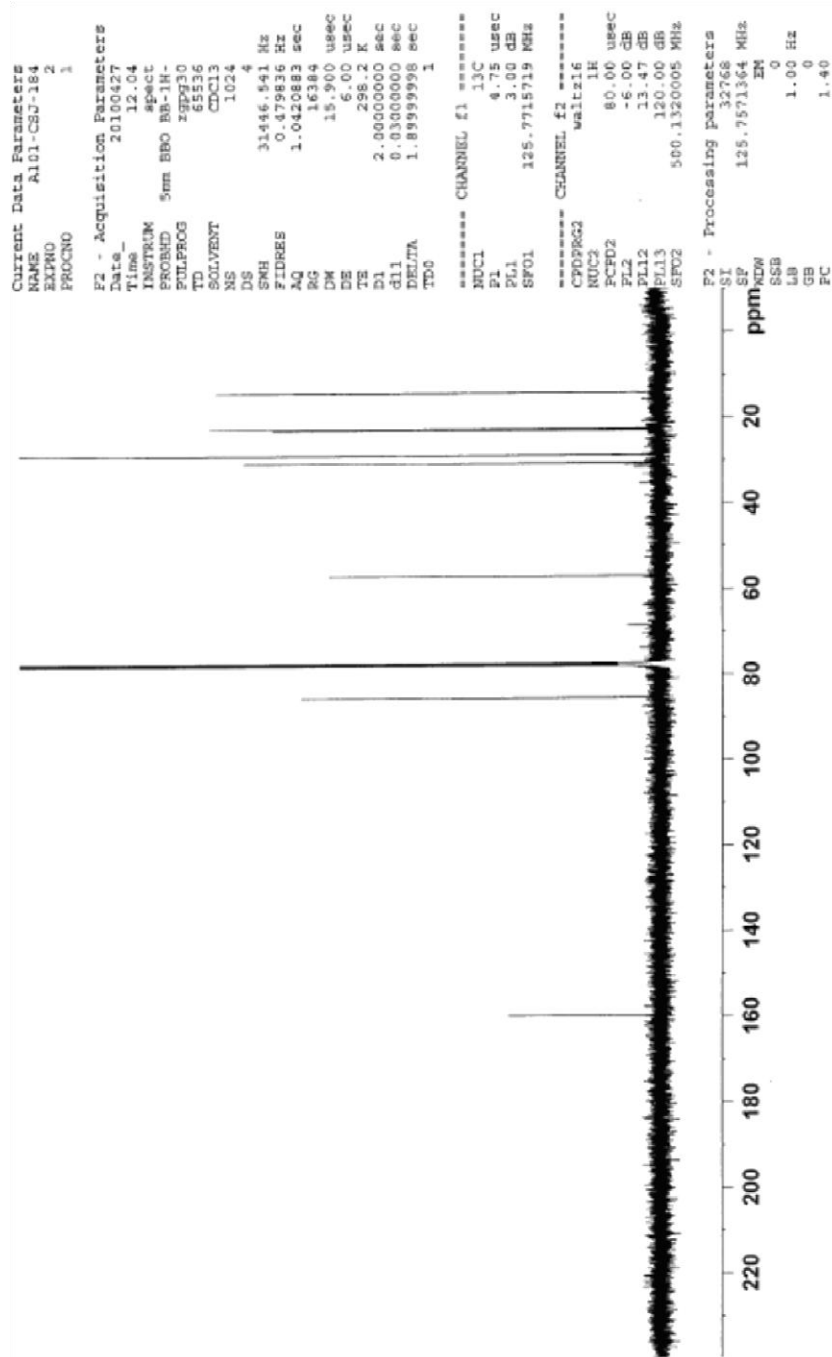


Figure 63. $^{13}\text{C}\{^1\text{H}\}$ NMR (125 MHz) spectrum of *t*-butyl (pentylsulfonyl)diazoacetate (**191**) in CDCl_3 .

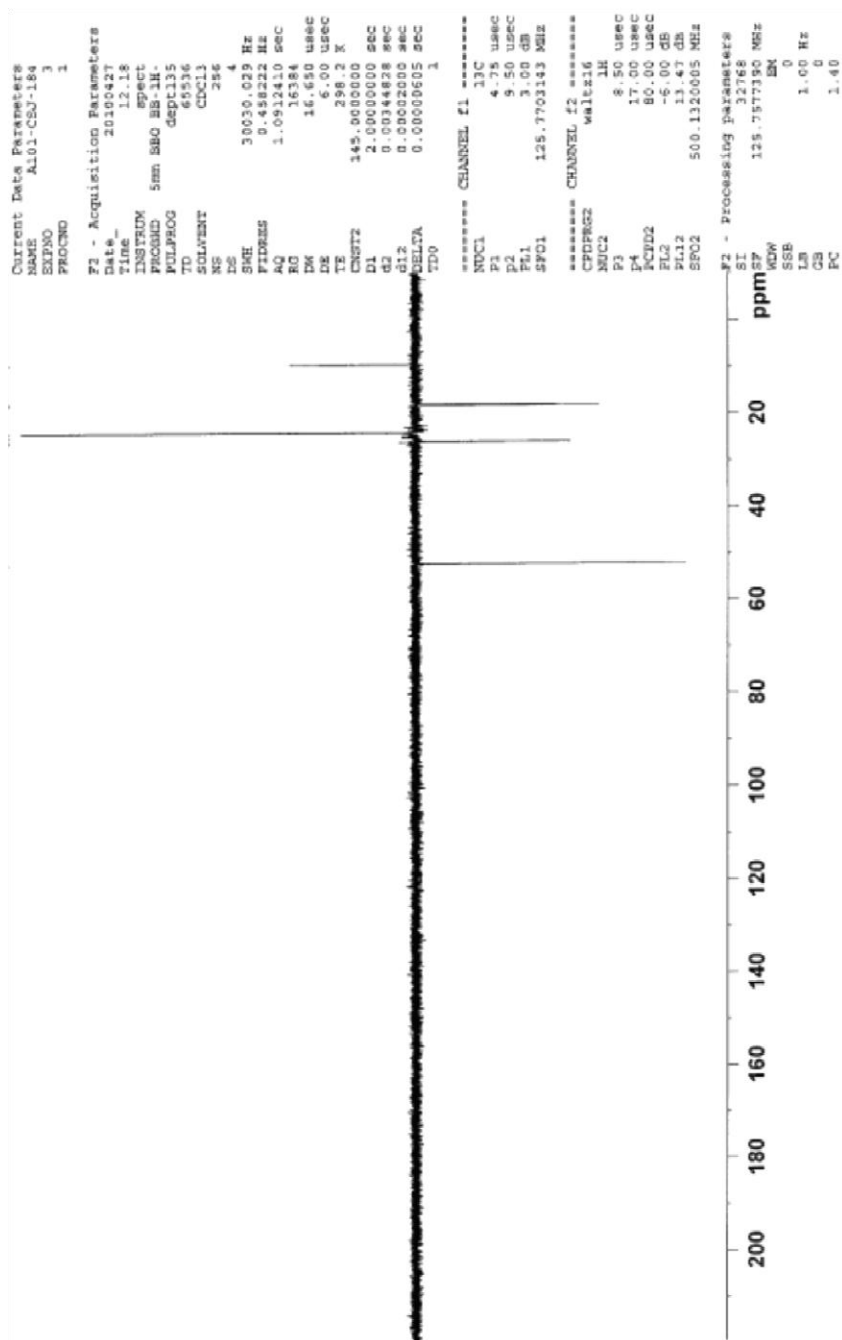


Figure 64. DEPT 135 NMR (125 MHz) spectrum of *t*-butyl (pentylsulfonyl)diazoacetate (**191**) in CDCl₃.

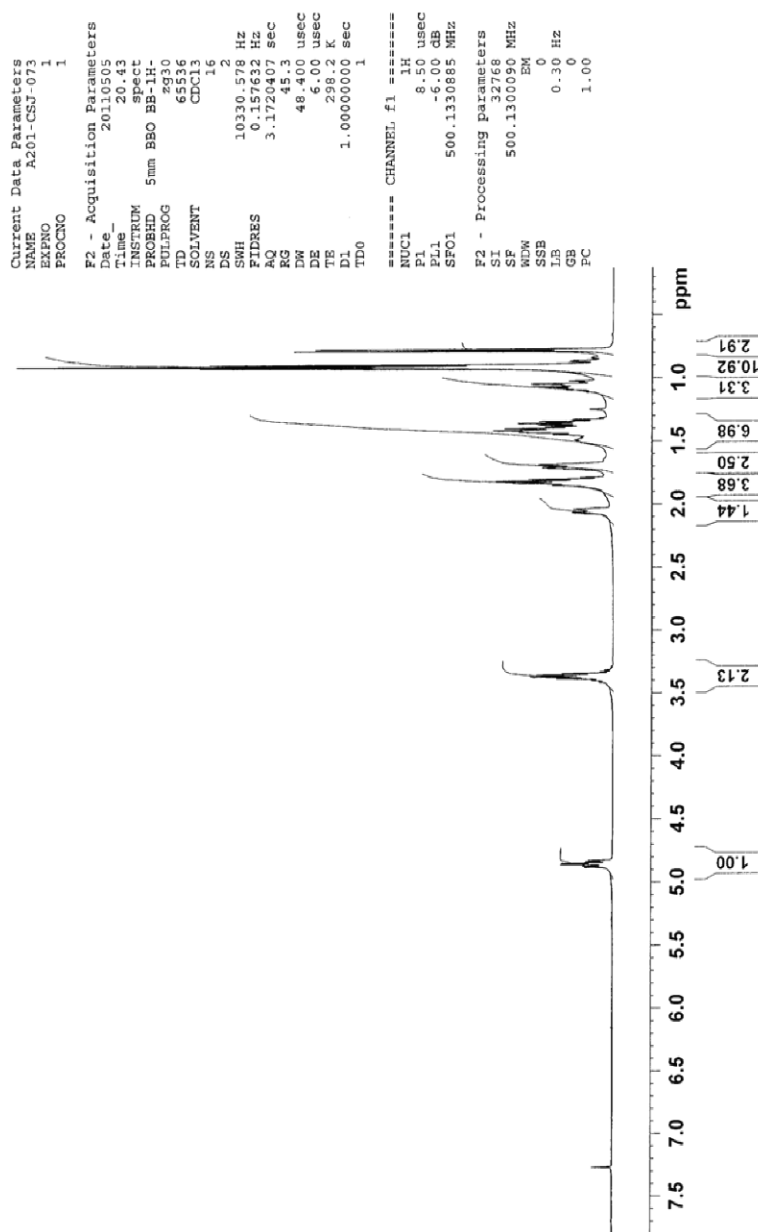


Figure 65. ^1H NMR (500 MHz) spectrum of (1*R*,2*S*,5*R*)-2-isopropyl-5-methylcyclohexyl (pentylsulfonyl)diazoacetate (**193**) in CDCl_3 .

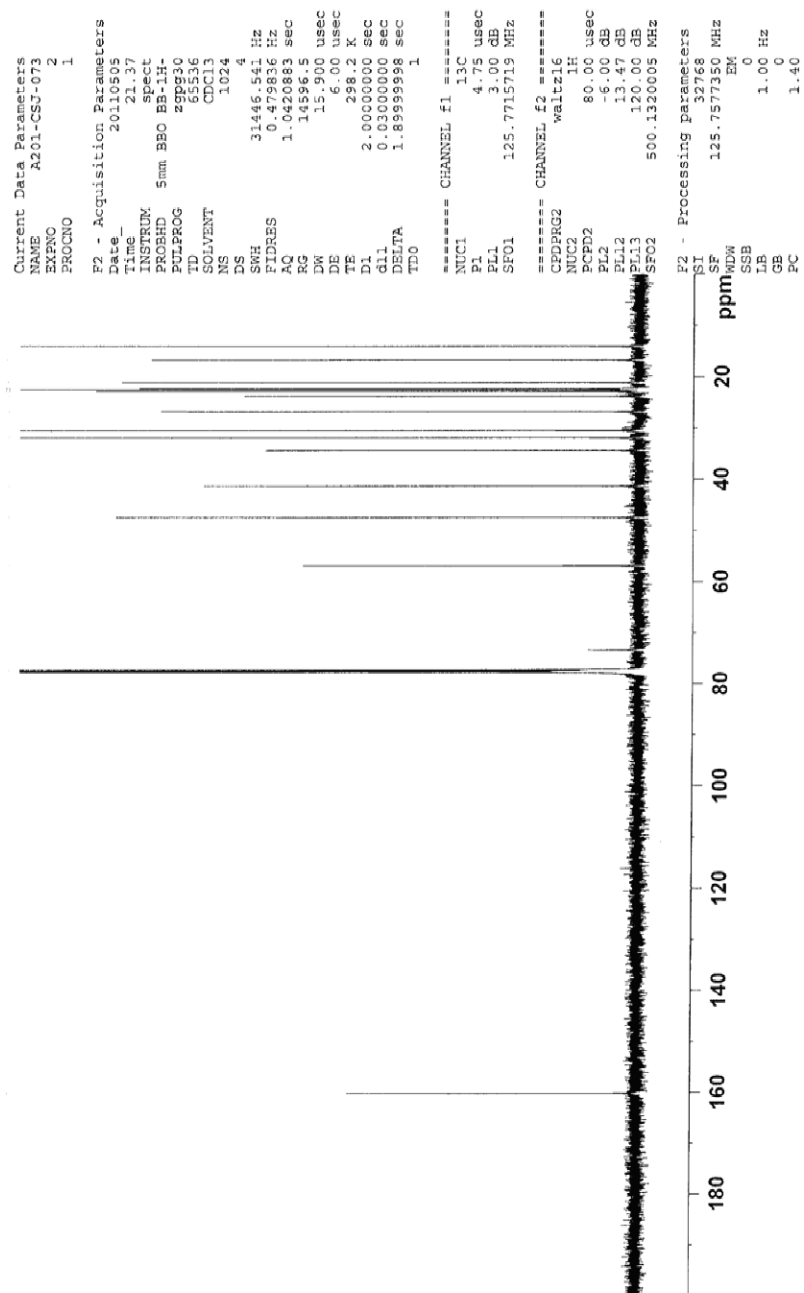


Figure 66. $^{13}\text{C}\{^1\text{H}\}$ NMR (500 MHz) spectrum of (1*R*,2*S*,5*R*)-2-isopropyl-5-methylcyclohexyl (pentylsulfonyl)diazoacetate (**193**) in CDCl_3 .

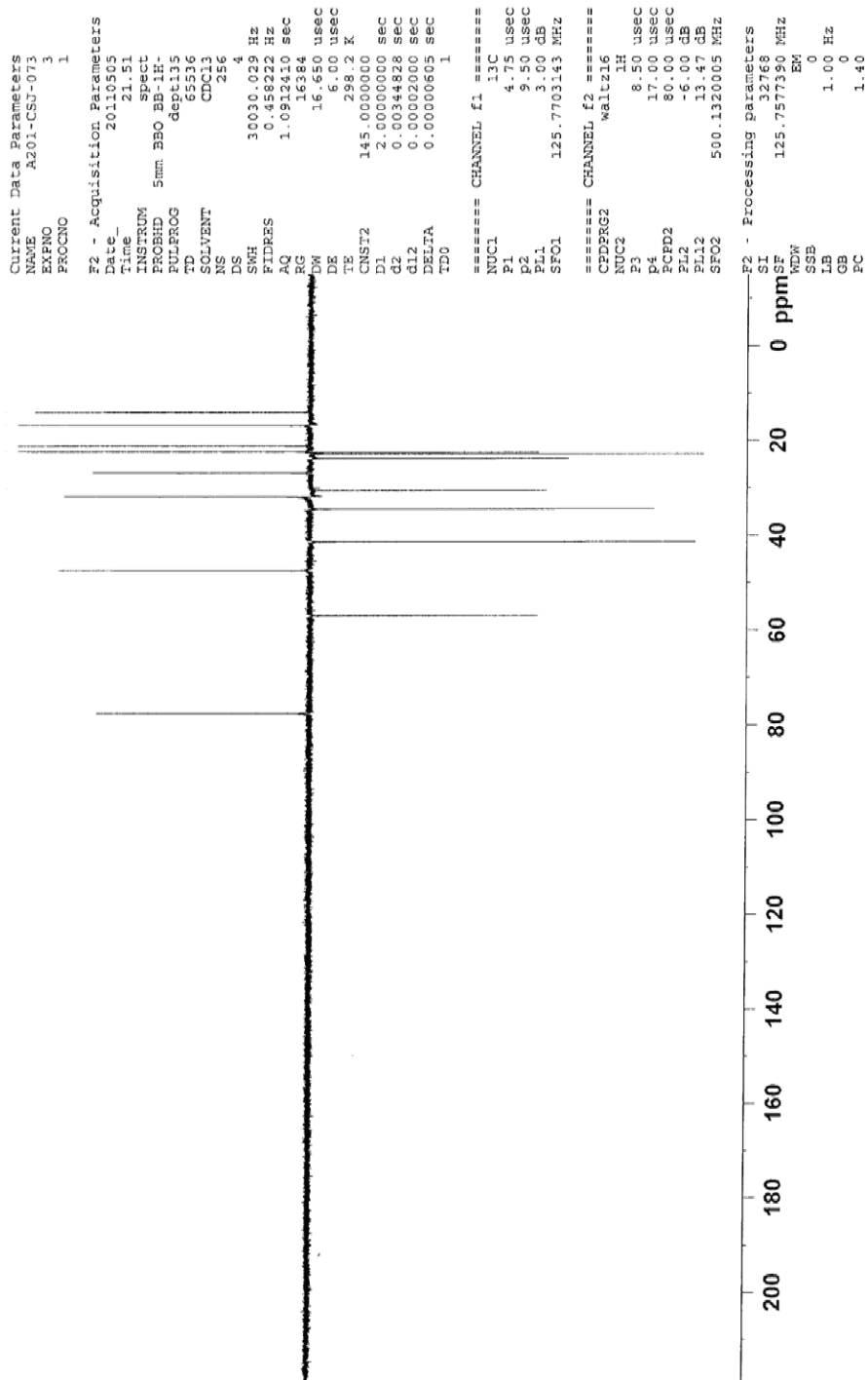


Figure 67. DEPT 135 NMR (500 MHz) spectrum of (1*R*,2*S*,5*R*)-2-isopropyl-5-methylcyclohexyl (pentylsulfonyl)diazoacetate (**193**) in CDCl₃.

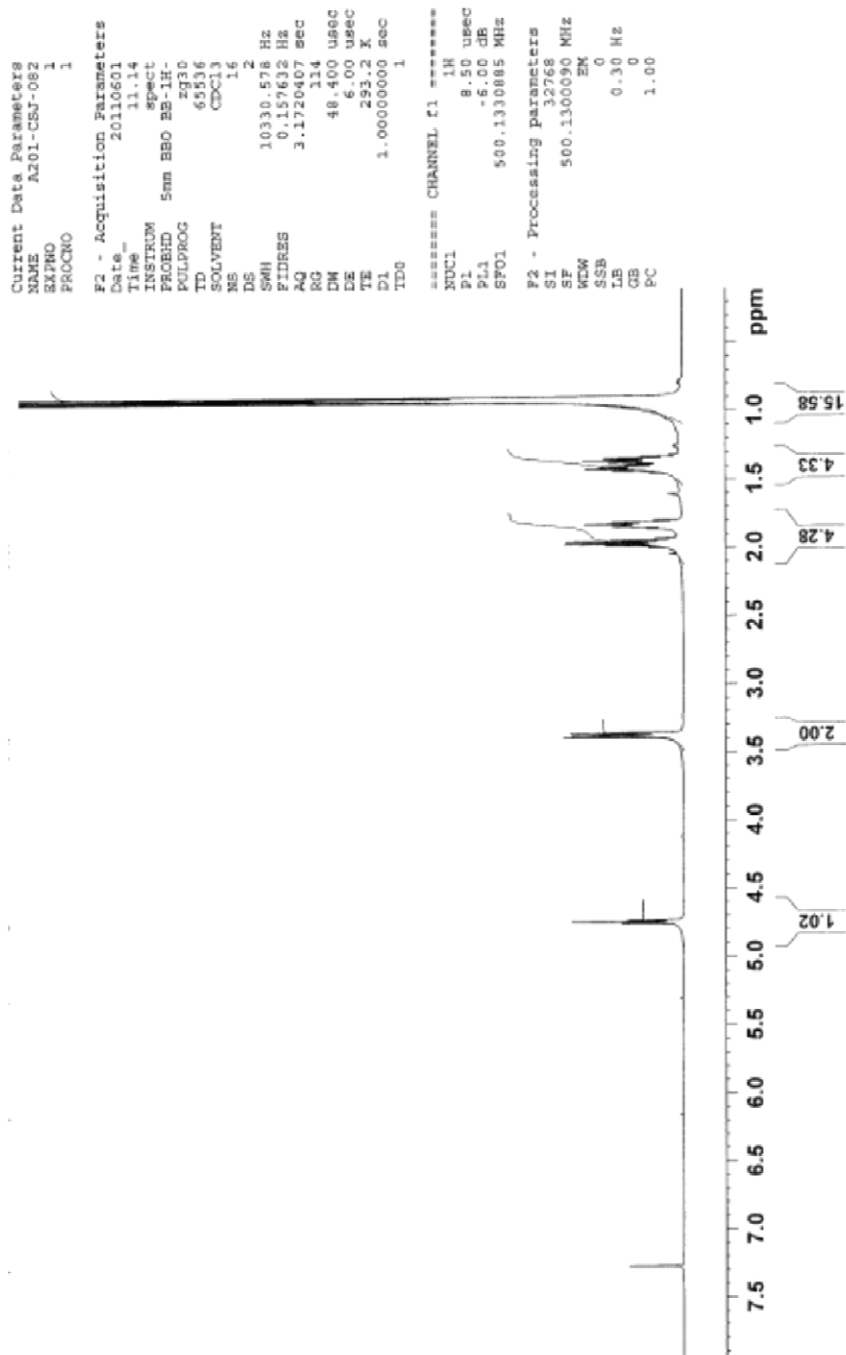


Figure 68. ^1H NMR (500 MHz) spectrum of 2,4-dimethyl-3-pentyl (pentylsulfonyl)diazoacetate (**194**) in CDCl_3 .

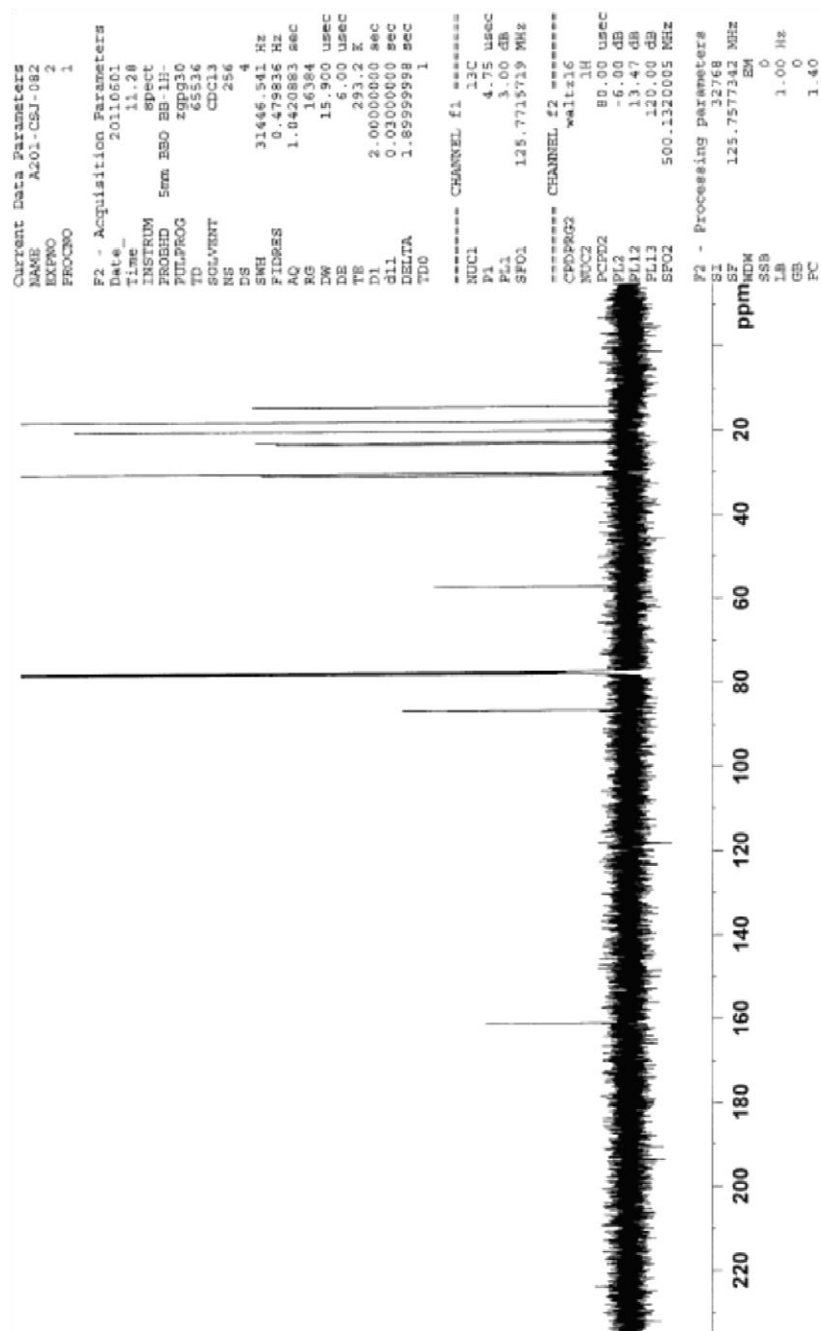


Figure 69. $^{13}\text{C}\{^1\text{H}\}$ NMR (500 MHz) spectrum of 2,4-dimethyl-3-pentyl(pentylsulfonyl)diazoacetate (**194**) in CDCl_3 .

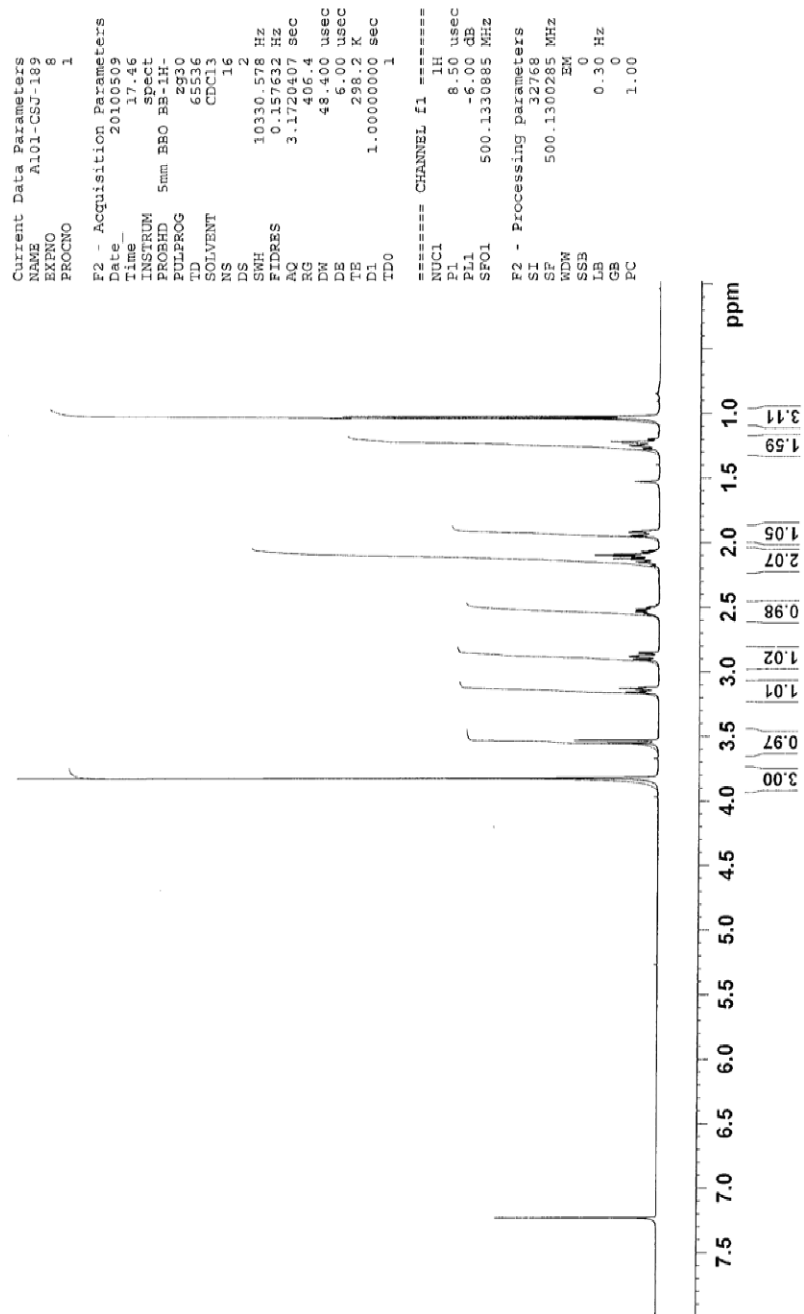


Figure 71. ^1H NMR (500 MHz) spectrum of *trans*-methyl 3-methyltetrahydro-2H-thiopyran-1,1-dioxide-2-carboxylate (**195**) in CDCl_3 .

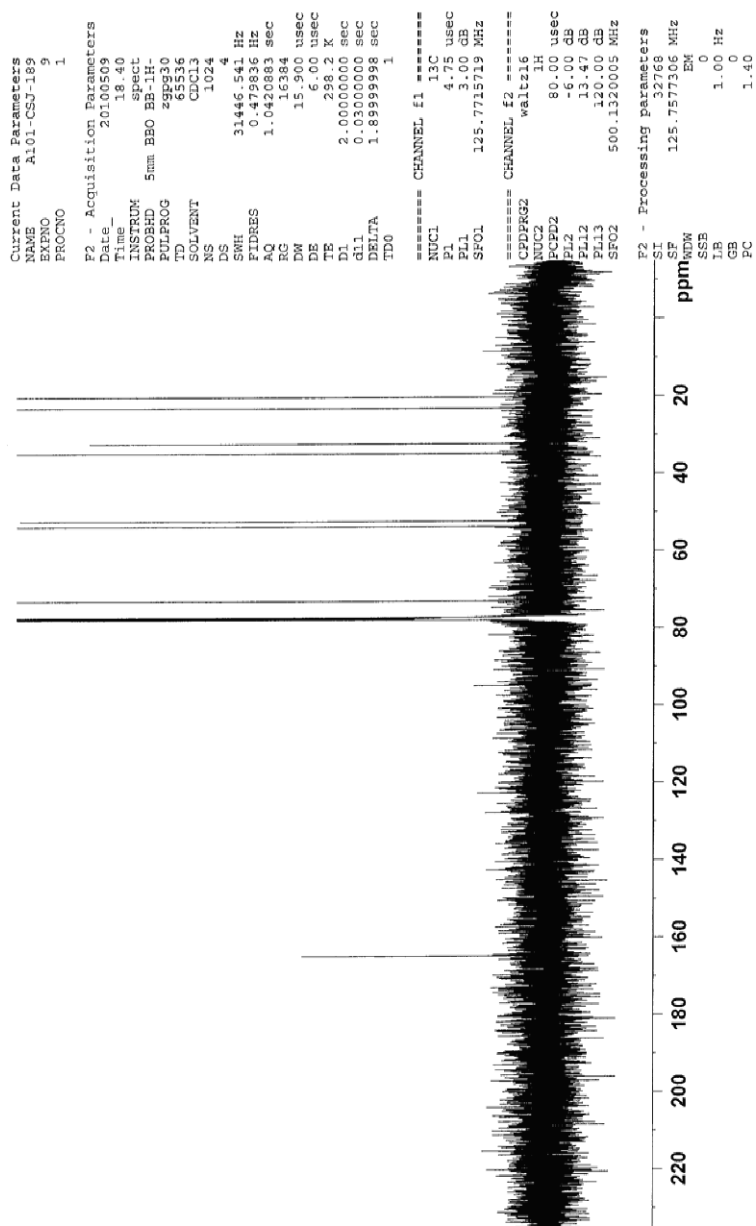


Figure 72. $^{13}\text{C}\{^1\text{H}\}$ NMR (125 MHz) spectrum of *trans*-methyl 3-methyltetrahydro-2*H*-thiopyran-1,1-dioxide-2-carboxylate (**195**) in CDCl_3 .

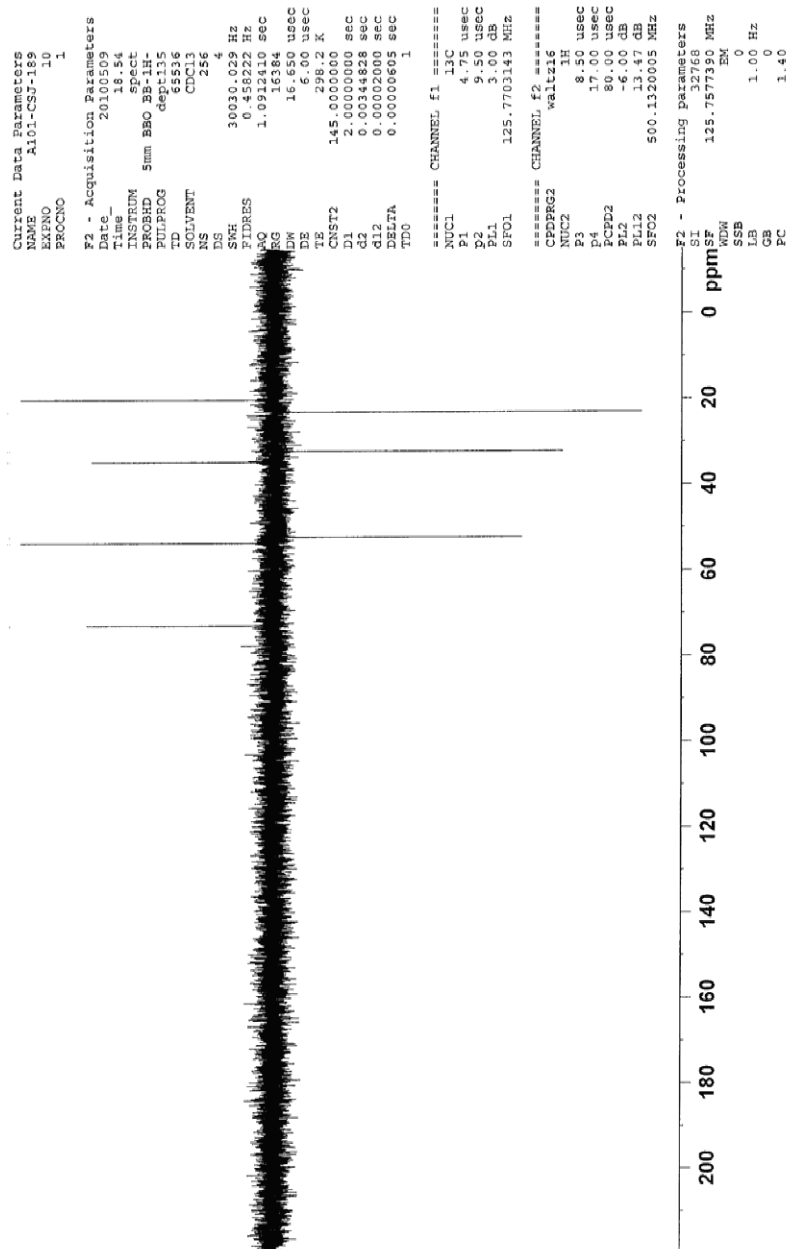


Figure 73. DEPT 135 NMR (125 MHz) spectrum of *trans*-methyl 3-methyltetrahydro-2*H*-thiopyran-1,1-dioxide-2-carboxylate (**195**) in CDCl₃.

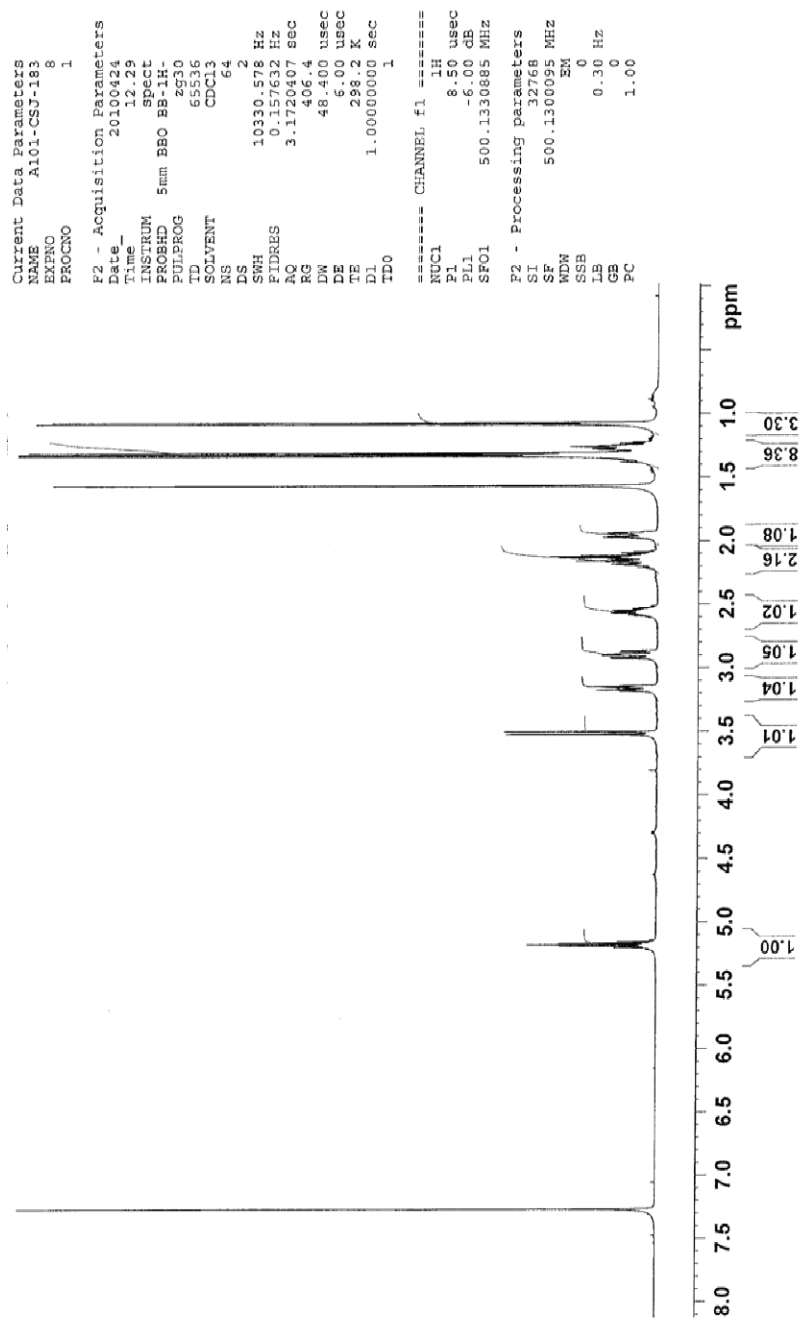


Figure 74. ^1H NMR (500 MHz) spectrum of *trans*-isopropyl 3-methyltetrahydro-2*H*-thiopyran-1,1-dioxide-2-carboxylate (**196**) in CDCl_3 .

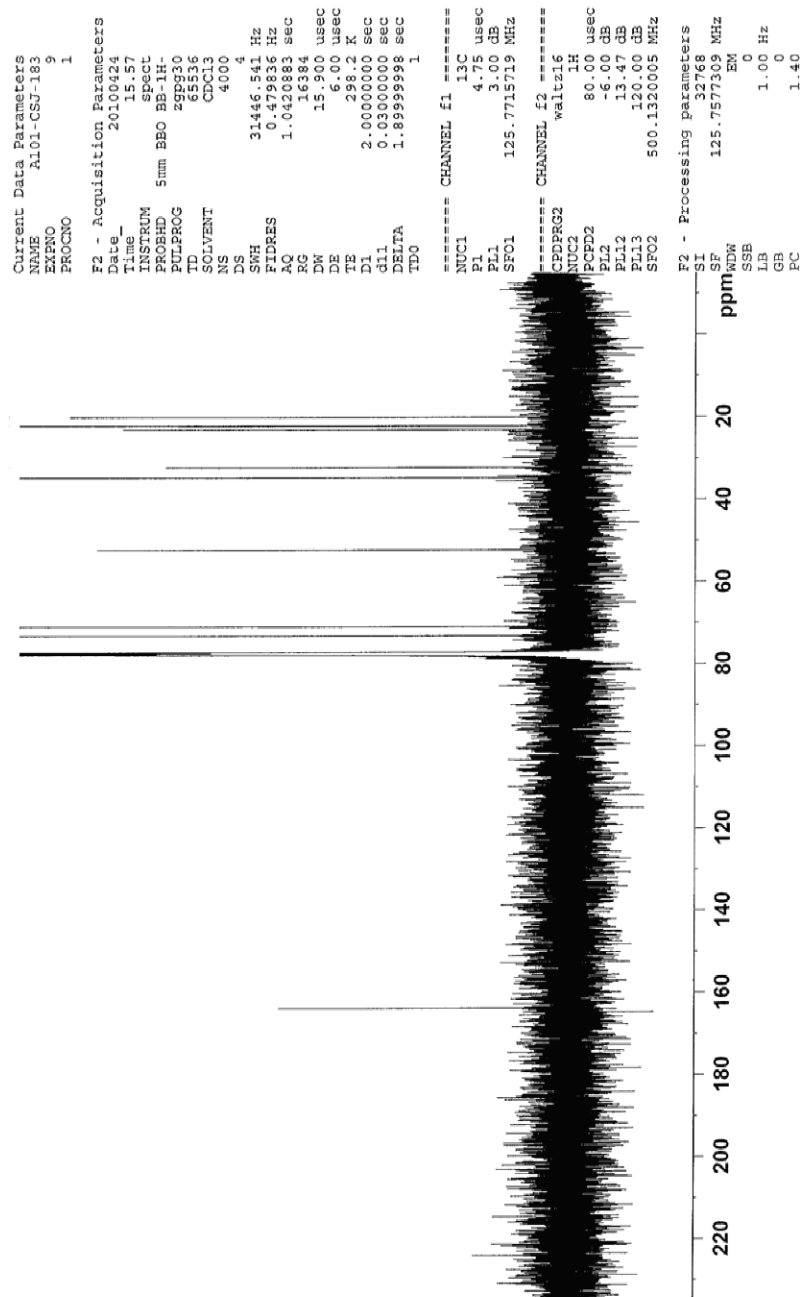


Figure 75. $^{13}\text{C}\{^1\text{H}\}$ NMR (125MHz) spectrum of *trans*-isopropyl 3-methyltetrahydro-2H-thiopyran-1,1-dioxide-2-carboxylate (**196**) in CDCl_3 .

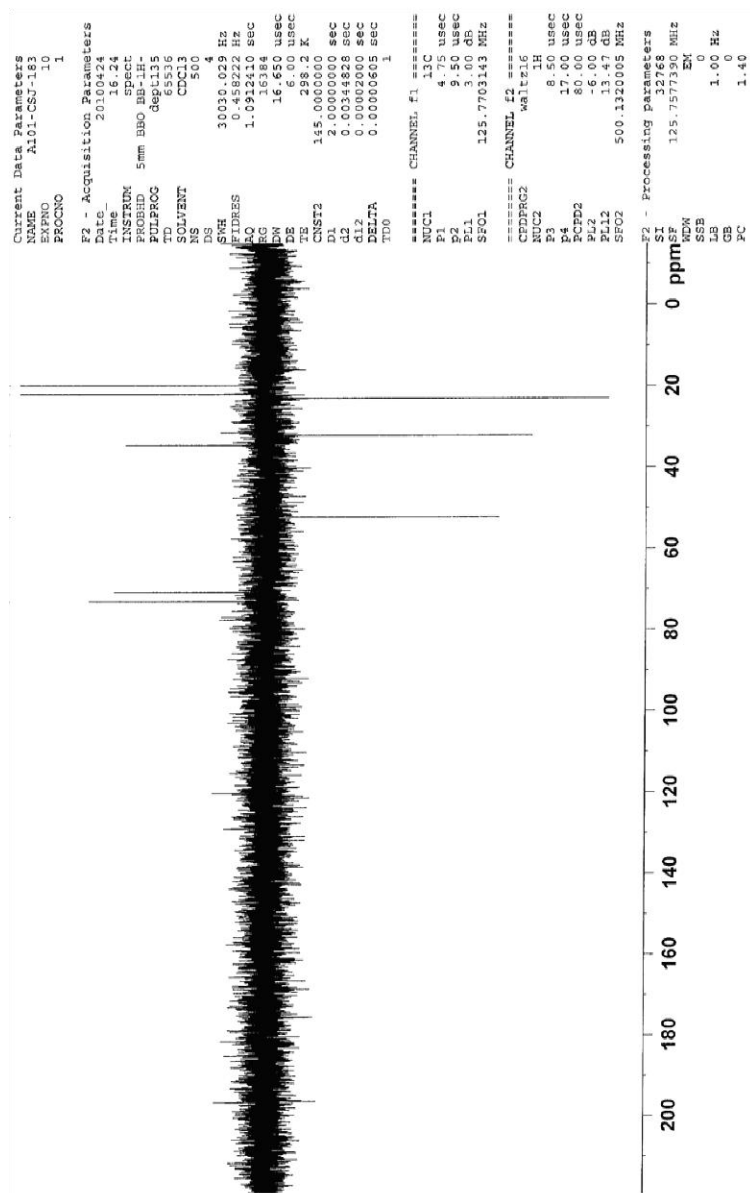


Figure 76. DEPT 135 NMR (125MHz) spectrum of *trans*-isopropyl 3-methyltetrahydro-2*H*-thiopyran-1,1-dioxide-2-carboxylate (**196**) in CDCl₃.

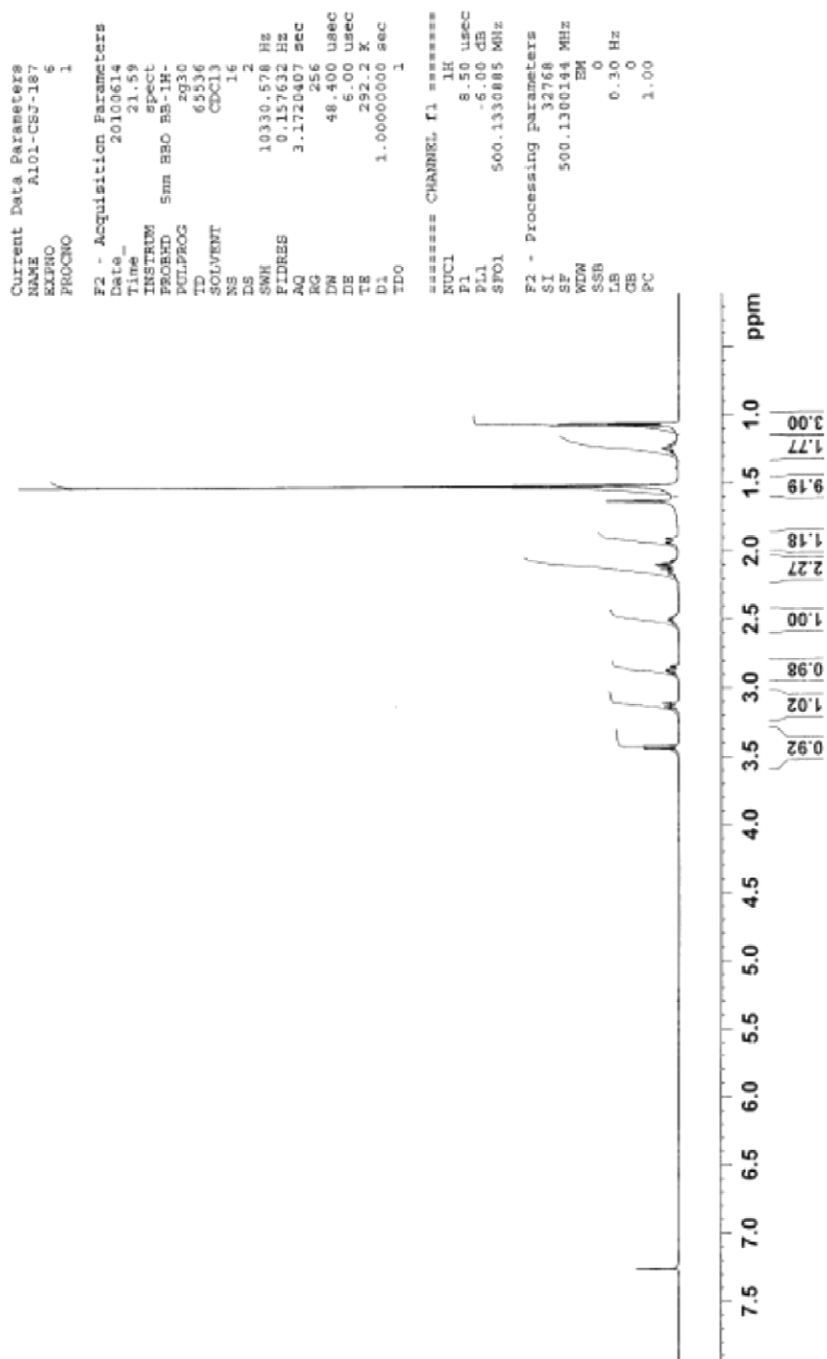


Figure 77. ^1H NMR (500 MHz) spectrum of *trans-t*-butyl 3-methyltetrahydro-2*H*-thiopyran-1,1-dioxide-2-carboxylate (**197**) in CDCl_3 .

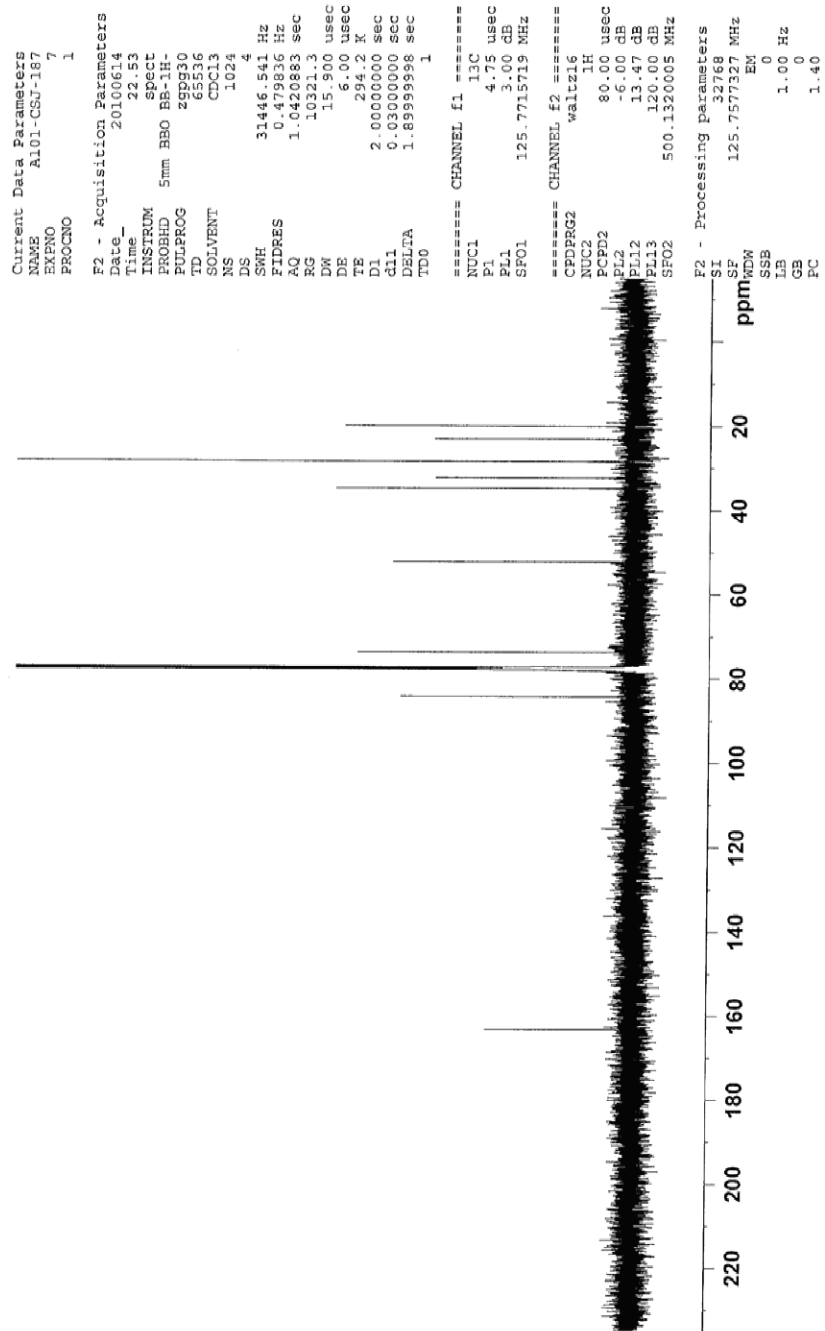


Figure 78. $^{13}\text{C}\{^1\text{H}\}$ NMR (125 MHz) spectrum of *trans-t*-butyl 3-methyltetrahydro-2*H*-thiopyran-1,1-dioxide-2-carboxylate (**197**) in CDCl_3 .

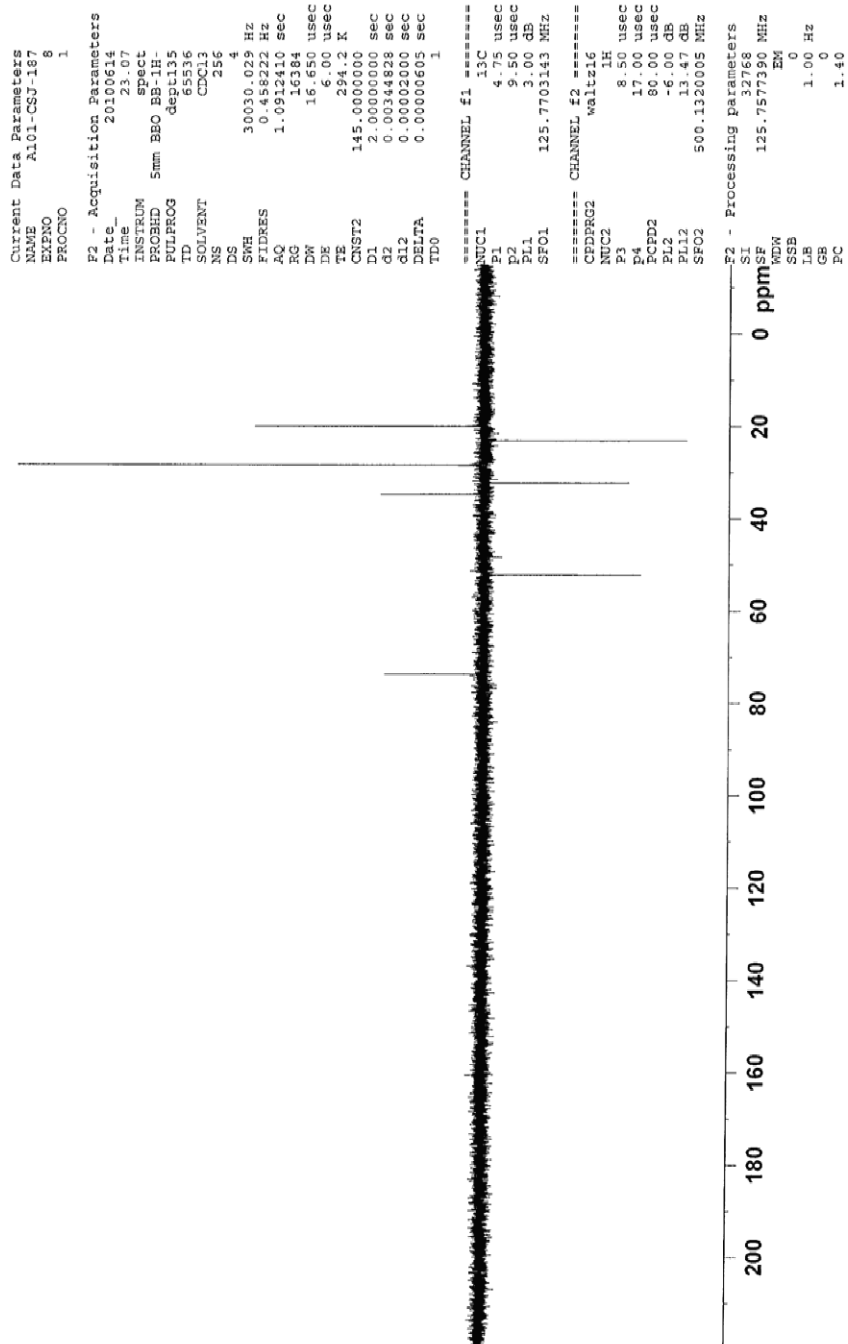


Figure 79. DEPT 135 NMR (125 MHz) spectrum of *trans-t*-butyl 3-methyltetrahydro-2*H*-thiopyran-1,1-dioxide-2-carboxylate (**197**) in CDCl₃.

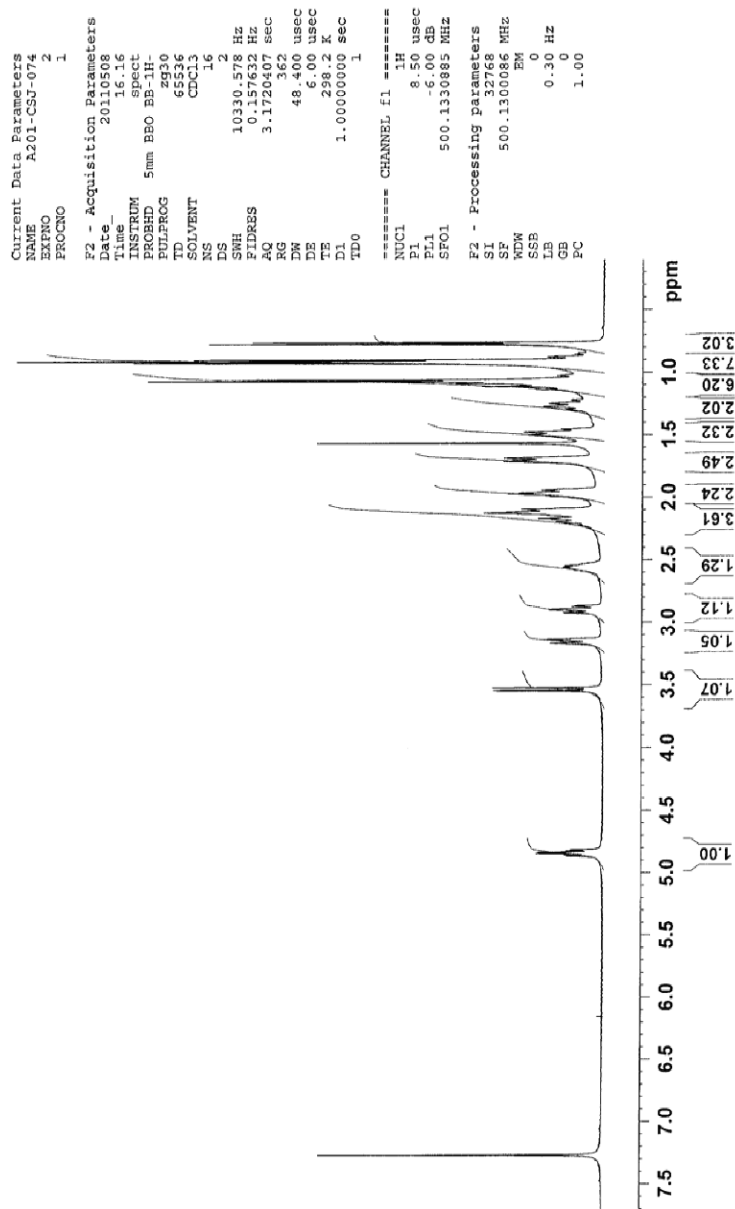


Figure 80. ^1H NMR (500 MHz) spectrum of (1*R*,2*S*,5*R*)-2-isopropyl-5-methylcyclohexyl (2*R*,3*R*) 3-methyltetrahydro-2*H*-thiopyran-1,1-dioxide-2-carboxylate (**199**) in CDCl_3

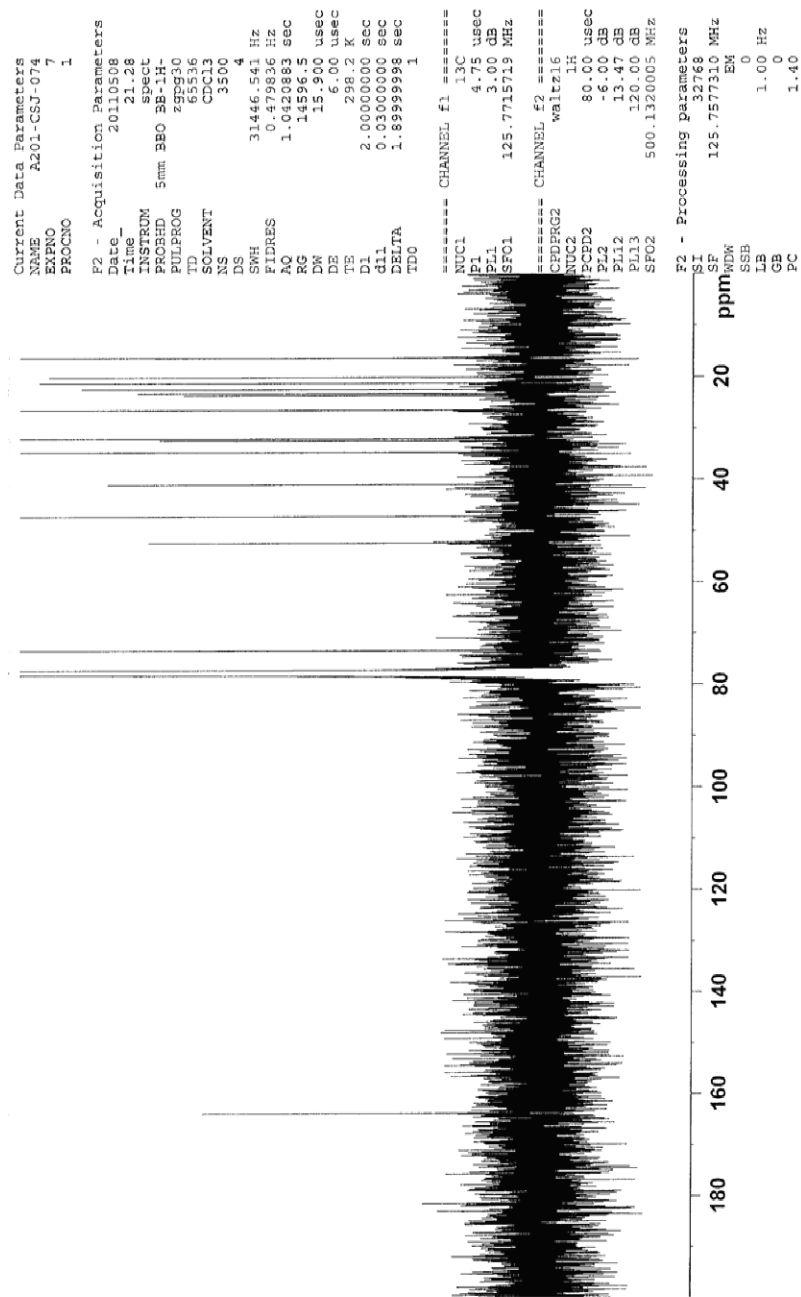


Figure 81. $^{13}\text{C}\{^1\text{H}\}$ NMR (125 MHz) spectrum of (1*R*,2*S*,5*R*)-2-isopropyl-5-methylcyclohexyl (2*R*,3*R*) 3-methyltetrahydro-2*H*-thiopyran-1,1-dioxide-2-carboxylate (**199**) in CDCl_3 .

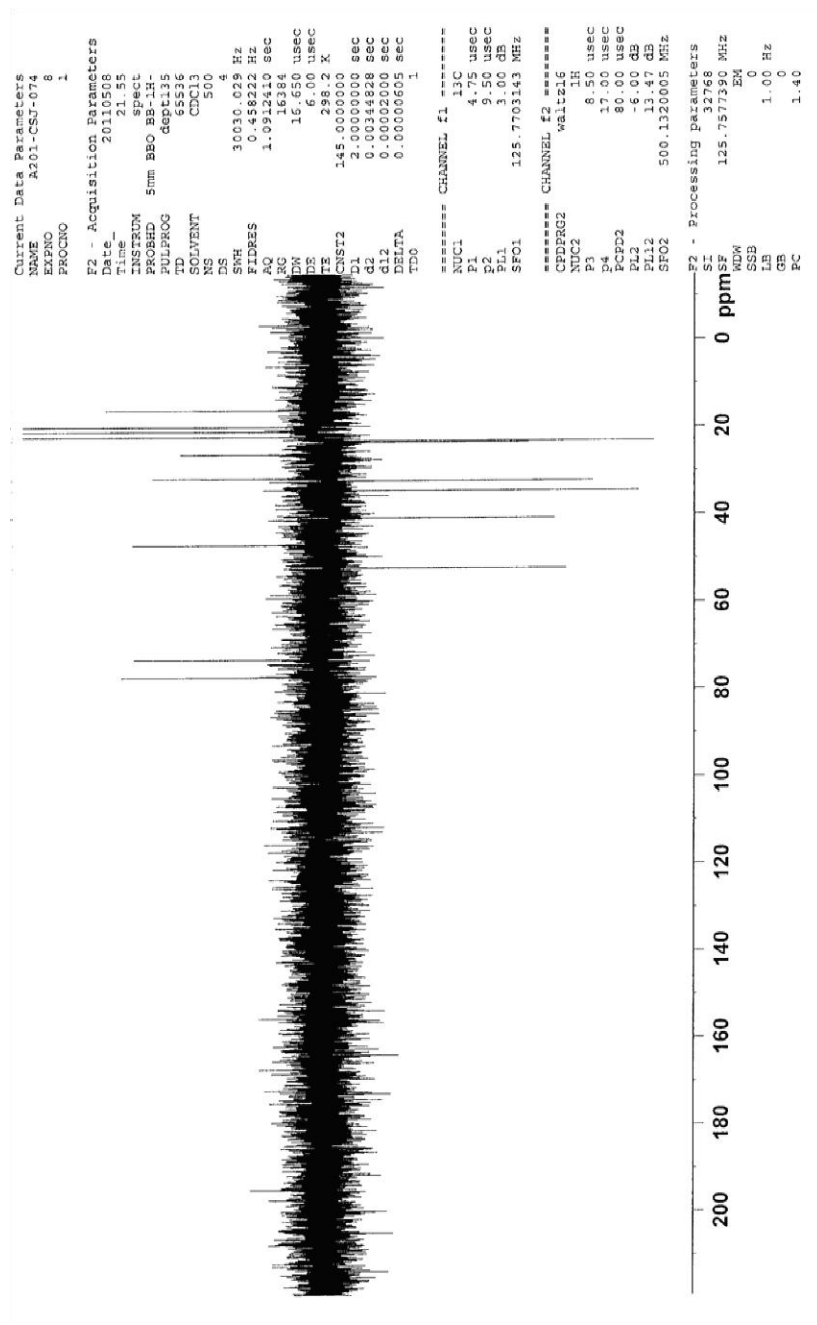


Figure 82. DEPT 135 NMR (125 MHz) spectrum of (1*R*,2*S*,5*R*)-2-isopropyl-5-methylcyclohexyl (2*R*,3*R*) 3-methyltetrahydro-2*H*-thiopyran-1,1-dioxide-2-carboxylate (**199**) in CDCl₃.

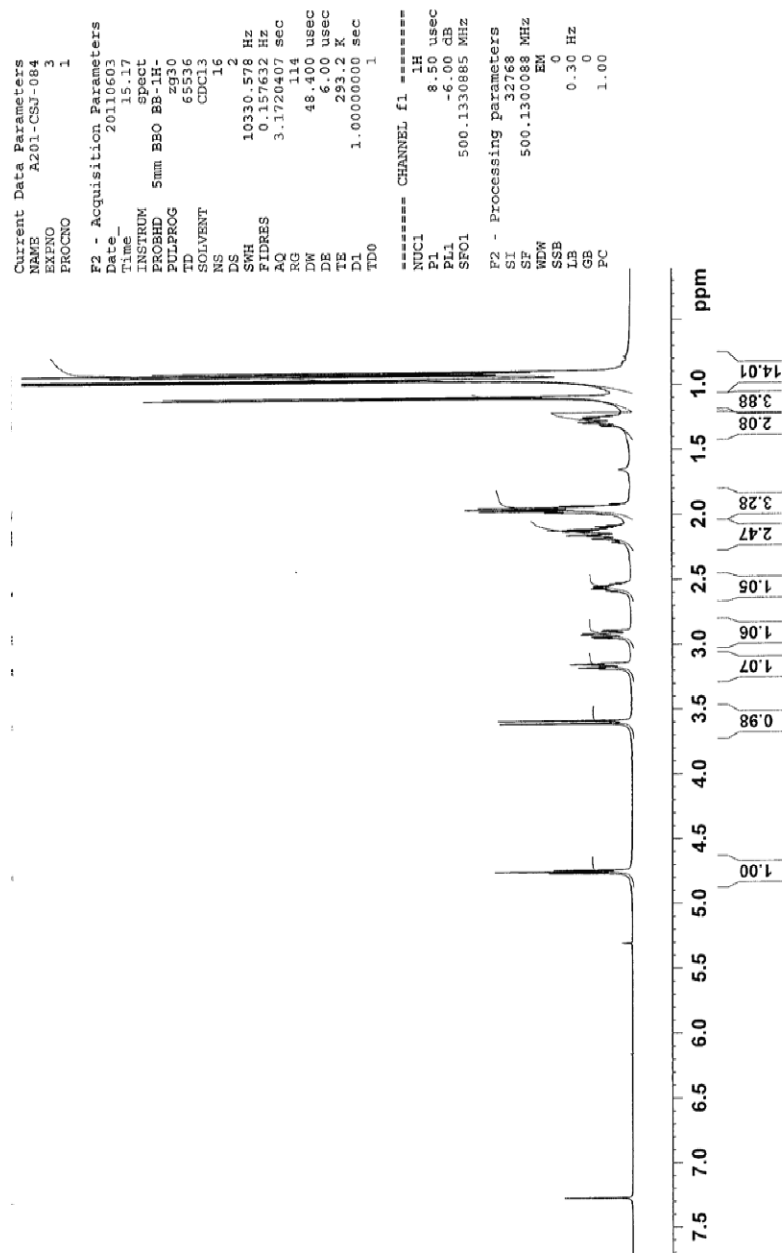


Figure 83. ^1H NMR (500 MHz) spectrum of *trans*-2,4-dimethyl-3-pentyl 3-methyltetrahydro-2*H*-thiopyran-1,1-dioxide-2-carboxylate (**200**) in CDCl_3 .

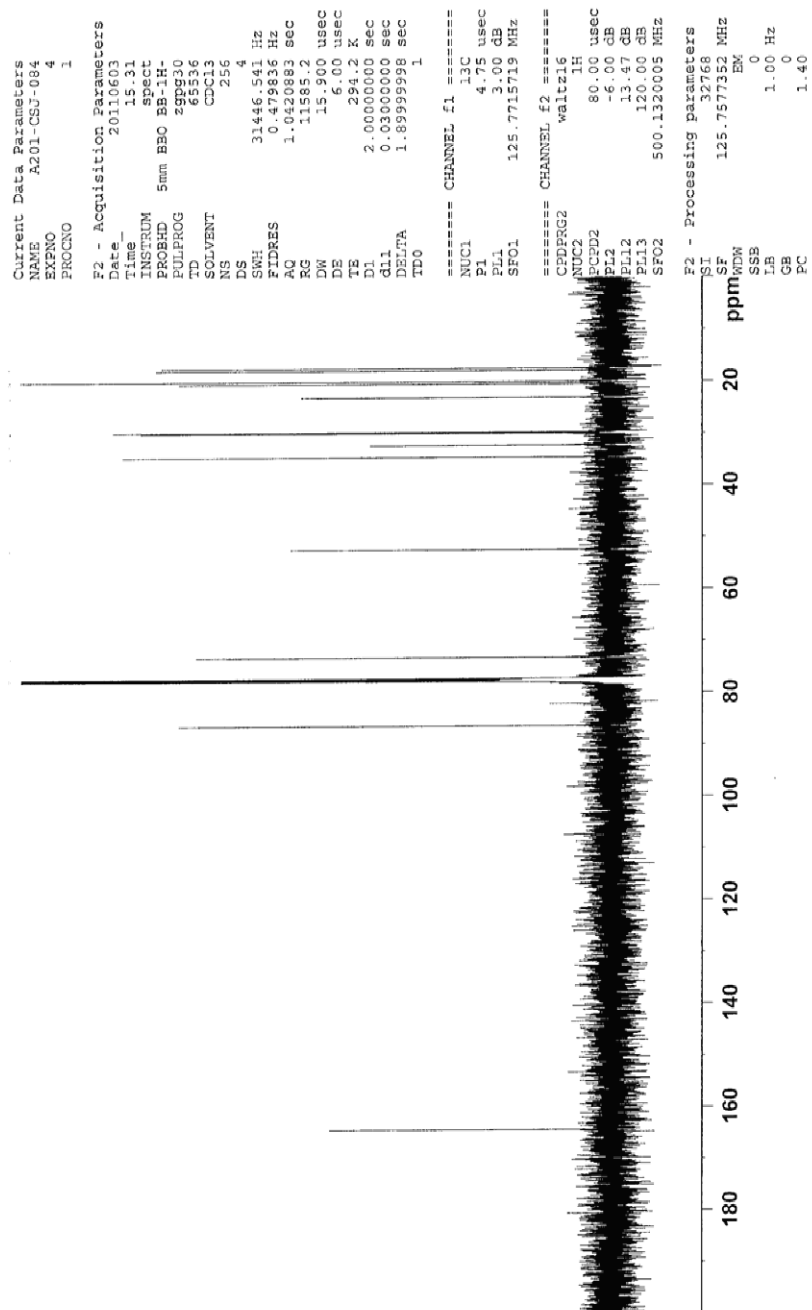


Figure 84. $^{13}\text{C}\{^1\text{H}\}$ NMR (125 MHz) spectrum of *trans*-2,4-dimethyl-3-pentyl 3-methyltetrahydro-2*H*-thiopyran-1,1-dioxide-2-carboxylate (**200**) in CDCl_3 .

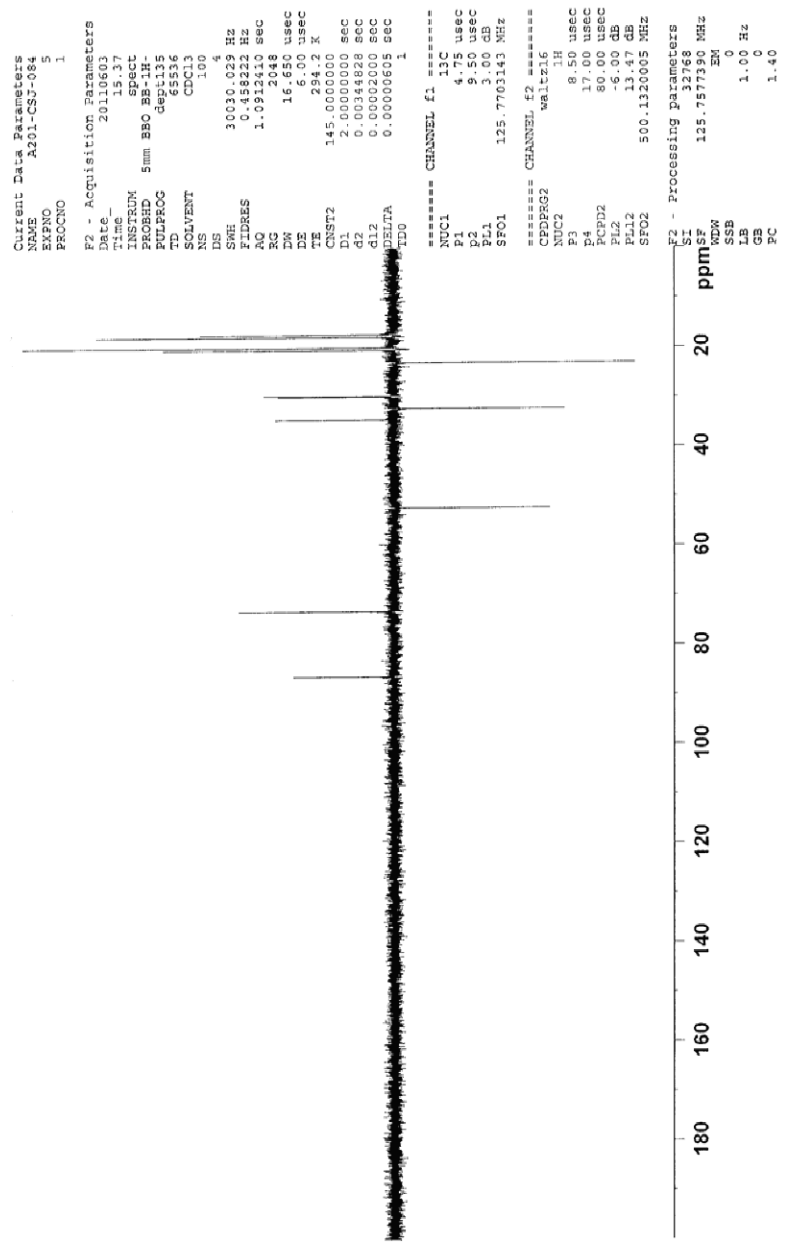


Figure 85. DEPT 135 NMR (125 MHz) spectrum of *trans*-2,4-dimethyl-3-pentyl 3-methyltetrahydro-2*H*-thiopyran-1,1-dioxide-2-carboxylate (**200**) in CDCl₃.

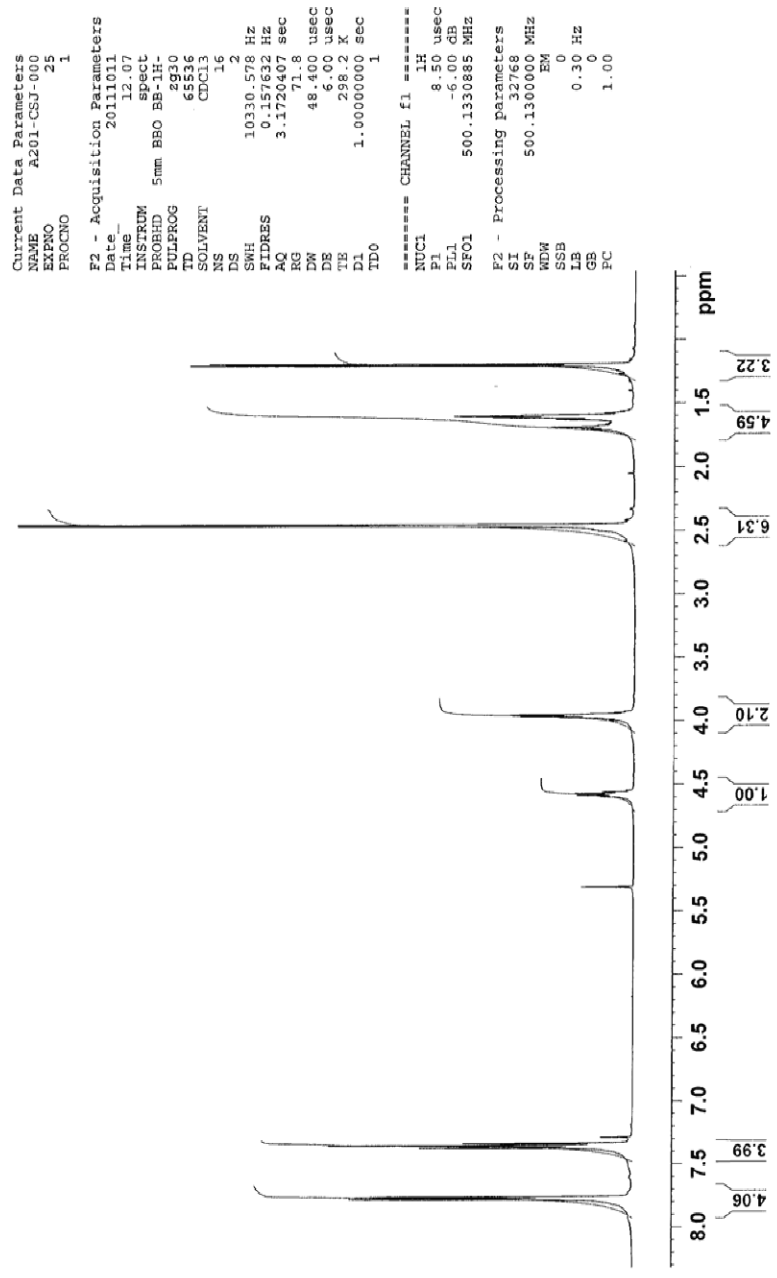


Figure 86. ¹H NMR (500 MHz) spectrum of (*R*)-1,4-bis(4-toluenesulfonyloxy)pentane (**202**) in CDCl₃.

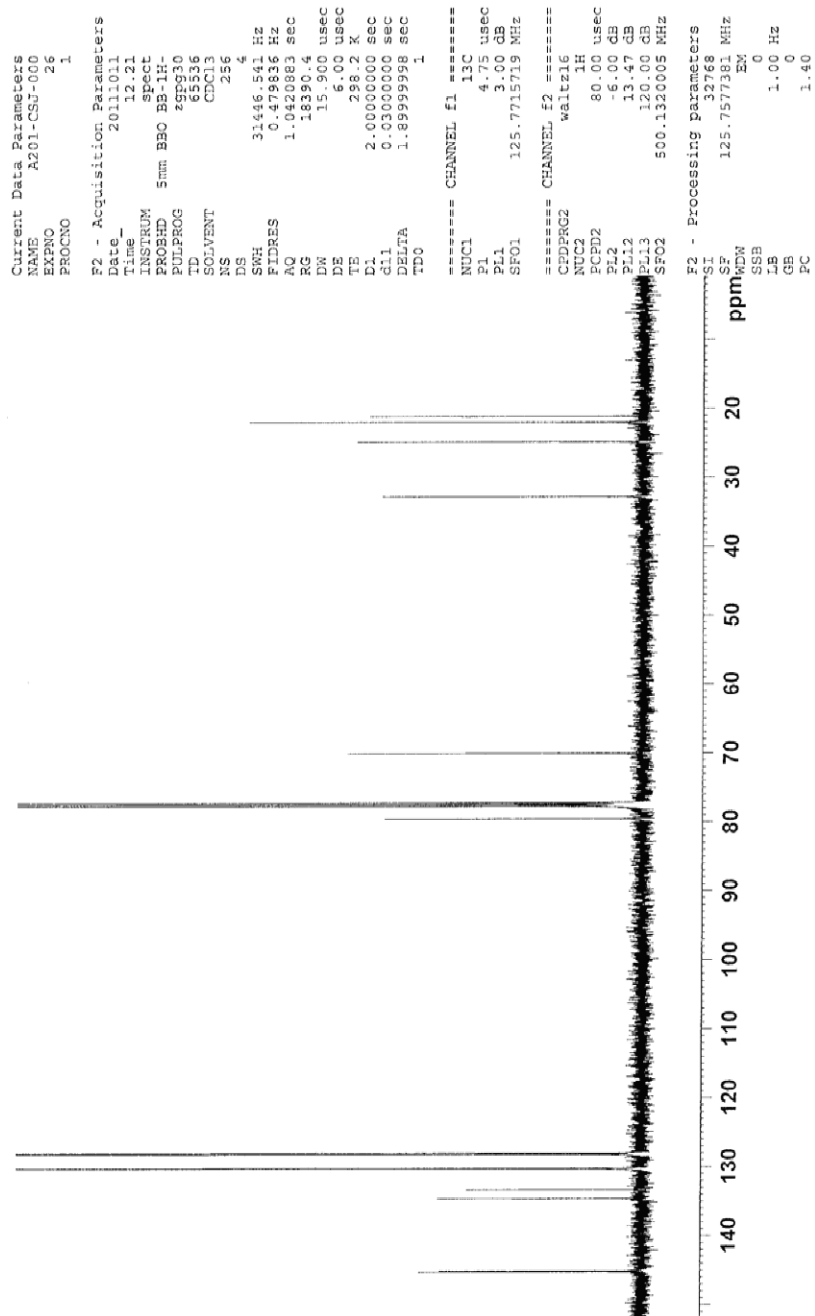


Figure 87. $^{13}\text{C}\{^1\text{H}\}$ NMR (125 MHz) spectrum of (*R*)-1,4-bis(4-toluenesulfonyloxy)pentane (**202**) in CDCl_3 .

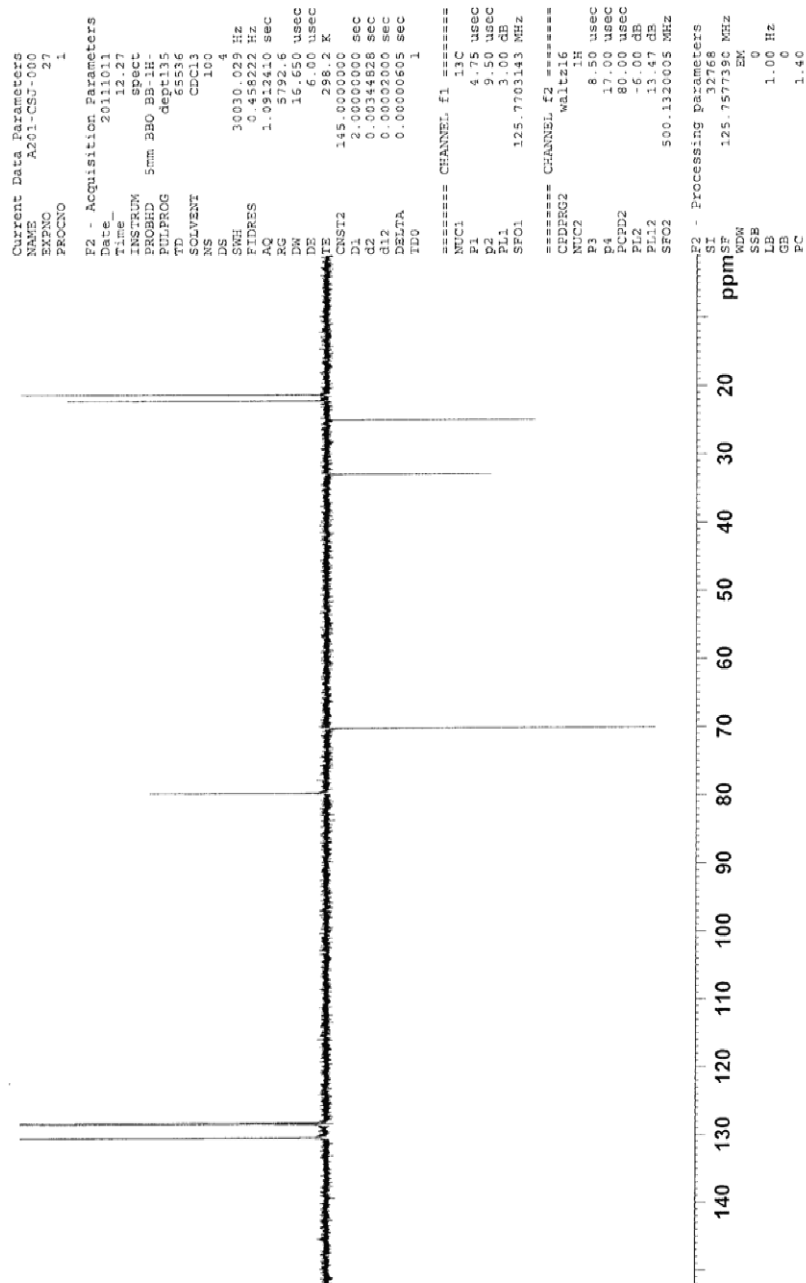


Figure 88. DEPT 135 NMR (125 MHz) spectrum of (*R*)-1,4-bis(4-toluenesulfonyloxy)pentane (**202**) in CDCl₃.

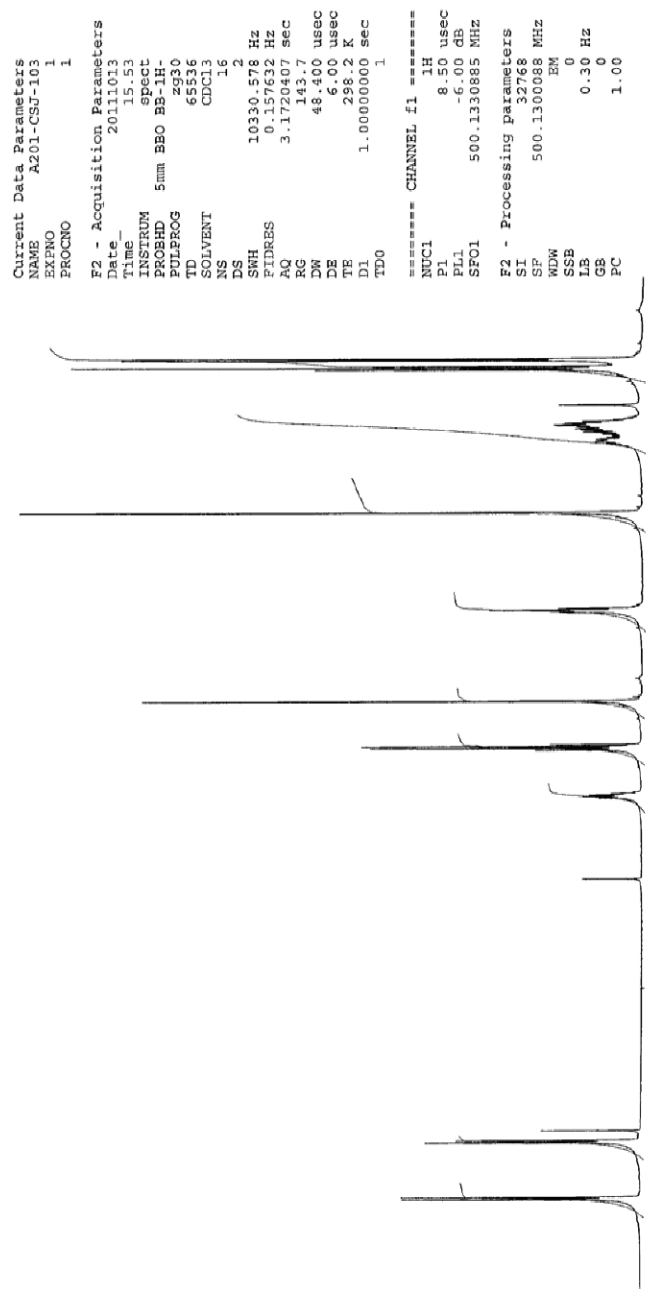


Figure 89. ¹H NMR (500 MHz) spectrum of (*R*)-ethyl [4-(4-toluenesulfonyloxy)pentylsulfonyl]acetate (**203**) in CDCl₃.

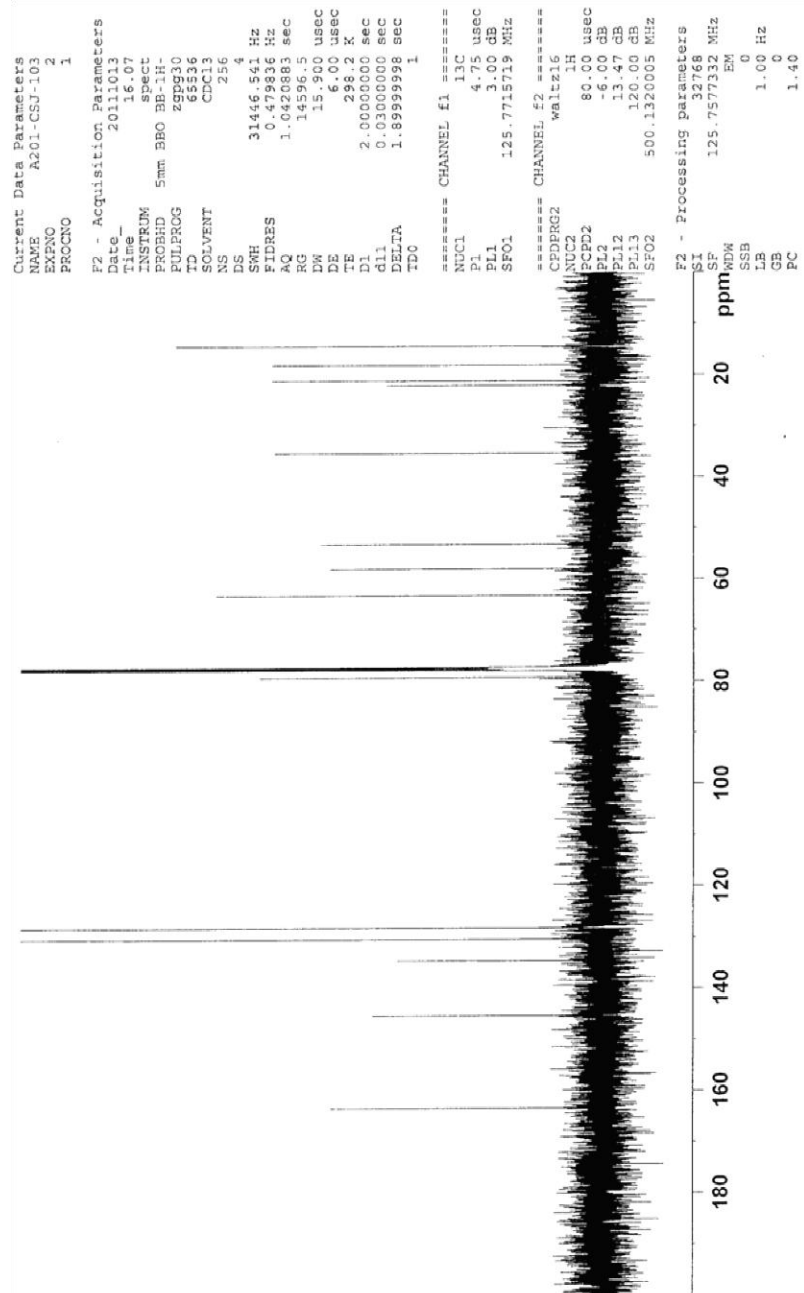


Figure 90. $^{13}\text{C}\{^1\text{H}\}$ NMR (125 MHz) spectrum of (*R*)-ethyl [4-(4-toluenesulfonyloxy)pentylsulfonyl]acetate (**203**) in CDCl_3 .

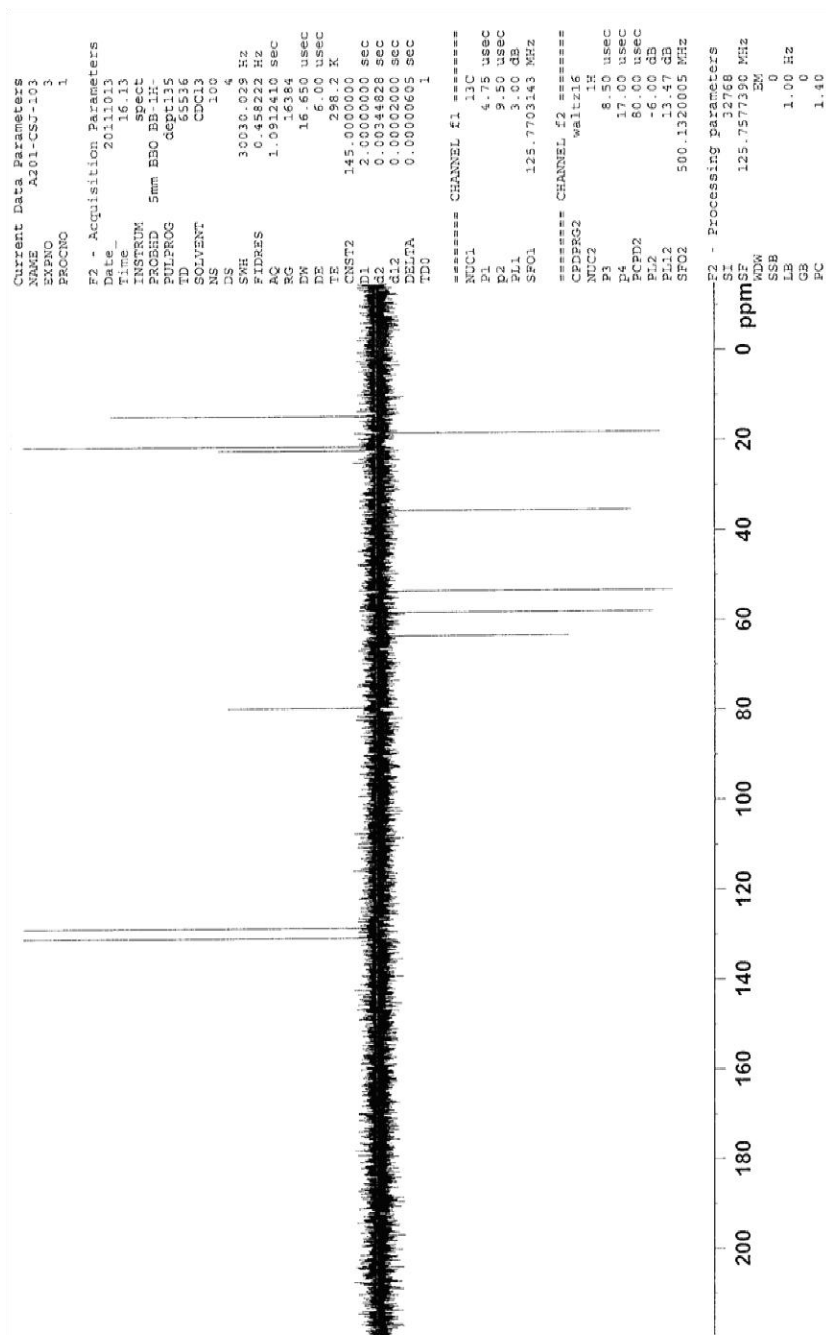


Figure 91. DEPT 135 NMR (125 MHz) spectrum of (*R*)-ethyl [4-(4-toluenesulfonyloxy)pentylsulfonyl]acetate (**203**) in CDCl₃.

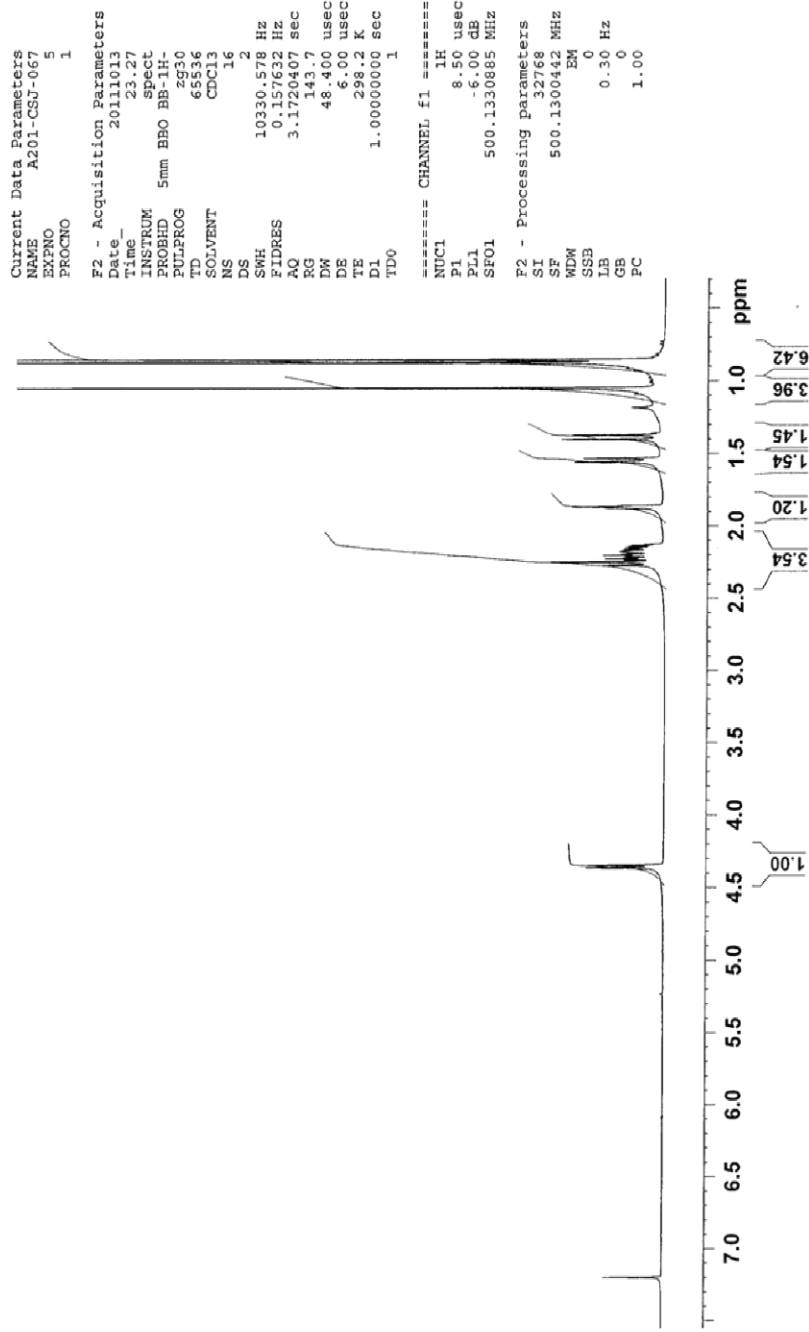


Figure 92. ¹H NMR (500 MHz) spectrum of 7,8,8-trimethyl-4-oxatricyclo[4.2.1.0^{3,7}]nonan-5-one (**225**) in CDCl₃.

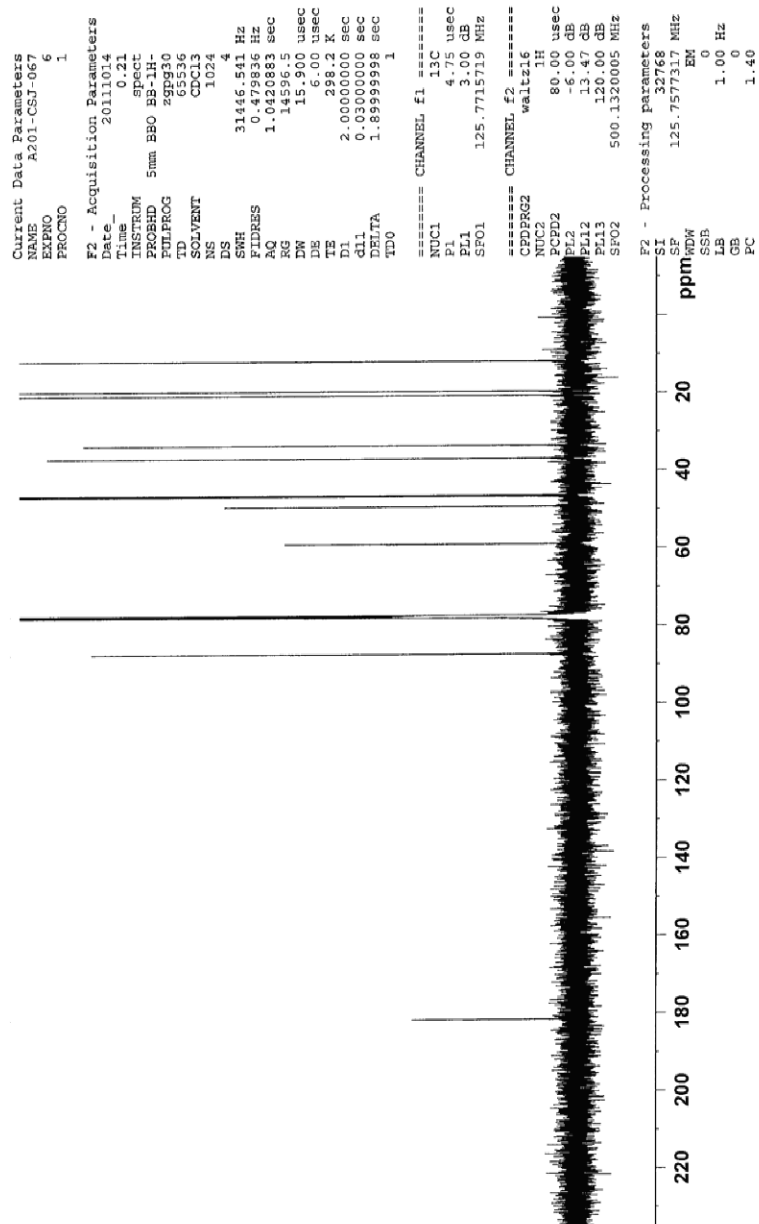


Figure 93. $^{13}\text{C}\{^1\text{H}\}$ NMR (125 MHz) spectrum of 7,8,8-trimethyl-4-oxatricyclo[4.2.1.0^{3,7}]nonan-5-one (**225**) in CDCl_3 .

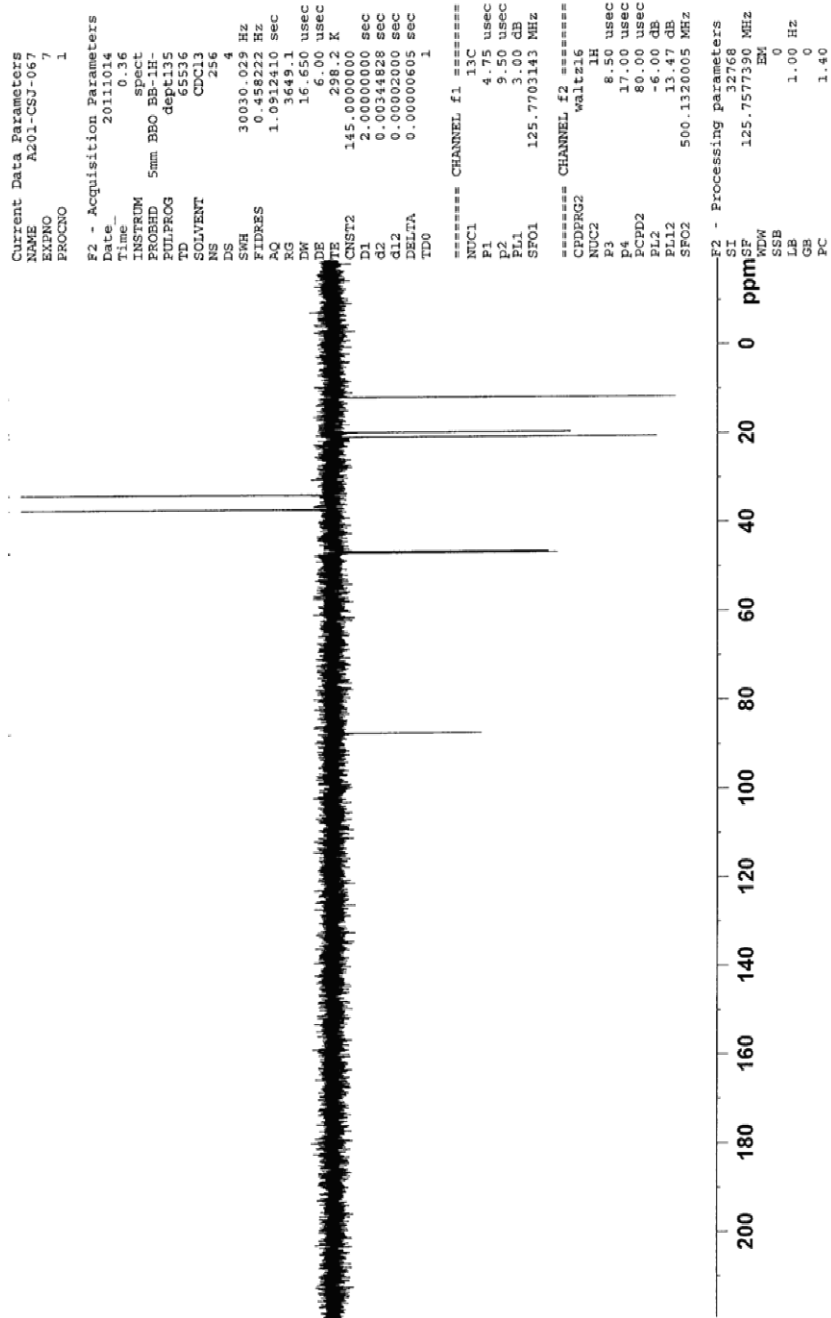


Figure 94. DEPT-135 NMR (125 MHz) spectrum of 7,8,8-trimethyl-4-oxatricyclo[4.2.1.0^{3,7}]nonan-5-one (**225**) in CDCl₃

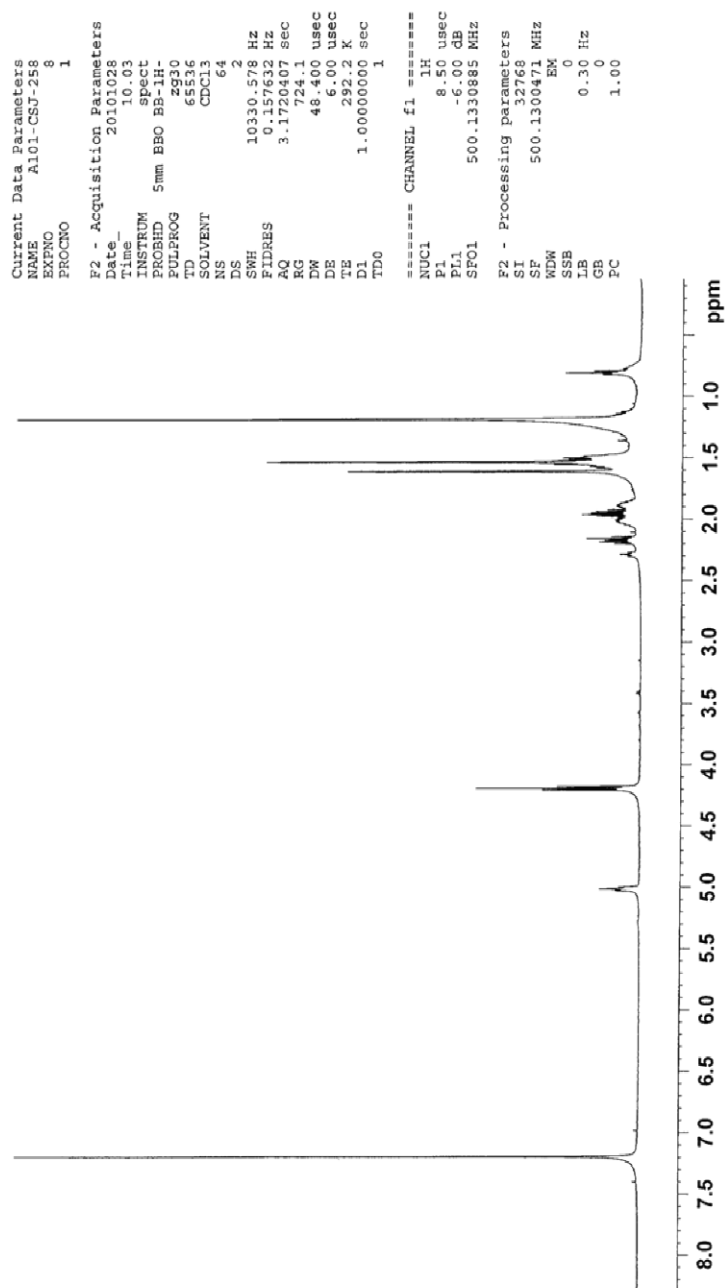


Figure 95. ^1H NMR (500 MHz) spectrum of 3-methyl-3-(4-methyl-3-pentenyl)dihydrofuran-2-one (**226**) in CDCl_3 .

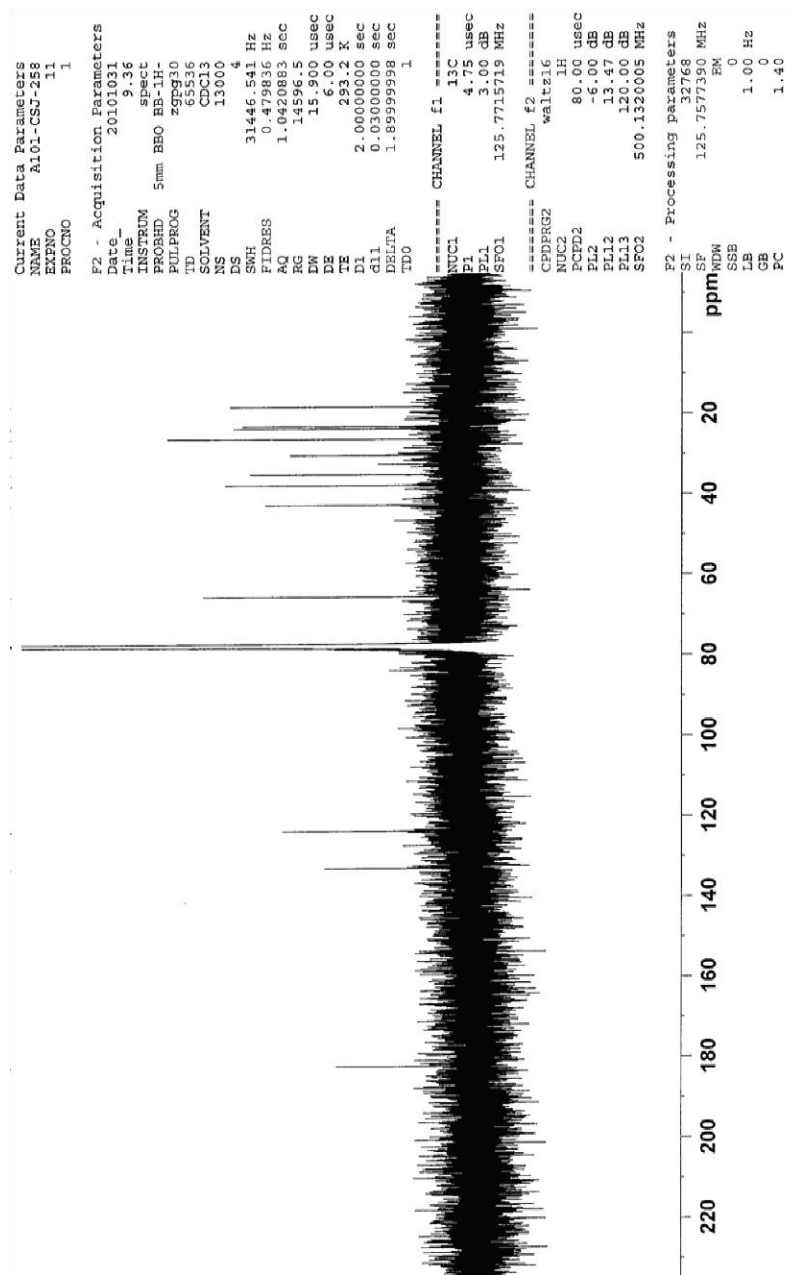


Figure 96. $^{13}\text{C}\{^1\text{H}\}$ NMR (125 MHz) spectrum of 3-methyl-3-(4-methyl-3-pentenyl)dihydrofuran-2-one (**226**) in CDCl_3 .

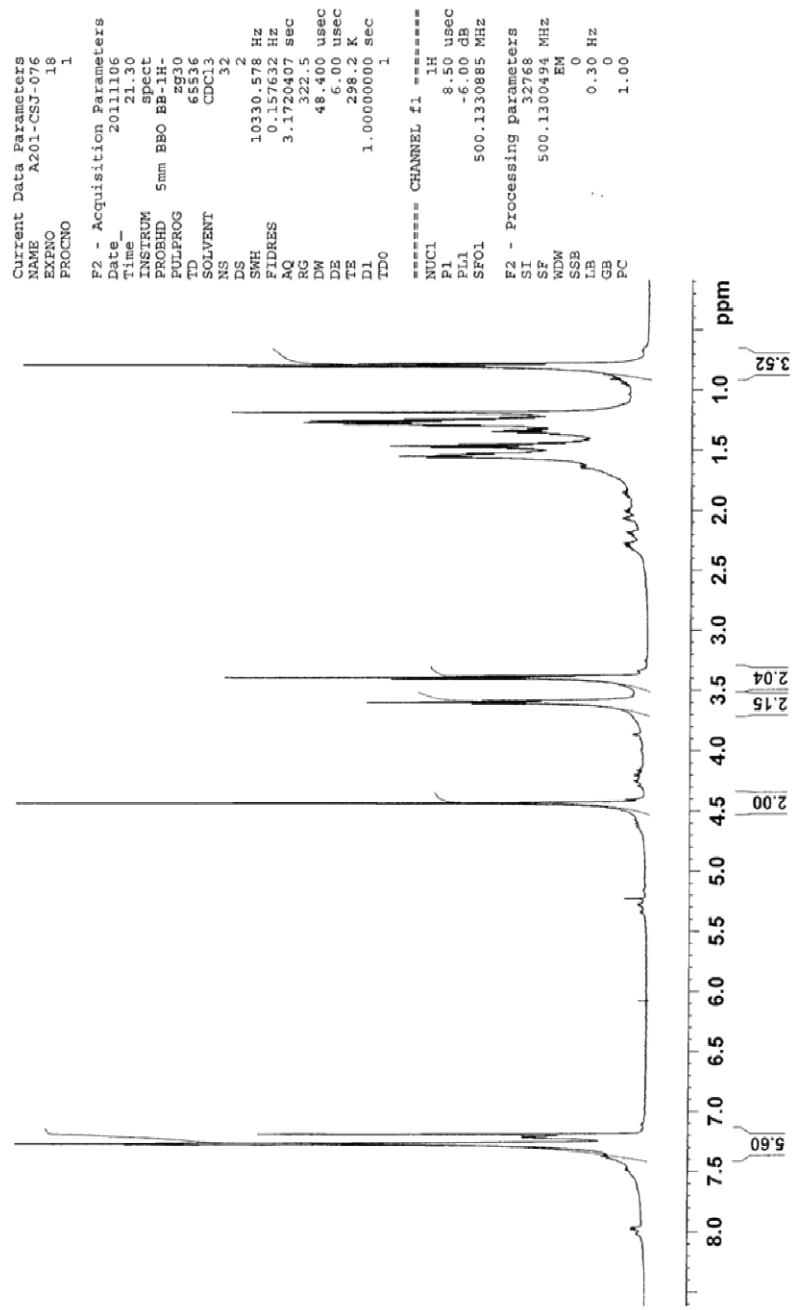


Figure 97. ¹H NMR (500 MHz) spectrum of 3-(3-benzyloxypropyl)-3-ethyldihydrofuran-2-one (**227**) in CDCl₃.

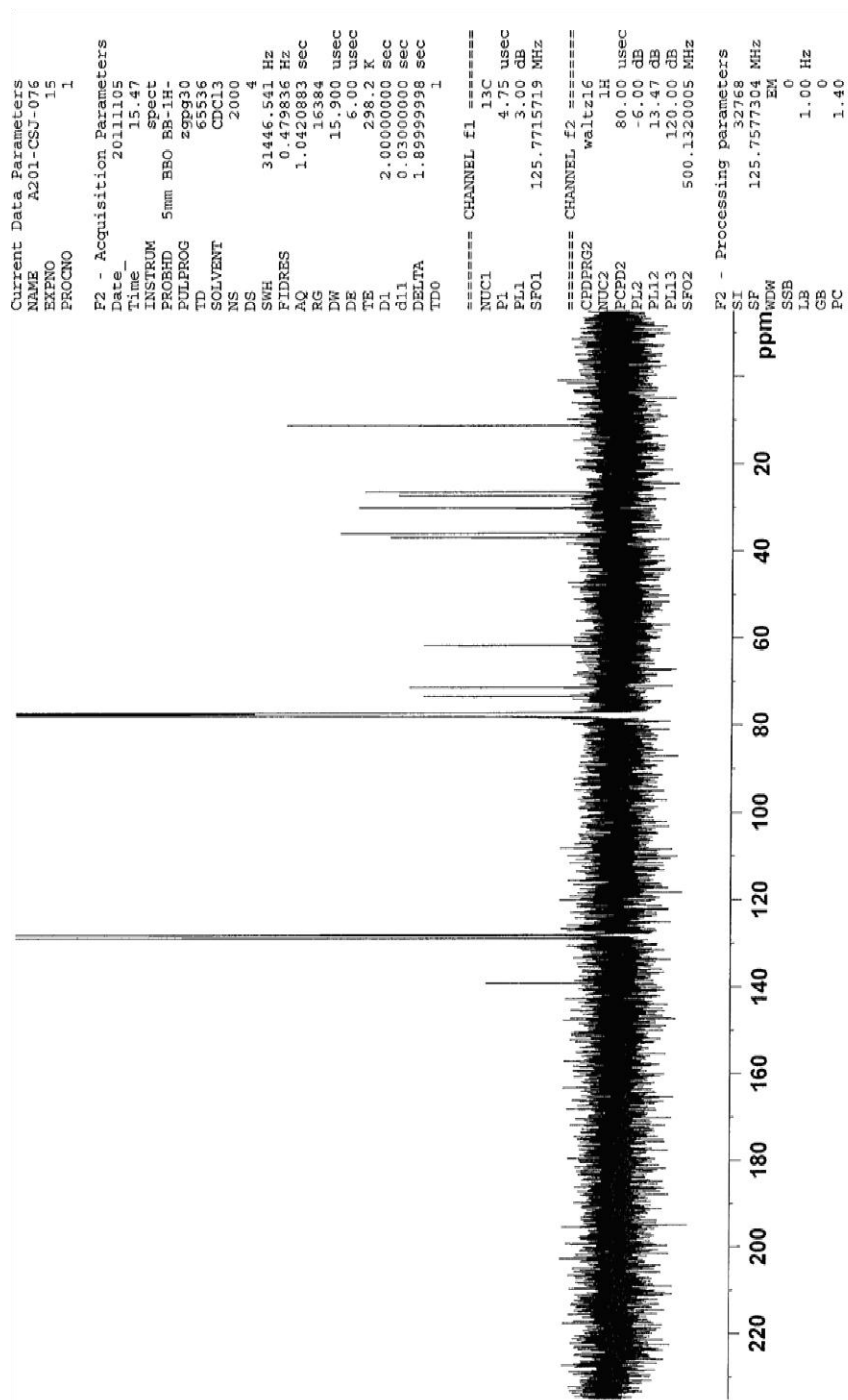


Figure 98. $^{13}\text{C}\{^1\text{H}\}$ NMR (125 MHz) spectrum of 3-(3-benzyloxypropyl)-3-ethylidihydrofuran-2-one (**227**) in CDCl_3 .

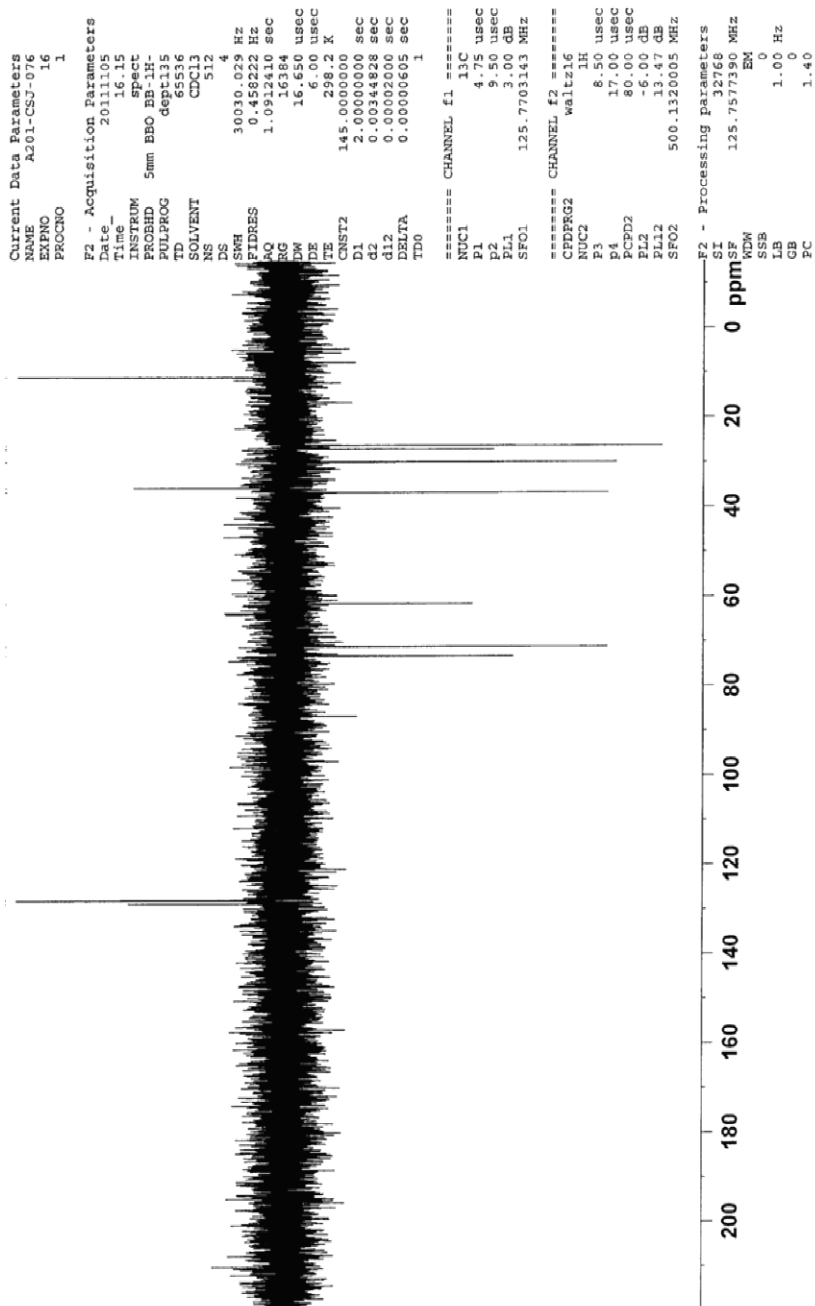


Figure 99. DEPT 135 NMR (125 MHz) spectrum of 3-(3-benzyloxypropyl)-3-ethylidihydrofuran-2-one (**227**) in CDCl₃.

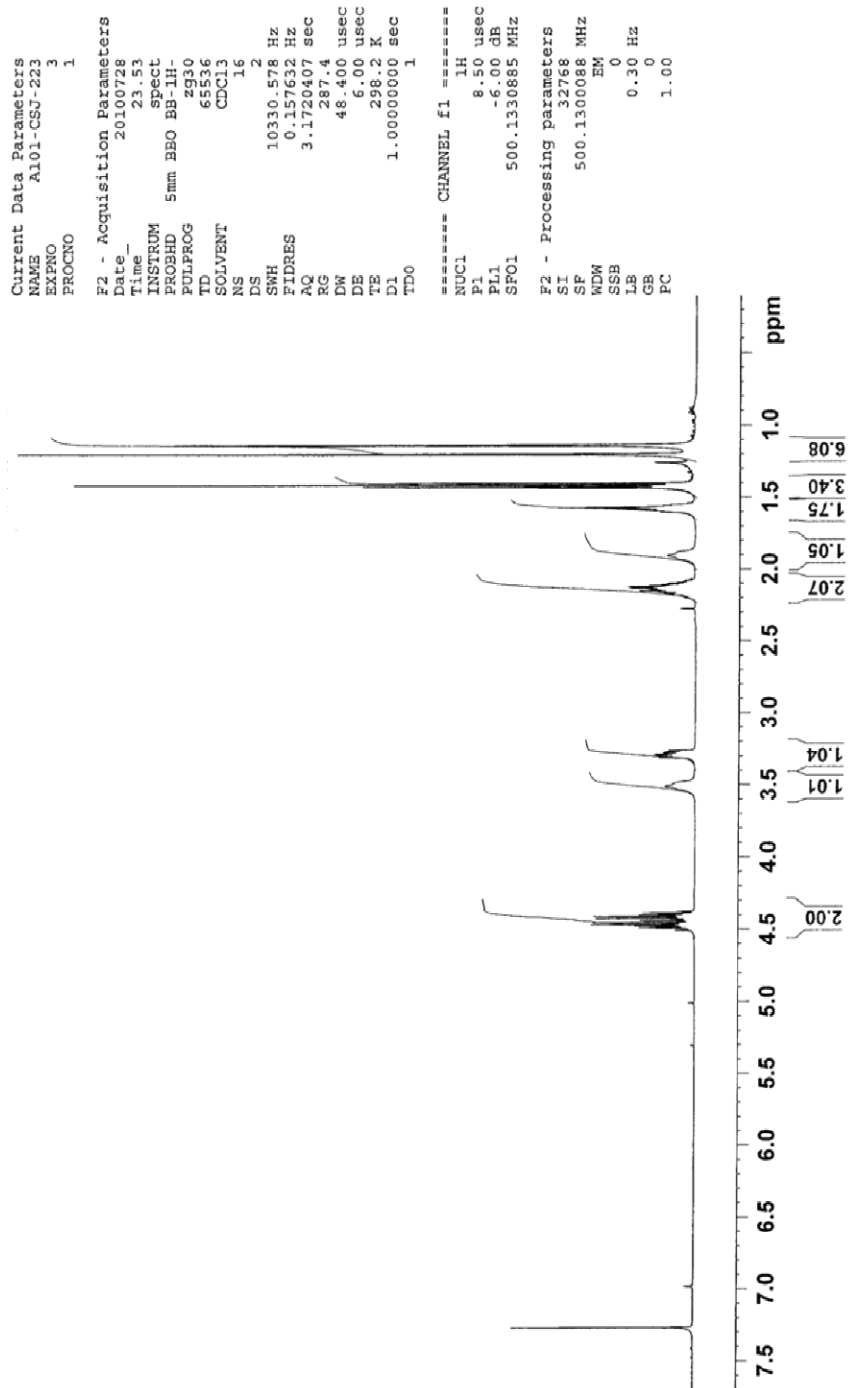


Figure 100. ^1H NMR (500 MHz) spectrum of 2-azido-2-carbethoxy-3,3-dimethylthiane-1,1-dioxide (**239**) in CDCl_3 .

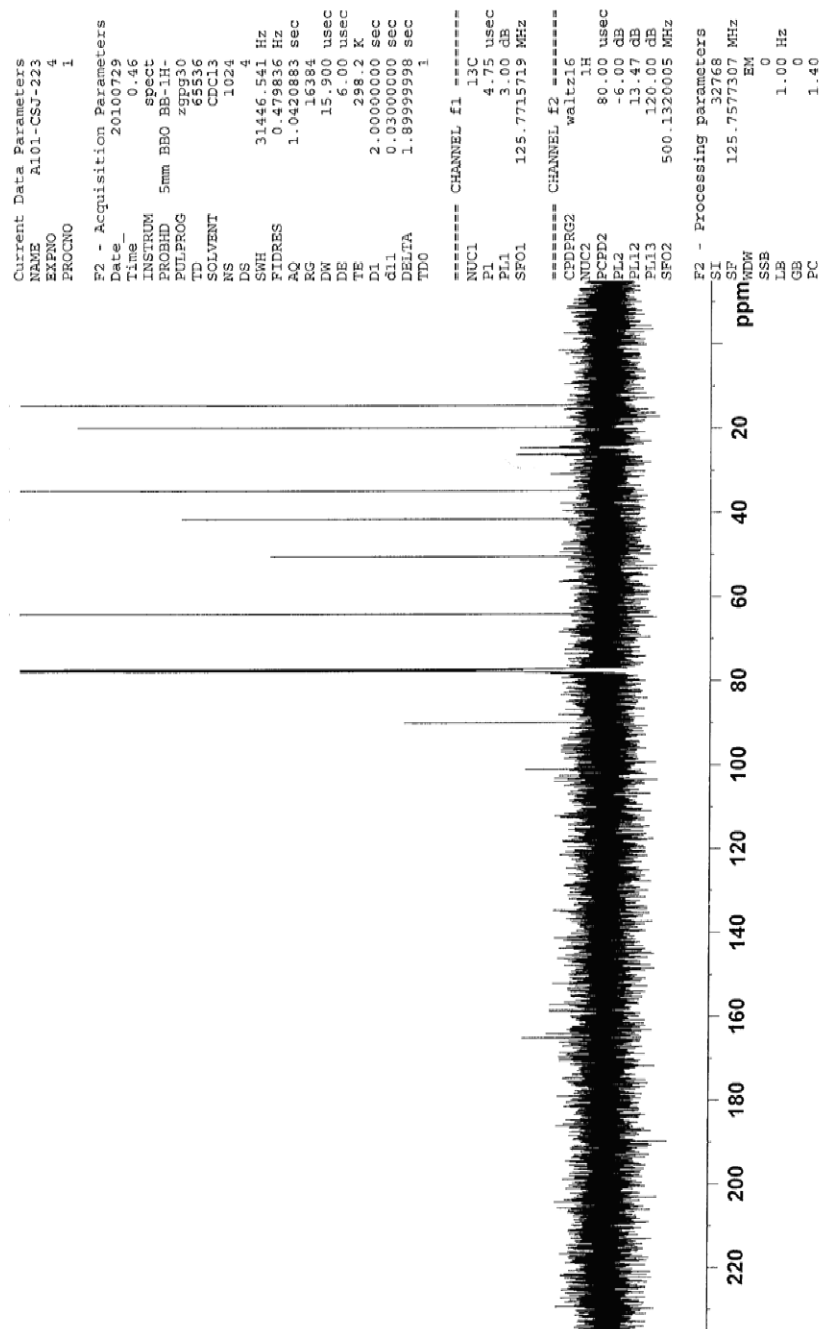


Figure 101. $^{13}\text{C}\{^1\text{H}\}$ NMR (125 MHz) spectrum of 2-azido-2-carbethoxy-3,3-dimethylthiane-1,1-dioxide (**239**) in CDCl_3 .

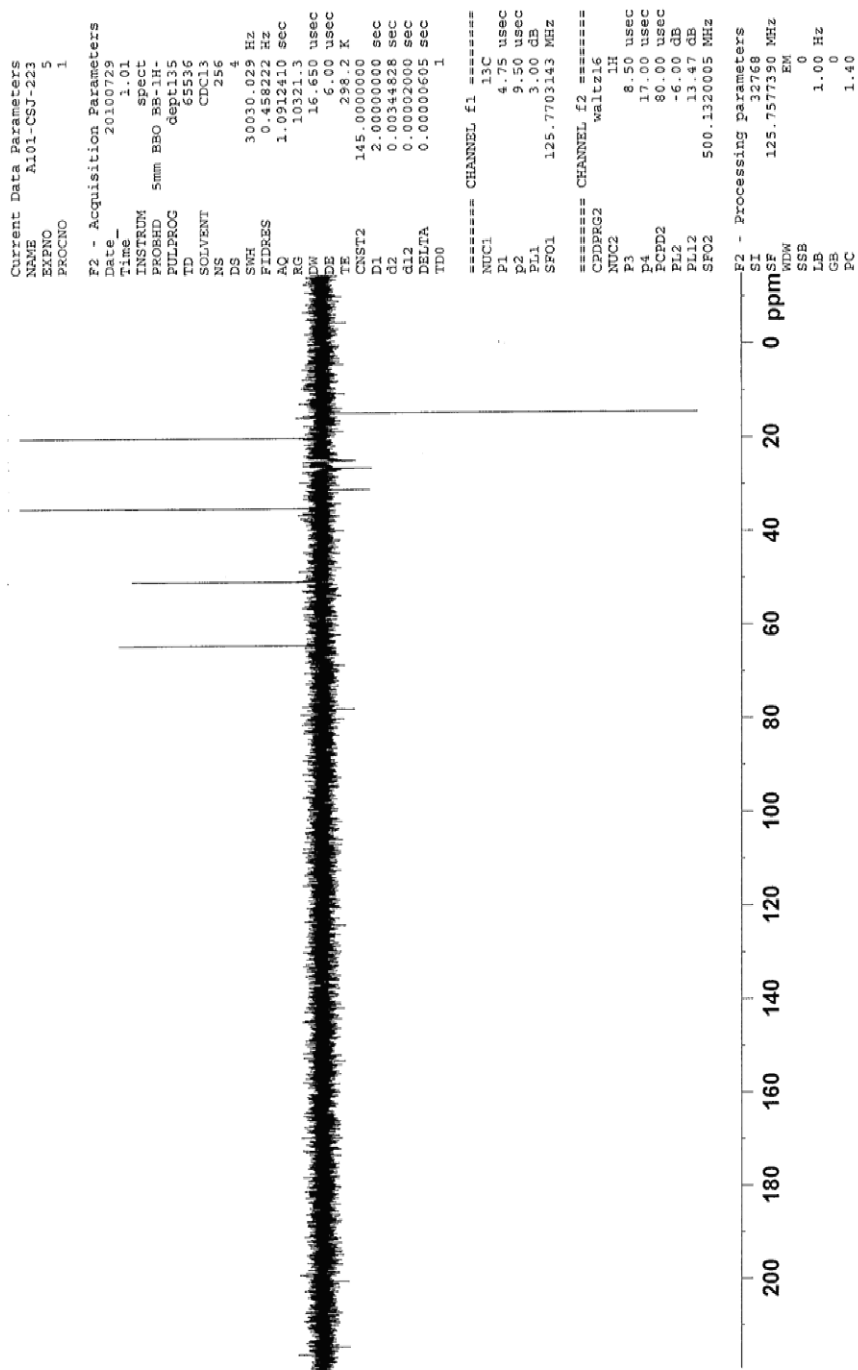


Figure 102. DEPT 135 NMR (125 MHz) spectrum of 2-azido-2-carbethoxy-3,3-dimethylthiane-1,1-dioxide (**239**) in CDCl₃.

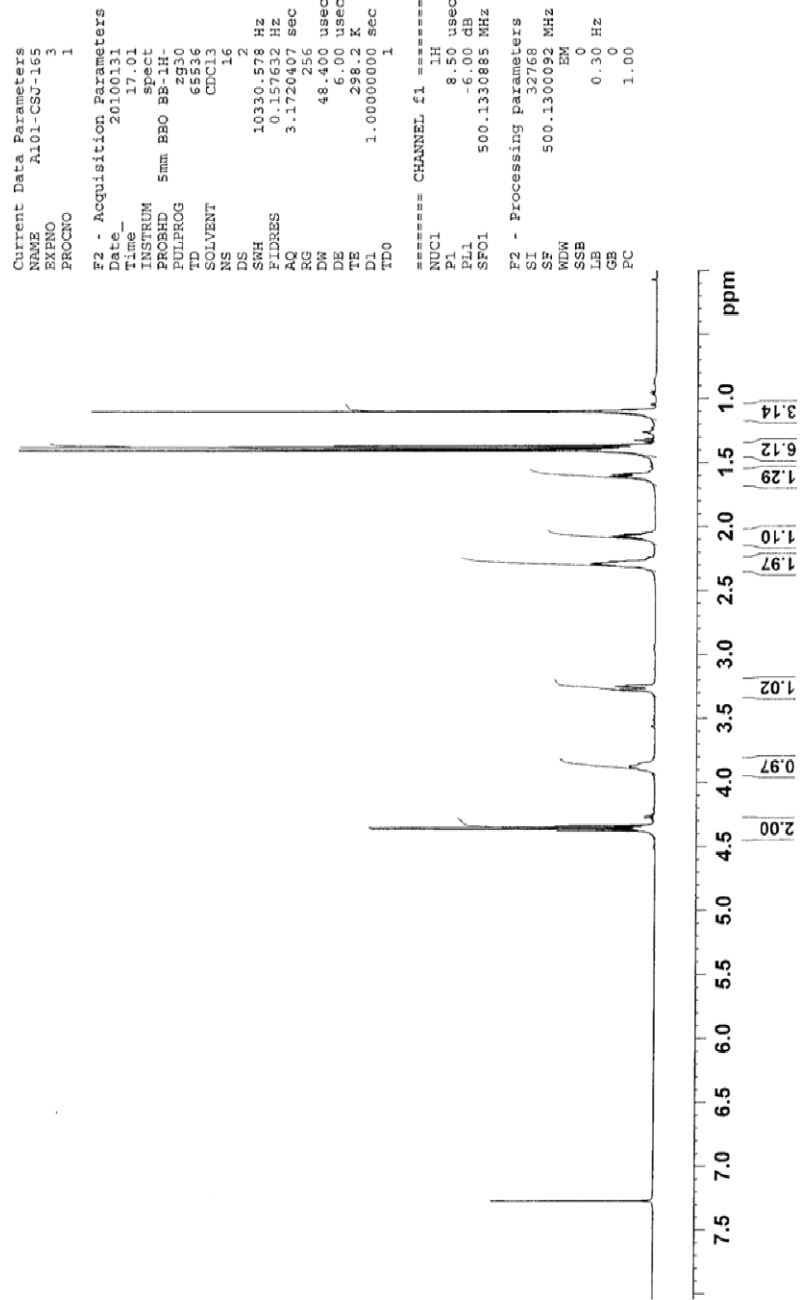


Figure 103. ¹H NMR (500 MHz) spectrum of 2-chloro-2-carbethoxy-3,3-dimethylthiane-1,1-dioxide (**240**) in CDCl₃.

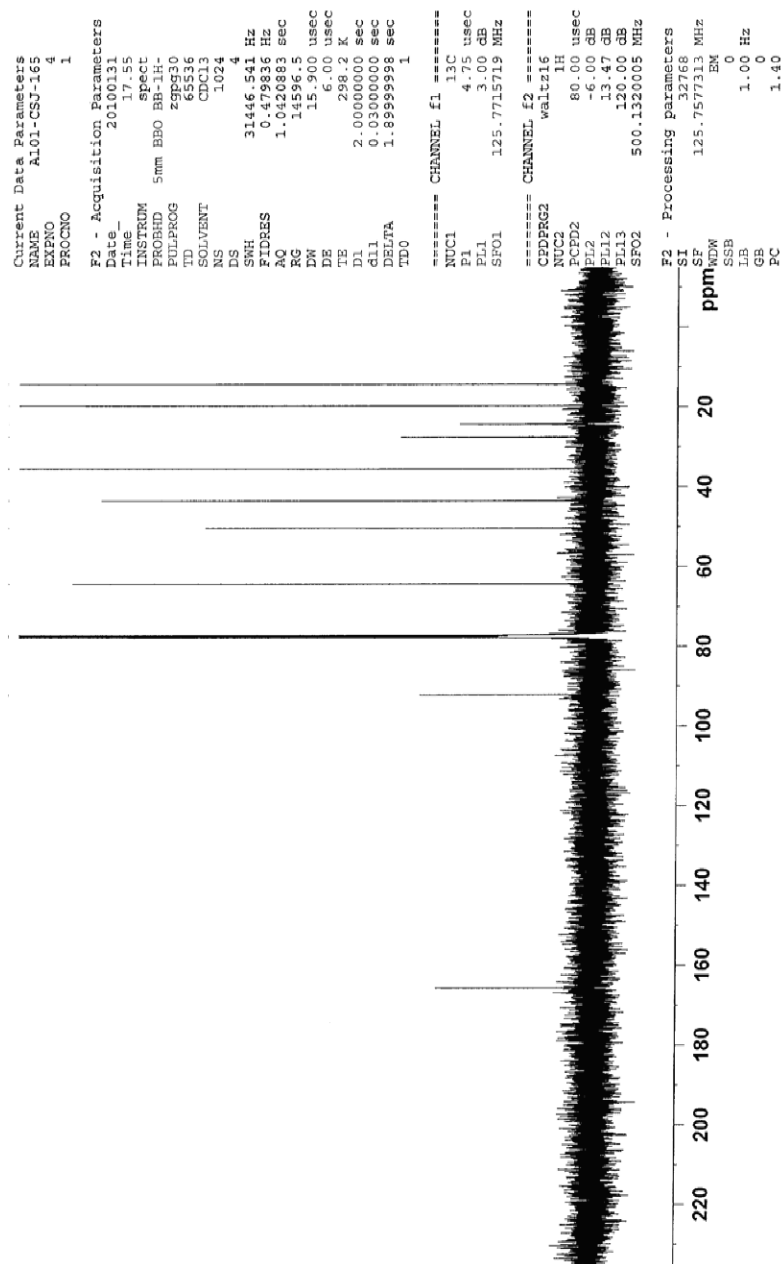


Figure 104. $^{13}\text{C}\{^1\text{H}\}$ NMR (125 MHz) spectrum of 2-chloro-2-carbethoxy-3,3-dimethylthiane-1,1-dioxide (**240**) in CDCl_3 .

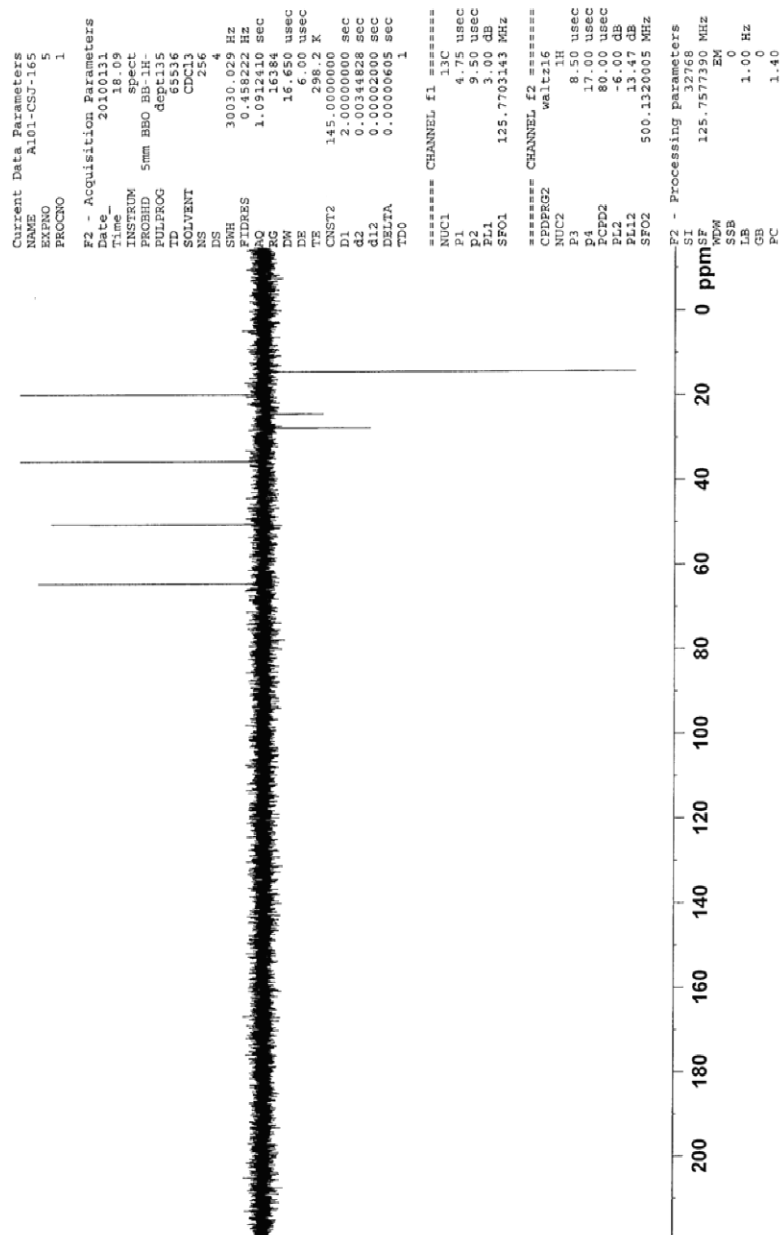


Figure 105. DEPT 135 NMR (125 MHz) spectrum of 2-chloro-2-carbethoxy-3,3-dimethylthiane-1,1-dioxide (**240**) in CDCl_3 .

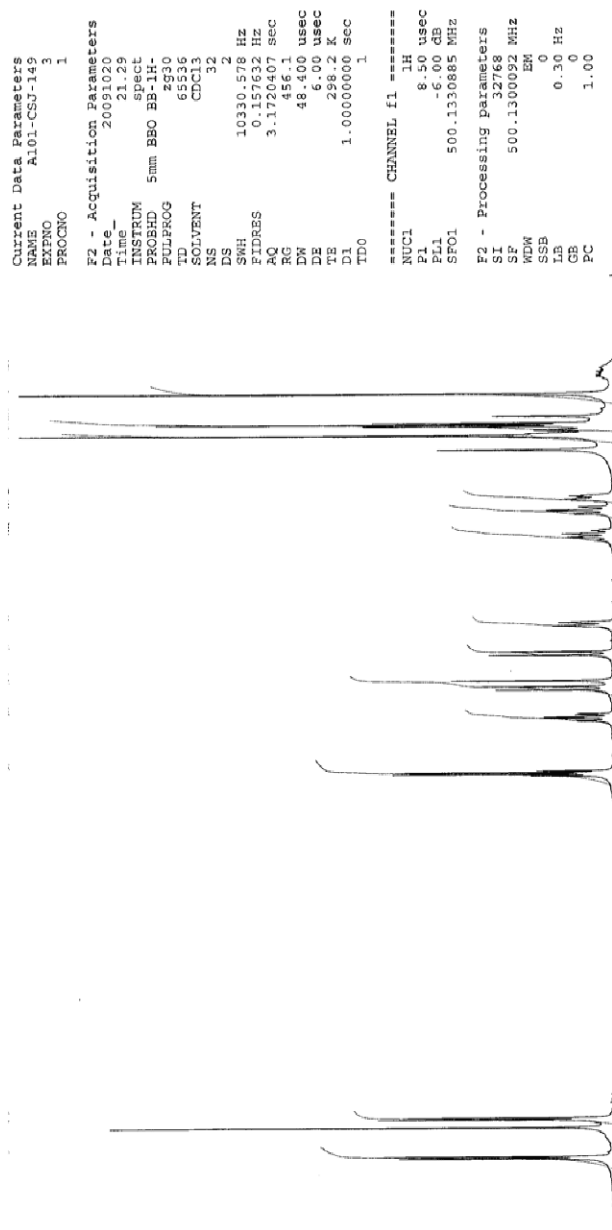


Figure 106. ^1H NMR (500 MHz) spectrum of 2-(4-chlorobenzyl)-2-carbethoxy-3,3-dimethylthiane-1,1-dioxide (**241**) in CDCl_3 .

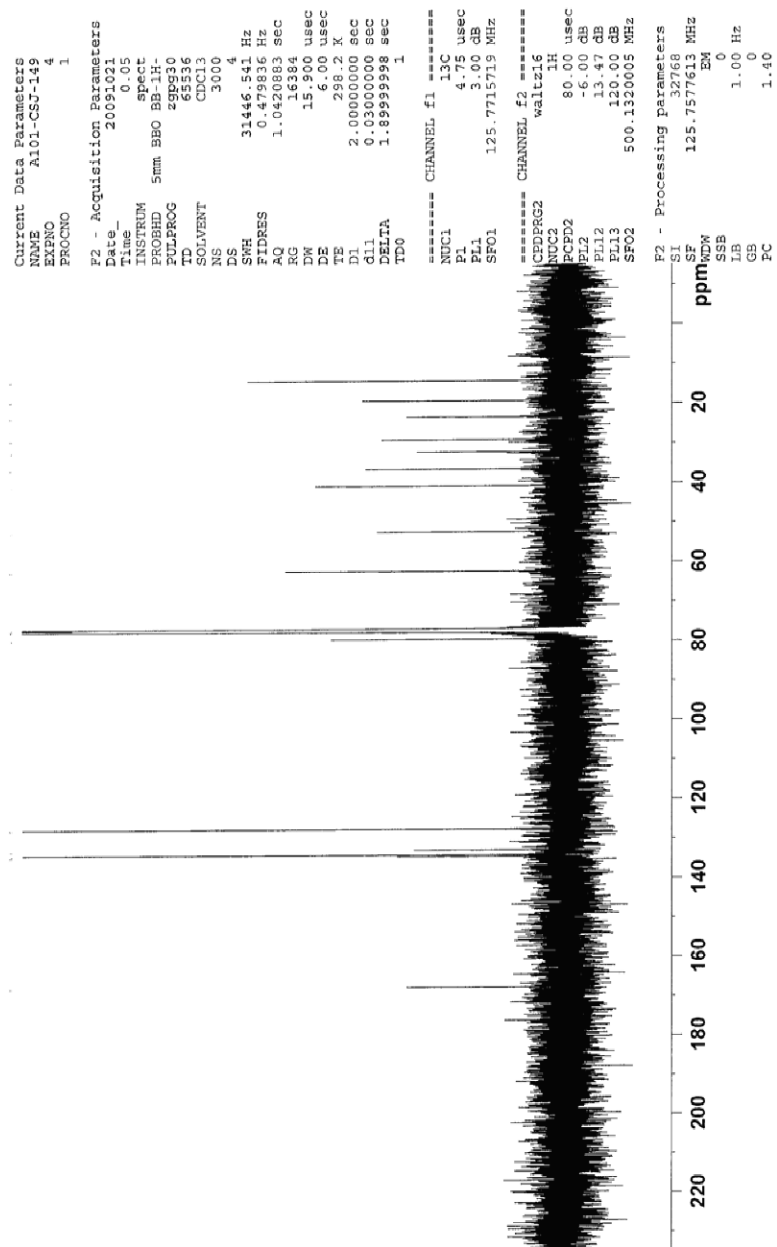


Figure 107. $^{13}\text{C}\{^1\text{H}\}$ NMR (125 MHz) spectrum of 2-(4-chlorobenzyl)-2-carbethoxy-3,3-dimethylthiane-1,1-dioxide (**241**) in CDCl_3 .

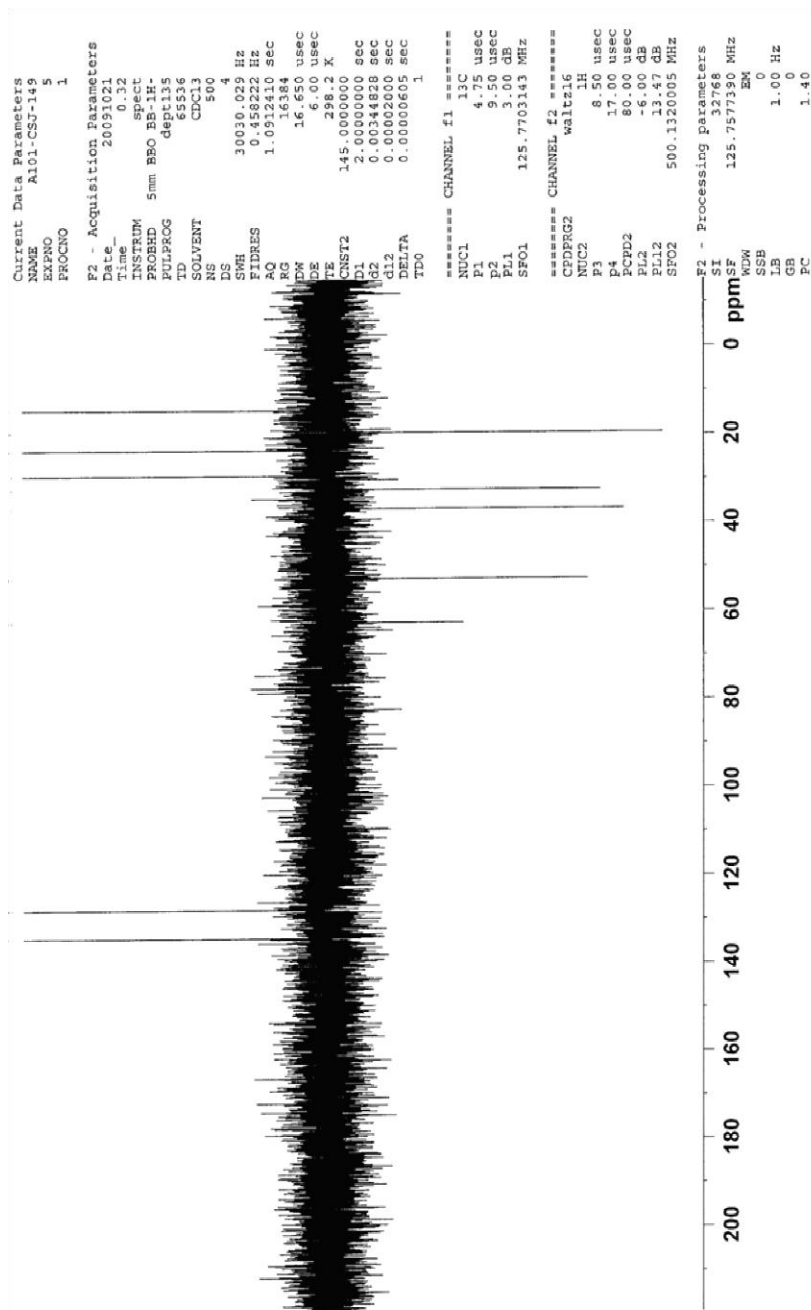


Figure 108. DEPT 135 NMR (125 MHz) spectrum of 2-(4-chlorobenzyl)-2-carbethoxy-3,3-dimethylthiane-1,1-dioxide (**241**) in CDCl₃.

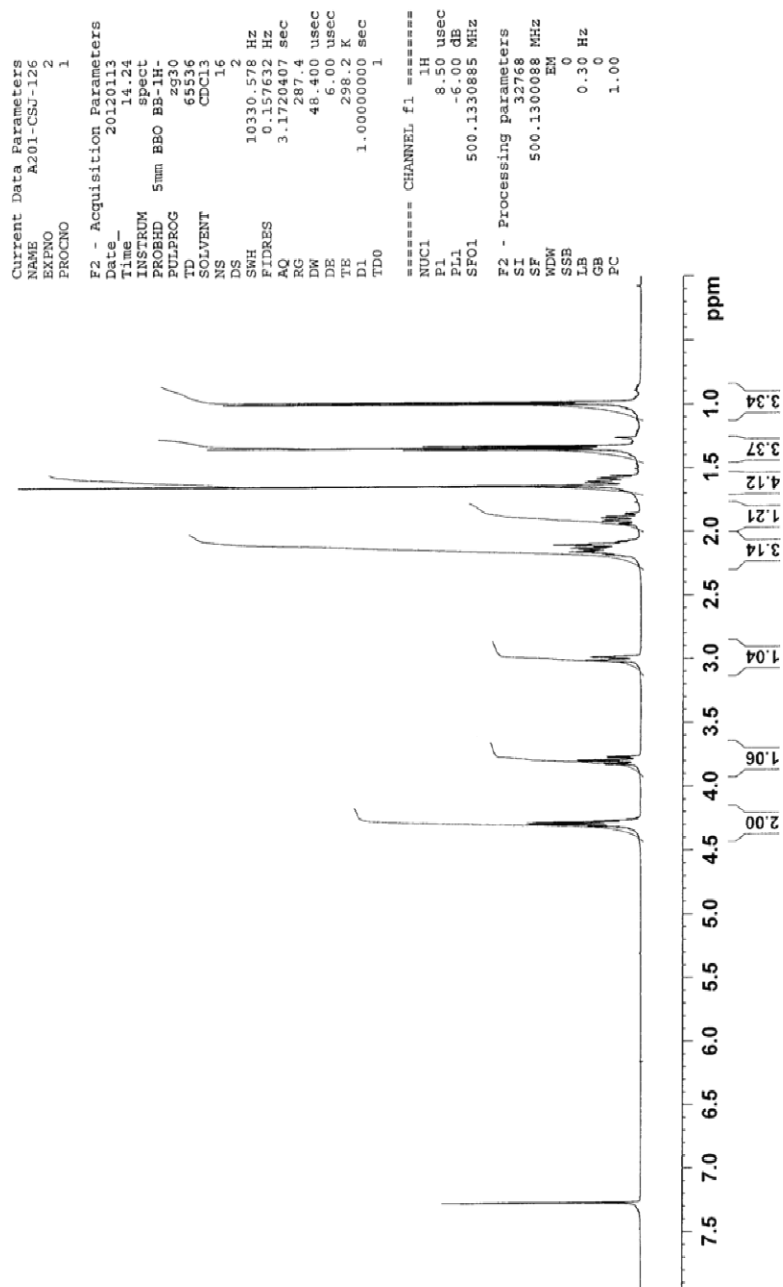


Figure 109. ^1H NMR (500 MHz) spectrum of 2-methyl-2-carbethoxy-3,3-dimethylthiane-1,1-dioxide (**242**) in CDCl_3 .

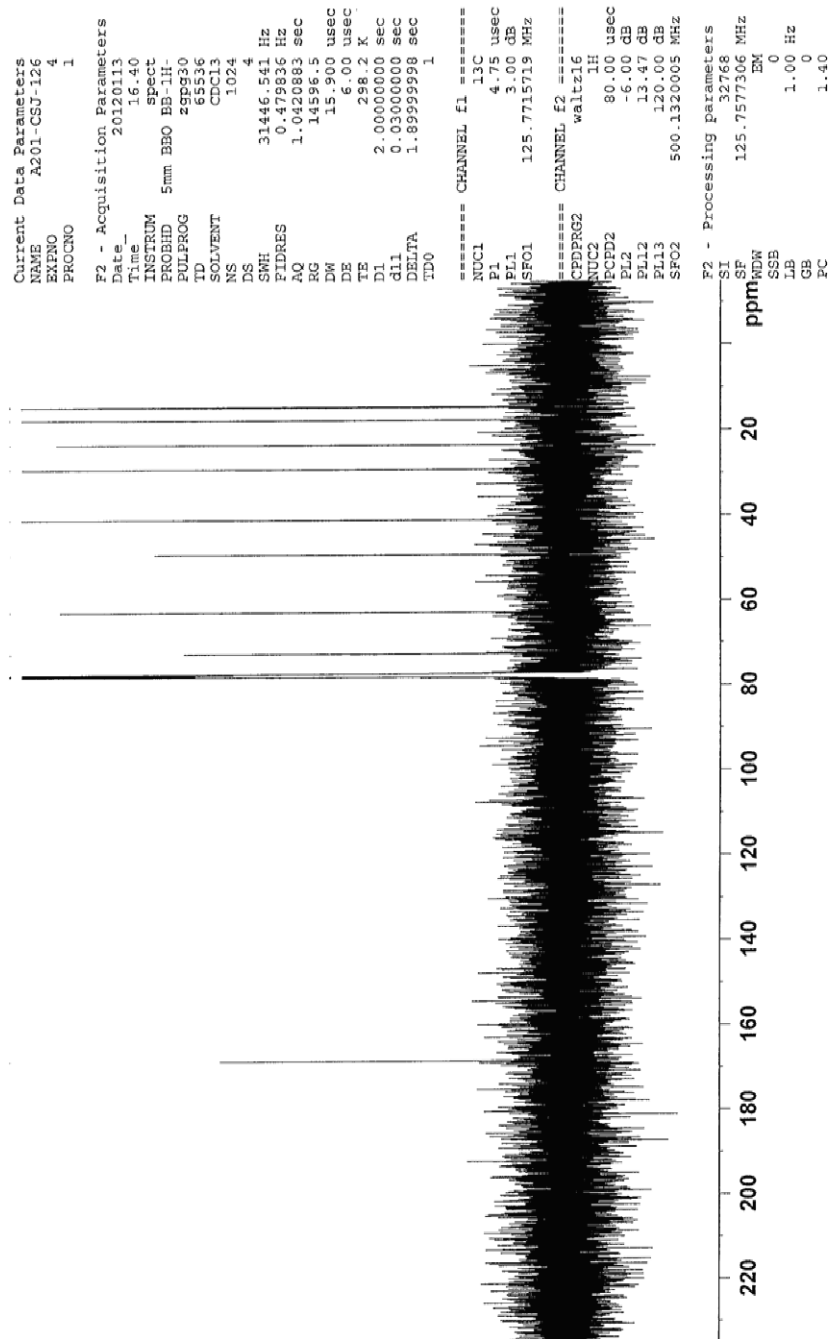


Figure 110. $^{13}\text{C}\{^1\text{H}\}$ NMR (125 MHz) spectrum of 2-methyl-2-carboxy-3,3-dimethylthiane-1,1-dioxide (**242**) in CDCl_3 .

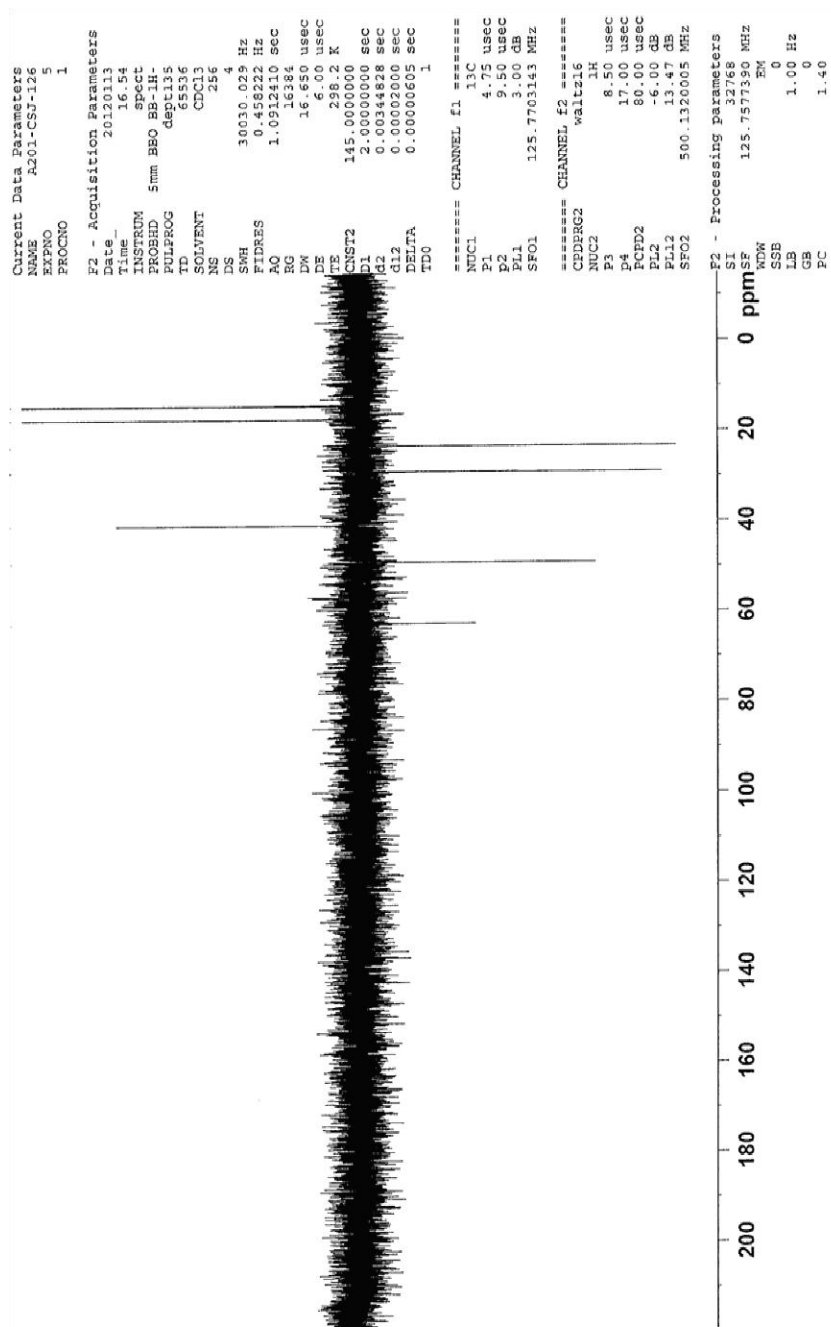


Figure 111. DEPT 135 NMR (125 MHz) spectrum of 2-methyl-2-carboxy-3,3-dimethylthiane-1,1-dioxide (**242**) in CDCl_3 .

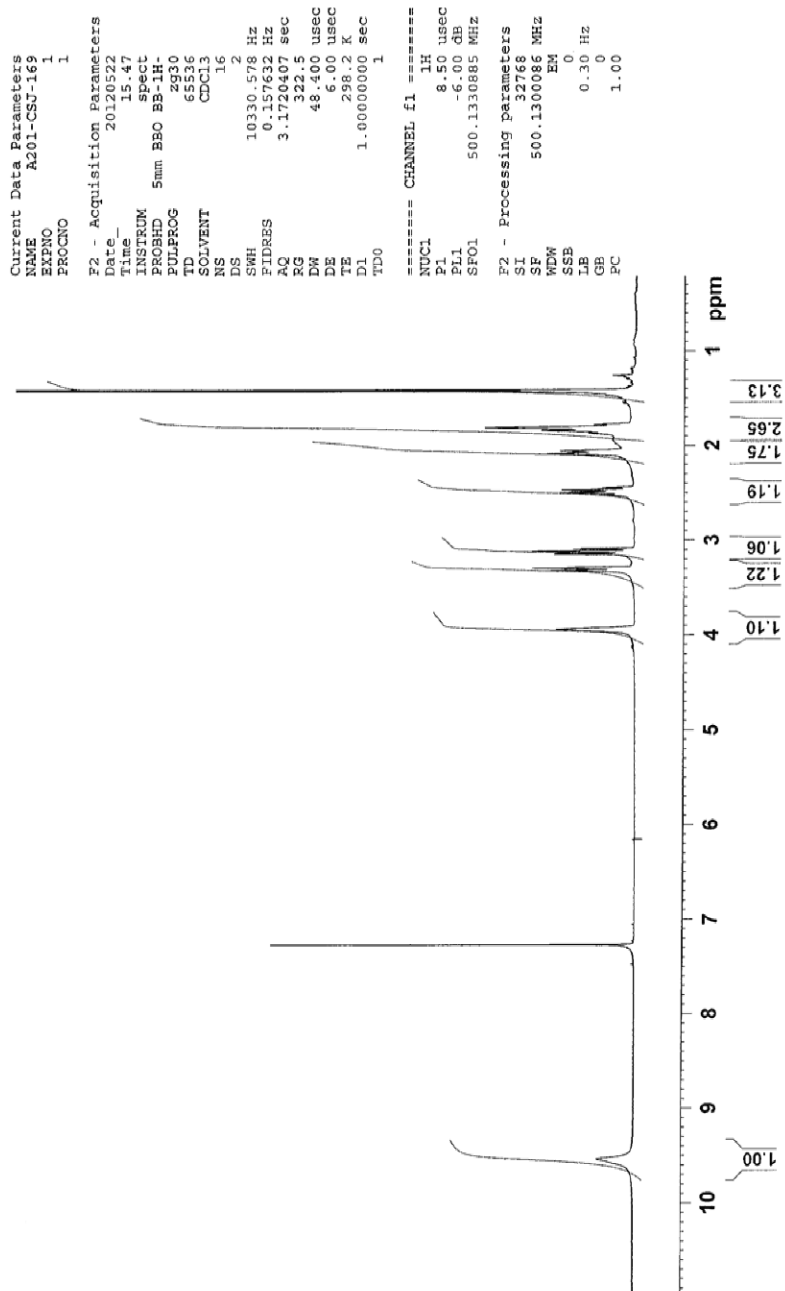


Figure 112. ^1H NMR (500 MHz) spectrum of 2-hydroxyimino-3-methylthiane-1,1-dioxide (**254**) in CDCl_3 .

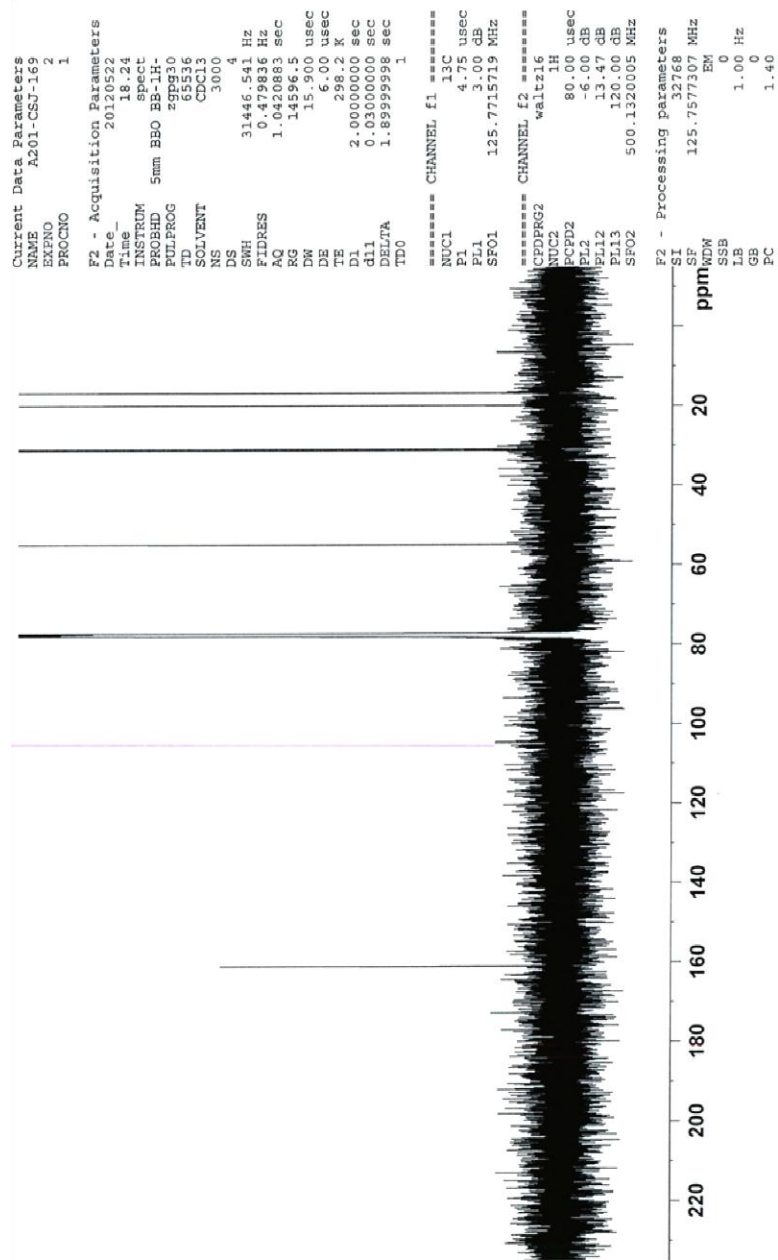


Figure 113. $^{13}\text{C}\{^1\text{H}\}$ NMR (125 MHz) spectrum of 2-hydroxyimino-3-methylthiane-1,1-dioxide (**254**) in CDCl_3 .

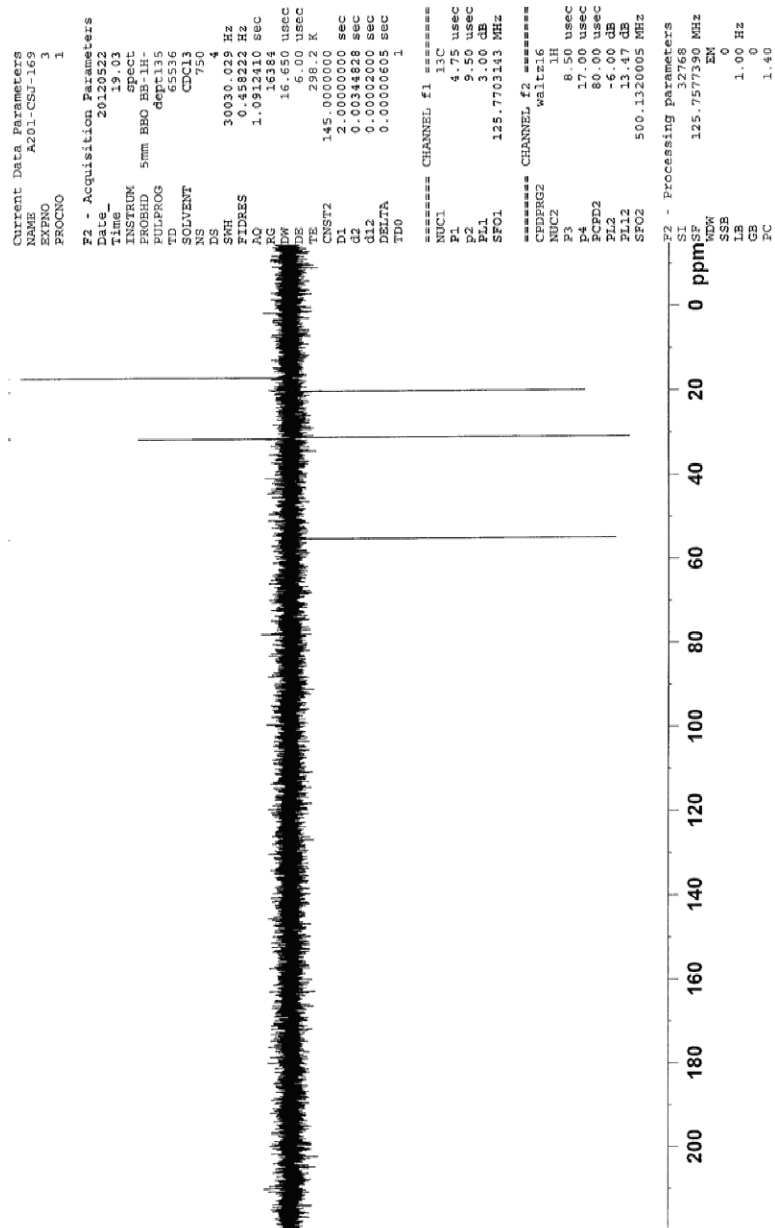


Figure 114. DEPT 135 NMR (125 MHz) spectrum of 2-hydroxyimino-3-methylthiane-1,1-dioxide (**254**) in CDCl_3 .

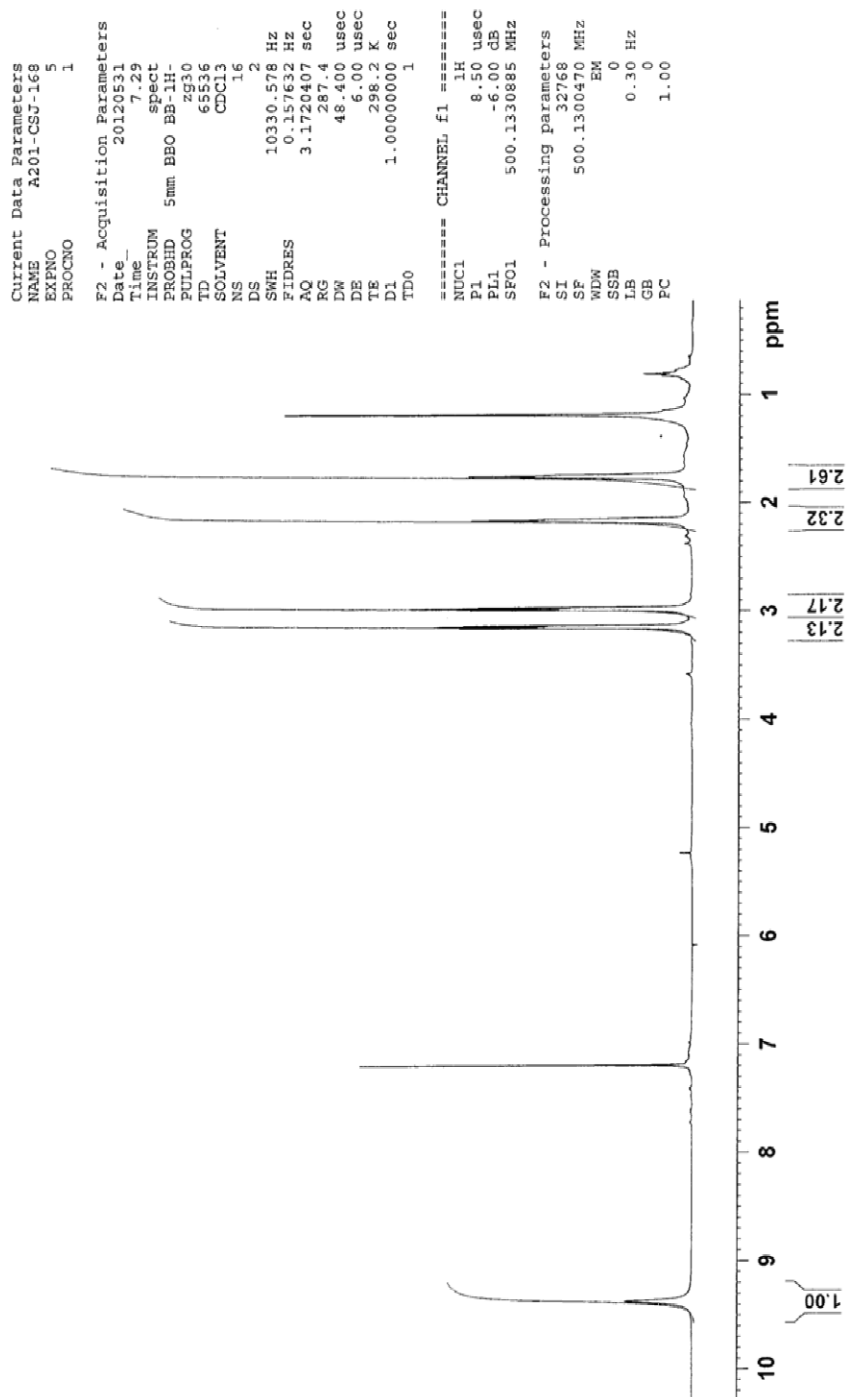


Figure 115. ^1H NMR (500 MHz) spectrum of 2-hydroxyiminothiane-1,1-dioxide (**255**) in CDCl_3 .

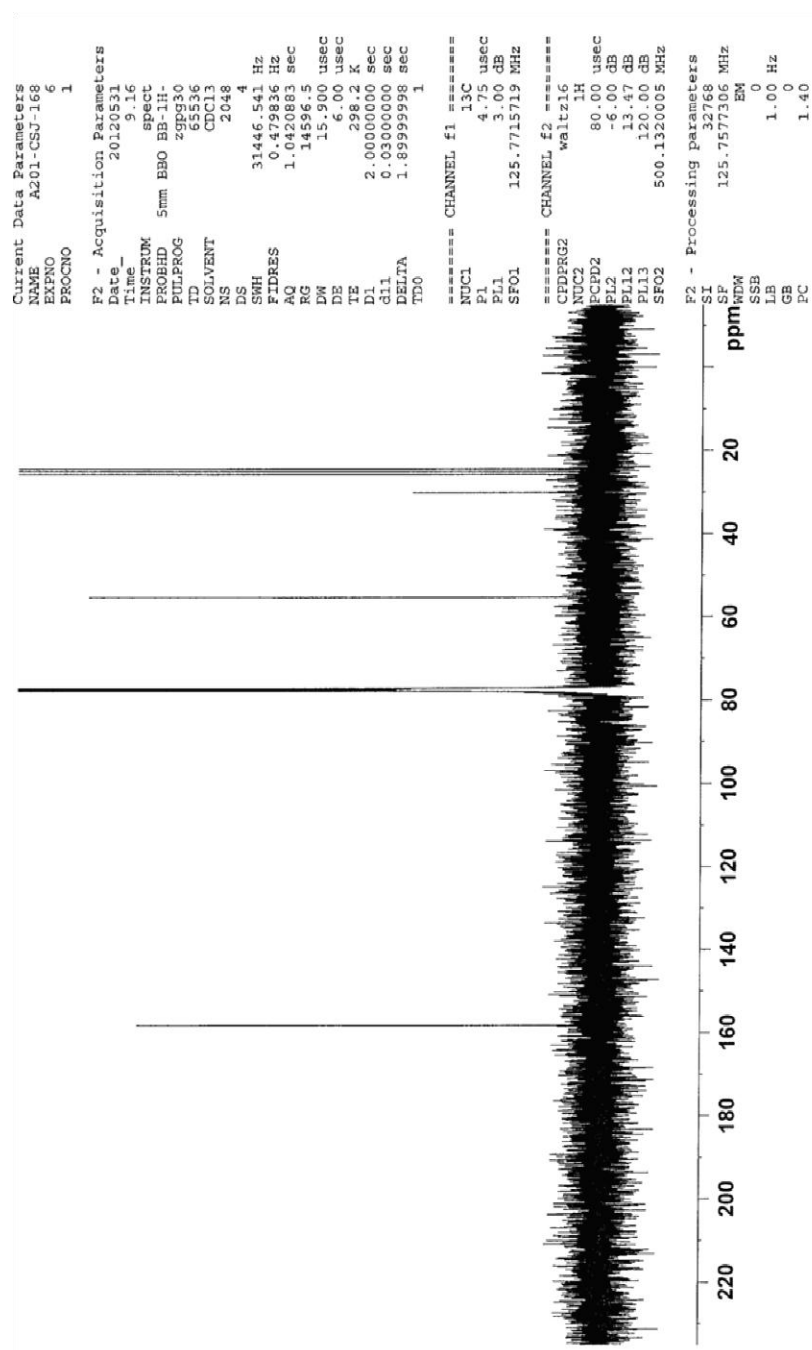


Figure 116. $^{13}\text{C}\{^1\text{H}\}$ NMR (500 MHz) spectrum of 2-hydroxyiminothiane-1,1-dioxide (255) in CDCl_3 .

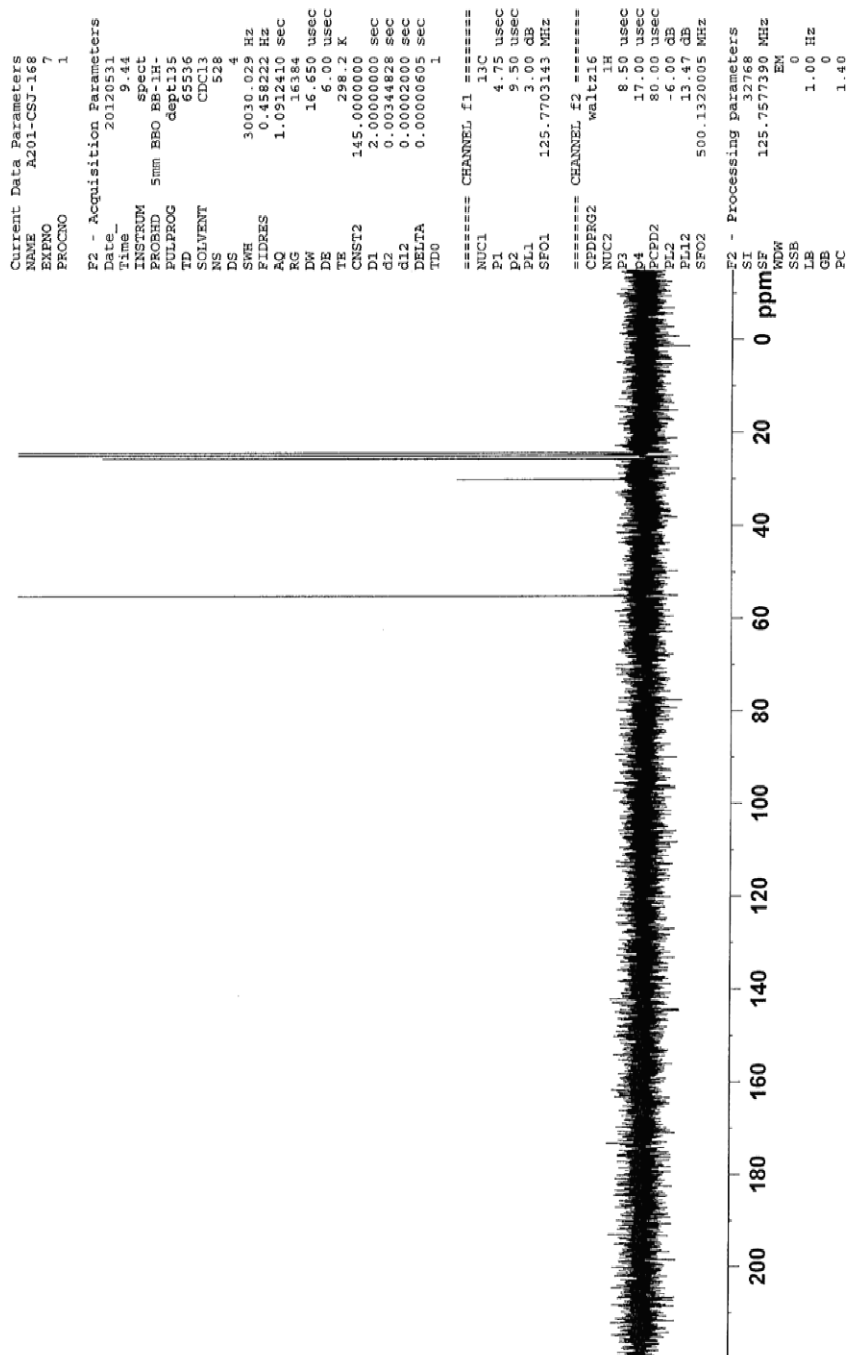


Figure 117. DEPT 135 NMR (500 MHz) spectrum of 2-hydroxyiminothiane-1,1- dioxide (255) in CDCl_3 .

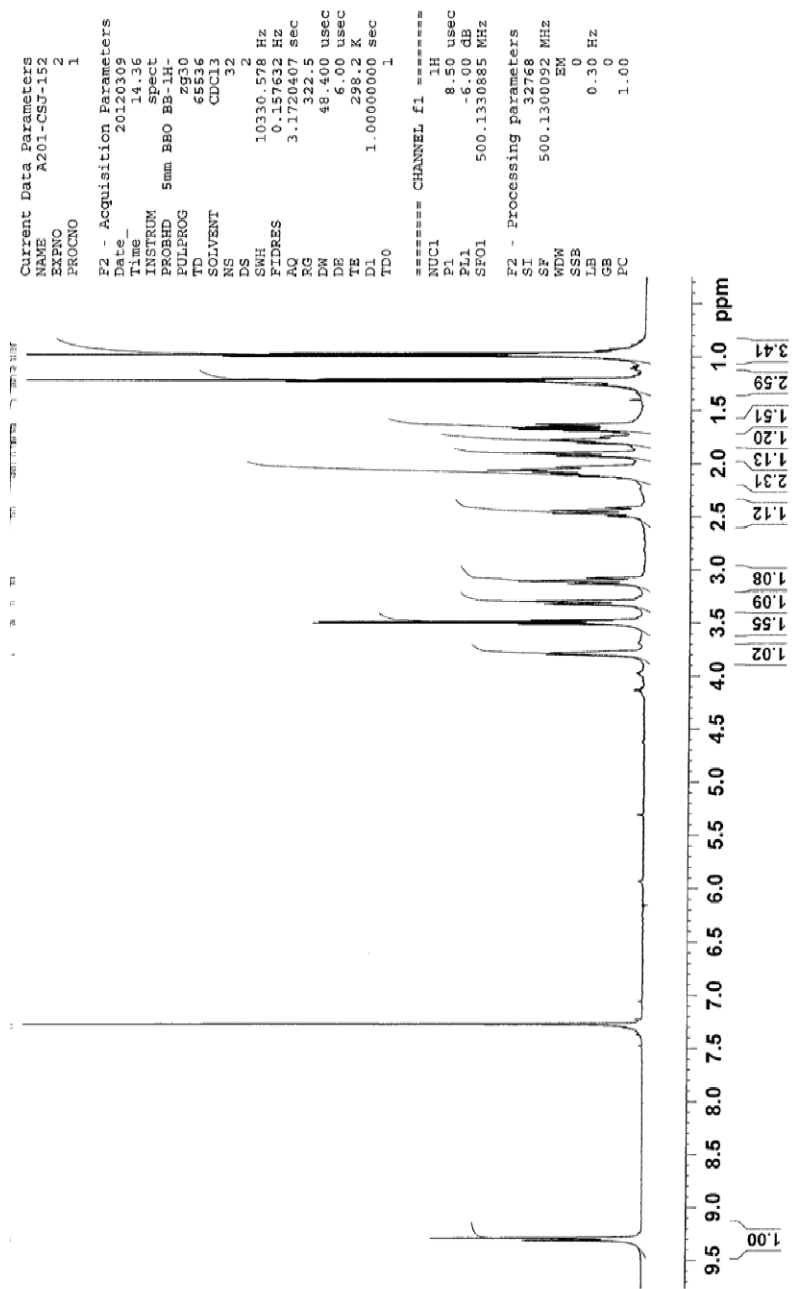


Figure 118. ^1H NMR (500 MHz) spectrum of 2-hydroxyimino-3-ethylthiane-1,1-dioxide (**256**) in CDCl_3 .

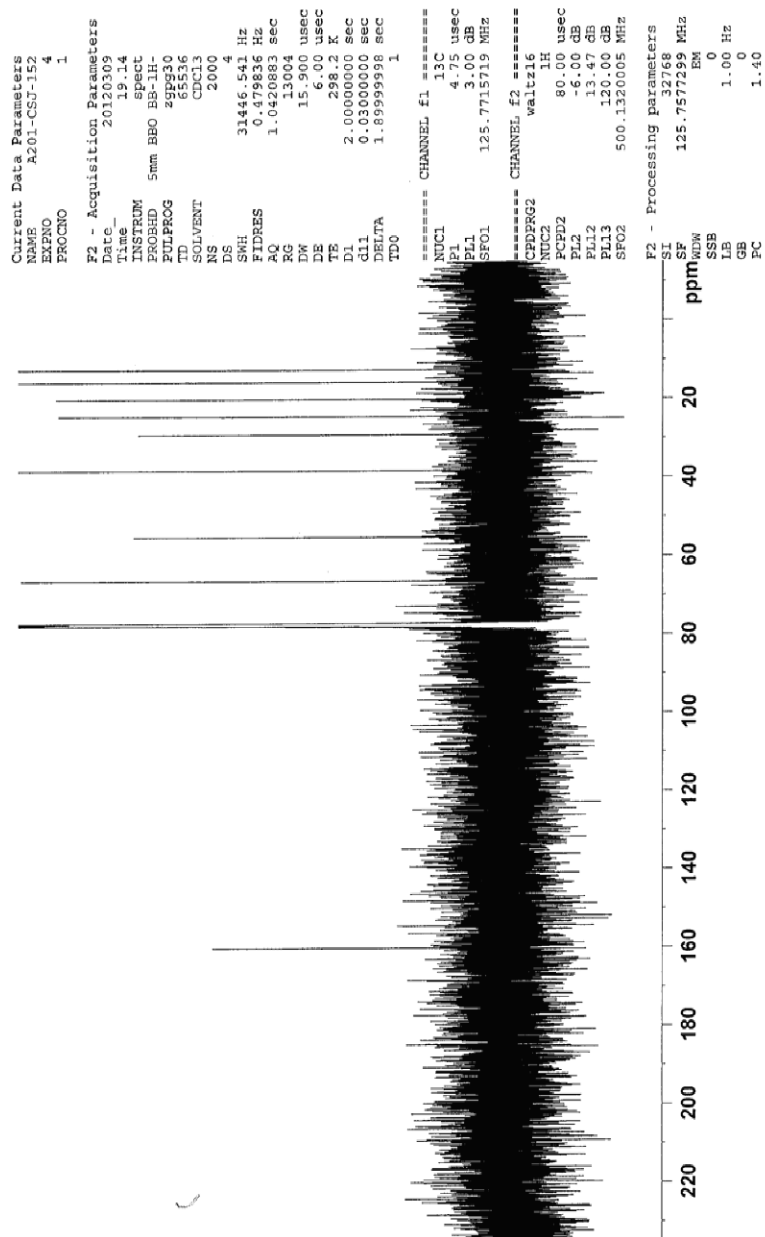


Figure 119. $^{13}\text{C}\{^1\text{H}\}$ NMR (125 MHz) spectrum of 2-hydroxyimino-3-ethylthiane-1,1-dioxide (**256**) in CDCl_3 .

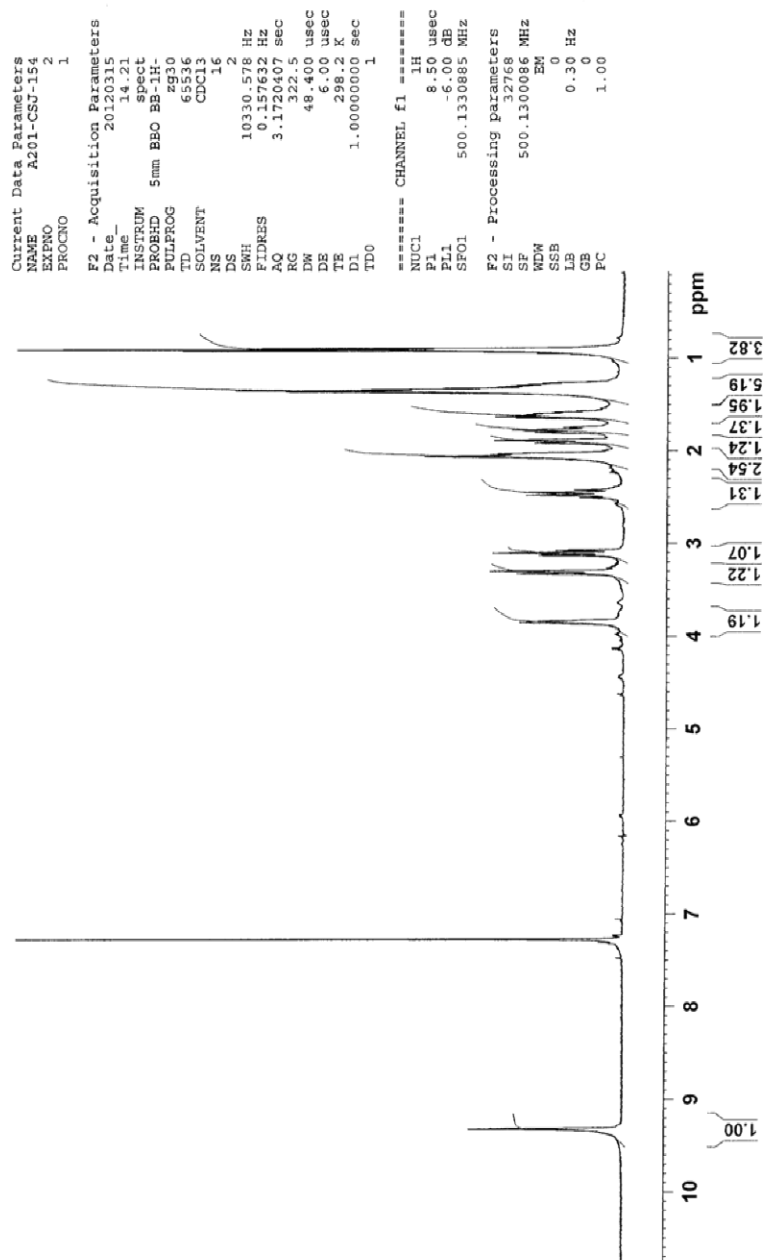


Figure 121. ¹H NMR (500 MHz) spectrum of 2-hydroxyimino-3-butylthiane-1,1-dioxide (257) in CDCl₃.

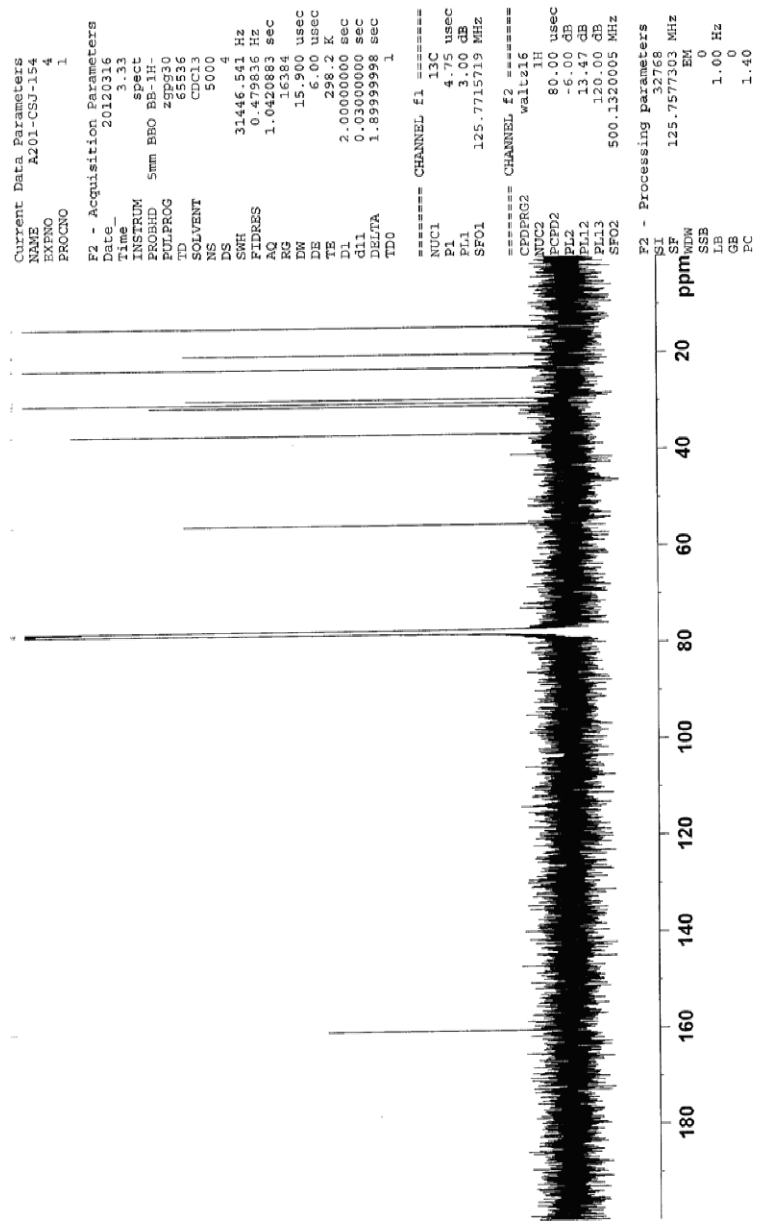


Figure 122. $^{13}\text{C}\{^1\text{H}\}$ NMR (125 MHz) spectrum of 2-hydroxyimino-3-butylthiane-1,1-dioxide (**257**) in CDCl_3 .

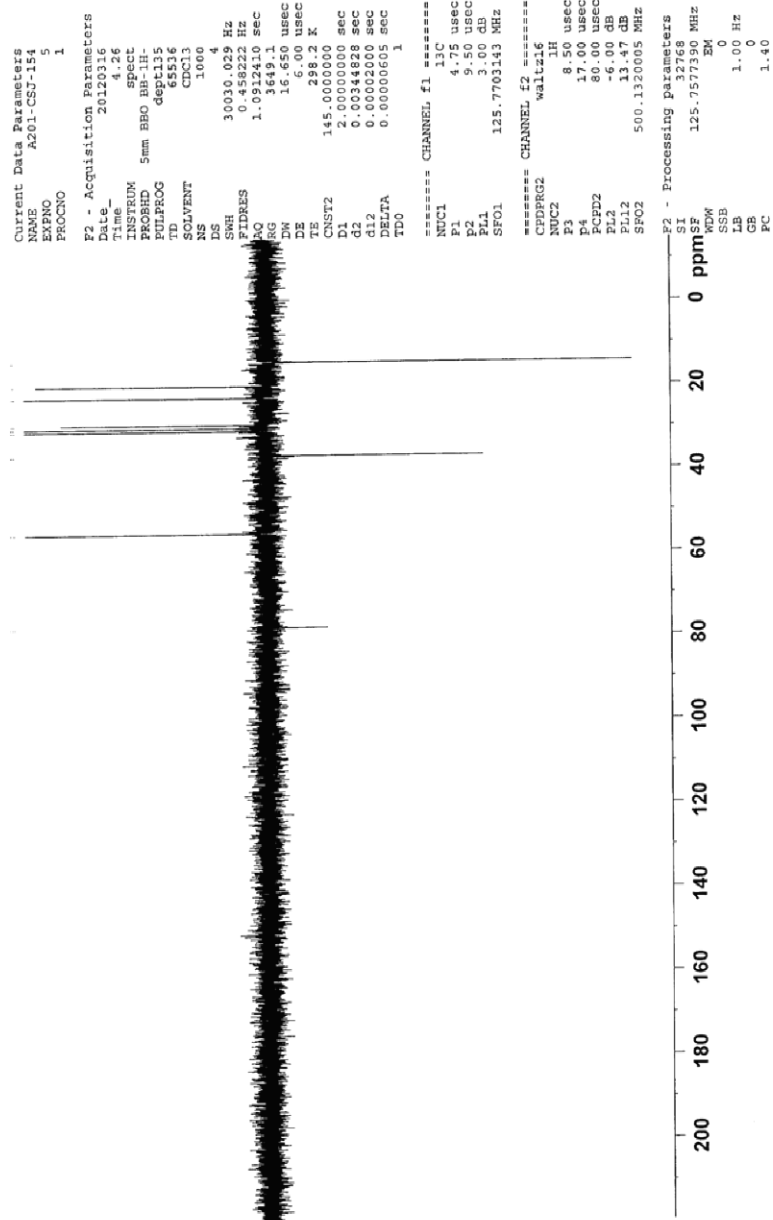


Figure 123. DEPT 135 NMR (125 MHz) spectrum of 2-hydroxyimino-3-butylthiane-1,1-dioxide (**257**) in CDCl_3 .

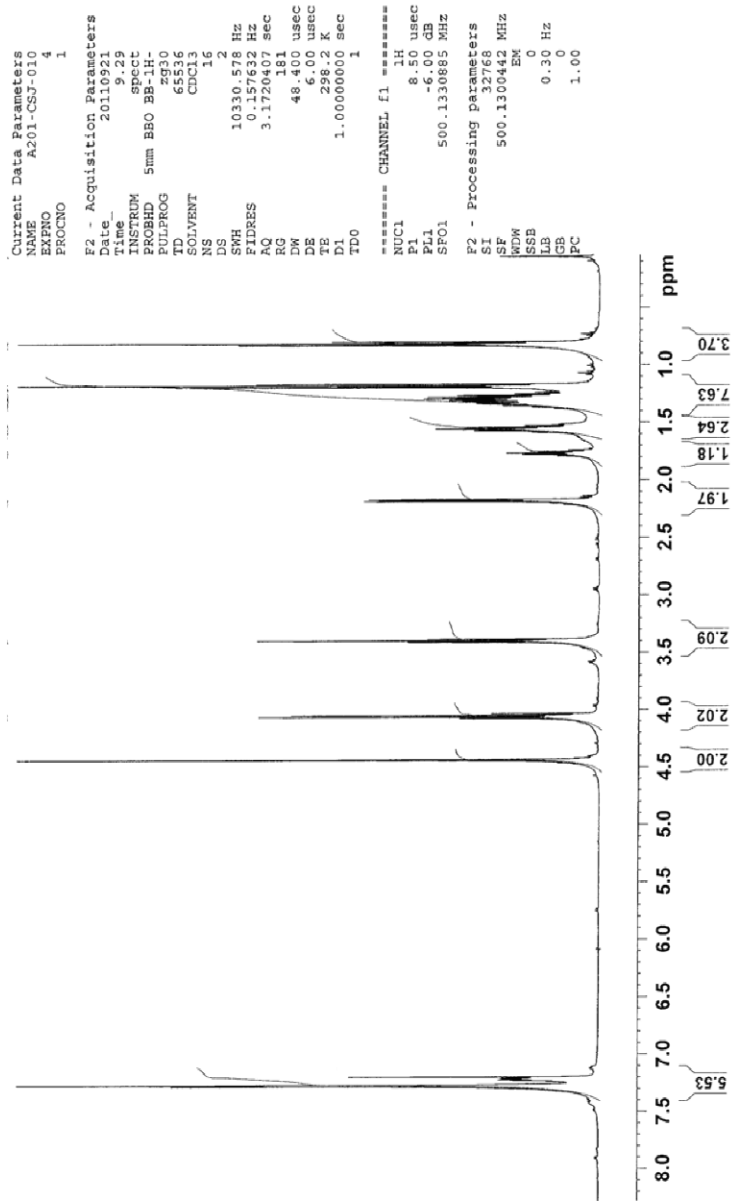


Figure 124. ^1H NMR (500 MHz) spectrum of ethyl 6-benzyloxy-3-ethylhexanoate (**294**) in CDCl_3 .

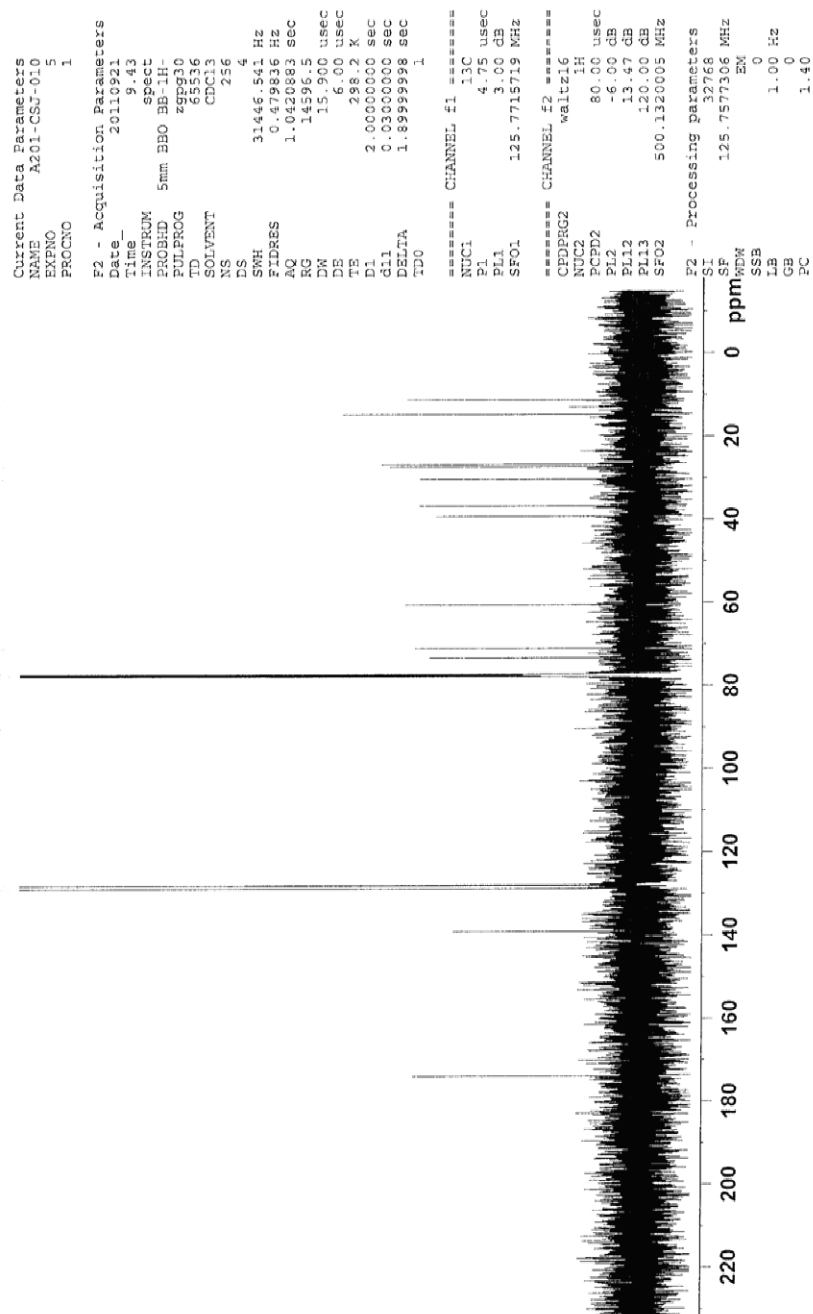


Figure 125. $^{13}\text{C}\{^1\text{H}\}$ NMR (125 MHz) spectrum of ethyl 6-benzyloxy-3-ethylhexanoate (**294**) in CDCl_3 .

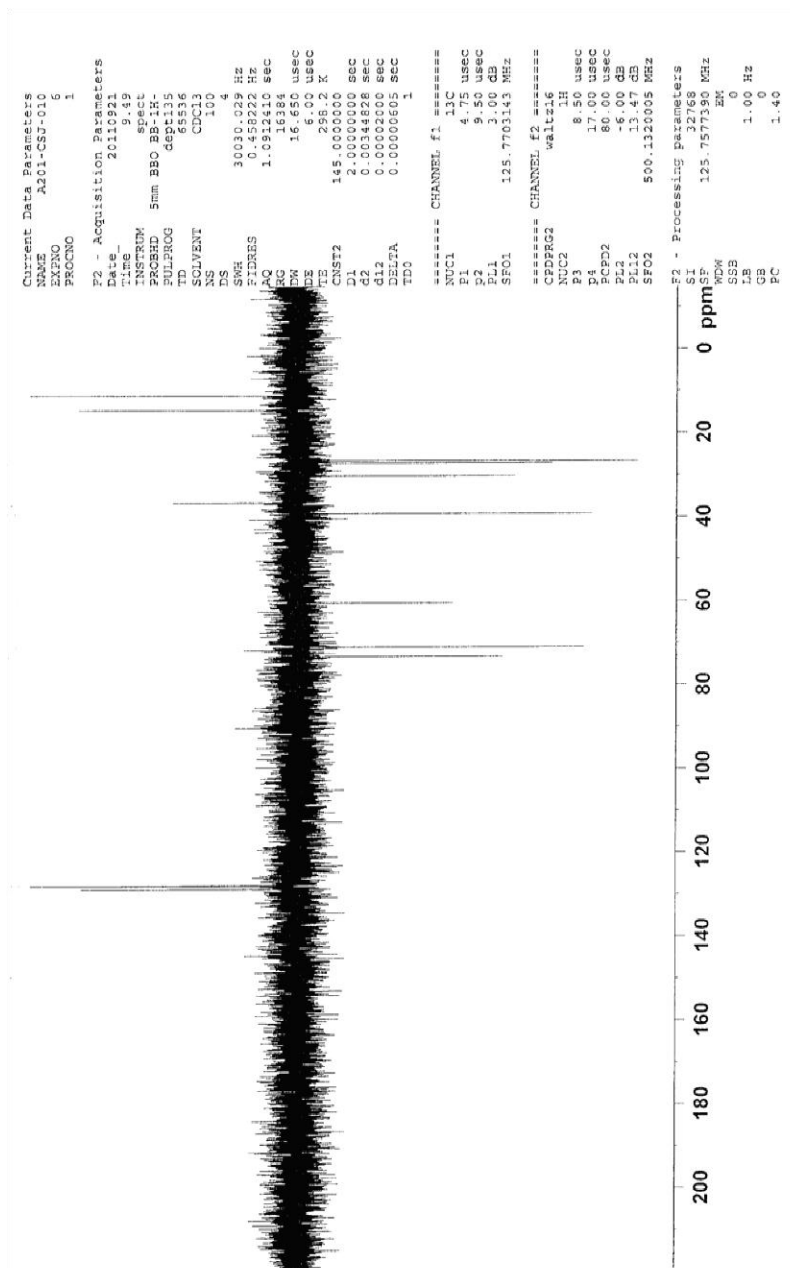


Figure 126. DEPT 135 NMR (125 MHz) spectrum of ethyl 6-benzyloxy-3-ethylhexanoate (**294**) in CDCl_3 .

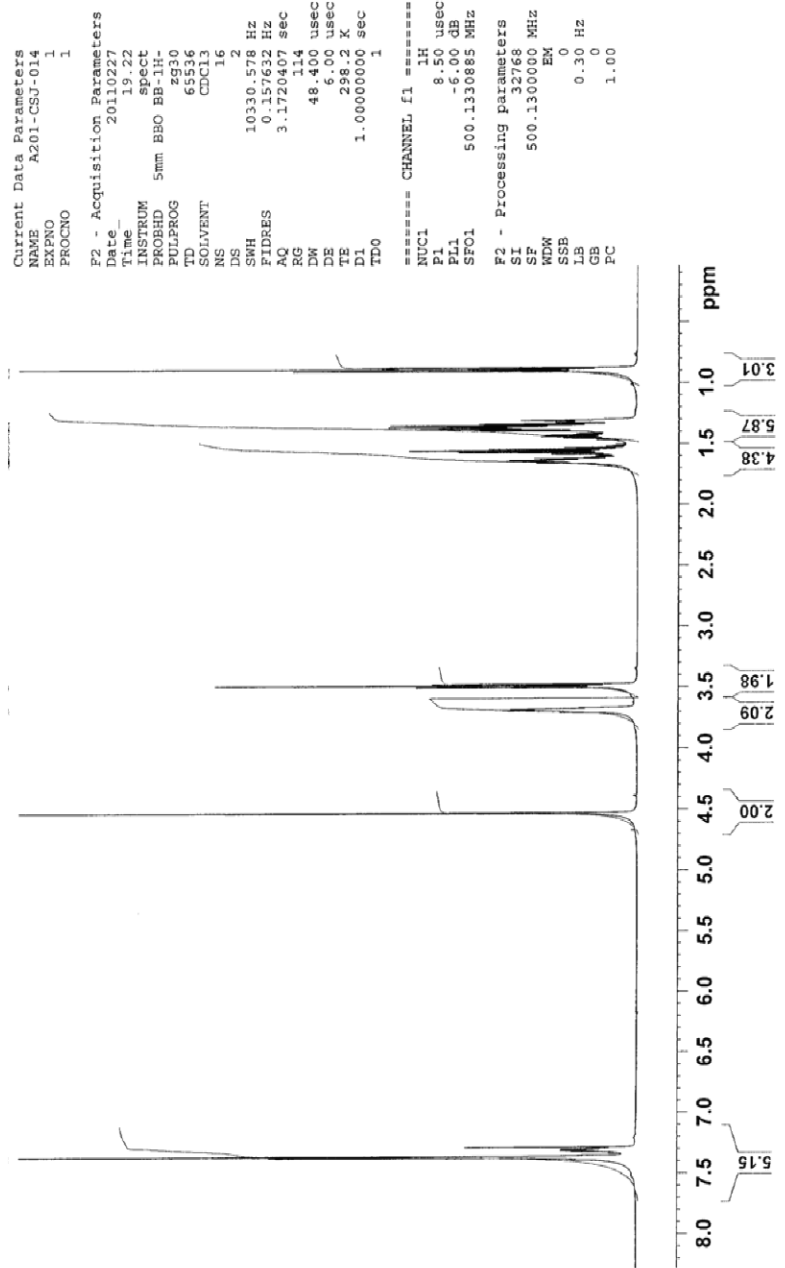


Figure 127. ¹H NMR (500 MHz) spectrum of 6-benzyloxy-3-ethyl-1-hexanol (**289**) in CDCl₃.

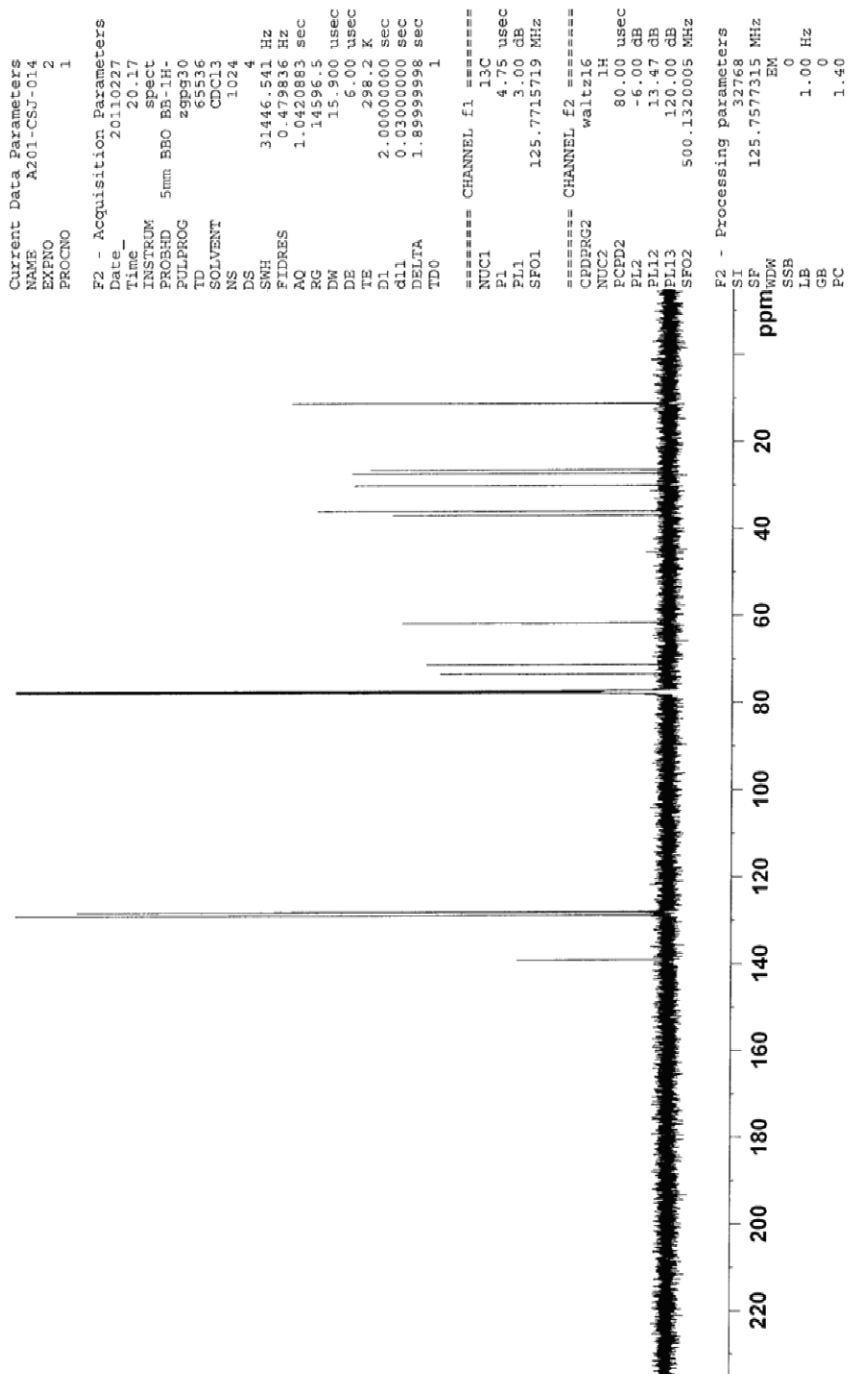


Figure 128. $^{13}\text{C}\{^1\text{H}\}$ NMR (500 MHz) spectrum of 6-benzyloxy-3-ethyl-1-hexanol (**589**) in CDCl_3 .

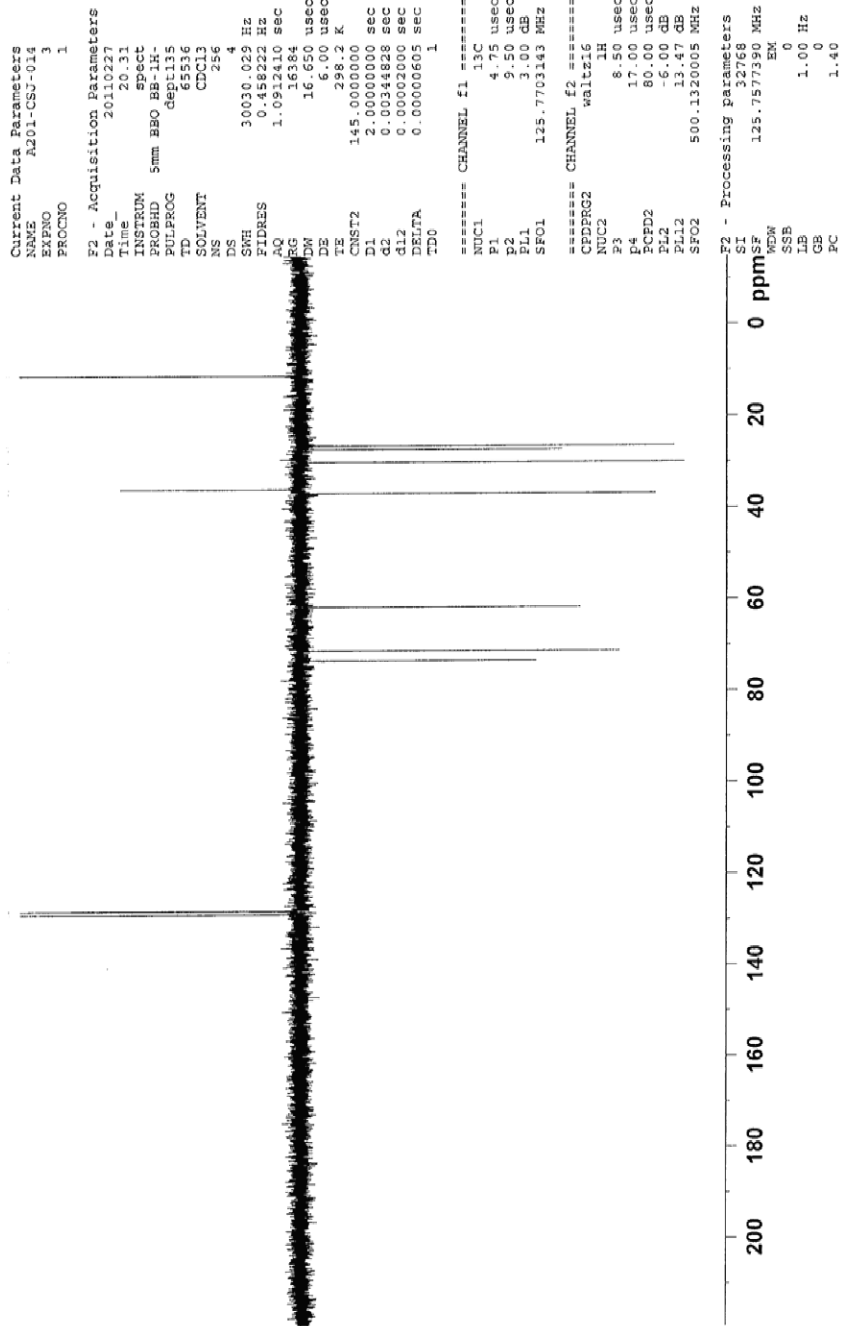


Figure 129. DEPT 135 NMR (500 MHz) spectrum of 6-benzyloxy-3-ethyl-1-hexanol (289) in CDCl_3 .

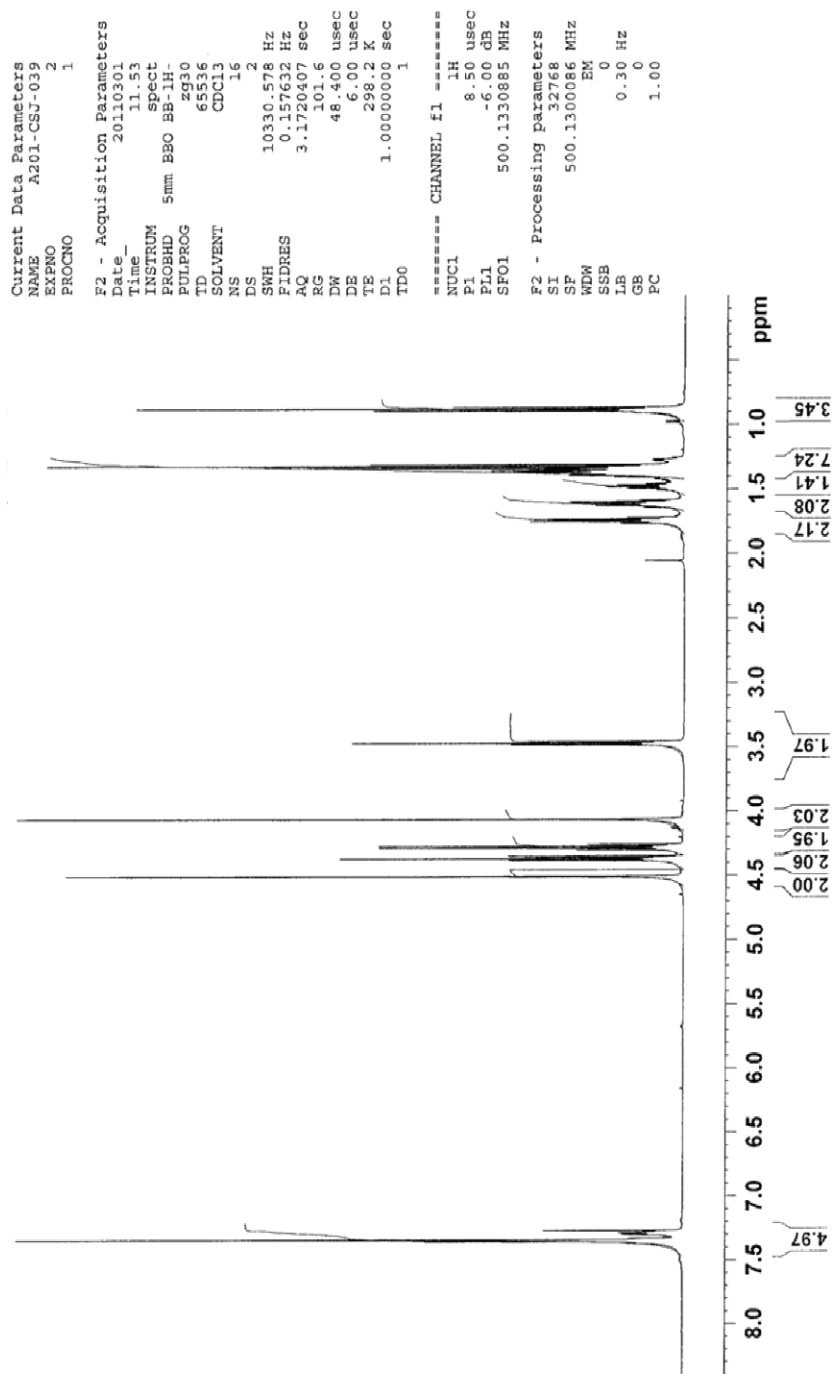


Figure 130. ^1H NMR (500 MHz) spectrum of ethyl [(6-benzyloxy-3-ethyl)hexyloxysulfonyl]acetate (**295**) in CDCl_3 .

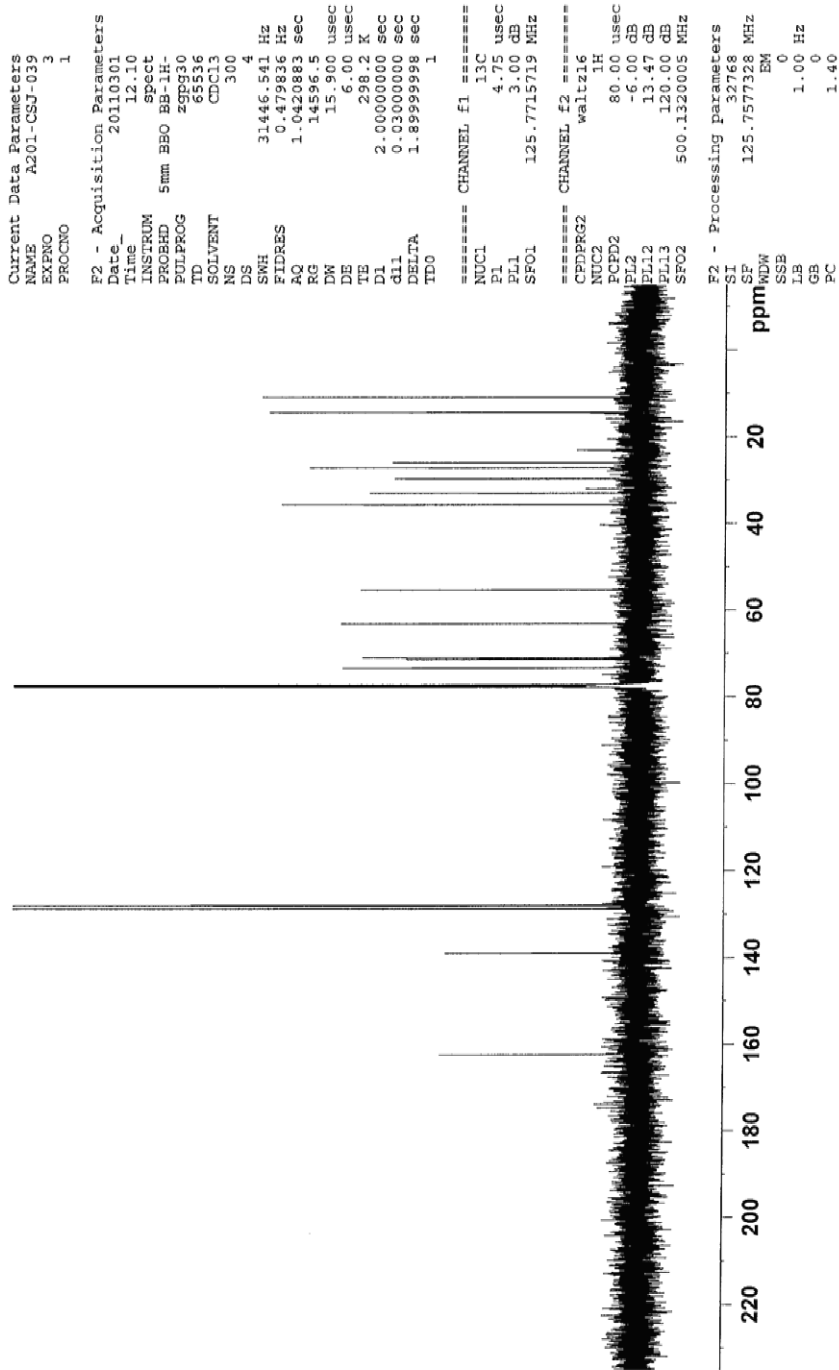


Figure 131. $^{13}\text{C}\{^1\text{H}\}$ NMR (125 MHz) spectrum of ethyl [(6-benzyloxy-3-ethyl)hexyloxysulfonyl]acetate (**295**) in CDCl_3 .

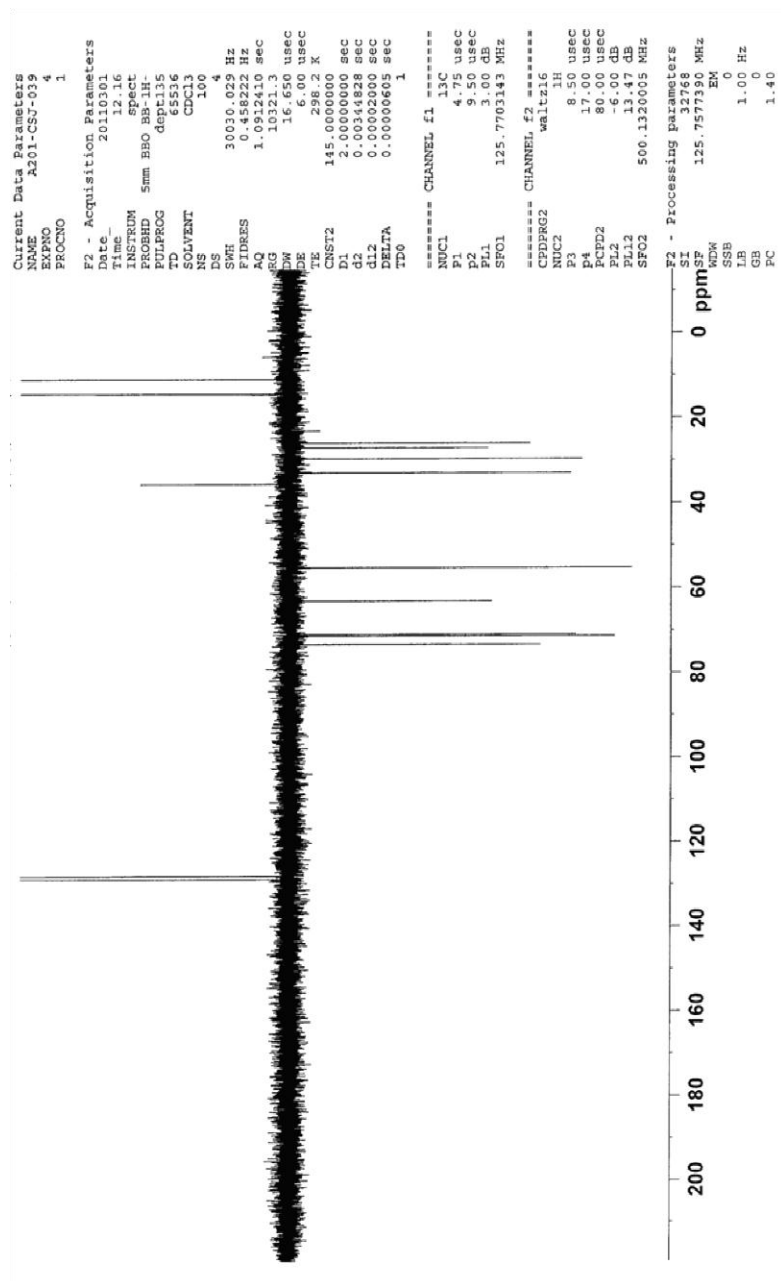


Figure 132. DEPT 135 NMR (125 MHz) spectrum of ethyl [(6-benzyloxy-3-ethyl)hexyloxysulfonyl]acetate (**295**) in CDCl₃.

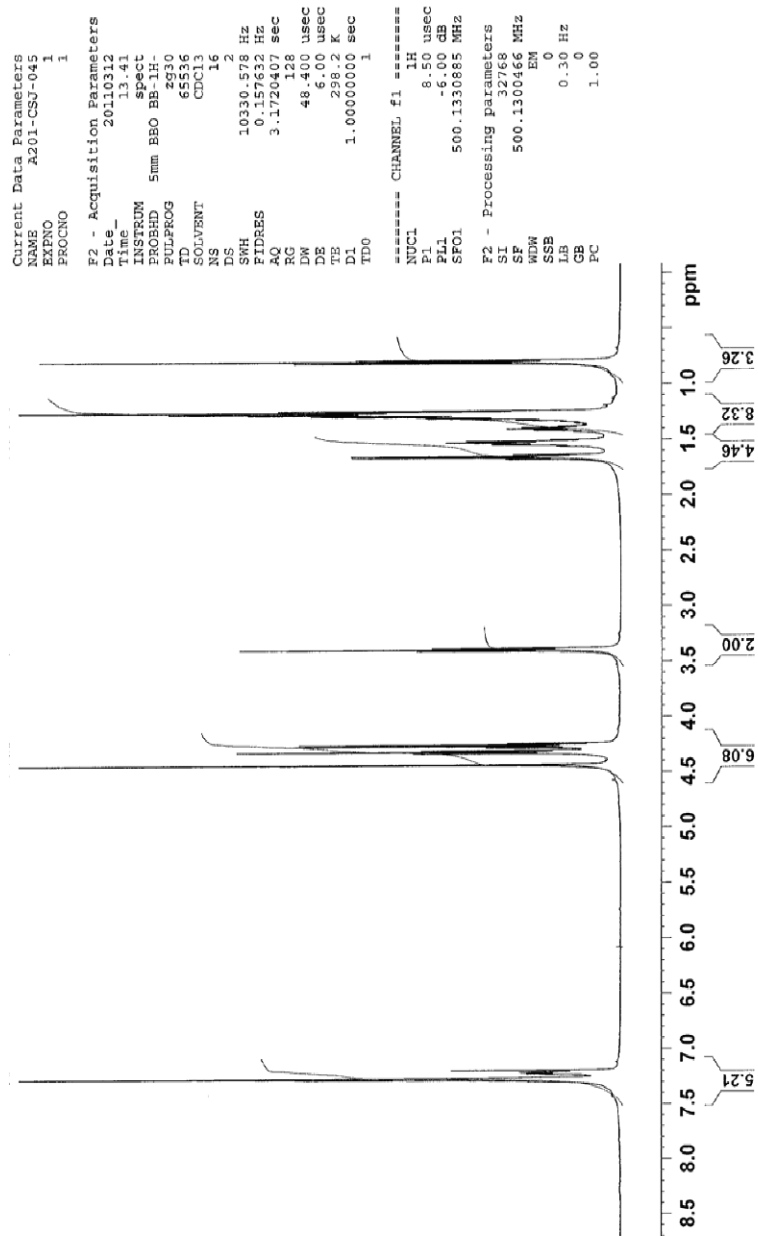


Figure 133. ^1H NMR (500 MHz) spectrum of ethyl [(6-benzyloxy-3-ethyl)hexyloxysulfonyl]diazoacetate (**296**) in CDCl_3 .

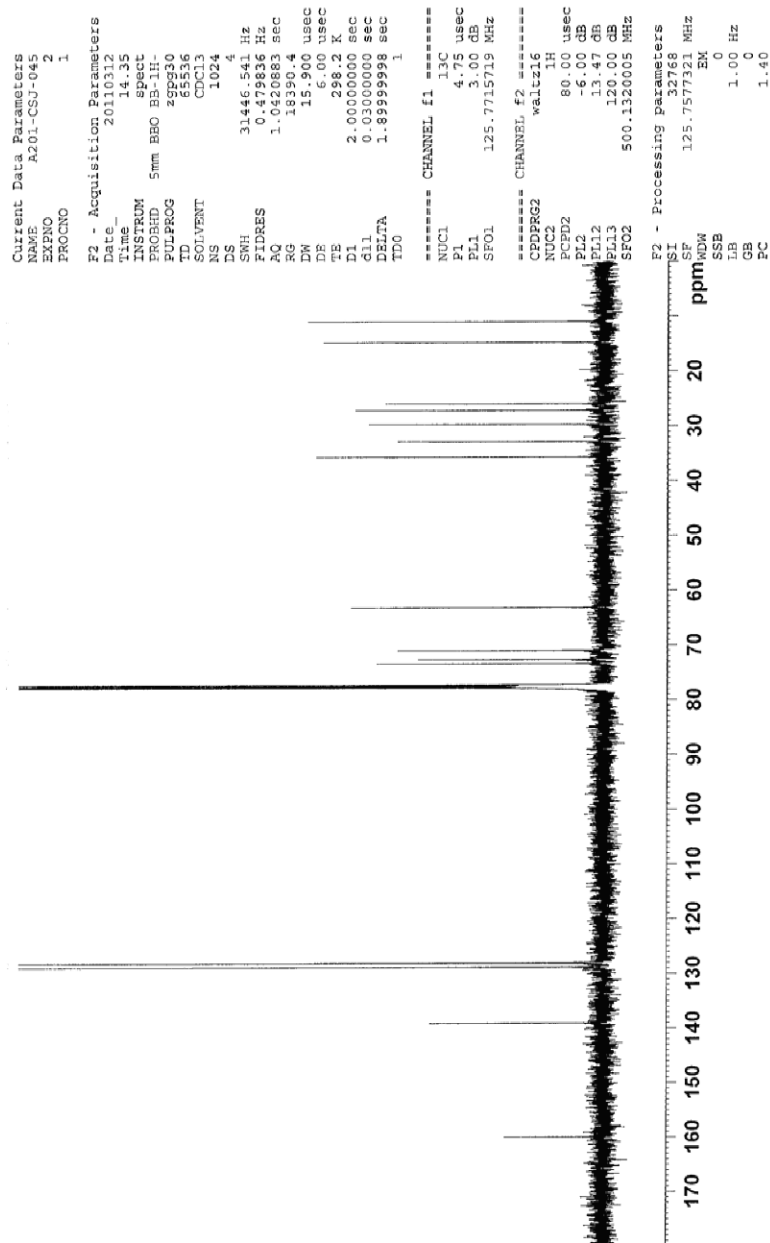


Figure 134. $^{13}\text{C}\{^1\text{H}\}$ NMR (125 MHz) spectrum of ethyl [(6-benzyloxy-3-ethyl)hexyloxysulfonyl]diazoacetate (**296**) in CDCl_3 .

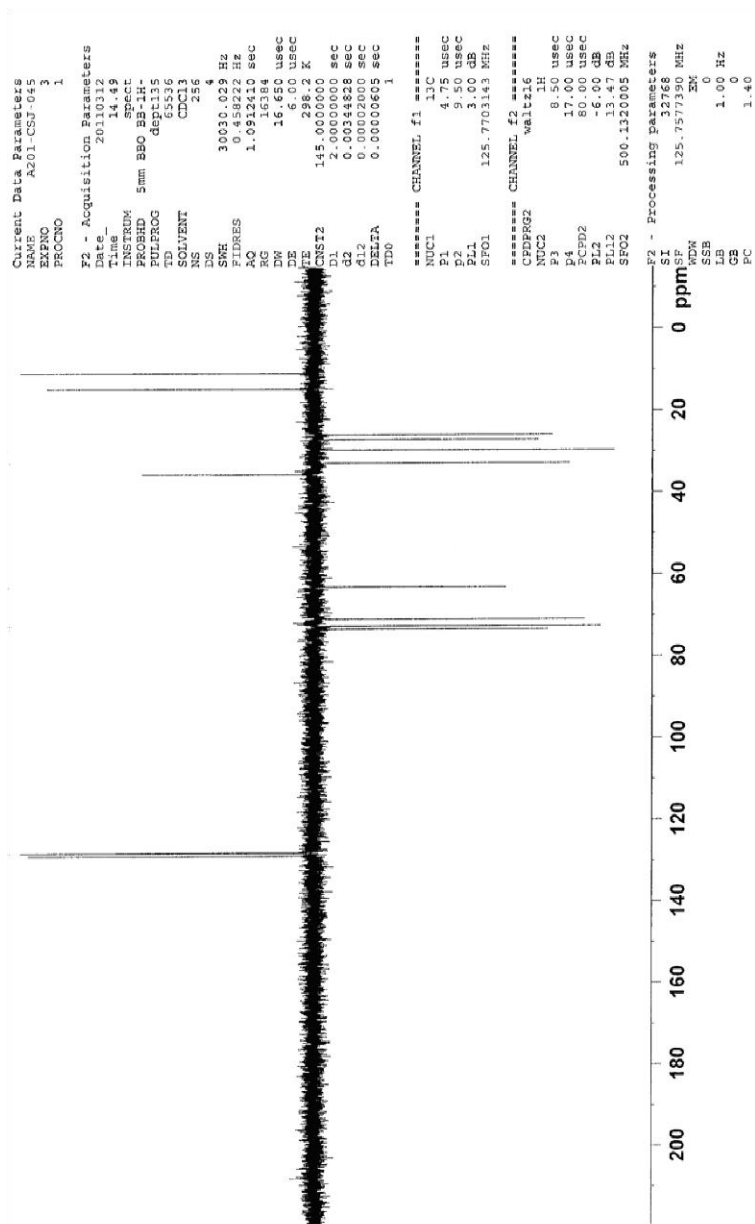


Figure 135. DEPT 135 NMR (125 MHz) spectrum of ethyl [(6-benzyloxy-3-ethyl)hexyloxysulfonyl]diazoacetate (**296**) in CDCl_3 .

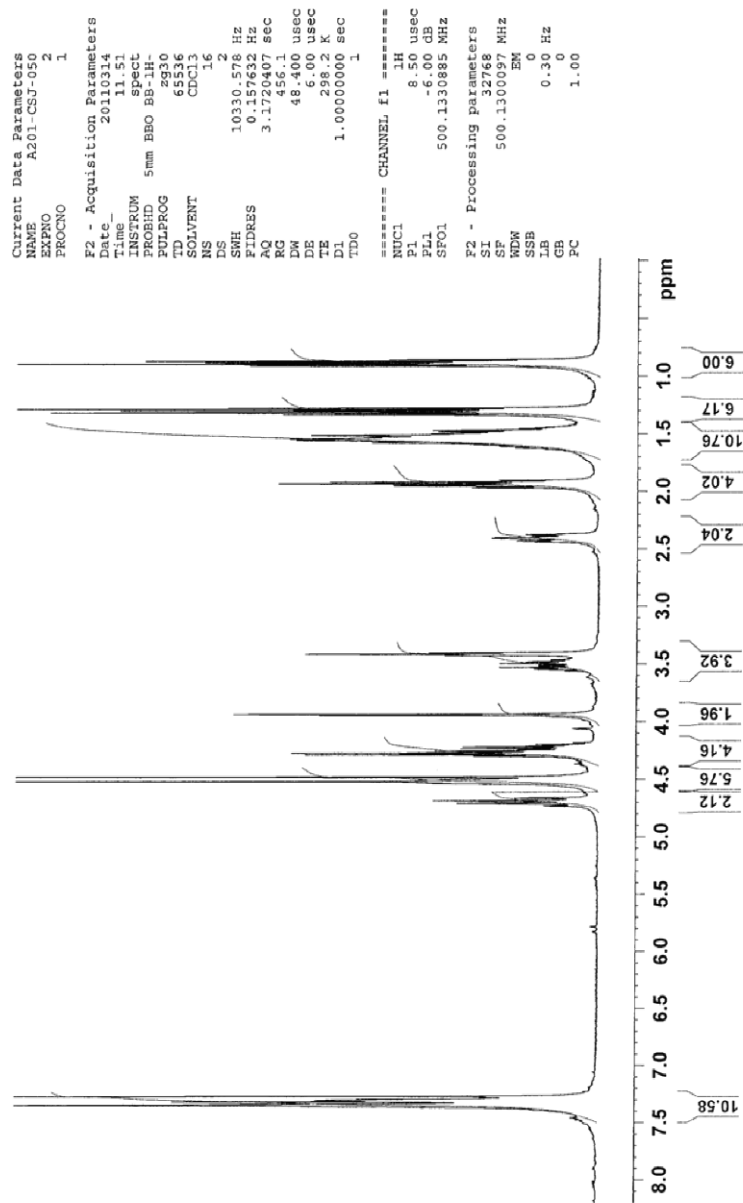


Figure 136. ^1H NMR (500 MHz) spectrum of 3-carbethoxy-4-(3-benzyloxy)propyl-4-ethyl-1,2-oxathiane-2,2-dioxide (**223**) in CDCl_3 .

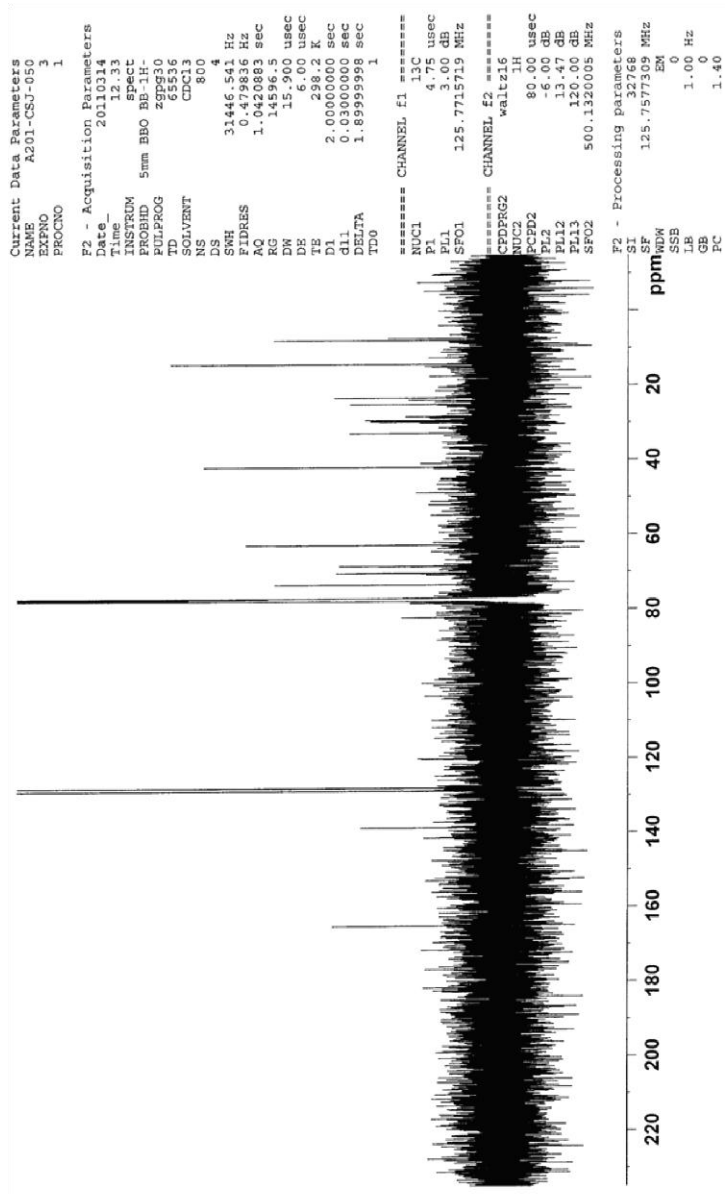


Figure 137. $^{13}\text{C}\{^1\text{H}\}$ NMR (500 MHz) spectrum of 3-carbethoxy-4-(3-benzyloxy)propyl-4-ethyl-1,2-oxathiane-2,2-dioxide (**223**) in CDCl_3 .

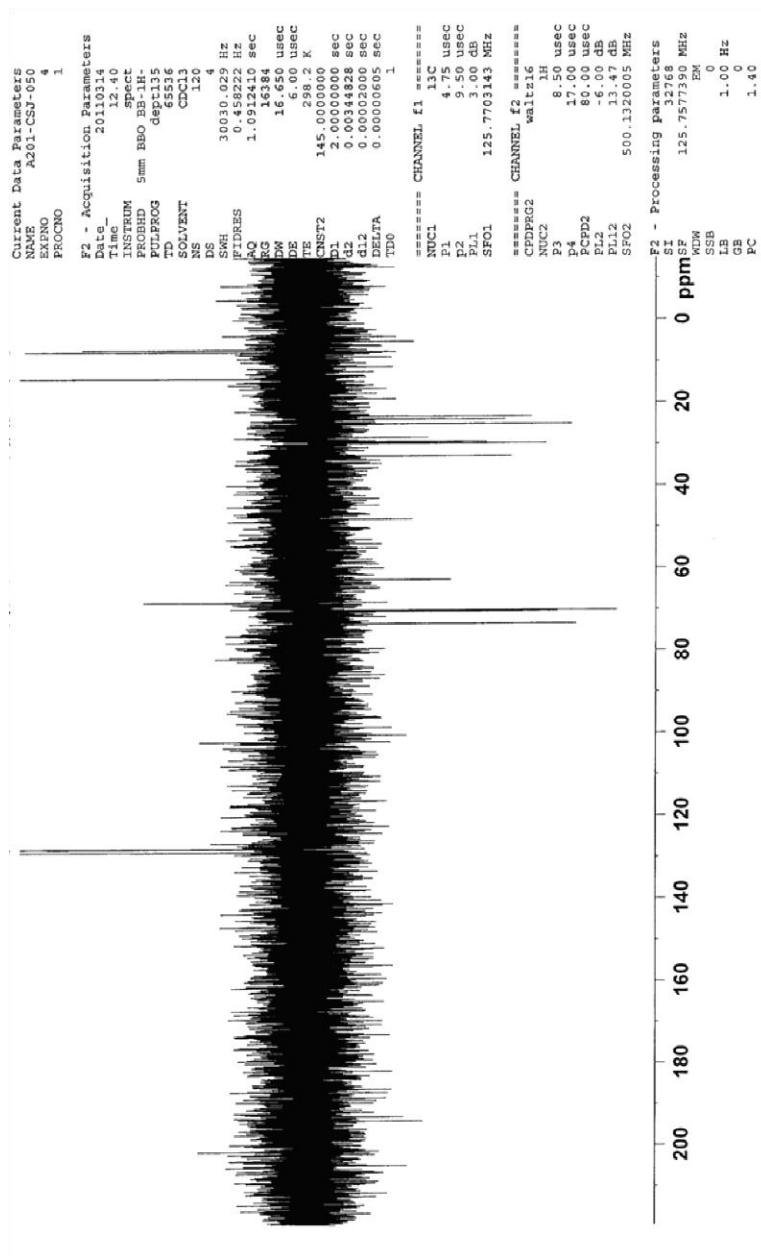


Figure 138. DEPT 135 NMR (500 MHz) spectrum of 3-carbethoxy-4-(3-benzyloxy)propyl-4-ethyl-1,2-oxathiane-2,2-dioxide (**223**) in CDCl₃.

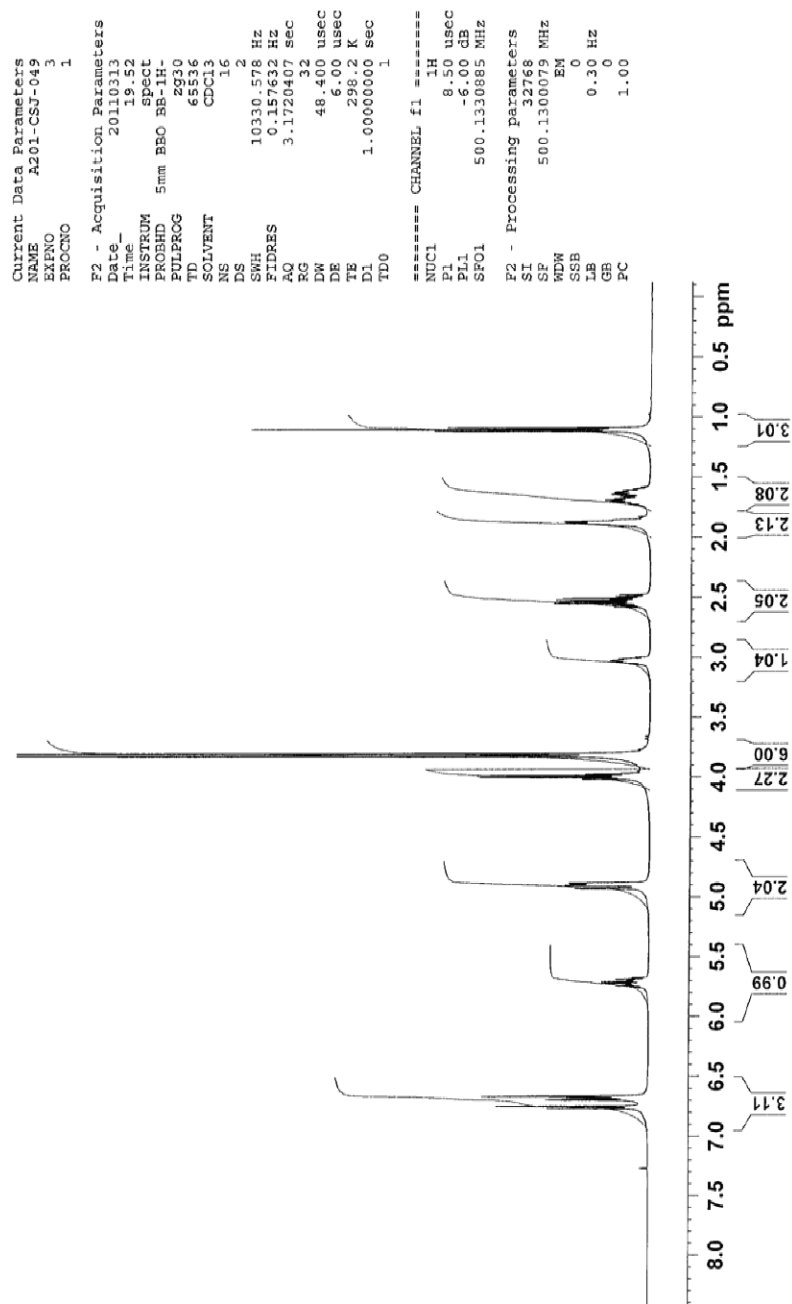


Figure 139. ^1H NMR (500 MHz) spectrum of ethyl 3-(3,4-dimethoxy)phenyl-6-heptenoate (**303**) in CDCl_3 .

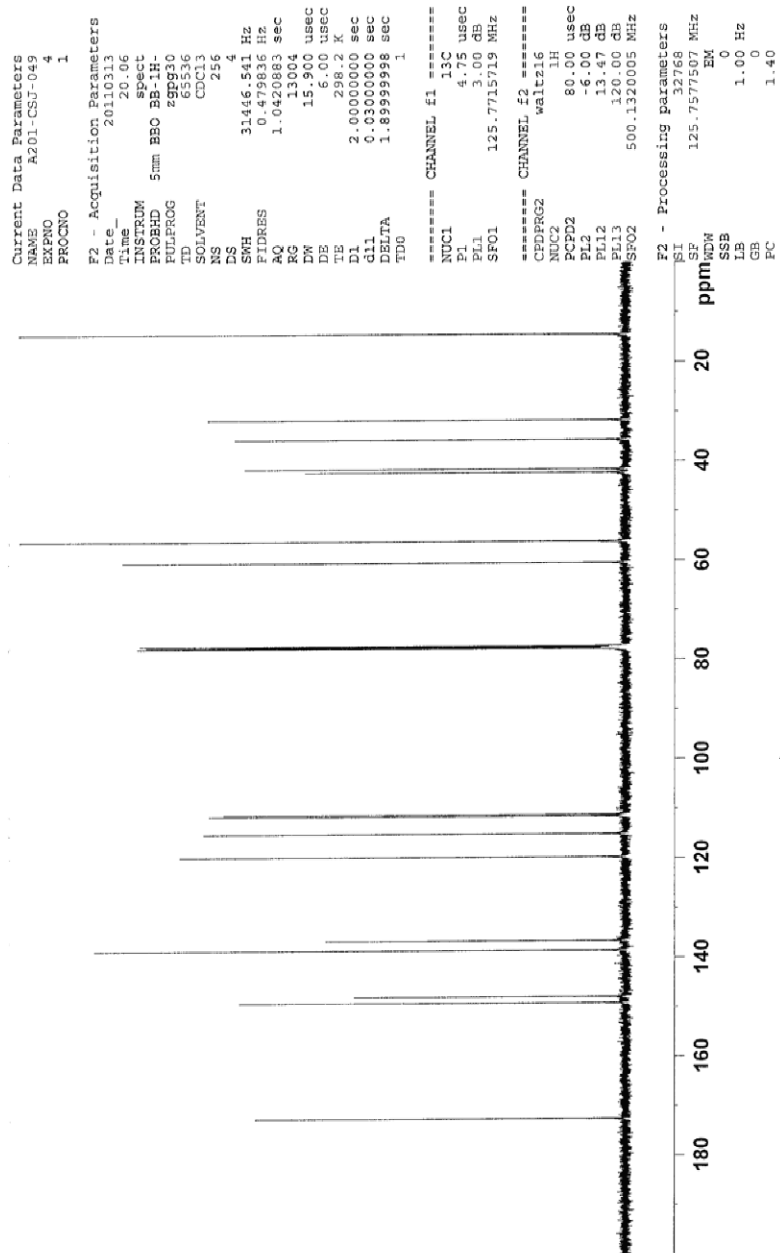


Figure 140. $^{13}\text{C}\{^1\text{H}\}$ NMR (125 MHz) spectrum of ethyl 3-(3,4-dimethoxy)phenyl-6-heptenoate (**303**) in CDCl_3 .

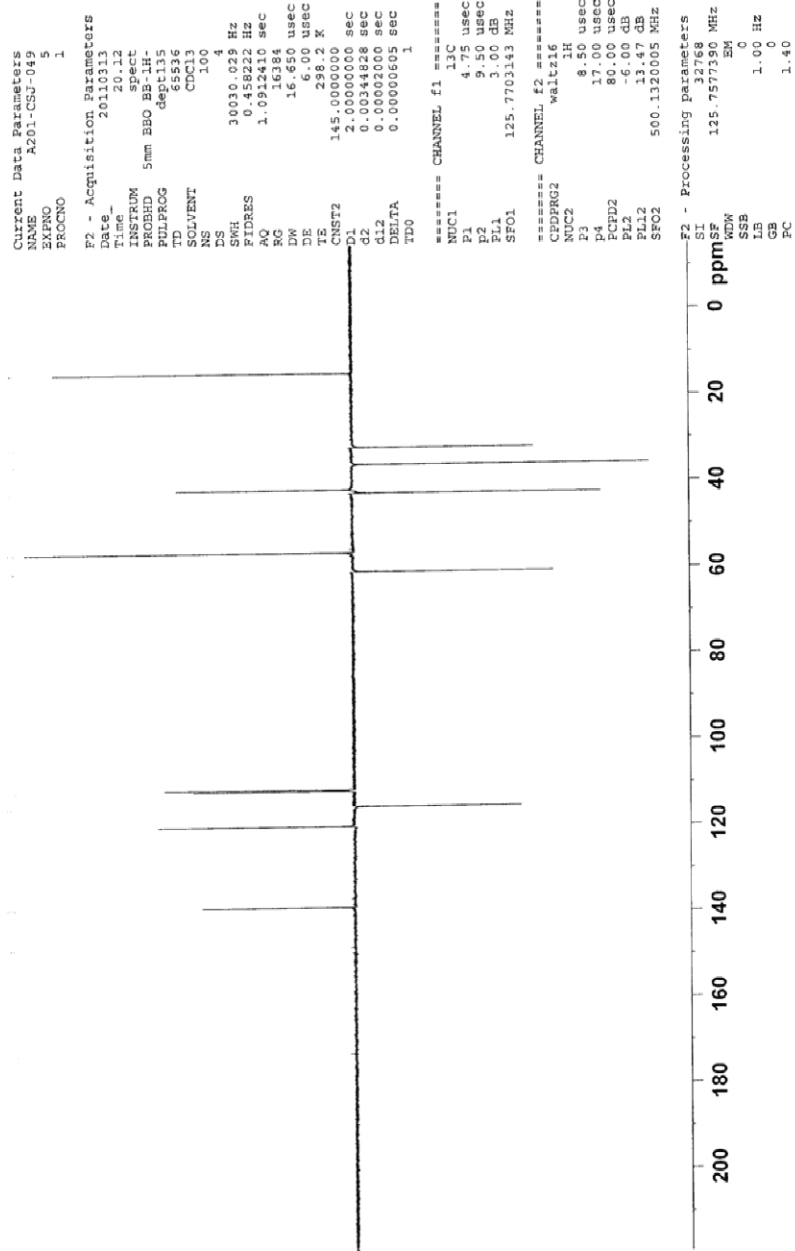


Figure 141. DEPT 135 NMR (125 MHz) spectrum of ethyl 3-(3,4-dimethoxy)phenyl-6-heptenoate (**303**) in CDCl₃.

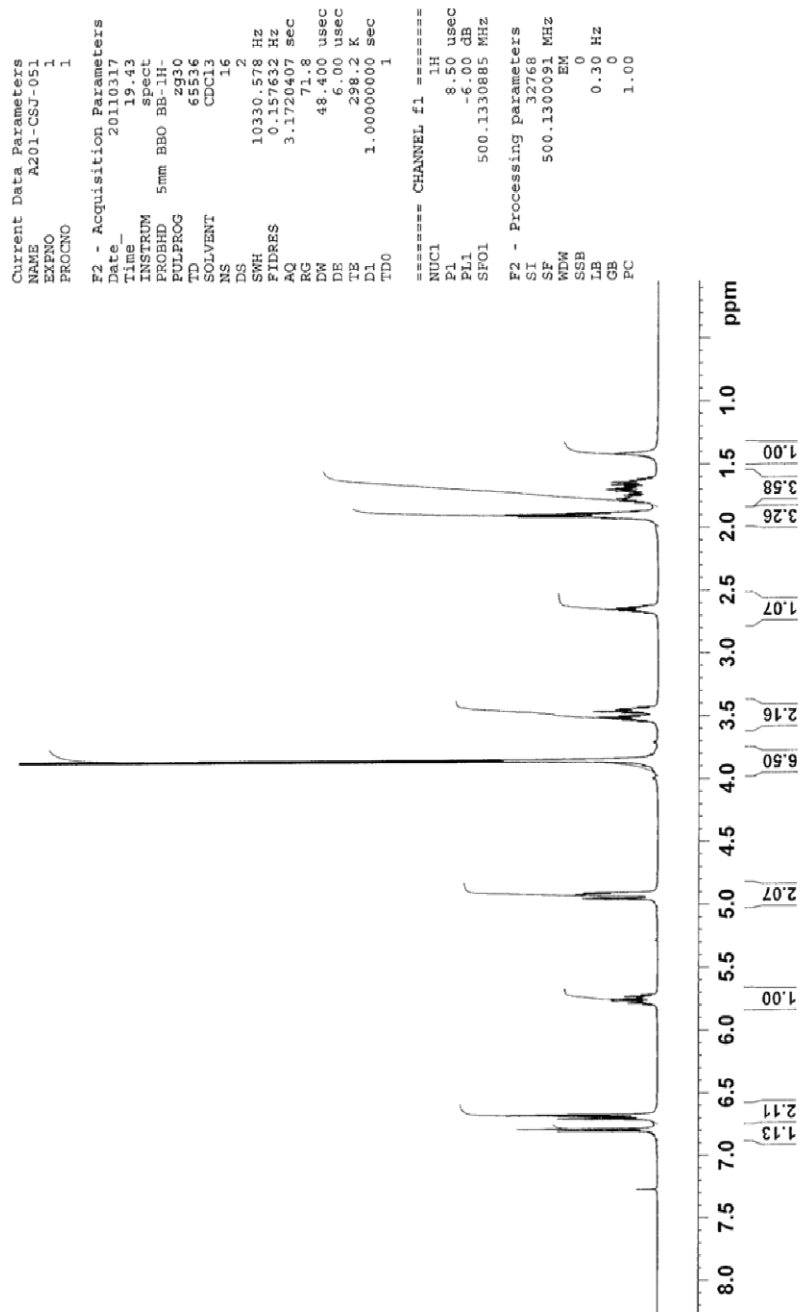


Figure 142. ^1H NMR (500 MHz) spectrum of 3-(3,4-dimethoxy)phenyl-hept-6-en-1-ol (**300**) in CDCl_3 .

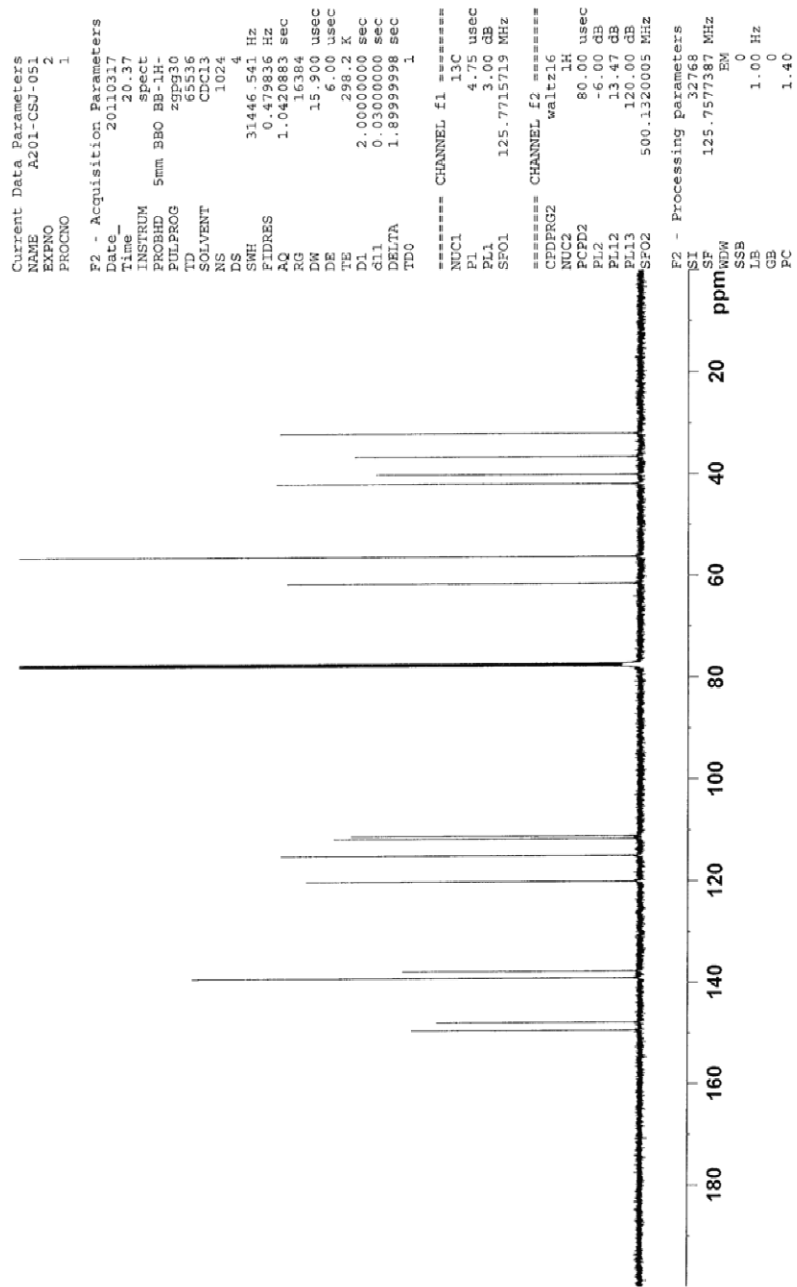


Figure 143. $^{13}\text{C}\{^1\text{H}\}$ NMR (125 MHz) spectrum of 3-(3,4-dimethoxy)phenylhept-6-en-1-ol (**300**) in CDCl_3 .

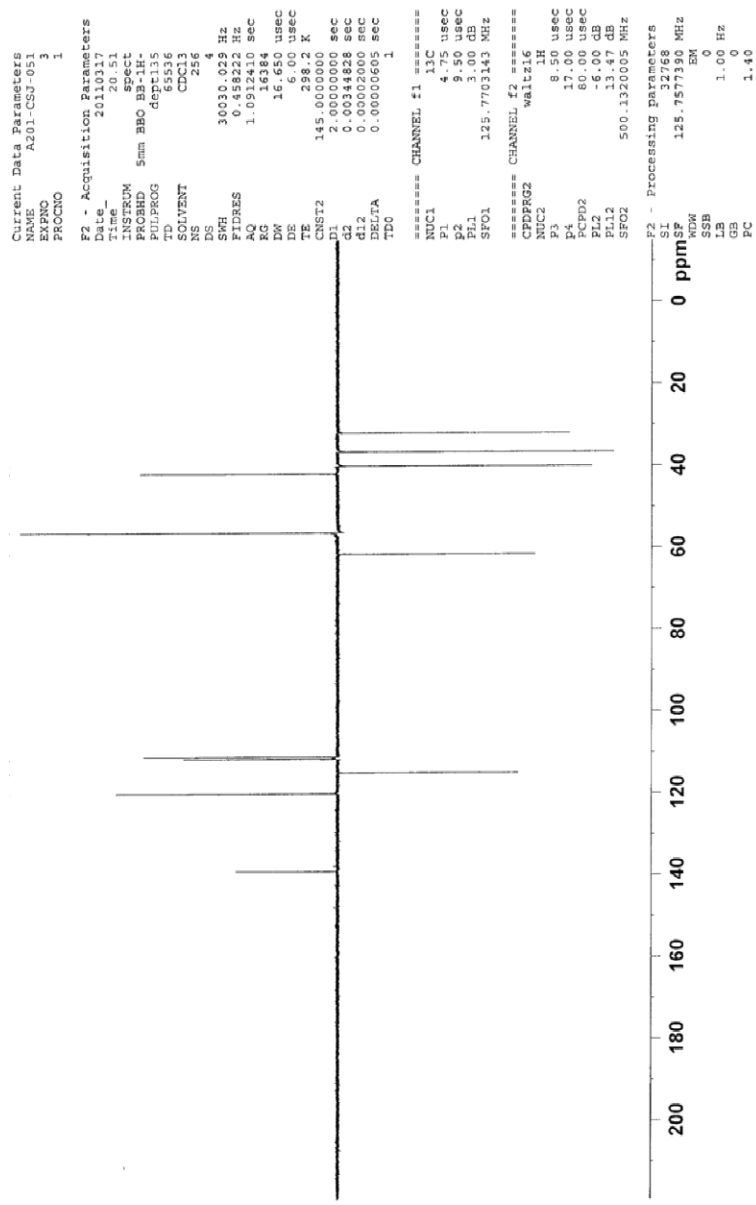


Figure 144. DEPT 135 NMR (125 MHz) spectrum of 3-(3,4-dimethoxy)phenylhept-6-en-1-ol (**300**) in CDCl_3 .

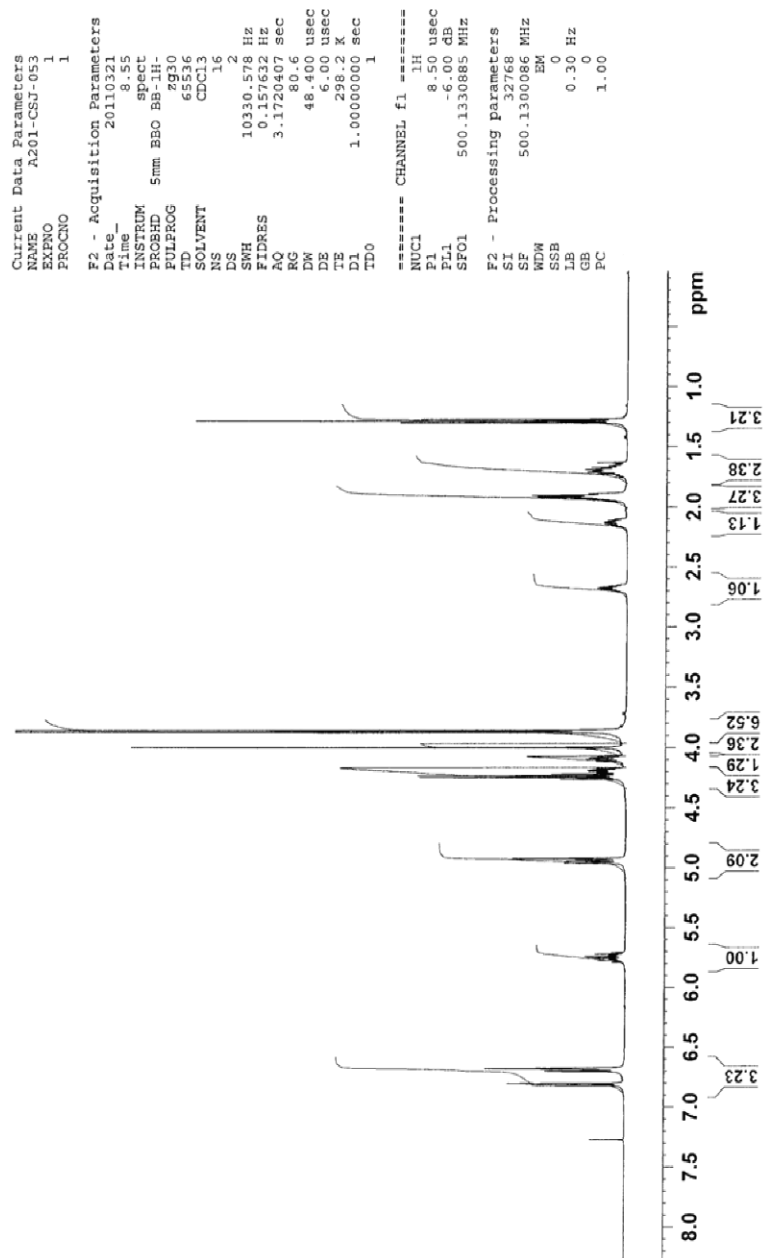


Figure 145. ^1H NMR (500 MHz) spectrum of ethyl [3-(3,4-dimethoxy)phenyl-6-heptenyloxysulfonyl]acetate (**304**) in CDCl_3 .

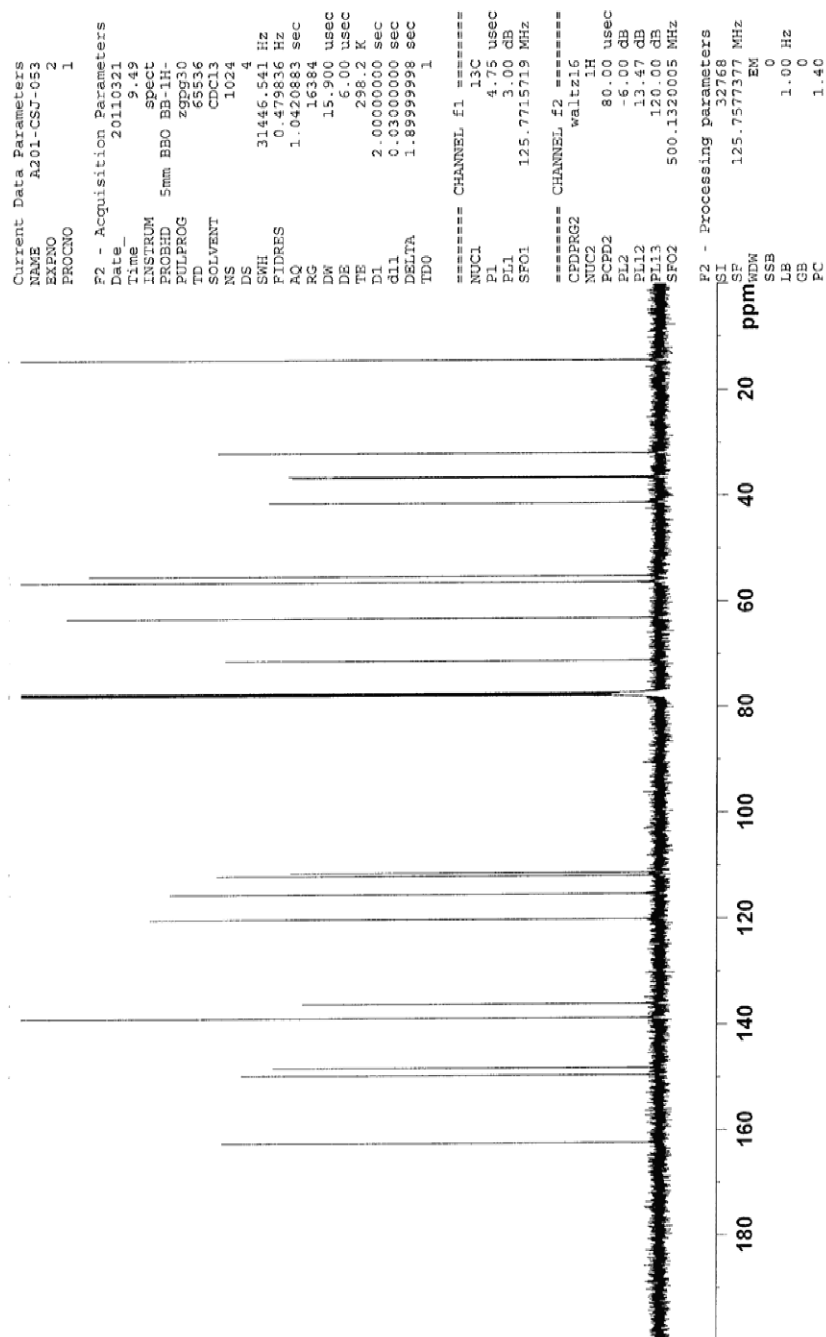


Figure 146. $^{13}\text{C}\{^1\text{H}\}$ NMR (125 MHz) spectrum of ethyl [3-(3,4-dimethoxy)phenyl-6-heptenyloxysulfonyl]acetate (**304**) in CDCl_3 .

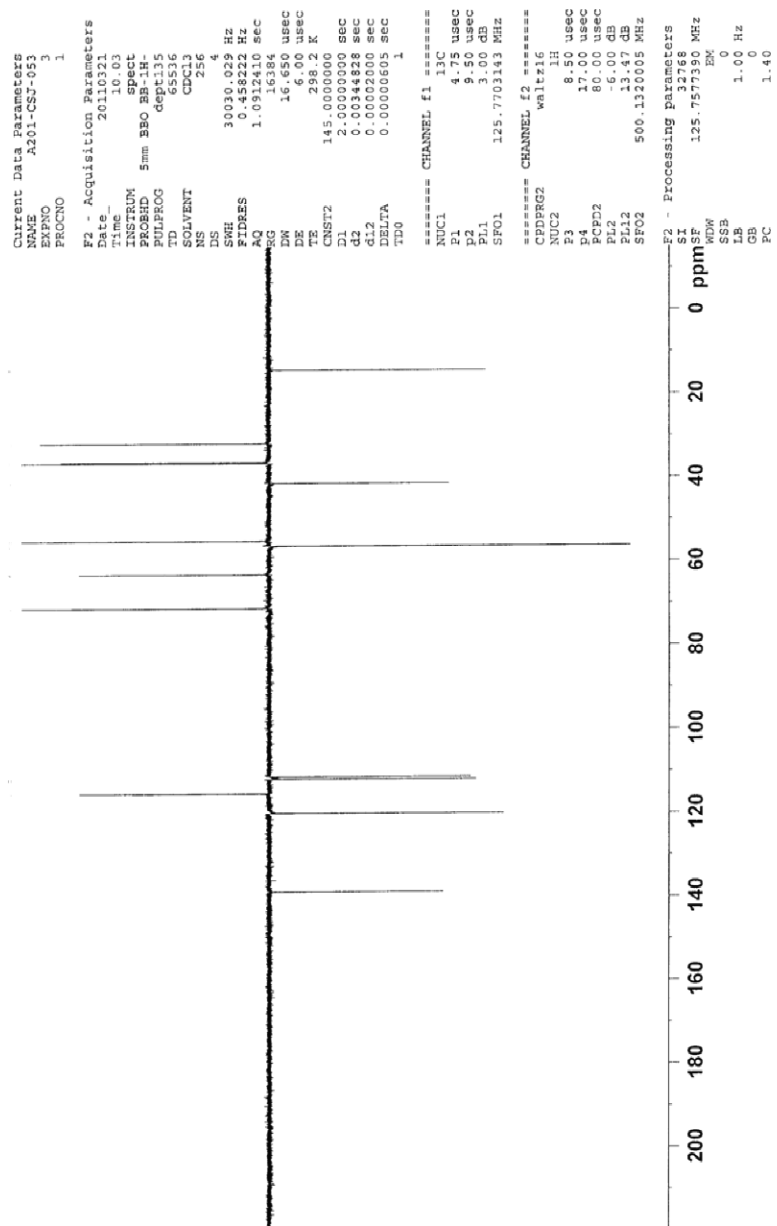


Figure 147. DEPT 135 NMR (125 MHz) spectrum of ethyl [3-(3,4-dimethoxy)phenyl-6-heptenyloxysulfonyl]acetate (**304**) in CDCl₃.

```

Current Data Parameters
NAME      A201-CSJ-055
EXPNO     2
PROCNO    1

F2 - Acquisition Parameters
Date_     20110405
Time      20.02
INSTRUM   Spect
PROBHD    5mm BBO BB-LH-
PULPROG   zgpg30
TD         65536
SOLVENT   CDCl3
NS         2
DS         2
SMH       10330.578 Hz
FIDRES    0.157632 Hz
AQ         3.1720407 sec
RG         128
DM         48.400 usec
DE         6.00 usec
TE         298.2 K
D1         1.00000000 sec
TDO        1

===== CHANNEL f1 =====
NUC1       1H
P1         8.50 usec
PL1        -6.00 dB
SFO1       500.1330885 MHz

F2 - Processing Parameters
SI         32768
SF         500.1300086 MHz
WDW        EM
SSB        0
LB         0.30 Hz
GB         0
PC         1.00

```

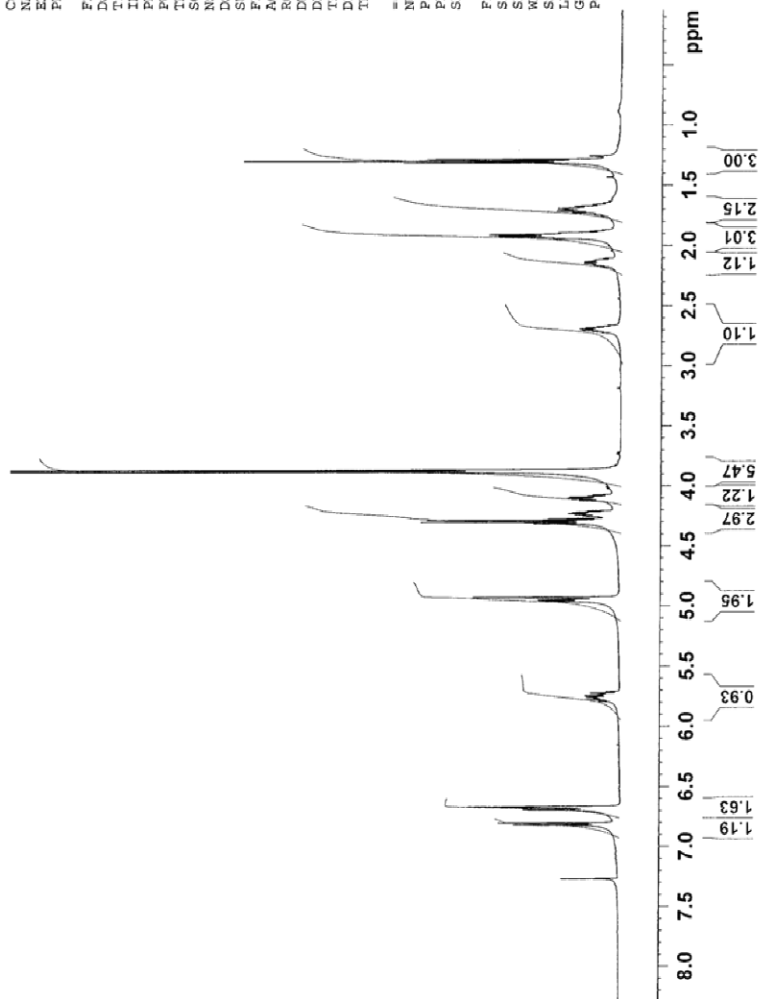


Figure 148. ¹H NMR (500 MHz) spectrum of ethyl [3-(3,4-dimethoxy)phenyl]-6-heptenyloxysulfonyl diazoacetate (**305**) in CDCl₃.

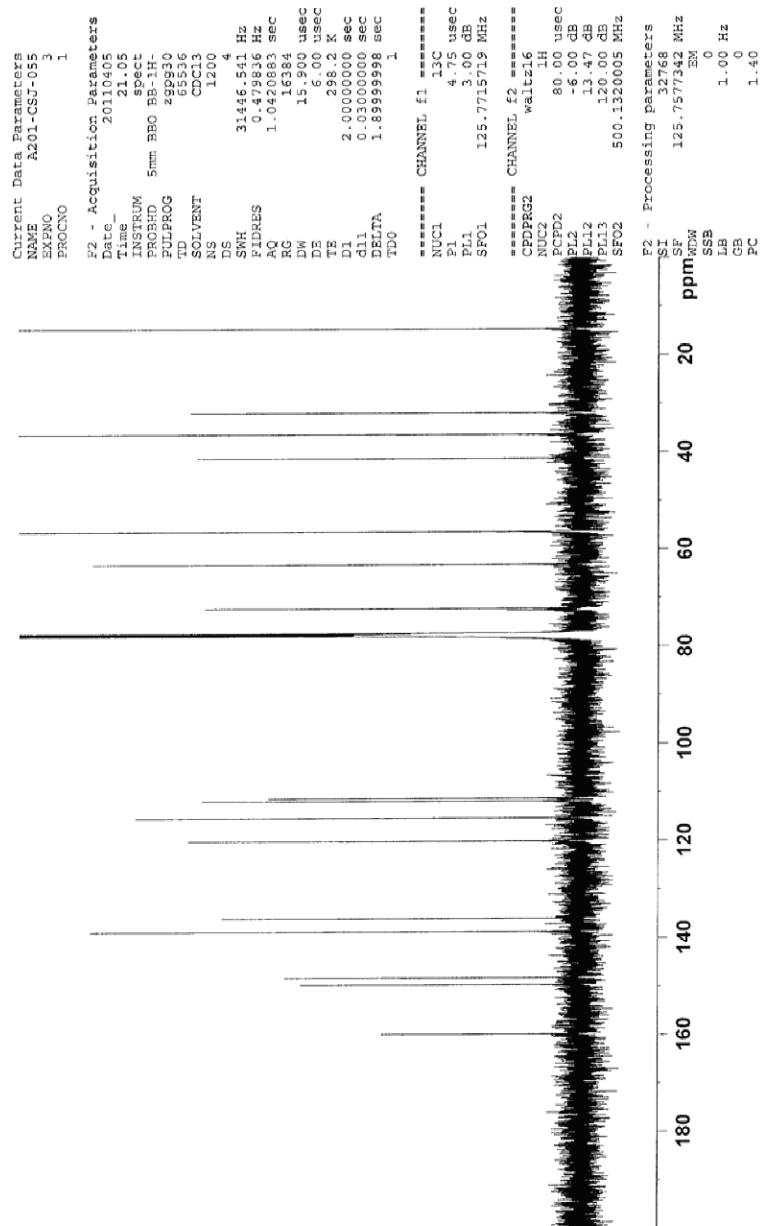


Figure 149. $^{13}\text{C}\{^1\text{H}\}$ NMR (125 MHz) spectrum of ethyl [3-(3,4-dimethoxy)phenyl-6-heptenyloxysulfonyl]diazoacetate (**305**) in CDCl_3 .

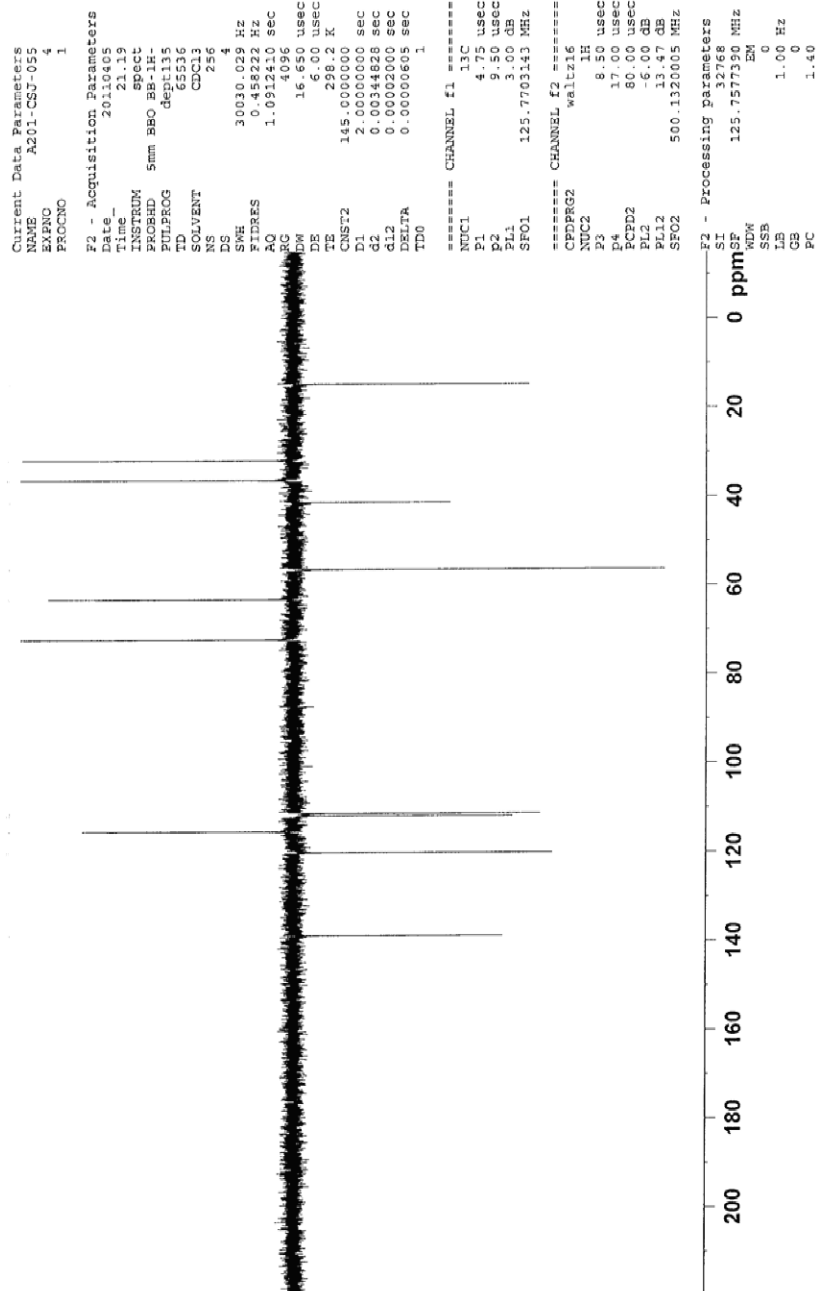


Figure 150. DEPT 135 NMR (125 MHz) spectrum of ethyl [3-(3,4-dimethoxy)phenyl-6-heptenyloxysulfonyl]diazoacetate (**305**) in CDCl_3 .

REFERENCES

1. <http://www.Fda.Gov/aboutfda/reportsmanualsforms/reports/ucm276385.Htm>. (Accessed 04/09/2012).
2. Davies, H. M. L.; Dick, A. R. Functionalization of carbon–hydrogen bonds through transition metal carbenoid insertion. *Top. Curr. Chem.* **292**, 303–345.
3. Davies, H. M. L.; Du, B. J.; Yu, J. Q. C–H functionalization in organic synthesis. *Chem. Soc. Rev.* **2011**, *40*, 1855–1856.
4. Doyle, M. P. Catalytic methods for metal carbene transformations. *Chem. Rev.* **1986**, *86*, 919–940.
5. Godula, K.; Sames, D. C–H bond functionalization in complex organic synthesis. *Science* **2006**, *312*, 67–72.
6. Labinger, J. A.; Bercaw, J. E. Understanding and exploiting C–H bond activation. *Nature* **2002**, *417*, 507–514.
7. Kakiuchi, F.; Chatani, N. Catalytic methods for C–H bond functionalization: Application in organic synthesis. *Adv. Synth. Catal.* **2003**, *345*, 1077–1101.
8. Sezen, B.; Sames, D. Diversity synthesis via C–H bond functionalization: Concept-guided development of new C-arylation methods for imidazoles. *J. Am. Chem. Soc.* **2006**, *128*, 8364.
9. White, M. C. Adding aliphatic C–H bond oxidations to synthesis. *Science*. **2012**, *335*, 807–809.
10. Dick, A. R.; Sanford, M. S. Transition metal catalyzed oxidative functionalization of carbon–hydrogen bonds. *Tetrahedron* **2006**, *62*, 2439–2463.
11. Chen, M. S.; White, M. C. A predictably selective aliphatic C–H oxidation reaction for complex molecule synthesis. *Science* **2007**, *318*, 783–787.
12. Doyle, M. P. Catalytic methods for metal carbene transformations. *Chem. Rev.* **1986**, *86*, 919–939.

13. Davies, H. M. L.; Manning, J. R. Catalytic C–H functionalization by metal carbenoid and nitrenoid insertion. *Nature* **2008**, *451*, 417–424.
14. Doyle, M. P.; Duffy, R.; Ratnikov, M.; Zhou, L. Catalytic carbene insertion into C–H bonds. *Chem. Rev.* **2011**, *110*, 704–724.
15. Doyle, M. P. Electrophilic metal carbenes as reaction intermediates in catalytic reactions. *Acc. Chem. Res.* **1986**, *19*, 348–356.
16. Xu, X.; Hu, W.-H.; Zavalij, P. Y.; Doyle, M. P. Divergent outcomes of carbene transfer reactions from dirhodium- and copper-based catalysts separately or in combination. *Angew. Chem., Int. Ed.* **2011**, *50*, 11152–11155.
17. Doyle, M. P. *In Asymmetric cyclopropanation*; VCH: 1993; pp 63–99.
18. Deng, G.; Xu, B.; Wang, J. A new method for the synthesis of 2-cyclopenten-1-one-5-carboxylic ester derivatives via Rh₂(OAc)₄-mediated intramolecular C–H insertion reaction of 4-vinyl-diazo-keto esters. *Tetrahedron* **2005**, *61*, 10811–10817.
19. Davies, H. M. L.; Morton, D. Guiding principles for site selective and stereoselective intermolecular C–H functionalization by donor/acceptor rhodium carbenes. *Chem. Soc. Rev.* **2011**, *40*, 1857–1869.
20. Fiori, K. W.; Du, B. J. *In Development of a Rh-catalyzed intermolecular C–H amination reaction*; American Chemical Society: 2006; pp 489.
21. Taber, D. F.; You, K. K.; Rheingold, A. L. Predicting the diastereoselectivity of Rh-mediated intramolecular C–H insertion. *J. Am. Chem. Soc.* **1996**, *118*, 547–556.
22. Nadeau, E.; Ventura, D. L.; Brekan, J. A.; Davies, H. M. L. Controlling factors for C–H functionalization versus cyclopropanation of dihydronaphthalenes. *J. Org. Chem.* **2010**, *75*, 1927–1939.
23. Sezen, B.; Franz, R.; Sames, D. C–C bond formation via C–H bond activation: Catalytic arylation and alkenylation of alkane segments. *J. Am. Chem. Soc.* **2006**, *128*, 25, 8364.
24. Aumann, R. Formation of carbon–carbon double bonds by novel insertion reactions of allenes, heterocumulenes and acid amides into metal–carbon double bond of Fischer carbene complexes. *Adv. Met.* **1989**, *269*, 211–231.
25. Arndtsen, B. A.; Bergman, R. G.; Mobley, T. A.; Peterson, T. H. Selective intermolecular carbon–hydrogen bond activation by synthetic metal complexes in homogeneous solution. *Acc. Chem. Res.* **1995**, *28*, 154–162.

26. Jia, C.; Kitamura, T.; Fujiwara, Y. Catalytic functionalization of arenes and alkanes via C–H bond activation. *Acc. Chem. Res.* **2001**, *34*, 633–639.
27. Jia, C.; Piao, D.; Oyamada, J.; Lu, W.; Kitamura, T.; Fujiwara, Y. Efficient activation of aromatic C–H bonds for addition to C–C multiple bonds. *Science* **2000**, *287*, 1992–1995.
28. Sezen, B.; Sames, D. Selective and catalytic arylation of *N*-phenylpyrrolidine: sp³ C–H bond functionalization in the absence of a directing group. *J. Am. Chem. Soc.* **2006**, *128*, 3102.
29. Keuseman, K. J.; Smoliakova, I. P.; Dunina, V. V. Cyclopalladation of (*S*)-4-*tert*-butyl-2-methyl-2-oxazoline: An unprecedented case of (sp³) C–H bond activation resulting in exo-palladacycle formation. *Organometallics* **2005**, *24*, 4159–4169.
30. Mawo, R. Y.; Mustakim, S.; Young Jr, V. G.; Hoffmann, M. R.; Smoliakova, I. P. Endo-effect-driven regioselectivity in the cyclopalladation of (*S*)-2-*tert*-butyl-4-phenyl-2-oxazoline. *Organometallics* **2007**, *26*, 1801–1810.
31. Chatani, N.; Amishiro, N.; Morii, T.; Yamashita, T.; Murai, S. Pd-catalyzed coupling reaction of acetylenes, iodotrimethylsilane, and organozinc reagents for the stereoselective synthesis of vinylsilanes. *J. Org. Chem.* **1995**, *60*, 1834–1840.
32. Hawari, J.; Davis, S.; Engel, P.; Gilbert, B.; Griller, D., The free radical reaction between alkanes and carbon tetrachloride. *J. Am. Chem. Soc.* **1985**, *107*, 4721–4724.
33. Atkinson, R.; Aschmann, S. M. OH radical reaction rate constants for polycyclic alkanes: Effects of ring strain and consequences for estimation methods. *Int. J. Cheml. Kinet.* **1992**, *24*, 983–989.
34. Davies, H. M. L.; Beckwith, R. E. J. Catalytic enantioselective C–H activation by means of metal-carbenoid-induced C–H insertion. *Chem. Rev.* **2003**, *103*, 2861–2903.
35. Lewis, J. C.; Bergman, R. G.; Ellman, J. A. Direct functionalization of nitrogen heterocycles via Rh-catalyzed C–H bond activation. *Acc. Chem. Res.* **2008**, *41*, 1013–1025.
36. Arndtsen, B. A.; Bergman, R. G. Unusually mild and selective hydrocarbon C–H bond activation with positively charged iridium(III) complexes. *Science* **1995**, *270*, 1970–1973.
37. Chatani, N.; Fukumoto, Y.; Ida, T.; Murai, S. Ruthenium-catalyzed reaction of 1, 6-diyne with hydrosilanes and carbon monoxide: A third way of incorporating CO. *J. Am. Chem. Soc.* **1993**, *115*, 11614–11615.

38. Shilov, A. E.; Shul'pin, G. B. Activation of C–H bonds by metal complexes. *Chem. Rev.* **1997**, *97*, 2879–2932.
39. Crabtree, R. H. The organometallic chemistry of alkanes. *Chem. Rev.* **1985**, *85*, 245–269.
40. Crabtree, R. H., Organometallic alkane C–H activation. *J. Organomet. Chem.* **2004**, *689*, 4083–4091.
41. Maguire, J. A.; Petrillo, A.; Goldman, A. S. Efficient transfer-dehydrogenation of alkanes catalyzed by rhodium trimethylphosphine complexes under dihydrogen atmosphere. *J. Am. Chem. Soc.* **1992**, *114*, 9492–9498.
42. Davies, H. M. L. Recent advances in catalytic enantioselective intermolecular C–H functionalization. *Angew. Chem., Int. Ed.* **2006**, *45*, 6422–6425.
43. Pastine, S. J.; Gribkov, D. V.; Sames, D. sp^3 C–H bond arylation directed by amidine protecting group: C-arylation of pyrrolidines and piperidines. *J. Am. Chem. Soc.* **2006**, *128*, 14220–14221.
44. Chatani, N.; Asaumi, T.; Yorimitsu, S.; Ikeda, T.; Kakiuchi, F.; Murai, S. $Ru_3(CO)_{12}$ -catalyzed coupling reaction of sp^3 C–H bonds adjacent to a nitrogen atom in alkylamines with alkenes. *J. Am. Chem. Soc.* **2001**, *123*, 10935–10941.
45. Taber, D. F.; Petty, E. H., General route to highly functionalized cyclopentane derivatives by intramolecular C–H insertion. *J. Org. Chem.* **1982**, *47*, 4808–4809.
46. Doyle, M. P. New catalysts and methods for highly enantioselective metal carbene reactions. *Pure Appl. Chem.* **1998**, *70*, 1123–1128.
47. Doyle, M. P., Chiral rhodium(II) carboxamides. Remarkably effective catalysts for enantioselective metal carbene transformations. *ACS Symp. Ser.* **1993**, *517*, 40–57.
48. Davies, H. M. L.; Long, M. S. Recent advances in catalytic intramolecular C–H aminations. *Angew. Chem., Int. Ed.* **2005**, *44*, 3518–3520.
49. Davies, H. M. L.; Denton, J. R. Application of donor/acceptor-carbenoids to the synthesis of natural products. *Chem. Soc. Rev.* **2009**, *38*, 11, 3061–3071.
50. Davies, H. M. L. C–H insertion reactions, cycloadditions, and ylide formation of diazo compounds. *Compr. Asymmetric Catal., Suppl.* **2004**, *1*, 83–94.
51. Sulikowski, G. A.; Cha, K. L.; Sulikowski, M. M. Stereoselective intramolecular carbon-hydrogen insertion reactions of metal carbenes. *Tetrahedron: Asymmetry* **1998**, *9*, 3145–3169.

52. Arduengo, A., Looking for stable carbenes: The difficulty in starting anew. *Acc. Chem. Res.* **1999**, *32*, 913–921.
53. Bourissou, D.; Guerret, O.; Gabbai, F. P.; Bertrand, G. Stable carbenes. *Chem. Rev.* **2000**, *100*, 39–92.
54. Arduengo III, A. J.; Dias, H. V. R.; Harlow, R. L.; Kline, M. Electronic stabilization of nucleophilic carbenes. *J. Am. Chem. Soc.* **1992**, *114*, 5530–5534.
55. Nakamura, E.; Yoshikai, N.; Yamanaka, M. Mechanism of C–H bond activation/C–C bond formation reaction between diazo compound and alkane catalyzed by dirhodium tetracarboxylate. *J. Am. Chem. Soc.* **2002**, *124*, 7181–7192.
56. Taber, D. F.; You, K.; Song, Y. A simple preparation of α -diazo esters. *J. Org. Chem.* **1995**, *60*, 1093–1094.
57. Padwa, A.; Austin, D. J.; Price, A. T.; Semones, M. A.; Doyle, M. P.; Protopopova, M. N.; Winchester, W. R.; Tran, A. Ligand effects on dirhodium(II) carbene reactivities. Highly effective switching between competitive carbenoid transformations. *J. Am. Chem. Soc.* **1993**, *115*, 8669–8680.
58. Taber, D. F.; Tian, W. Rhodium-catalyzed intramolecular C–H insertion of α -aryl- α -diazo ketones. *J. Org. Chem.* **2007**, *72*, 3207–3210.
59. Wang, P.; Adams, J. Model studies of the stereoelectronic effect in Rh(II) mediated carbenoid C–H insertion reactions. *J. Am. Chem. Soc.* **1994**, *116*, 3296–3305.
60. Hansen, J.; Autschbach, J.; Davies, H. M. L. Computational study on the selectivity of donor/acceptor-substituted rhodium carbenoids. *J. Org. Chem.* **2009**, *74*, 6555–6563.
61. Hansen, J.; Autschbach, J.; Davies, H. M. L. Computational study on the selectivity of donor/acceptor-substituted rhodium carbenoids. *J. Org. Chem.* **2009**, *74*, 6555–6563.
62. Reddy, R. P.; Lee, G. H.; Davies, H. M. L. Dirhodium tetracarboxylate derived from adamantylglycine as a chiral catalyst for carbenoid reactions. *Org. Lett.* **2006**, *8*, 3437–3440.
63. Slattery, C. N.; Ford, A.; Maguire, A. R. Catalytic asymmetric C–H insertion reactions of α -diazocarbonyl compounds. *Tetrahedron* **2009**, *34*, 6681–6705.
64. Hansen, J.; Davies, H. M. L. High symmetry dirhodium(II) paddlewheel complexes as chiral catalysts. *Coord. Chem. Rev.* **2008**, *252*, 545–555.

65. Doyle, M. P.; Winchester, W. R.; Hoorn, J. A. A.; Lynch, V.; Simonsen, S. H.; Ghosh, R. Dirhodium(II) tetrakis(carboxamidates) with chiral ligands. Structure and selectivity in catalytic metal-carbene transformations. *J. Am. Chem. Soc.* **1993**, *115*, 9968–9978.
66. Doyle, M. P.; Winchester, W. R.; Protopopova, M. N. Tetrakis[(4*S*)-4-phenyloxazolidin-2-one]dirhodium(II) and its catalytic applications for metal carbene transformations. *Helv. Chim. Acta.* **1993**, *76*, 2227–2235.
67. Davies, H. M. L.; Hodges, L. M. Rhodium carboxylate catalyzed decomposition of vinyl diazoacetates in the presence of heterodienes: Enantioselective synthesis of the 6-azabicyclo[3.2.2]nonane and 6-azabicyclo[3.2.2]nonanone ring systems. *J. Org. Chem.* **2002**, *67*, 5683–5689.
68. Demonceau, A.; Noels, A.; Hubert, A.; Teyssie, P. Transition-metal-catalysed reactions of diazoesters. Insertion into C–H bonds of paraffins catalysed by bulky rhodium(II) carboxylates: Enhanced attack on primary C–H bonds. *B. Soc. Chim. Belg.* **1984**, *93*, 945–948.
69. Maas, G., Transition-metal catalyzed decomposition of aliphatic diazo compounds: New results and applications in organic synthesis. *Top. Curr. Chem.* **1987**, *137*, 75–253.
70. Padwa, A.; Austin, D. J. Ligand effects on the chemoselectivity of transition metal catalyzed reactions of α -diazo carbonyl compounds. *Angew. Chem. Int. Edit.* **1994**, *33*, 1797–1815.
71. Pirrung, M. C.; Morehead Jr, A. T. Electronic effects in dirhodium(II) carboxylates. Linear free energy relationships in catalyzed decompositions of diazo compounds and CO and isonitrile complexation. *J. Am. Chem. Soc.* **1994**, *116*, 8991–9000.
72. Hashimoto, S.; Watanabe, N.; Ikegami, S., Dirhodium(II) tetra(triphenylacetate): A highly efficient catalyst for the site-selective intramolecular carbon-hydrogen insertion reactions of α -diazo-keto esters. *Tetrahedron Lett.* **1992**, *33*, 2709–2712.
73. Doyle, M. P.; Westrum, L. J.; Wolthuis, W. N. E.; See, M. M.; Boone, W. P.; Bagheri, V.; Pearson, M. M. Electronic and steric control in carbon-hydrogen insertion reactions of diazoacetoacetates catalyzed by dirhodium(II) carboxylates and carboxamides. *J. Am. Chem. Soc.* **1993**, *115*, 958–964.
74. Taber, D. F.; Malcolm, S. C. Rhodium-mediated intramolecular C–H insertion: Probing the geometry of the transition state. *J. Org. Chem.* **1998**, *63*, 3717–3721.
75. Davies, H. M. L.; Pelphrey, P. M. Intermolecular C–H insertions of carbenoids. *Org. React.* **1998**, *75*, 75–211.

76. Davies, H. M. L.; Loe, O. Intermolecular C–H insertions of donor/acceptor-substituted rhodium carbenoids: A practical solution for catalytic enantioselective C–H activation. *Synthesis* **2004**, 16, 2595–2608.
77. Davies, H. M. L.; Hedley, S. J. Intermolecular reactions of electron-rich heterocycles with copper and rhodium carbenoids. *Chem. Soc. Rev.* **2007**, 36, 1109–1119.
78. Candeias, N. R.; Gois, P. M. P.; Afonso, C. A. M. Rh(II)-catalyzed intramolecular C–H insertion of diazo substrates in water: Scope and limitations. *J. Org. Chem.* **2006**, 71, 5489–5497.
79. Davies, H. M. L.; Antoulinakis, E. G. Intermolecular metal-catalyzed carbenoid cyclopropanations. *Org. React.* **2001**, 57, 2150–2160.
80. Davies, H. M. L.; Hansen, T. Asymmetric intermolecular carbenoid C–H insertions catalyzed by rhodium(II) (*S*)-*N*-(*p*-dodecylphenyl) sulfonylprolinate. *J. Am. Chem. Soc.* **1997**, 119, 9075–9076.
81. Davies, H. M. L.; Hodges, L. M.; Matasi, J. J.; Hansen, T.; Stafford, D. G. Effect of carbenoid structure on the reactivity of rhodium-stabilized carbenoids. *Tetrahedron Lett.* **1998**, 39, 4417–4420.
82. Corey, E. J.; Gant, T. G. A catalytic enantioselective synthetic route to the important antidepressant sertraline. *Tetrahedron Lett.* **1994**, 35, 5373–5376.
83. Davies, H. M. L.; Dai, X. Application of the combined C–H activation/cope rearrangement as a key step in the total syntheses of the assigned structure of (+)-elisabethadione and a (+)-*p*-benzoquinone natural product. *Tetrahedron* **2006**, 62, 10477–10484.
84. Davies, H. M. L.; Stafford, D. G.; Hansen, T. Catalytic asymmetric synthesis of diarylacetates and 4,4-diarylbutanoates. A formal asymmetric synthesis of (+)-sertraline. *Org. Lett.* **1999**, 1, 233–236.
85. Davies, H. M. L.; Doan, B. D. Total synthesis of (±)-tremulenolide A and (±)-tremulenediol A via a stereoselective cyclopropanation/Cope rearrangement annulation strategy. *J. Org. Chem.* **1998**, 63, 657–660.
86. Larson, K. K.; Sarpong, R. Total synthesis of alkaloid (±)-GB 13 using a Rh(II)-catalyzed ketone hydroarylation and late-stage pyridine reduction. *J. Am. Chem. Soc.* **2009**, 131, 13244–13245.

87. Davies, H. M. L.; Beckwith, R. E. J.; Antoulinakis, E. G.; Jin, Q. New strategic reactions for organic synthesis: Catalytic asymmetric C–H activation to oxygen as a surrogate to the aldol reaction. *J. Org. Chem.* **2003**, *68*, 6126–6132.
88. Davies, H. M. L.; Venkataramani, C.; Hansen, T.; Hopper, D. W. New strategic reactions for organic synthesis: Catalytic asymmetric C–H activation to nitrogen as a surrogate for the Mannich reaction. *J. Am. Chem. Soc.* **2003**, *125*, 6462–6468.
89. Davies, H. M. L.; Ni, A. Enantioselective synthesis of α -amino esters and its application to the synthesis of the enantiomers of the antidepressant venlafaxine. *Chem. Commun.* **2006**, *29*, 3110–3112.
90. Hansen, J. H.; Gregg, T. M.; Ovalles, S. R.; Lian, Y.; Autschbach, J.; Davies, H. M. L. On the mechanism and selectivity of the combined C–H activation/Cope rearrangement. *J. Am. Chem. Soc.* *133*, 5076–5085.
91. Davies, H. M. L.; Loe, O.; Stafford, D. G. Sequential cycloaddition approach to the tricyclic core of vibsantin E. Total synthesis of (\pm)-5-*epi*-10-*epi*-vibsantin E. *Org. Lett.* **2005**, *7*, 5561–5563.
92. Davies, H. M. L.; Jin, Q. Catalytic asymmetric reactions for organic synthesis: The combined C–H activation/Cope rearrangement. *Proc. Natl. Acad. Sci.* **2004**, *101*, 15472–15475.
93. Davies, H. M. L.; Dai, X.; Long, M. S. Combined C–H activation/Cope rearrangement as a strategic reaction in organic synthesis: Total synthesis of (-)-colombiasin A and (-)-elisapterosin B. *J. Am. Chem. Soc.* **2006**, *128*, 2485–2490.
94. Davies, H. M. L.; Walji, A. M.; Townsend, R. J. Catalytic asymmetric C–H activation by methyl thiophen-3-yl diazoacetate applied to the synthesis of (+)-cetiedil. *Tetrahedron Lett.* **2002**, *43*, 4981–4983.
95. Davies, H. M. L.; Manning, J. R. Catalytic C–H functionalization by metal carbenoid and nitrenoid insertion. *Nature* **2008**, *451*, 417–424.
96. Davies, H. M. L.; Gregg, T. M. Asymmetric synthesis of (+)-indatraline using rhodium-catalyzed C–H activation. *Tetrahedron Lett.* **2002**, *43*, 4951–4953.
97. Wee, A. G. H. Rhodium(II)-catalyzed reaction of diazocompounds in the service of organic synthesis of natural and non-natural products. *Curr. Org. Synth.* **2006**, *3*, 499–555.

98. Xu, X.; Hu, W.-H.; Doyle, M. P. Highly enantioselective catalytic synthesis of functionalized chiral diazoacetates. *Angew. Chem. Int. Ed. Engl.* **1998**, *50*, 6392–6395.
99. Yoon, C. H.; Flanigan, D. L.; Chong, B.-D.; Jung, K. W. A novel synthetic route to chiral gamma-lactams from alpha-amino acids via Rh-catalyzed intramolecular C–H insertion. *J. Org. Chem.* **2002**, *67*, 6582–6584.
100. Taber, D. F.; You, K. K. Highly diastereoselective cyclopentane construction: Enantioselective synthesis of the dendrobatid alkaloid 251F. *J. Am. Chem. Soc.* **1995**, *117*, 5757–5762.
101. Taber, D. F.; Walter, R.; Meagley, R. P. Intramolecular C–H insertion by an alkylidene carbene: Diastereoselective synthesis of a taxol ring synthon. *J. Org. Chem.* **1994**, *59*, 6014–6017.
102. Taber, D. F.; Song, Y. Specific C–C bond construction by remote C–H activation: Synthesis of (-)-*trans*-cembranolide. *J. Org. Chem.* **1997**, *62*, 6603–6607.
103. Doyle, M. P.; Colyer, J. Steric balance within chiral dirhodium(II) carboxamidate catalysts enhances stereoselectivity. *J. Mol. Catal. A: Chem.* **2003**, *196*, 93–100.
104. Taber, D. F.; Hennessy, M. J.; Hoerrner, R. S.; Raman, K.; Ruckle, R. E., Jr.; Schuchardt, J. S. Cyclopentane construction by rhodium-catalyzed intramolecular C–H insertion: Scope and selectivity. *Chem. Ind.* **1990**, *40*, 43–60.
105. Zhang, B.; Wee, A. G. H. Di- and trisubstituted β -lactams via Rh(II)-carbenoid reaction of branched, *N*-bis(trimethylsilyl)methyl-diazoamides. Synthesis of (\pm)-allokainic acid. *Org. Lett.* **2001**, *14*, 2654.
106. Taber, D. F.; Tian, W. Synthesis of (-)-hamigeran B. *J. Org. Chem.* **2008**, *73*, 7560–7564.
107. Kurosawa, W.; Kan, T.; Fukuyama, T., Stereocontrolled total synthesis of (-)-ephedradine A (orantine). *J. Am. Chem. Soc.* **2003**, *125*, 8112–8113.
108. Doyle, M. P.; May, E. J., Enantioselective γ -lactone formation from phenyldiazoacetates via catalytic intramolecular carbon-hydrogen insertion. *Synlett* **2001**, 967–969.
109. Doyle, M. P.; Oon, S. M.; Van, H. F. R.; Brown, C. B. β -Lactam formation via rhodium(II) catalyzed carbon-hydrogen insertion reactions of α -diazo amides. *Bioorg. Med. Chem. Lett.* **1993**, *3*, 2409–2414.
110. Doyle, M. P.; Hu, W. Enantioselective carbon-hydrogen insertion is an effective and efficient methodology for the synthesis of (*R*)-(-)-baclofen. *Chirality* **2002**, *14*, 169–172.

111. Liu, W.-J.; Chen, Z.-L.; Chen, Z.-Y.; Hu, W.-H. Dirhodium catalyzed intramolecular enantioselective C–H insertion reaction of *N*-cumyl-*N*-(2-*p*-anisylethyl)diazoacetamide: Synthesis of (-)-rolipram. *Tetrahedron: Asymmetry* **2005**, *16*, 1693–1698.
112. Doyle, M. Enantiocontrol in catalytic metal carbene reactions. *Russ. Chem. B⁺* **1999**, *48*, 16–20.
113. Taber, D. F.; Schuchardt, J. L. Intramolecular carbon-hydrogen insertion: Synthesis of (±)-pentalenolactone E methyl ester. *J. Am. Chem. Soc.* **1985**, *107*, 5289–5290.
114. White, J. D.; Hrcnciar, P.; Stappenbeck, F. Asymmetric synthesis of (+)-morphine. The phenanthrene route revisited. *J. Org. Chem.* **1997**, *62*, 5250–5251.
115. Srikrishna, A.; Gharpure, S. J. An intramolecular rhodium carbenoid C–H insertion approach to chiral isotwistanes. Synthesis of (-)-neopupukean-4,10-dione and (-)-neopupukean-10-one. *Chem. Commun.* **1998**, *15*, 1589–1590.
116. Babu, S. D.; Hrytsak, M. D.; Durst, T. Intramolecular rhodium carbenoid insertions into aromatic carbon-hydrogen bonds. Preparation of 1,3-dihydrothiophene 2,2-dioxides fused onto aromatic rings. *Can. J. Chem.* **1989**, *67*, 1071–1076.
117. Hrytsak, M.; Etkin, N.; Durst, T. Intramolecular rhodium carbenoid insertions into aromatic C–H bonds. Preparation of 1-carboalkoxy-1,3-dihydrobenzo[*c*]thiophene 2,2-dioxide. *Tetrahedron Lett.* **1986**, *27*, 47, 5679–5682.
118. Zalatan, D. N.; Du Bois, J. A chiral rhodium carboxamidate catalyst for enantioselective C–H amination. *J. Am. Chem. Soc.* **2008**, *130*, 9220–9221.
119. Wehn, P. M.; Lee, J.; Du Bois, J. Stereochemical models for Rh-catalyzed amination reactions of chiral sulfamates. *Org. Lett.* **2003**, *5*, 4823–4826.
120. Espino, C. G.; Du Bois, J. A Rh-catalyzed C–H insertion reaction for the oxidative conversion of carbamates to oxazolidinones. *Angew. Chem.* **2001**, *113*, 618–620.
121. Fiori, K. W.; Du Bois, J. Catalytic intermolecular amination of C–H bonds: Method development and mechanistic insights. *J. Am. Chem. Soc.* **2007**, *129*, 562–568.
122. John, J. P.; Novikov, A. V. Selective formation of six-membered cyclic sulfones and sulfonates by C–H insertion. *Org. Lett.* **2007**, *9*, 61–63.
123. Wolckenhauer, S. A.; Devlin, A. S.; Du, B. J. δ -sultone formation through Rh-catalyzed C–H insertion. *Org. Lett.* **2007**, *9*, 4363–4366.

124. Jungong, C. S.; John, J. P.; Novikov, A. V. Formation of six- versus five-membered cyclic sulfones by C–H insertion. *Tetrahedron Lett.* **2009**, *50*, 1954–1957.
125. Catino, A. J.; Forslund, R. E.; Doyle, M. P. Dirhodium(II) caprolactamate: An exceptional catalyst for allylic oxidation. *J. Am. Chem. Soc.* **2004**, *126*, 13622–13623.
126. Flynn, C. J.; Elcoate, C. J.; Lawrence, S. E.; Maguire, A. R. Highly enantioselective intramolecular copper catalyzed C–H insertion reactions of α -diazosulfones. *J. Am. Chem. Soc.* *132*, 4, 1184–1185.
127. Wee, A. G. H.; Duncan, S. C.; Fan, G.-J. Intramolecular asymmetric C–H insertion of *N*-arylalkyl, *N*-bis(trimethylsilyl)methyldiazoamides mediated by chiral rhodium(II) catalysts. Synthesis of (*R*)-benzyl- γ -aminobutyric acid. *Tetrahedron: Asymmetry* **2006**, *17*, 297–307.
128. Taber, D. F.; Raman, K.; Gaul, M. D. Enantioselective ring construction: Synthesis of (+)-estrone methyl ether. *J. Org. Chem.* **1987**, *52*, 28–34.
129. Taber, D. F.; Petty, E. H.; Raman, K., Enantioselective ring construction: Synthesis of (+)-cuparenone. *J. Am. Chem. Soc.* **1985**, *107*, 196–199.
130. Adams, J.; Poupart, M. A.; Grenier, L. Diastereoselectivity in the synthesis of 3 (*2H*)-furanones. Total synthesis of (+)-muscarine. *Tetrahedron Lett.* **1989**, *30*, 1753–1756.
131. Doyle, M. P. Asymmetric syntheses with catalytic enantioselective metal carbene transformations. *Izv. Akad. Nauk, Ser. Khim.* **1994**, *11*, 1879–1892.
132. Wee, A. G. H.; Duncan, S. C. The bis(trimethylsilyl)methyl group as an effective *n*-protecting group and site-selective control element in rhodium(II)-catalyzed reaction of diazoamides. *J. Org. Chem.* **2005**, *70*, 8372–8380.
133. Davies, H. M. L.; Stafford, D. G.; Doan, B. D.; Houser, J. H. Tandem asymmetric cyclopropanation/cope rearrangement. A highly diastereoselective and enantioselective method for the construction of 1, 4-cycloheptadienes. *J. Am. Chem. Soc.* **1998**, *120*, 3326–3331.
134. Reddy, R. P.; Davies, H. M. L. Dirhodium tetracarboxylates derived from adamantylglycine as chiral catalysts for enantioselective C–H aminations. *Org. Lett.* **2006**, *8*, 5013–5016.
135. House, H. O.; Larson, J. K. The use of beta-ketone sulfones as synthetic intermediates. *J. Org. Chem.* **1968**, *33*, 61–65.

136. Trost, B. M.; Verhoeven, T. R. New synthetic reactions. Catalytic vs. Stoichiometric allylic alkylation. Stereocontrolled approach to steroid side chain. *J. Am. Chem. Soc.* **1976**, *98*, 630–632.
137. Lee, G. H.; Lee, H. K.; Choi, E. B.; Kim, B. T.; Pak, C. S. An efficient Julia olefination mediated by magnesium in ethanol. *Tetrahedron Lett* **1995**, *36*, 5607–5608.
138. Molander, G. A.; Hahn, G. Lanthanides in organic synthesis. Reduction of alpha-heterosubstituted ketones. *J. Org. Chem.* **1986**, *51*, 1135–1138.
139. Duffy, L. A.; Matsubara, H.; Procter, D. J. A ring size-selective reduction of lactones using SmI₂ and H₂O. *J. Am. Chem. Soc.* **2008**, *130*, 1136–1137.
140. Jungong, C. S.; John, J. P.; Bequette, J. P.; Novikov, A. V. Synthetically useful transformations of δ-sultones and thiane-1,1-dioxides obtained by C–H insertion. *Heterocycles* **2009**, *78*, 2531–2539.
141. Deacon, G. B.; Forsyth, C. M.; Sun, J. Regiospecific replacement of fluorine by hydrogen in an aromatic ring induced by a rare earth organometallic. *Tetrahedron Lett.* **1994**, *35*, 1095–1098.
142. Tsutsui, H.; Ichikawa, T.; Narasaka, K. Preparation of primary amines by the alkylation of O-sulfonyloximes of benzophenone derivatives with Grignard reagents. *B. Chem. Soc. Jpn.* **1999**, *72*, 1869–1878.
143. Watanabe, H.; Mao, C. L.; Hauser, C. R. Beckmann rearrangement of some benzophenone oximes having an ortho-*N*-substituted carboxamide or sulfonamide group leading to cyclization. *J. Org. Chem.* **1969**, *34*, 1786–1791.
144. Ryu, I.; Kuriyama, H.; Miyazato, H.; Minakata, S.; Komatsu, M.; Yoon, J. Y.; Kim, S. Zinc-induced deoxygenation of α,β-dioxo-type oximes and oxime ethers leading to α,β-diketo esters. *B. Chem. Soc. Jpn.* **2004**, *77*, 1407–1408.
145. Rao, A.; Bhalla, V.; Nayak, U.; Dev, S. Meroterpenoids: *Psoralea corylifolia* absolute configuration of (+)-bakuchiol. *Tetrahedron* **1973**, *29*, 1127–1130.
146. Labb, Ñ, C.; Faini, F.; Coll, J.; Connolly, J. D. Bakuchiol derivatives from the leaves of *Psoralea glandulosa*. *Phytochemistry* **1996**, *42*, 1299–1303.
147. Erazo, S.; Gonzalez, V.; Zaldivar, M.; Negrete, R. Antimicrobial activity of *Psoralea glandulosa*. *Pharm. Biol.* **1997**, *35*, 385–387.

148. Chen, H.; Du, X.; Tang, W.; Zhou, Y.; Zuo, J.; Feng, H.; Li, Y. Synthesis and structure immunosuppressive activity relationships of bakuchiol and its derivatives. *Bioorg. Med. Chem.* **2008**, *16*, 2403–2411.
149. Adhikari, S.; Joshi, R.; Patro, B.; Ghanty, T.; Chintalwar, G.; Sharma, A.; Chattopadhyay, S.; Mukherjee, T. Antioxidant activity of bakuchiol: Experimental evidences and theoretical treatments on the possible involvement of the terpenoid chain. *Chem. Res. Toxicol.* **2003**, *16*, 1062–1069.
150. Ryu, S. Y.; Choi, S. U.; Lee, C. O.; Zee, O. P. Antitumor activity of *psoralea corylifolia*. *Archives of Pharmacal Research* **1992**, *15*, 356–359.
151. Ferrandiz, M. L.; Gil, B.; Sanz, M. J.; Ubeda, A.; Erazo, S.; Gonzalez, E.; Negrete, R.; Pacheco, S.; Payaa, M.; Alcaraz, M. J., Effect of bakuchiol on leukocyte functions and some inflammatory responses in mice. *Journal of Pharmacy and Pharmacology* **1996**, *48*, 975–980.
152. Takano, S.; Shimazaki, Y.; Ogasawara, K., Enantiocontrolled synthesis of natural (+)-bakuchiol. *Tetrahedron Lett.* **1990**, *31*, 3325–3326.
153. Sakakiyama, S.; Yamamoto, K.; Asaoka, M. A new synthesis of (+)-bakuchiol. *Natural Product Lett.* **1999**, *14*, 1–4.
154. Esumi, T.; Shimizu, H.; Kashiya, A.; Sasaki, C.; Toyota, M.; Fukuyama, Y. Efficient construction of a chiral all-carbon quaternary center by asymmetric 1, 4-addition and its application to total synthesis of (+)-bakuchiol. *Tetrahedron Lett* **2008**, *49*, 6846–6849.
155. Du, X. L.; Chen, H. L.; Feng, H. J.; Li, Y. C., Stereoselective total synthesis of natural (S)-bakuchiol and its enantiomer. *Hel. Chim. Acta.* **2008**, *91*, 371–378.
156. Bequette, J. P.; Jungong, C. S.; Novikov, A. V. Enantioselective synthesis of bakuchiol using diazosulfonate C–H insertion to install the quaternary center. *Tetrahedron Lett.* **2009**, *50*, 6963–6964.
157. Deutsch, H. F.; Evenson, M. A.; Drescher, P.; Sparwasser, C.; Madsen, P. O. Isolation and biological activity of aspidospermine and quebrachamine from an aspidosperma tree source. *J. Pharm. Biomed. Anal.* **1994**, *12*, 1283–1287.
158. Stork, G.; Dolfini, J. E. The total synthesis of dl-aspidospermine and of dl-quebrachamine. *J. Am. Chem. Soc.* **1963**, *85*, 2872–2873.
159. Starke, K.; Borowski, E.; Endo, T., Preferential blockade of presynaptic adrenoceptors by yohimbine. *Eur. J. Pharmacol.* **1975**, *34*, 385–388.

160. Markey, S.; Biemann, K., Isolation of rhazidine and akuammidine from *aspidosperma quebracho blanco*. The structure of rhazidine. *Tetrahedron Lett.* **1967**, *2*, 157.
161. De Araajo, J. X.; Antheaume, C.; Trindade, R. C. P.; Schmitt, M.; Bourguignon, J. J.; Santâ Ana, A. E. G. Isolation and characterisation of the monoterpene indole alkaloids of *Aspidosperma pyriforme*. *Phytochem. Rev.* **2007**, *6*, 183–188.
162. Campos, A. R.; Lima, R. C. P.; Uchoa, D. E. A.; Silveira, E. R.; Santos, F. A.; Rao, V. S. N., Pro-erectile effects of an alkaloidal rich fraction from *aspidosperma* root bark in mice. *J. Ethnopharmacol.* **2006**, *104*, 240–244.
163. Bajtos, B.; Pagenkopf, B. L., Total synthesis of (±)-quebrachamine via [3+2] cycloaddition and efficient chloroacetamide photocyclization. *Eur. J. Org. Chem.* **2009**, *7*, 1072–1077.
164. Shikanga, E. A.; Viljoen, A.; Combrinck, S.; Marston, A. Isolation of scelletium alkaloids by high-speed countercurrent chromatography. *Phytochem. Lett.* **2011**, *4*, 190–193.
165. Shikanga, E. A.; Hamman, J. H.; Chen, W.; Combrinck, S.; Gericke, N.; Viljoen, A. M. In vitro permeation of mesembrine alkaloids from *Scelletium tortuosum* across porcine buccal, sublingual, and intestinal mucosa. *Planta Medica* **2012**, *78*, 260–268.